Università degli Studi di Ferrara

UCA Universidad de Cádiz

International Ph.D. Course
in
Earth and Marine Sciences

CYCLE XXXI

DIRECTOR Prof. Massimo Coltorti

The role of internal waves in ancient carbonate systems

Scientific/Disciplinary Sector (SDS) _GEO_/_02

Candidate
Dott.ssa Kiani Harchegani, Farkhondeh

_____
(signature)

Supervisors
Prof. Morsilli, Michele

Prof. Izquierdo González, Alfred

_____
(signature)

Abstract

Internal waves are perturbations propagating along the pycnocline, a boundary layer between two different density water masses. Although they are well known by oceanographers, their impact on the sedimentary record still poorly documented. In siliciclastic systems, breaking of internal waves on a sloping surface creates repetitive high-turbulent events and consequently erosion and transport of sediments along the shelves and continental slopes. In carbonate settings, internal waves can influence the carbonate production at the depth of pycnocliene by pumping the nutrient-rich waters to the carbonate buildups and create an ideal setting where the metazoan communities can thrive. The base of pycnocline is usually associated with the chlorophyll-maximum zone which corresponds to the lower part of the photic zone. The light penetration is one of the fundamental factor controlling loci, amount and type of carbonate productions. The light zones are named "euphotic", "oligophotic" or "mesophotic", and "aphotic". Recently, the role of internal waves, as a source of water turbulence, has been considered as a useful tool in the interpretation of mesophotic carbonate communities. During the Late Jurassic and Late Oligocene, extensive carbonate reefs have been developed along the Tethys. In this PhD project, two case studies from the Upper Jurassic stromatoporoid-rich facies and Late Oligocene (Chattian) coral-rich facies have been studied in order to study the role of internal waves in development of these carbonate communities. The Upper Jurassic stromatoporoid-rich facies of Monte Sacro Limestones (MSL) crop out along the platform margin of Apulia Carbonate Platform (ACP) in Gargano area. The stromatoporoid buildups in MSL are characterized by high percentage of high-energy debris-rich facies associated with low-energy facies. The origin of these high-energy facies are still matter of debates. The MSL is characterized by three lithofacies LF1- stromatoporoid-rich facies, LF2- stromatoporoid-coral facies, and LF3- stromatoporoid-microbial facies. LF1 is the main lithofacies developed in MSL and characterized by stromatoporoids growth in low-energy mesophotic condition (LF1-S1) associated with high-energy intraclastic-bioclastic rich facies (LF1-S2). The stromatoporoid-rich buildups (LF1) in ACP can be categorized as phototrophic-heterotrophic reefs generated in a pure carbonate environment. The light penetration was confined, resulted in the high development of light-independent micro-encrusters (*Tubiphytes morronensis*), in a mesophotic condition, where the environment was not ideal for light-dependent microencrusters (*Lithocodium-Bacinella*) to grow. The origin of high-energy facies developed associated with mesophotic

stromatoporoid buildups in MSL can be linked to the effect of internal waves. Firstly, internal waves can provide nutrient-rich water needed by stromatoporoid buildups to grow. Latterly, the buildups can be affected by high-energy turbulence, producing a large amount of high-energy debris rich facies (LF1-S2) in MSL. Moving on to a different age, the Late Oligocene (Chattian) coral-rich facies are well developed in Grotta San Michele Limestone (GSML) Gargano, Italy, as well as Asmari Formation, Zagros, Iran. The corals in GSML are surrounded by a mud-dominated matrix, indicating development in low-energy environments. The corals, are associated with meso-oligophotic components such as non-articulate red algae, rhodolith and *Polystrata alba*. However, the euphotic components such as articulated red-algae, and rare miliolids are associated with corals. Although these mesophotic corals can be mixed with euphotic components shed down from the shallower depth, the internal waves can be a factor to provide nutrient-rich water for coral colonies to develop in this low-energy settings. In the Zagros basin, Iran, the coral buildups are very well developed along the depositional profile. These coral buildups are characterized by a low-energy mud-dominated matrix and show the characteristics of cluster reefs. The corals are strongly encrusted by red algae and also associated with meso-oligophotic components such as non-articulated red algae, *Neorotalia* and *Nephrolepidina* suggesting mesophotic conditions. The internal waves can affect these mesophotic corals by two ways: provide the nutrient-rich water to buildups and produce high-energy turbulence responsible for the development of high-energy flank facies associated with coral buildups.

Keywords: Apulia Carbonate Platform (ACP); Internal waves; Stromatoporoid facies; Upper Jurassic reef; Mesophotic corals; Late Oligocene, Zagros Basin

Il ruolo delle onde interne in sistemi carbonatici antichi

Riassunto: Le onde interne sono delle perturbazioni che si propagano lungo la picnoclina, la superficie che delimita due masse d'acqua a differente densità. Sebbene siano ben note dagli oceanografi e dai biologi marini, il loro impatto sul record sedimentario è ancora poco conosciuto e documentato, e in alcuni casi completamente ignorato da Sedimentologi e Stratigrafi.

Nei sistemi silicoclastici, la frangenza delle onde interne su di una qualsiasi superficie inclinata crea ripetuti eventi di alta turbolenza con conseguente erosione e trasporto di sedimento sia verso l'alto che verso il basso, influenzando notevolmente i processi sedimentari sia sulle piattaforme continentali che lungo le adiacenti scarpate.

Nei sistemi carbonatici le onde interne, oltre a creare gli stessi effetti idrodinamici dei sistemi silicoclastici, possono influenzare la produzione carbonatica in prossimità della picnoclina attraverso il pompaggio di acque più o meno ricche di nutrienti, creando un contesto ideale in cui le comunità bentoniche di metazoi possano proliferare. Infatti, la base della picnoclina è comunemente associata con la zona di massima concentrazione della clorofilla e che in alcuni contesti coincide con la parte bassa della zona fotica.

Un altro fattore di controllo importante nei sistemi carbonatici è la penetrazione della luce che condiziona il tipo, la quantità e il luogo di produzione carbonatica. La zona Fotica è distinta usualmente in due zone principali denominate dall'alto verso il basso zona eufotica e oligofotica o mesofotica, per passare infine alla zona afotica.

Recentemente, le onde interne sono state considerate come potenziale processo che potrebbe spiegare la presenza e sviluppo di numerose *carbonate factories* meso/oligophotiche e le loro peculiari associazioni di facies.

Durante il Giurassico Superiore e l'Oligocene superiore, diversi sistemi carbonatici si sono sviluppati lungo i margini della Tetide o dell'area Mediterranea. In questo progetto di dottorato, sono stati considerati tre casi studio ricadenti in questo intervallo temporale allo scopo di caratterizzare le facies di margine biocostruito e il possibile ruolo delle onde interne nello sviluppo e ubicazione di questi sistemi carbonatici.

Le facies ricche di stromatoporoidi del Giurassico Superiore dei Calcari di Monte Sacro (MSL) affiorano lungo il margine della Piattaforma Carbonatica Apula (ACP) nel Promontorio del Gargano. La MSL è caratterizzata da tre facies LF1-stromatoporoidi-rich, facies LF2-stromatoporoidi-coralli e facies LF3-stromatoporoidi-microbialiti. LF1 è la litofacies principale sviluppata nei MSL e caratterizzata dalla crescita di stromatoporoidi in condizioni mesofotiche a bassa energia (LF1-S1) associate a facies di alta energia intraclastiche-bioclastiche (LF1-S2). L'origine delle facies ad alta energia in MSL può essere collegata all'azione delle onde interne. In primo luogo, le onde interne possono fornire i nutrienti necessari per la crescita dei buildup a stromatoporoidi. Questi accumuli possono essere influenzati periodicamente da turbolenza, producendo una grande quantità di facies detritiche di alta energia (LF1-S2).

Per i sistemi dell'Oligocene superiore sono stati scelti due sistemi carbonatici caratterizzati da facies con abbondanti coralli, ubicati rispettivamente nel Promontorio del Gargano e nell'Iran Centrale (Monti Zagros). La facies ricca di coralli dell'Oligocene superiore (Cattiano) è ben sviluppata nei Calcari di Grotta di San Michele (GSML) nel Gargano, e nella Formazione di Asmari, Monti Zagros, Iran.

I coralli della GSML sono circondati da una matrice dominata da sedimenti fini fangosi, e che indica un ambiente a bassa energia. Sebbene questi coralli mesofotici possano essere mescolati con componenti eufotici le onde interne possono essere un fattore per fornire acqua ricca di nutrienti per le colonie di coralli che si sviluppino in queste condizioni a bassa energia. Nel bacino di Zagros, in Iran, gli accumuli di coralli sono molto sviluppati lungo il profilo deposizionale. Anche in questo caso, questi accumuli di coralli sono caratterizzati da una matrice dominata da fango carbonatico. Le onde interne possono influenzare questi coralli mesofotici in due modi: fornire l'acqua ricca di nutrienti alle comunità bentoniche e produrre eventi turbolenti responsabili dello sviluppo di facies detritiche sul fianco delle biocostruzioni.

Acknowledgment

I would like to extend thanks to the many people who so generously contributed to the work presented in this thesis.

Special mention goes to my enthusiastic supervisor, Prof. Michele Morsilli, who patiently supported me during my PhD period, as a professor, as a friend, as a family member. He has shown me, by his example, what a good scientist and person should be.

I will always remember the good and tough days that he spent with me during these years. I also would like to thank my supervisor, Prof. Alfredo Izquierdo González from University of Cadiz for his supports and considerations during my PhD period. Special thanks to Prof. Francisco Javier Gracia Prieto for all his support during my visit to Cadiz University and afterward.

I would especially like to thank Prof. Piero Gianolla, the chairman of my PhD committee, for all the support he did during my PhD defense processes and also the most beautiful days I worked with him in Dolomite.

I also would like to thank the geological team from National Iranian Oil Company (Dr. Ghabeishavi, Dr. Shabafrooz and Dr. Allahkaram-Dill for their kindly support during the fieldwork in Iran.

Special thanks to my PhD thesis referees, Prof. Luca Basilone from University of Palermo and Prof. Fabrizio Berra from University of Milan, whose comments greatly improved the thesis.

Nobody has been more important to me in the pursuit of this project than the members of my family. I would like to thank my parents, whose love and guidance are with me in whatever I pursue. They are the ultimate role models. I would also dedicate my thesis to my sister, Farideh, my brothers Farshad and Farhad, and their lovely children. To my best nieces Farnaz and Behnaz.

At the end I want to say to my best friend Amirhossein, thank you, for everything, for being with me in happiness and sadness, for all your support, without you it was impossible to continue. And also to my lovely friends, Arezoo, Naghmeh, you made my life happier during my PhD period and I will always remember you.

I would also like to thank my best officemate Gabriella for all the days we worked together in office and all good memories during the field work.

And Mina, you brought the happiness to the department when you came, your presence beside me always gave me strength.

Special thanks to Brunella, Paola and Matteo to host me in her house as one of family member, all the time and during the fieldwork, with you all, I always felt that I am at home.

TABLE OF CONTENTS

Chapter 1

Introduction

1-1-Carbonate platforms

Carbonate Platform is a general term referred to carbonate sequences deposited in a variety of geotectonic settings (along passive continental margins, failed rifts and foreland basins) and also to any depositional surface that shallow-water carbonate can develop on (Tucker and Wright, 1990; Pomar, 2001; Bosence, 2005). Carbonate platforms range from several to hundreds of kilometers wide and may be several kilometers thick (Schlager, 2005). Five types of carbonate platforms are: ramp, rimmed shelf, epeiric, isolated and drowned platforms (Fig.1-1).

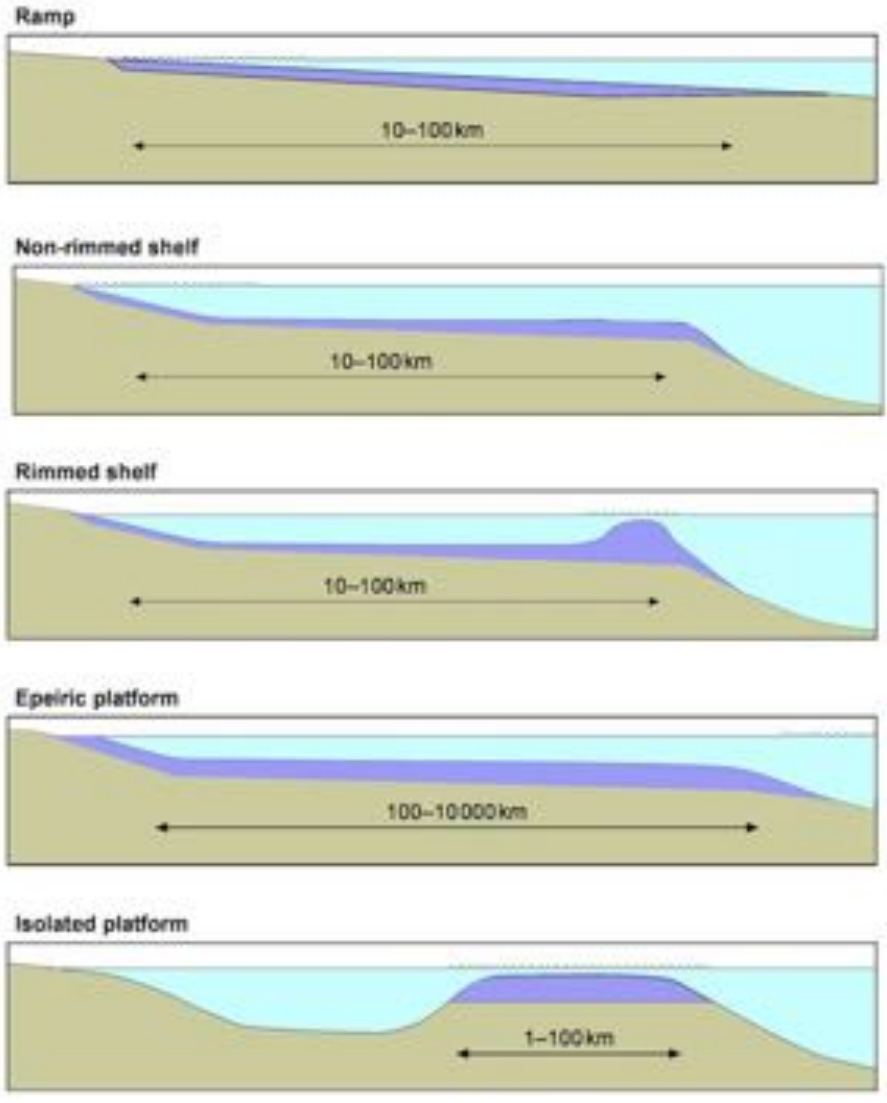

Figure.1-1- Figure shows different type of carbonate platforms (Nichols, 2009).

1-1-1-Carbonate ramps

Carbonate ramps develop in both cool- temperate and warm tropical marine environments and indicates by spatial differences in the size and type of grains with increased distance from the shoreline to the basin (Handford & Loucks, 1993).

In this setting, the different carbonate facies belts are differentiated preliminary by the level of energy (fair-weather wave base and storm wave base), different of ramp topography and sediment displace and transport by storms, waves and tides (Flügel, 2004). The ramp generally represents by high energy inner ramp passing basinward to a low- energy and deeper water outer ramp setting (Tucker, 2001). The ramp has been classified into two types: 1- homoclinal ramps and 2- distally steepened ramps. Homoclinal ramps are characterized by uniform and gentle slope (<1°) without shelf break passing to deeper outer ramp setting (Read, 1998) (Fig.1-2).

It is suggested that dominant mud-producing biota create a homoclinal ramp resulting from the low angle of repose of fine-grained sediments (Pomar, 2001). The distally steepened ramps are identified by a slope break separated shallow ramp from deeper water (Flügel, 2004). According to Pomar (2001), distally steepened ramp can be dominated by coarse-grained sediment produced deeper in the oligophotic zone.

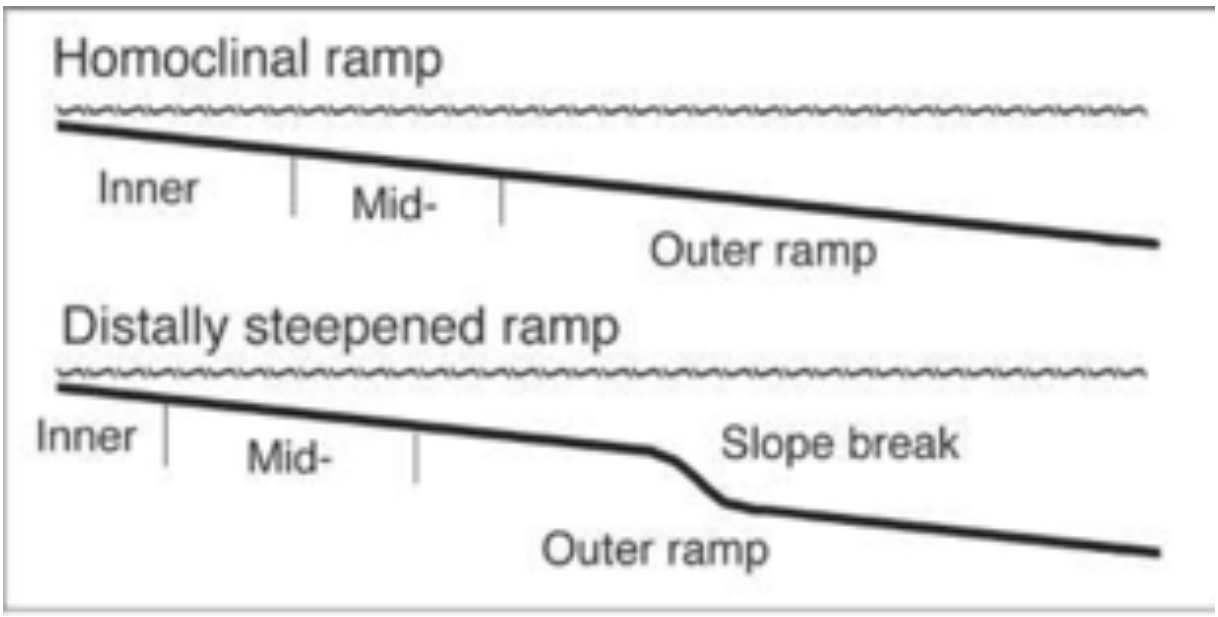

Figure.1-2- Figure shows two type of carbonate ramp (Flügel,2004)

The carbonate ramps are divided in 1- inner ramp 2- middle ramp and 3- outer ramp.

The inner ramp is generally composed of euphotic zone which located between upper shoreface and the fair-weather wave base and characterized by effect of wave action on the sea floor where dominated by high energy sand shoals or organic barriers. The middle ramp is located between fair-weather basin (FWWB) and storm wave base (SWB). The sediment deposited in this setting is characterized by some degree of storm influence base on the depth and bottom relief. In this part, the oolitic and bioclastic sand shoals are common and organic buildups are mostly represent by pinnacle reefs and mounds (Flügel, 2004). The outer ramp is considered the zone below storm wave base (SWB) with the water depth of ten meters to several hundreds of meters to the basin, and characterized by low-energy environments.

1-1-2-Rimmed shelf

The rimmed shelfs are shallow water carbonate platforms that characterized by distinct break in slope (commonly several, to > 60 °) (Fig.1-3). Reefs and carbonate buildups placed in the high energy shelf margin and restrict the water circulation behind the shelf (Tucker, 2001). Rimmed carbonate shelves can be flat tops (Ginsburg & James, 1974) or develop a margin that they are mostly represent by reefs. Depending on topography, type of biota and changes in relative sea-level, euphotic frame-building biota, such as large skeletons and encrusting organisms resist wave action at the high energy shelf margin and then they can develop barriers of organic buildups and carbonate sand bodies (Ginsburg & James, 1974; Pomar, 2001). Carbonate platforms with rimmed margin are characterized by continues or isolated reefs bodies that can act as barriers (< 10 m deep) (Hine, 1983). Carbonate reefs can be explained as a wave-resistant build-up that is generally associated with high wave energy, shallow water (or deep water) environments and formed by the interplay of organic frame-building, erosion, sedimentation and cementation (Longman, 1981; Wright & Burchette, 1996; Schlager, 2005). The rigid rim at the platform margin may be produced either by organic skeleton-built framestone, by chemical and biochemical cement-stone, or by both (Pomar, 2001). The basic factors controlling the geometry of reefs can be: upward growth of the organic framework; the influence of wave and current energy causing destruction and/or cementation; and sediment export by the reef factory (Schlager, 2005).

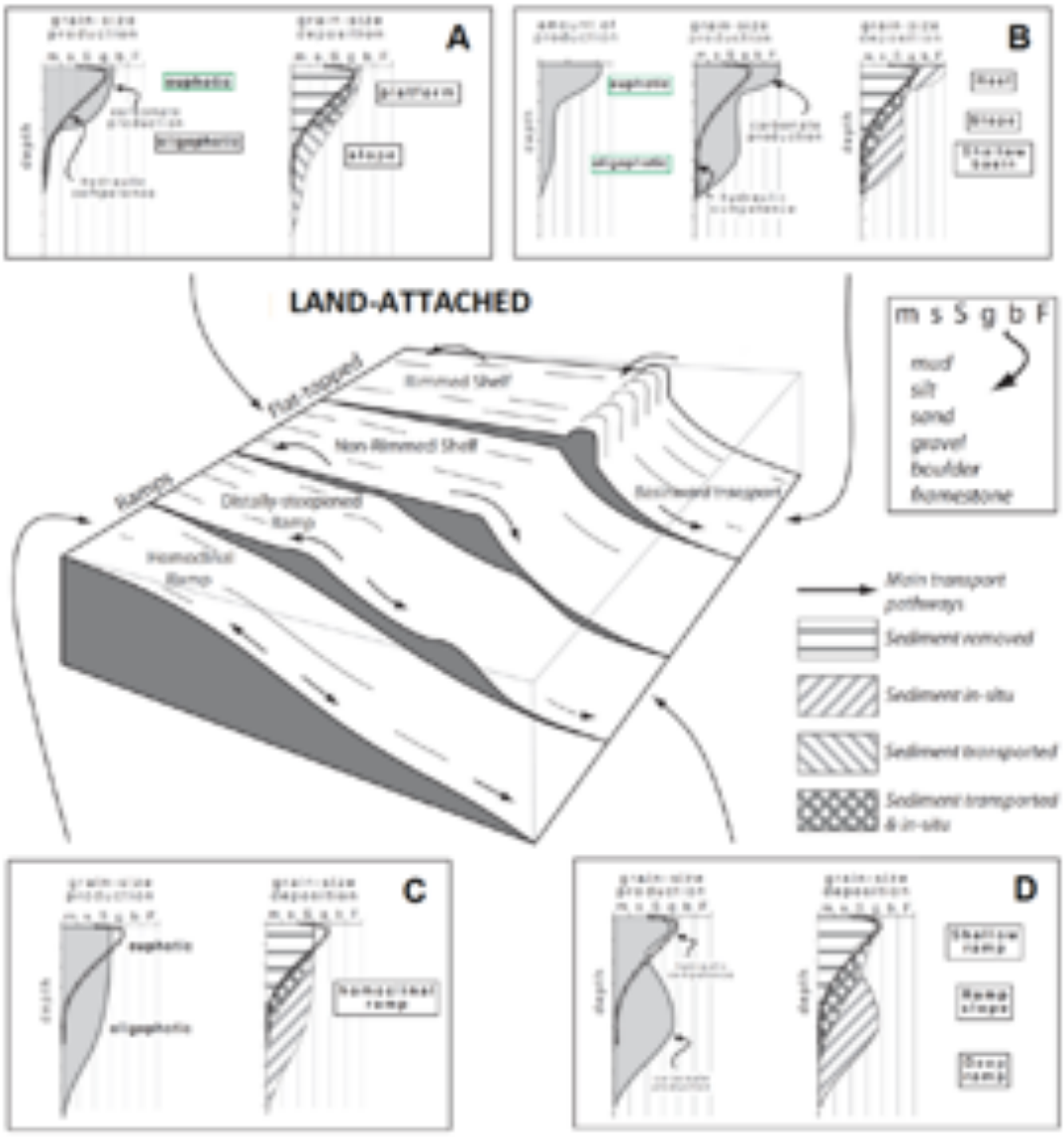

Figure.1-3- Main types of carbonate platforms and facies belts among the spectrum of depositional profiles as proposed by Pomar (2001).

1-1-3-Epeiric platforms

The epeiric platforms are generally developed as extensive cratonic flat area, (100-10000 km across) which covered by a shallow sea (Fig.1-4). Epeiric seas first flooded the margins and later the interior of tectonically stable cratons (Flügel, 2004). They may have a gentle margin (ramp like) or steep slope (shelf-like) to the basin (Tucker, 2001). This kind of platform is dominated by low energy shallow subtidal-intertidal sequences. The dominant processes are storms and tidal currents. The main sediments in the distal and proximal part of epeiric ramps are burrowed fine-

grained carbonate which can develop as a mud flats close the coast and more distal seagrass area. Grain-dominated sediments deposited as result of storms are mainly destroyed by the action of bioturbation. This happened due to high concentration of trophic resource levels, from low mesotrophic to eutrophic (Flügel, 2004).

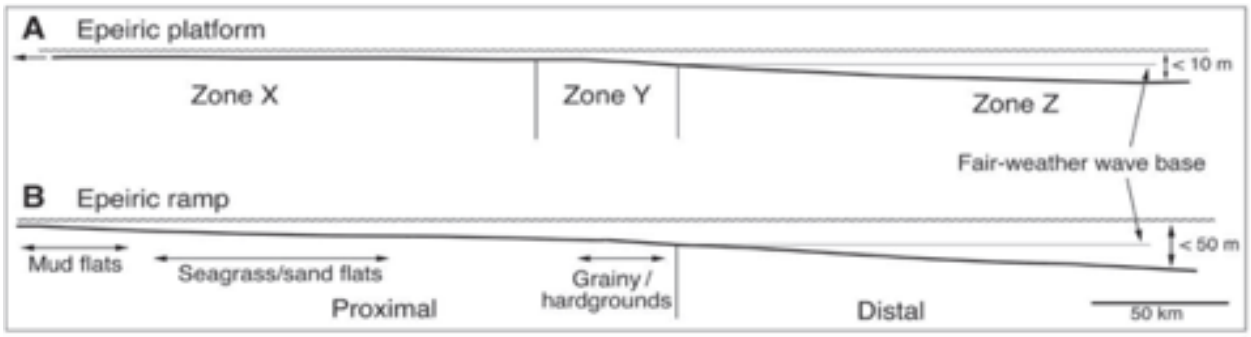

Figure.1-4- Epeiric platform and epeiric ramp models (Flügel, 2004).

1-1-4-Isolated carbonate platforms:

The isolated carbonate platforms are characterized by the accumulations of shallow-marine carbonates surrounded by steep margin, frequently tectonically inherited, and deep-water sediments (Flügel, 2004. The most isolated carbonate platforms characterized by steep margins and slopes passing to the deep to very deep water. The outer part of the platform is characterized by high-energy condition where the environment is good enough to marginal reefs or sand bodies to develop and they strongly affected by storm. This high carbonate production along the platform margin may be resulted to development of rimmed isolated platform with a lagoon in center ('empty bucket' *sensu* Schlager (1993). One of the most famous example of isolated carbonate platform is from the Triassic carbonate buildups of Dolomite reported by Bosellini, (1989).

1-1-5-Drowned platforms

This type of platform is characterized by continuous and rapid sea-level rise so the deeper water facies can deposited over the shallow water facies. The drowning of shallow marine platforms and reefs occure when rising sea level or tectonic subsidence outpaces carbonate cases (Schlager 1981). The pelagic carbonate platform is one of the specific type of drowning carbonate platform (Flügel, 2004). Drowned platform, which developed below the euphotic zone, shows stratigraphic succession of neritic deposits followed by pelagic deposition (Schlager, 1981). The

boundary between shallow water carbonate and deep water sediments are typically characterized by unconformity associated locally with hardground or karsts. The drowning unconformities show same geometric characteristics regardless whether they caused by subaerial exposure or if they are related to sea-level rise (Schlager, 1989).

The different rate of sea level change can affect the carbonate factory in different ways. They may show a progradation when the platform shifts basinward, aggradation when platform stack vertically or show retrogradation when it moves leeward. The figure 1-5 shows the different evolution phases of the carbonate factory.

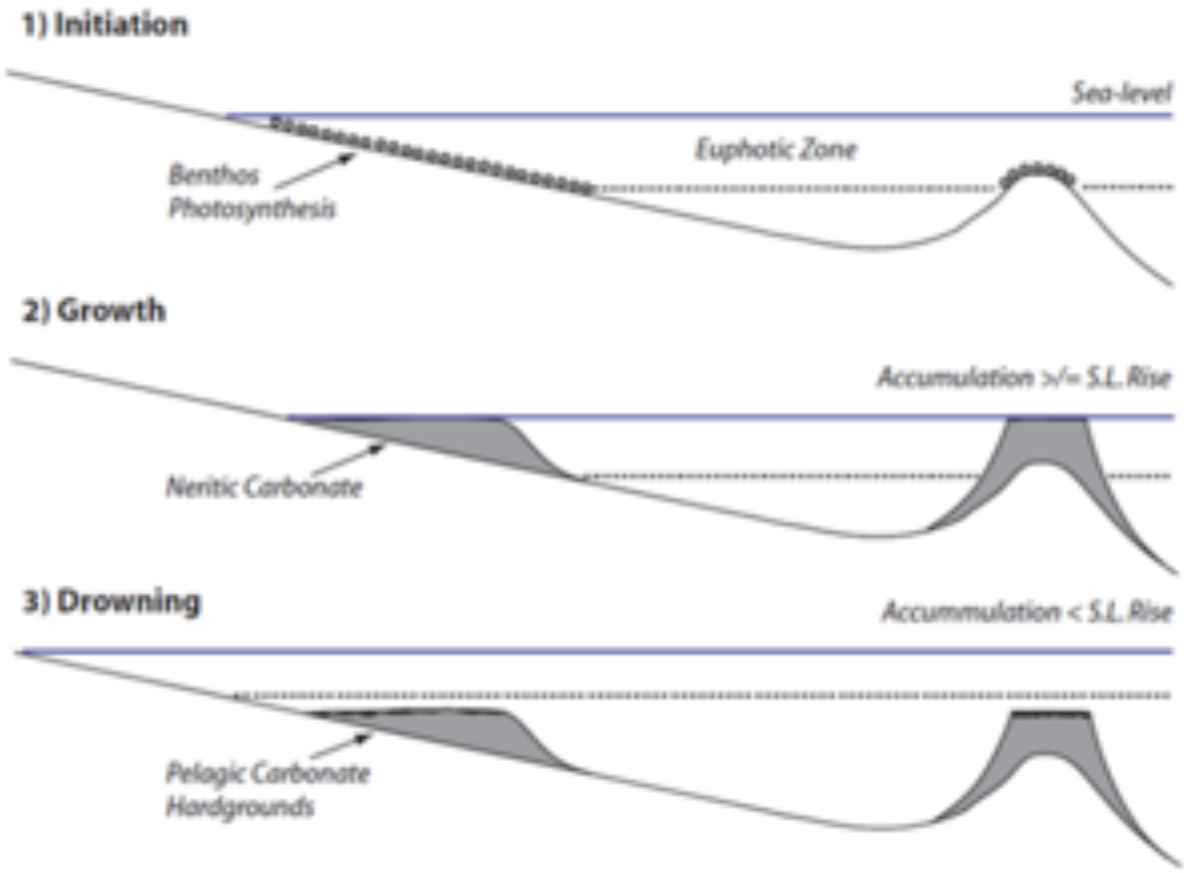

Figure.1-5- Schematic diagram showing initiation, growth and drowning of carbonate platform margins (Schlager, 1981).

1-2-Factor controlling the generation of carbonate platforms

The shallow water carbonate sedimentation is controlled by several factors such as oceanography, geotechtonic, temperature, nutrient source, salinity, water depth and sea-level changes. These

factors determine the ecology of carbonate-producing organisms, the hydrodynamic conditions which can affect the depositional geometry of a carbonate platforms (Wilson, 1975; Bathurst, 1975; Tucker and Wright; 1990; Pomar, 2001; Bosence, 2005; Shlager, 2005).

The tectonic setting, more than any other factor, affects the overall shape of the carbonate platform (i.e., rimmed shelf, ramp, epeiric or isolated platform (Read, 1982).

Bosence (2005) discussed that the overall morphology, size and stratigraphic development of carbonate platform can be controlled by tectonic setting. While climate, sea-level, chemistry and biological impact (Pomar, 2001) play an important role in facies type, depositional sequences and some futures of platform margins, but they are not affect the platform in large scale futures. The classification of Bosence (2005) is based on the major tectonic controls on the origin of platform instead of the platform margin morphology basis of classification of into rimmed-shelves and ramps (Wilson, 1975). The main eight types of carbonate platforms discussed by Bosence (2005) are: Fault-Block, Salt Diapir, Subsiding Margin, Offshore Bank, Volcanic Pedestal, Thrust-Top, Delta-Top and Foreland Margin carbonate platforms.

On the other hand, Benthic carbonate communities are the most important producers in carbonate platforms (Pomar, 2001). In the deeper part of carbonate platforms, planktonic communities considered also a main carbonate producer. In shallow- water environments, non-skeletal grains (ooids, peloids) can be main components in these depths (Pomar, 2001). Carbonate production is strongly related to the presence of light needed by organism to develop. These organisms can be authotrophic or mixotrophs or they can be heterotroph organisms (Pomar, 2001). The concept of the tropical carbonate factory is associated with the carbonate production that occurs in oligotrophic, warm and well- illuminated waters of the tropics and subtropics (Schlager, 2000, 2003; Hallock, 2005). In this condition, the light penetration is one of the fundamental factor controlling loci, amount and type of carbonate production, and can be used as a useful tool to reconstruct different zone in the rock record (Bosscher and Schlager, 1992; Pomar, 2001; Wilson and Vecsei, 2005; Morsilli et al., 2012; Pomar et al., 2015; Michel et al., 2018). These zones are named “euphotic”, “oligophotic” or “mesophotic”, and “aphotic”. The bathymetric position of these light zones is variable and depends on water transparency and latitude, and they associate with the development of some autotrophic organisms. The range of modern seagrasses and, non-dasyclad green algae can be used to define the euphotic zone, and the deepest occurrence of *in-situ* red algae define the lower limit of the oligophotic zone (Pomar, 2001; Morsilli et al., 2012).

(Fig.1-6) In addition to light, nutrient availability also plays a major factor in controlling carbonate production and define as oligotrophic, mesotrophic, and eutrophic conditions (Hallock, 1987; 2015).

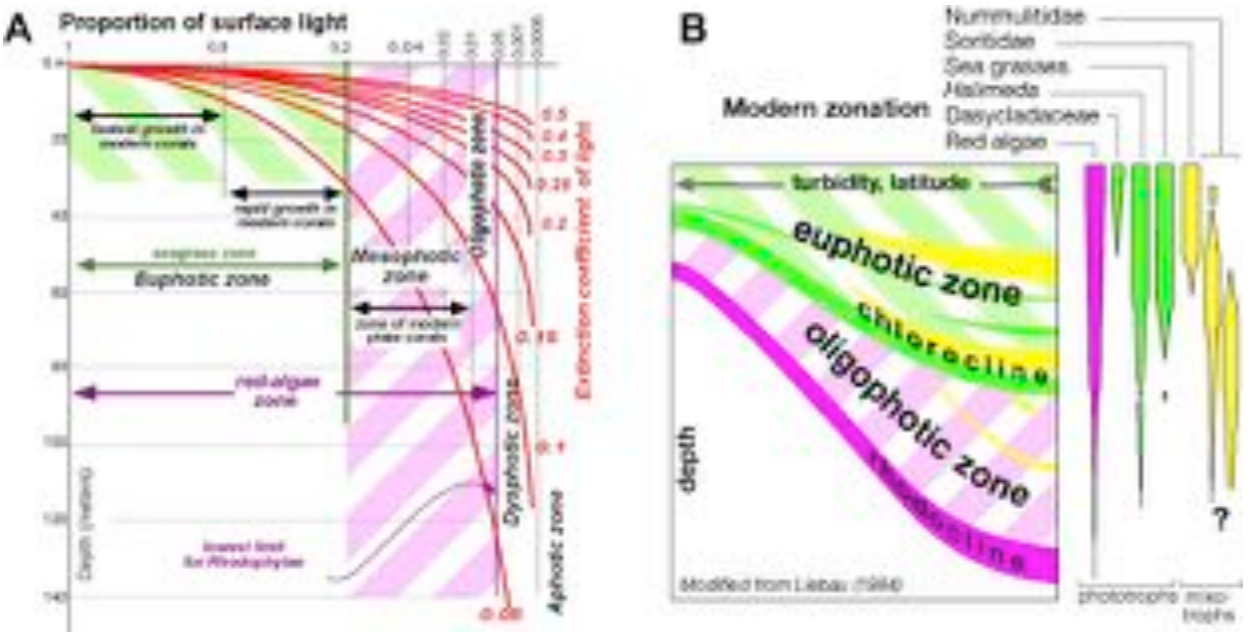

Figure. 1-6- Proportion of surface light with depth for different extinction coefficients of light, bathymetric light zones (*sensu* Pomar, 2001) based on the presence of in-situ photoautotrophs and mixotrophs, and growth rates of modern corals. B) Bathymetric light zones (*sensu* Pomar, 2001) and their lower boundaries (chlorocline and rhodocline) sensu Liebau, 1984). Chlorocline is the deepest occurrence of *in-situ* seagrasses and non-dasyclad green algae. Rhodocline is the deepest occurrence of in-situ red algae. The lower limit of these photic zones depends on turbidity and on latitude due to decreasing surface irradiance with latitude.

Schlager (2000, 2003) proposed three main types of carbonate production factories based on dominant type of benthic carbonate-producing biota. Each factory is characterized by different precipitation mode and mineralogy as well as different depth ranges. 1- tropical carbonate factory which represent by light-dependent communities, 2- cool-water carbonate factory associated with heterotrophic biotic components, and 3- mud mound factory which is characterized by microbial and abiotic precipitates. Figure 1-7 shows the model proposed by Schlager (2000, 2003) and their associated depth of carbonate production.

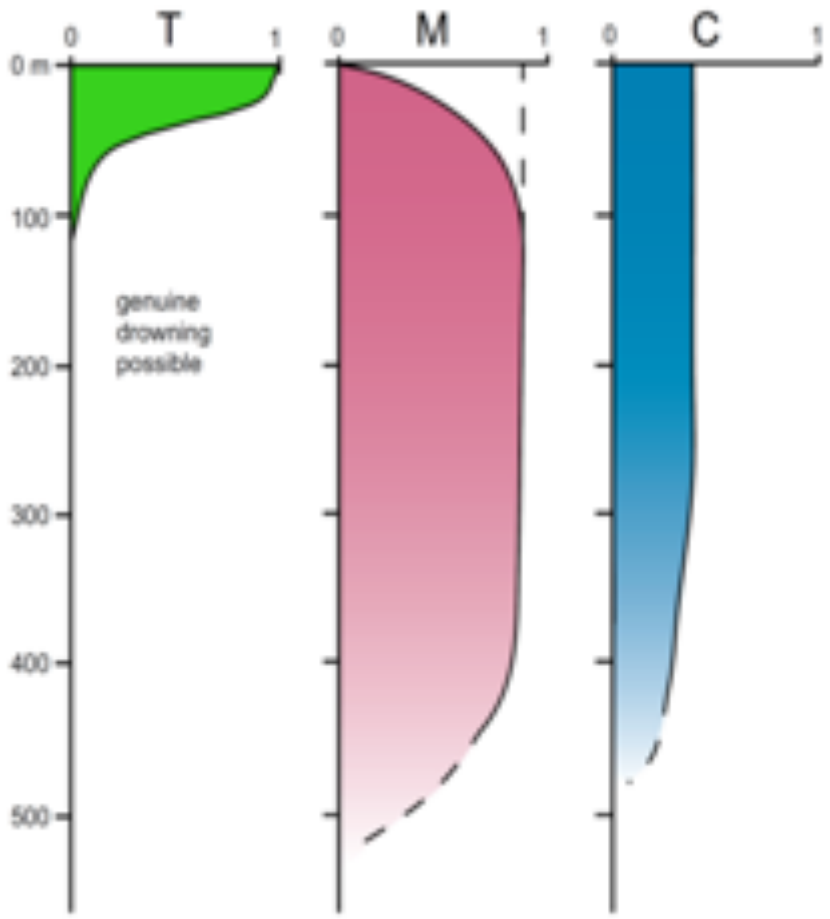

Figure.1-7-This figure shows the model proposed by Schlager (2000, 2003 for different carbonate factories. Tropica factory (T), mud mound factory (M) and cool-water carbonate factory (C). the shaded area is represented by different colors show the production rate of each carbonate factory at different depths.

According to Burgess (2010) carbonate platform architecture can be controlled based on the different carbonate factory proposed by Schlager (2000; 2003; 2005). Tropical carbonate factory, mud-mound carbonate factory and cool-water carbonate can generate different platform geometries (Pomar, 2001; Burgess & Wright, 2005; Schlager, 2005). Tropical factory is associated with rimmed shelf and cool-water carbonate factory are represent mostly by non-rimmed shelves. Instead, mud-mound factory is usually produce along the ramps (Schlager, 2005; see also Pomar, 2001). (Fig.1-3). This concept is applied in many studies which aim to sedimentological interpretation of depositional model. However, many examples from modern and ancient carbonate do not follow this concept (Burgess & Wright, 2005). The main factors controlling the

development of carbonate platform can be summarized in figure 1-8 proposed by Jones and Desrochers (1992). The carbonate factory is characterized by deposition of sediments in first phase. The sediment production is controlled by external factors such as climate, sea temperature and rate of siliciclastic input (Lomando & Harris, 1991). Also the production can be affected by several internal factors such as nutrient availability, water depth, salinity and oxygen level (Pomar, 2001; Handford & Loucks, 1993). After the final production, sediments can be affected by other factors including: waves, tides, storms and oceanic currents. The balance between carbonate production and transportation will affected the growth shape of platform (Jones & Desrochers, 1992). Carbonate platforms are strongly controlled by sea-level fluctuation and subsidence rate. A sea-level fall can be resulted in end of carbonate production and make an erosion or karstification. A sea-level rise can result in re-production of carbonate on the initial surface. The final vertical stacking of sediments is mostly controlled by sea-level changes and the shape of platform (Jones and Desrochers, 1992; Pomar 2001). Among other descriptive models, Pomar (2001), genetic approach to classifying carbonate platforms are more reliable when it comes to interpretation of the factors controlling the distribution of facies and depositional profile. This model also considers the relationship between carbonate-producing biota and production loci with hydrodynamic events. The hydrodynamic energy can control the depositional geometry and facies distribution and finally the platform architecture (Pomar, 2001). Therefore, this model can be applied widely in order to describe the carbonate platform classification.

1-3-Internal Waves

Internal solitary waves are characterized by a single isolated wave which ubiquitous in stratified fluids (Shanmugam, 2013). According to Apel, 2002, the internal waves (IWs) are a solitary waves that considered as nonsinusoidal, nonlinear and isolated waves with complex shape. Internal tides are internal waves at the tidal frequency (Shepard, 1975). Internal waves are known as internal tides at a tidal frequency. They are generated as the surface tides move stratified water up and down sloping topography, such as submarine canyons, producing an internal
wave that propagates along the density boundary layers (Shepard et al., 1979). In macrotidal range region with water depth no exceed 250 m, the average periods of these up-and
down-canyon currents are related to semidiurnal or diurnal tides. In microtidal range, bidirectional

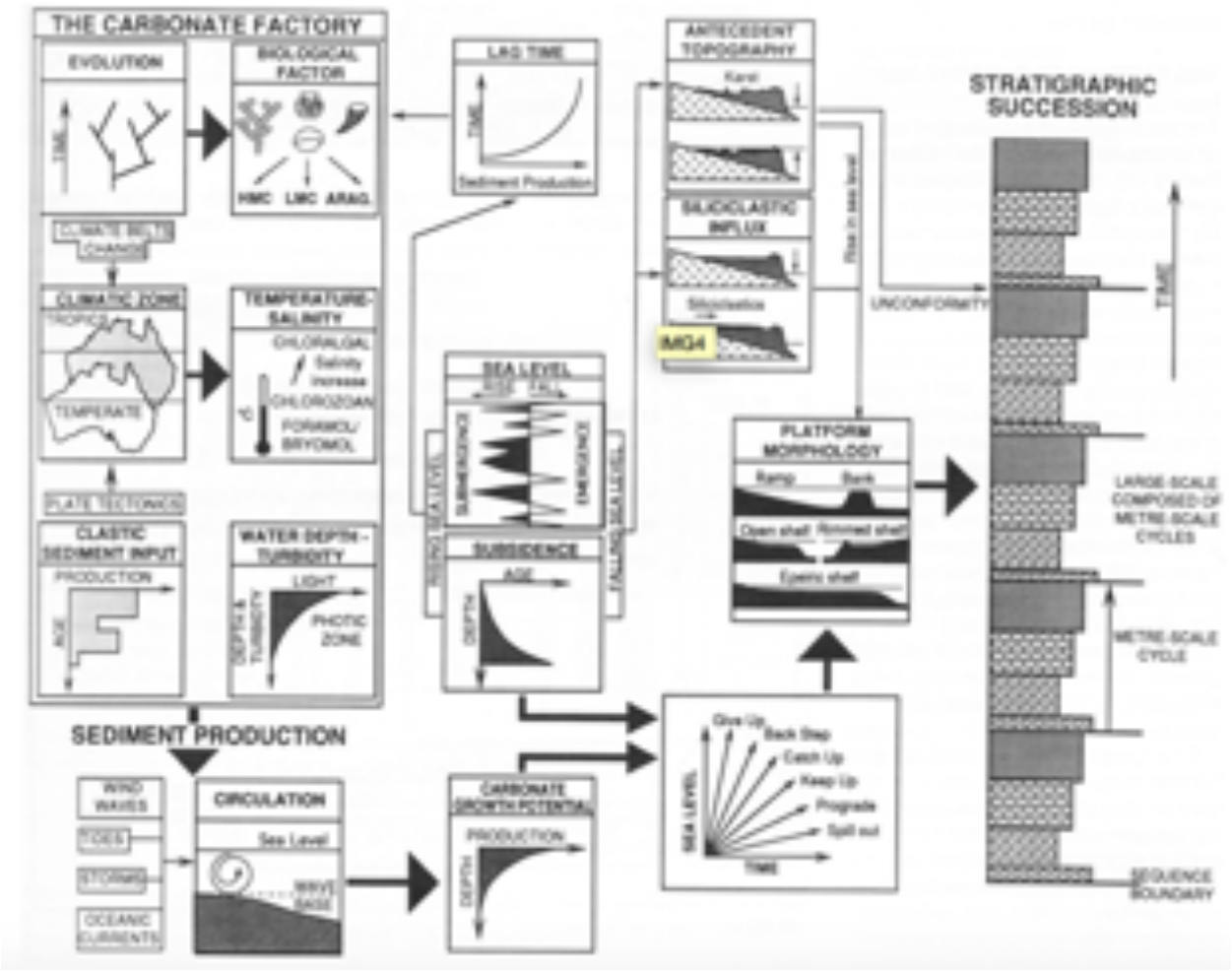

Figure.1-8-The figure shows the main factors controlling the development of carbonate platform according to Jones and Desrochers, (1992).

currents related to tides occur only in deeper water (Shepard et al., 1979).

Internal waves are responsible for ocean mixing, energy dissipation, and thermohaline circulation and often crash into nearshore ecosystems (Alford 2003; Garrett and Munk 1979; Nash et al. 2012; Ray and Mitchum 1996; Simmons et al. 2004; Zhao and Alford 2009). Nonlinear internal waves can transport significant amounts of waterbodies and characterized by increased turbulence and mixing (Woodson, 2018). The nonlinear internal waves can mix deep offshore water into nearshore The deep waters characterized by cold, low oxygen, high CO2 (low PH) and enrich of nutrients. So, IWs can change the environment condition, providing a high oxygen (hypoxia) or pH (acidification) conditions (Frieder et al. 2012).

Internal waves can be characterized by two parameters: wavelength (or frequency), λ (or f), and

the amplitude (or wave height). (Fig.1-9). The wavelengths in linear internal waves are considered by two factors. Coriolis parameter is responsible for setting maximum long-wavelength (lowest frequency), for sustained motion, and under this frequency internal waves will break down (Carter et al. 2005; Lerczak et al. 2001, 2003). Waves at the short-wavelength (high-frequency), do not have sufficient power and energy to overcome the stratification, as result setting a limit beyond which internal waves are rapidly dissipated (Woodson, 2018). The other important factor for internal waves is the fluid density change which also called stratification.

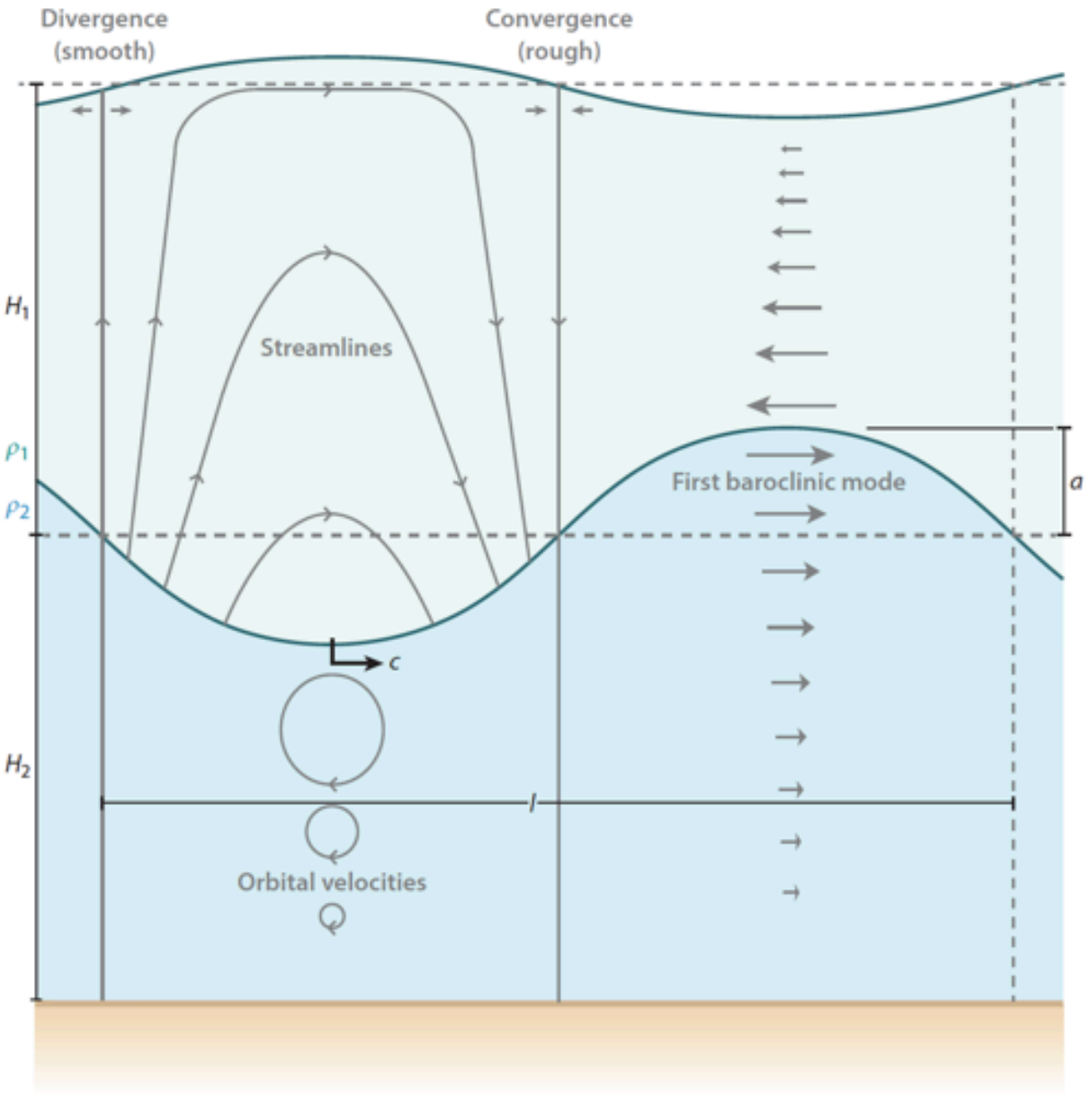

Figure.1-9- Schematic of an internal wave, along with definitions for a linear internal wave in deep water (Woodson, 2018).

Breaking of shoaling Internal solitary waves (ISWs) can be responsible for mixing and mass transport processes in oceans and lakes. Previous studies identified four breaker types: surging, plunging, collapsing, and fission. Nakayama et al (2019), illustrated the four different types of ISW breaker—fission, collapsing, plunging, and surging ISWs on the slope based on numerical experiment (Fig.1-10).

ISWs induce bottom stress, which may become sufficient to initiate sediment movement, and near-bed instability can re-suspend sediments (Boegman and Stastna, 2019). For large-amplitude waves over flat bottoms (e.g., Aghsaee and Boegman, 2015; Stastna and Lamb, 2008) and ISWs incident on steep slopes (collapsing, and plunging breakers; see the sidebar titled Classification of ISW Breaking Regimes) (Boegman et al. 2005), flow separation may occur in the adverse pressure gradient wake region behind the waves, driving strong turbulent burst events (Figure1-11) with maximum vertical velocities of ~0.1 m/s and enhanced sediment resuspension of ~100 g m2 per day (Hosegood and Van Haren,2004; Hosegood et al. 2004). When the ISW interact with topography, they create strong near bottom currents (Boegman and Stastna, 2019). Figure 1-11 showing the instability mechanisms for shoaling internal solitary waves (ISWs).

According to Garrett and Kunze, 2007, "Internal tides are internal gravity waves produced in stratified waters where the barotropic currents intersects the sea topography (Fig.1-12). Internal waves are usually produce high energy events in the coastal parts of ocean and also in the deeper parts. This high energy waves can vertically move the waters up to 100 meters and generate powerful currents and turbulence (Moum et al., 2003; Nash and Moum, 2005, Pomar et al., 2012). Episodic high-turbulence events can be generated as a result of breaking of the internal waves on the surface of slopes. This high-energy turbulence can erode and transport the sediments along the slope (Fig.1-12) (Apel, 2002, Boegman and Ivey, 2009; Lim et al., 2010, Pomar et al., 2012). The sediments deposited by the action of internal waves called "internalite" (Pomar et al., 2012).

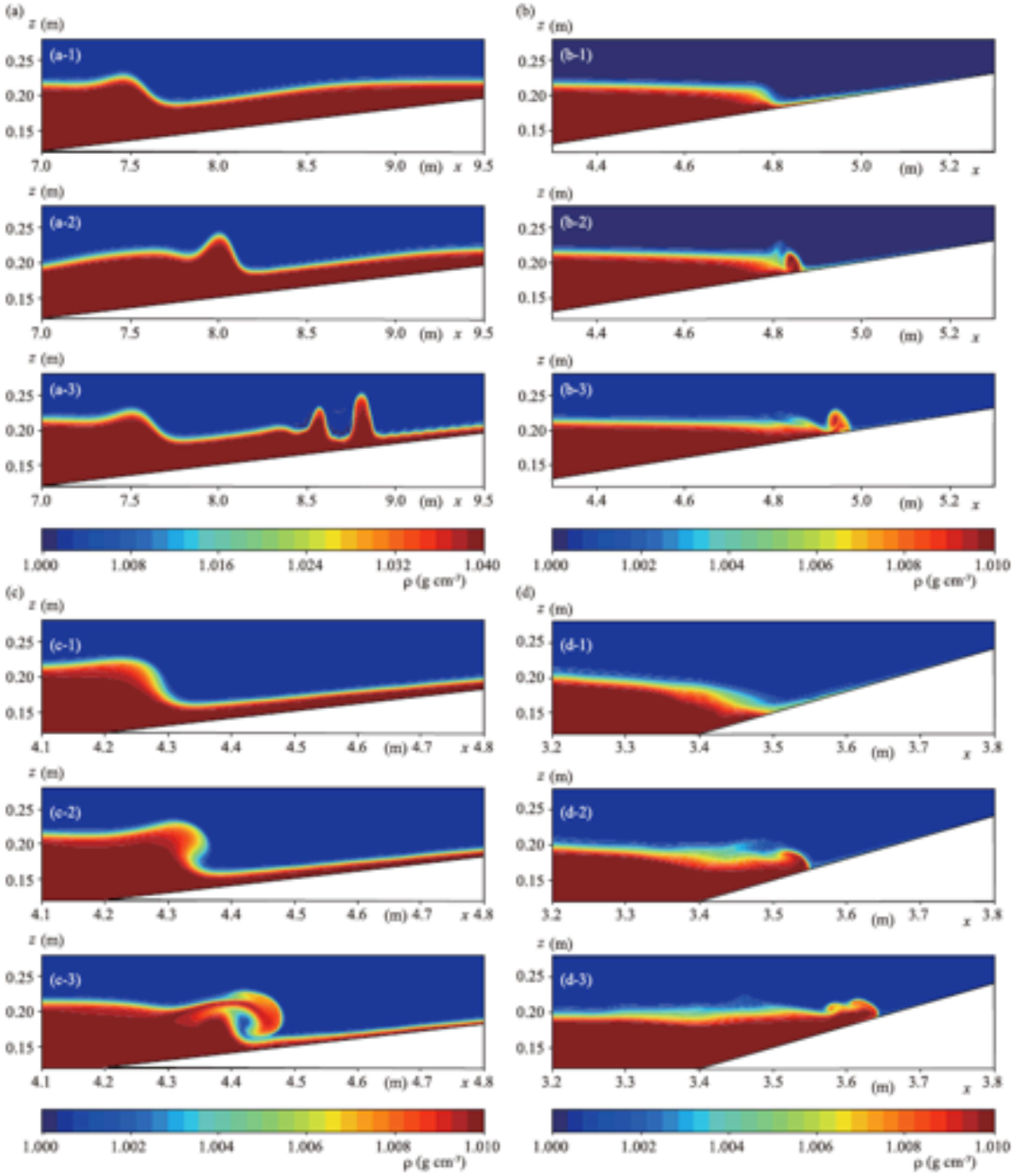

Figure. 1-10- Typical cases of different breaker types. A: Fission. B: Collapsing. C: Plunging. D: Surging. Contours indicate density (Nakayama et al., 2019).

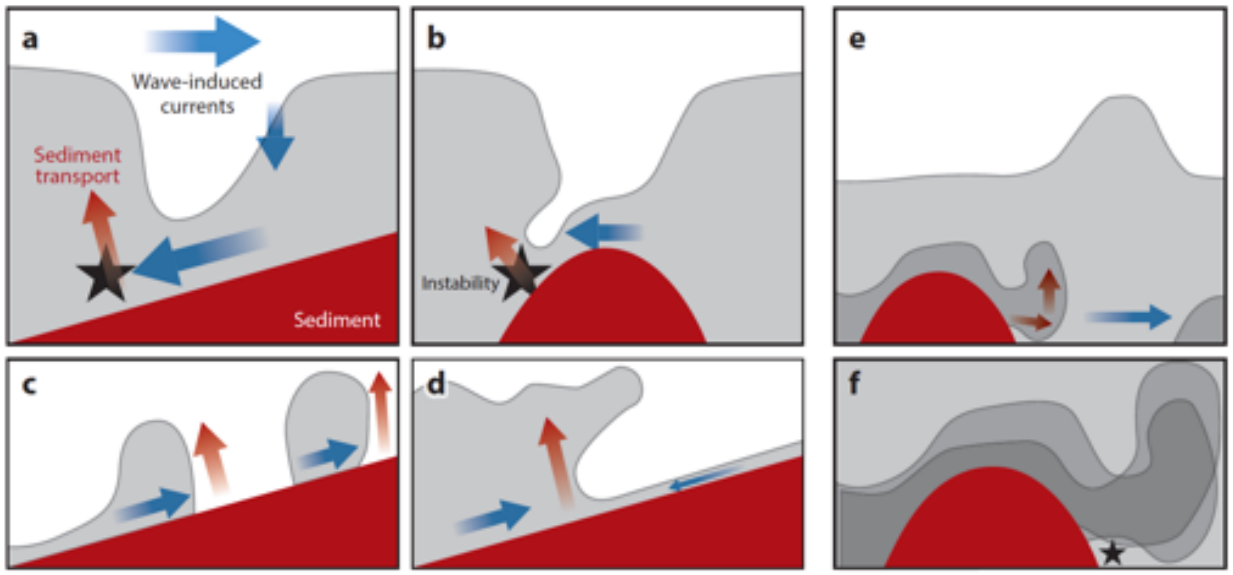

Figure.1-11- Schematic showing instability mechanisms for shoaling internal solitary waves (ISWs). A: The instability scenario for a shoaling ISW of depression propagating left to right. B: Instability and transport during passage of a wave of depression over large-amplitude, isolated topography. C: Systematic transport from the bottom boundary layer (BBL) by upslope-propagating boluses. D: Systematic transport from the BBL during downslope slumping (collapsing breaker). E: Instability and transport during passage of a wave of elevation over isolated topography when near-bottom stratification is present. F: Detail of panel e showing the location of Rayleigh–Taylor instability. Systematic transport of sediment from the BBL into the main water column is indicated by red gradient arrows in all panels (Boegman and Stastna, 2019).

1-3-1-Pycnocline

The pycnocline is the boundary surface between two different fluid layers with different density, or a layer where a vertical density-gradient is present (Pomar et al., 2012). As a result, the interval waves are propagating where the pycnocline is present. The primarily factor producing pycnocline in the modern oceans is the temperature and the secondary factor is the salinity gradients in the water column. In a “Greenhouse” time with mild temperature in the high-latitudes, the primarily factor controlled the pycnocline was halothermal (different water column defined by different salinity) (Nunes and Norris, 2006). Pycnocline can ocuure in shallow depth depend on seasonal thermocline or in the deeper parts on the continental slope when dependent on the permanent thermocline (Fig.1-13) (LaFond, 1962, Thorpe, 2005, Butman et al., 2006).

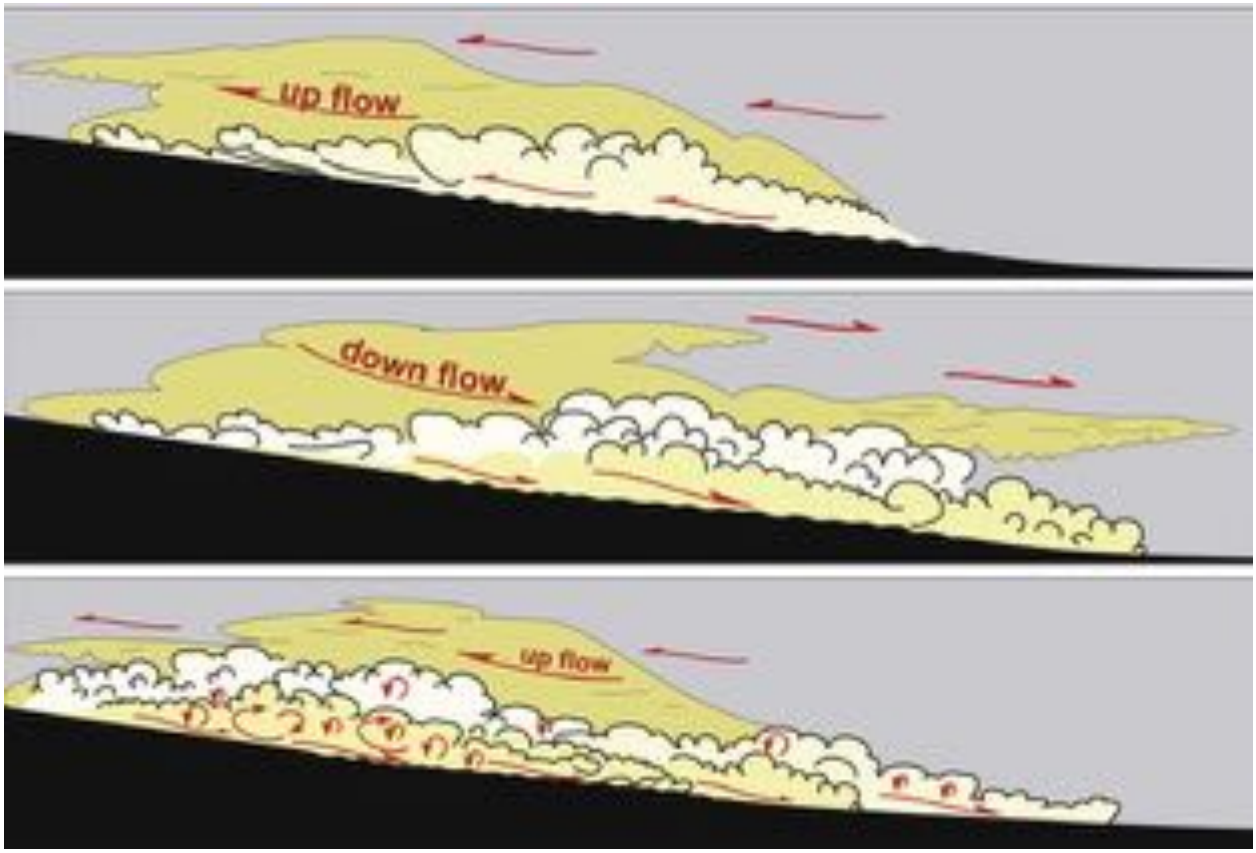

Figure.1-12- Breaking of internal waves on a shoaling surface. A: Sediment moves upslope by the breakers (swash run-up). B: The compensating return flow (backwash) mixes the fluid between breakers and moves the sediment down- slope. C: Breaking of internal waves creates turbulence and sediment erosion, transport and deposition under repetitive high-energy events (Pomar et al., 2012)

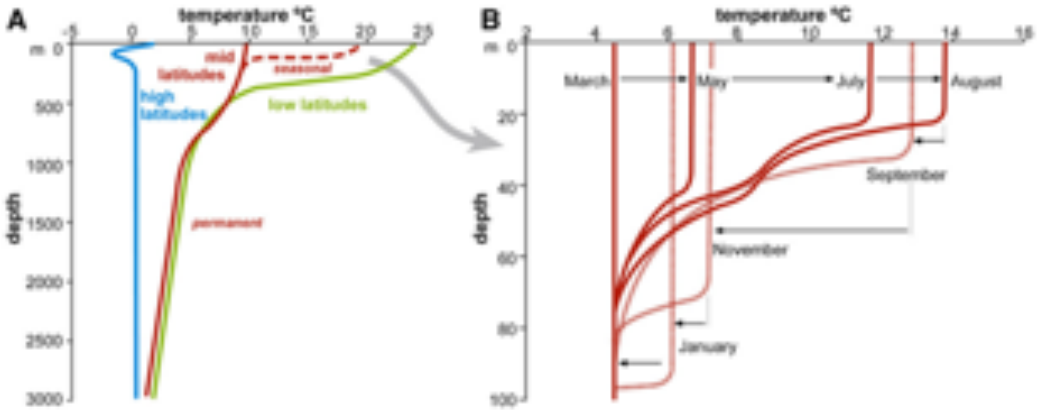

Figure.1-13- Typical temperature/depth profiles in open oceans (modified from Brown et al., 1989). (A) Mean temperature profile for different latitude. (B) Succession of temperature profiles showing the growth and decay of the seasonal thermocline in the Northern Hemisphere.

1-3-2-Tempestites and turbidites vs. internal waves deposits (internalites)

Surface storms, turbidity currents and internal waves generally show different characteristics regarding the generation processes and sediment transport direction. Also, they can occur at the different bathymetric ranges (Pomar et al., 2012). The lower limit of the tempestites is different based on several authors: equilibrium surface developed at or just below the storm-wave base (Seilacher, 1982), the shelf equilibrium profile (Swift and Thorne, 1991) and effective surface-wave base (Immenhauser, 2009). So, the depth of tempestites is different based on fetch of the basin, latitude and wind actions. Turbidites are the sediment deposited under action of turbidity currents. They generally deposited on the slope, continental and basin floors of passive and active margins. In contrast, internal waves can transport and redeposit the sediments in any depth where the pycnocline hit the seafloor (Butman et al., 2006).

Table 1-1. Comparison between tempestites, internal-wave deposits (internalites) and turbidites.
Turbulence (Pomar et al., 2012)

Turbulence events	Surface storms	Internal waves	Turbidity currents
Bathymetric range	Nearshore, down to the extreme storm-wave base	Depth of the pycnocline Mid-shelf settings (shallow pycnocline) Submarine canyons and continental slope (deeper pycnocline)	Commonly on the basin floor in passive margins, active margins or in depocenter of piggyback basins
Turbulence induction process	Gravity wave propagating along the sea surface	Breaking gravity wave propagating along the pycnocline	Sediment instability on the seafloor
Triggering mechanism	Commonly wind associated with atmospheric storms	Interaction of tidal currents with topography, wind stress fluctuations, tectonic events, and various other processes still poorly documented	Over-steepening of the sediment surface, storms and/or earthquakes, fluvial floods
Direction of transport	Preferentially alongshore but also seaward-directed	Onshore/offshore sediment reworking	Downdip
Deposits	Tempestites	Internalites	Turbidites

According to Al-Awwad and Pomar, 2015, from the reservoir geology point of view, the differentiation of different eventites deposited by surface storms, turbidity currents and internal waves is important tool to apply in order to better understanding of the relation between depositional architecture and reservoir plumbing system (Fig.1-14). In storm-dominated shelf tempestites generally as layers which thickening upward toward the shoreface facies. Instead, in turbidites, the most permeable layers develop in sequences which stacking patterns show the organization of lobes and channels, and can be distinguished from shoreline facies. In internalites

shelf model, grain-dominated facies with good permeability can develop as sets in mid-ramp muddy facies.

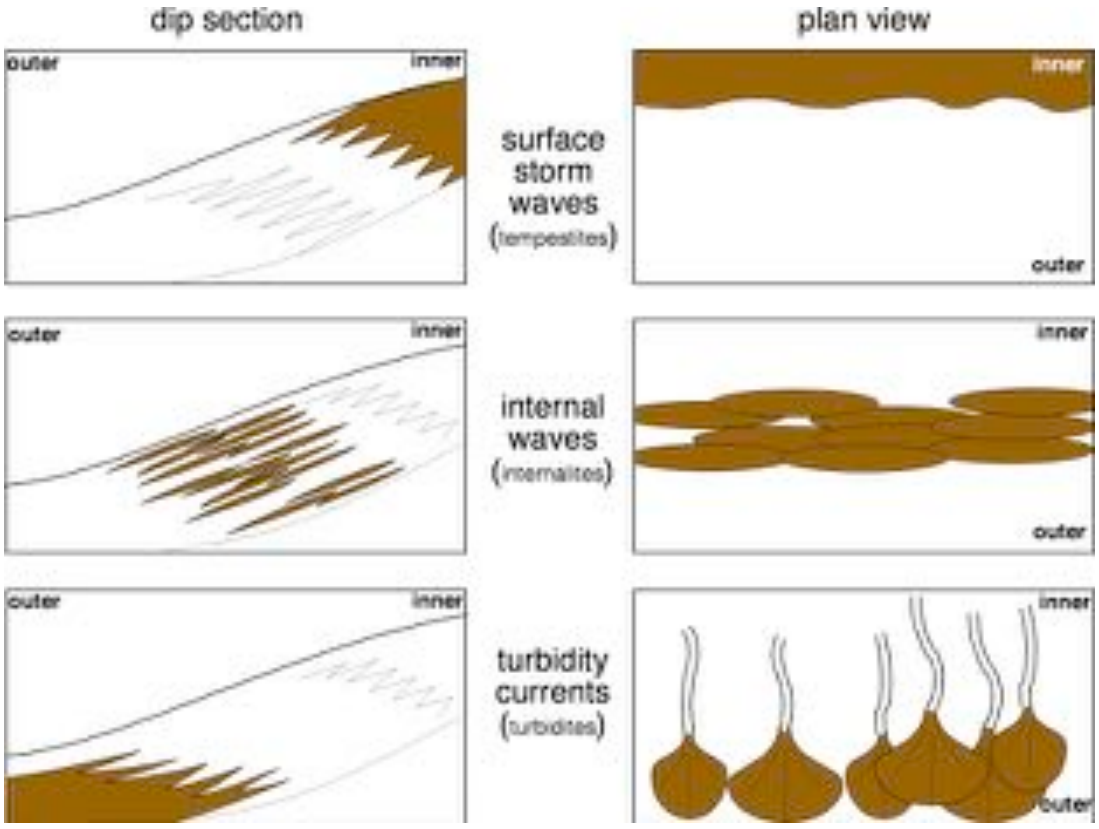

Figure.1-14- Differences in the stacking patterns of the rudstone–floatstone beds depending on the type of eventitic flow: storm-dominated are tied to the shoreline, internal wave deposits are incased in mid-ramp settings without connection to shallower or deeper deposits, and turbiditic flows occur as aprons or fans in deeper water settings (Al-Awwad and Pomar, 2015)

1-3-3-Internal waves and carbonate system

In carbonate systems, deposits of internal waves (internalites) and surface storm waves (tempestites) can be differentiated due to bathymetric position of many skeletal components. These carbonate grains can give information related to original environment of their deposition (Flügel, 2004, Pomar et al., 2012). In the environments close to pycnicline, internal waves act as an important mechanism for displacement the nutrient-rich waters, distribution of planktons and inducing ecological stress (Pomar et al., 2012). In shallow coastal zone, internal waves can bring the nutrient-rich deep water to shallow zone (Leichter et al., 2003, 2005). In general, two important

factors controlling the developments of carbonate buildups made by *zooxanthellate* corals, bryozoans, bivalves, or other heterotrophic calcifier: 1- nutrient source and delivery system like water motion (Pomar et al., 2017). In modern environments the development of aphotic corals takes place in association with area with subsurface currents where the thermocline and internal waves exist (Davies et al., 2009, Pomar et al., 2017).

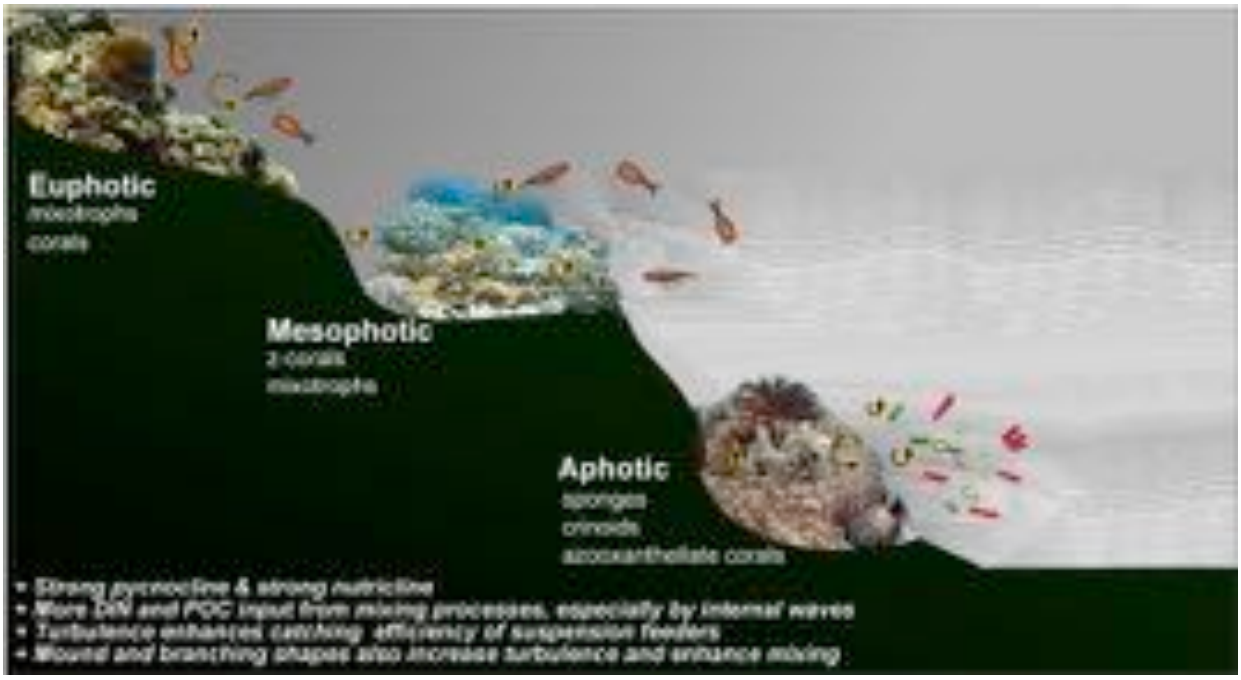

Figure 1-15- Occurrence of bioherms requires advantageous functionality. Skeletons of sessile metazoans, single or colonial, will produce mounded accumulations when there is 1) enough food availability (particulate organic carbon: POC) to promote growth and reproduction, and 2) water turbulence both to carry the plankton and to increase the impinging efficiency upon the feeding structures (Pomar et al., 2017).

Carbonate buildups dominated by autotrophic and mixotrophic biota show a balance between "trophic resources" and water transparency (Pomar et al., 2017). Water transparency usually limited due to abundant trophic resources and less amount of trophic resources means clear water and favorited conditions for photosynthesis to absorb the sunlight. According to Hallock, 2001, the best condition for modern carbonate buildups for accretion is where the waves and currents are moving upon mesotrophic condition (Fig.1-15). Mesophotic corals in modern environments tend to grow in the settings with clear surface water (oligotrophic condition) where the light can penetrate to depth 30-50 meters and more. In this settings, internal waves are mechanism for

displace the uppermost pycnocline waters to those depths and as a result provide the trophic resources needed by buildups to grow (Fig.1-16) (Pomar et al., 2017).

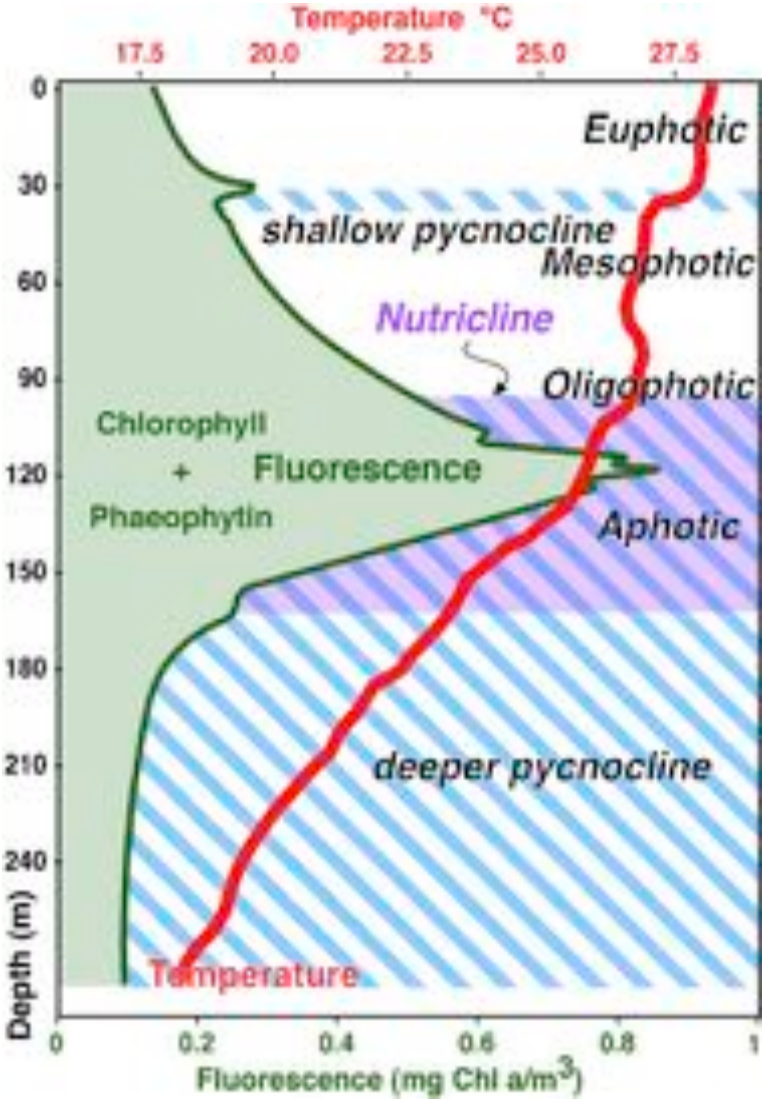

Fig.1-16- A peak in chlorophyll and phaeophytin (degrading chlorophyll) typically oc- curs at the nutricline, which coincides also with the top of pycnocline (Hallock et al., 1991). The nutricline generally begins in the lower part of the photic zone, where nutrient-rich (deeper) water can mix upward via upwelling or internal waves, and where available light energy, not nutrients, limits primary production (from Hallock and Pomar, 2008)

In the modern oceans, thermocline is primarily responsible for the pycnocline while in "greenhouse" time, the pycnocline was associated with halothermal conditions (Nunes and Norris, 2006). In the ocean, Chlorophyll maximum layers are coinciding with pycnocline (both seasonal or permanemt) (Fig.1-16) and in this zone, the concentrations of phytoplankton resulted in

accumulation of zooplankton (Richardson et al., 2000; Leichter et al., 2003; Ryan et al., 2005; Mann and Lazier, 2006). A peak in fluorescence, representing a maximum concentration in chlorophyll and phaeophytin (degrading chlorophyll), occurs at the nutricline, which also in accordance with the top of pycnocline (Hallock et al.,1991). The initiate zone of nutricline is generally in the lower part of the photic zone, where nutrient-rich water moves upward from deeper parts due to internal waves or upwelling where the growth of buildups limited by high concentarion of light. As a result, seasonal pycnocline and the upper part of the permanent pycnocline in lower latitude regions are associated with internal waves propagation and then high concentration of planktons (Hallock et al.,1991; Pomar et al., 2017). In modern oceans, internal waves are responsible of enhancing the inorganic nutrients and particulate organic carbon (POC) when they affect the shelf margin or upper slope (e.g. Florida Keys) (Leichter et al., 2003, 2008). The high turbulence produced by nutrient-rich internal waves resulted to strong vertical water displacement and then contribute to high biological productivity (Alford et al., 2015). In summary, the pycnocline is characterized by zone where both internal waves propogation and high plankton concentrations take place. Then, metazoans tend to produce buildups at the depth of pycnocline which can explain why Phanerozoic metazoan were mostly developed at mid- to outer ramp settings (e.g., Tucker andWright,1990; Burchette and Wright, 1992).

1-4- Impact of internal waves on Upper Jurassic –Lower Cretaceous and Late Oligocene Tethyan relams

While the role of internal waves is well-known for oceanographers and marine ecologists, their impact on the sedimentary records still very poorly documented. Recently, the source of turbulence has been highlighted in sedimentary systems linked to the internal waves and tides (Pomar et al., 2012; Shanmugam, 2013). These can help to interpret the development of some carbonate communities thrive in the mesophotic-oligophotic conditions where the buildups need nutrients and a water motion to grow (Pomar, 2017). During the Late Jurassic, an extensive coral and stromatoporoid reefs have been developed in northern and southern part of Tethys (Leinfelder et al., 2002). The Upper Jurassic reefs are characterized by high production of debris-rich facies associated with the carbonate buildups. However, the origin of these high-energy debris-rich facies is still matter of debate. In the Upper Jurassic-Lower Cretaceous Monte Sacro Limestones (MSL), Gagrano, Italy, the stromatoporoid-rich facies are accompanied by a high percentage of high-

energy intraclastic-bioclastic rich facies. Several outcrops of MSL located in platform margin of Apulia Carbonate Platfom (ACP) have been studied in order to study the main lithofacies distributed in study area. *The main aim of this study to examine the role of internal waves as a possible source of high-energy turbulence resulted in production of high-energy debris associated with stromatoporoid buildups.*

Moving to the other reef communities developed during the Cenozoic, abundant reef builders and carbonate producers were thrived specially through the Paleogene and Neogene (Pomar et al., 2017). During the Late Oligocene, the coral reefs were extensively spread along the Tethys realms (Frost, 1977; Frost et al., 1983) as well as in the Caribbean and the Indo-Pacific regions (Budd, 2000; Wilson, 2008). However, many studies use the modern Caribbean barrier-reef shelf-lagoon complex model for interpretation of the coral buildups developed during this time (e.g.: Frost, 1981). During the Late Oligocene, studies reported the coral buildups to be developed in mesophotic conditions (Pomar et al., 2017 and references therein). The study of modern deep-water mesophotic corals have been received an increased interest by ecologists (Kahng et al., 2017; Feldman et al., 2018; Rocha et al., 2018). However, the mesophotic corals have been poorly documented from sedimentary records during the geological periods (Morsilli et al., 2012). Recently, the role of internal waves, as a source of water turbulence, has been considered as a useful tool in interpretation of mesophotic carbonate communities (Morsilli et al., 2012, Pomar et al., 2017). The Late Oligocene coral-rich facies of Grotta San Michele Limestone (GSML) exposed along the platform margin of ACP. Also, during the Chattian age, extensive coral buildups were developed Asmari Formation, Zagros basin, Iran. Several outcrops of GSML and Chattian Asmari Formation have been studied in order to study the coral facies and their associated facies. *The main aim of this study to analyse the role of internal waves on formation and development of these mesophotic corals communities. Moreover, we also examine the possible role of internal waves as turbulence resulted in formation of high-energy flank facies associated with coral buildups.*

Chapter 2

Case study 1

Upper Jurassic- Lower Cretaceous Monte Sacro Limestones, Gargano, Italy

2-1- Introduction

The Late Jurassic was a period of extensive reef development, and it represents the peak in diversity of reef- builder organisms (Kiessling, 2002, 2009; Leinfelder et al., 2002; Cecca et al., 2005; Pomar and Hallock, 2008; Martin-Garin et al., 2012; Olivier et al., 2012). During this time the level of CO_2 was at least four times higher than the present and resulted in a high pressure of CO2 (pCO_2) and therefore a greenhouse condition (Holz, 2015), which favoured the development of abundant microbialite and benthic automicrite factory (Pomar and Hallock, 2008). Global sea-level rose until the end of the Kimmeridgian (Haq, 2018) and this rise was associated with the development of Upper Jurassic reefs domains especially on the european part of the northern Tethys Ocean (Leinfelder et al., 2002).

Upper Jurassic reefs have been studied in details with particular attention on northern part of Tethys and North Atlantic (Dupraz and Strasser, 1999, 2002; Insalaco, 1999; Olivier et al., 2004, 2007; 2012; Lathuilière et al., 2005; Reolid et al., 2007; Strasser and Védrine, 2009; Matyszkiewicz et al., 2012; San Miguel et al., 2017). On the contrary, southern and intra-Tethys reefs received less attention in the literatures (Catalano and D'Argenio, 1981; Turnšek et al., 1981; Morsilli and Bosellini, 1997; Leinfelder et al., 2005; Schlagintweit et al., 2005; Schlagintweit and Gawlick, 2008; Rusciadelli et al., 2011; Basilone and Sulli, 2016a; Hoffmann et al., 2017).

During the Late Jurassic, different types of reefs were developed along the northern and southern part of Tethys (Fig.2-1). Corals, sponges, and microbialites were the main bioconstructors, particularly in the northern Tethys margin and North Atlantic (Leinfelder et al., 2002), and depositional geometries and facies distribution were mainly ascribed to carbonate ramps (Leinfelder, 1993; Insalaco et al., 1997; Olóriz et al., 2003; San Miguel et al., 2017). Coral reefs widespread in the distal part of the inner ramp of north Tethys, while mid-ramp settings were characterized by mixed coral-siliceous sponge reefs (Leinfelder et al., 2002) as well as coral-microbial reefs in the western part of Tethys (Bádenas and Aurell, 2010). Instead, siliceous sponge mounds thrived in the outer-ramp setting (Dromart et al., 1994; Leinfelder et al., 2002; Olivier et al., 2007; Guo et al., 2011). In contrast, in the southern part of Tethys, including intra-Tethys, the stromatoporoids (inc. chaetetids) were more abundant than corals (Turnšek et al., 1981; Wood, 1999; Leinfelder et al., 2002). These buildups were mostly developed on the margin of isolated platforms (Morsilli and Bosellini, 1997; Rusciadelli et al., 2011) (Fig.2-1) as well as mid- ramp settings (Al-Awwad and Pomar, 2015).

According to various authors, during the middle to late Oxfordian, in the western and northern Tethys, coral reefs were mainly developed in shallow water settings accompanied with stromatoporoid as a minor constructor (Pandey and Fürsich, 2003; Lathuilière et al., 2005; Guo et al., 2011; Strasser et al., 2015). Microsolenid corals were also formed in the more distal part of the margin (Insalaco et al., 1997; Insalaco, 1999). Siliceous sponges- microbial mounds were widely distributed in the deeper shelf (Guo et al., 2011; Krajewski et al., 2016), while microbialite-rich reefs were expanded in western Tethys and North Atlantic (Reolid et al., 2005) (Fig.2-1). During the Kimmeridgian coral-microbial reefs flourished (Olivier et al., 2003, 2008; San Miguel et al., 2017) (Fig.2-1), instead siliceous sponges were developed locally (Leinfelder et al., 1993). In the North Atlantic, sponge reefs, mixed sponge-coral reefs, and bivalve reefs were dominant (Leinfelder et al., 2002). During the Tithonian, scatter coral reefs were distributed compared with Oxfordian to Kimmeridgian time (Leinfelder et al., 2002)

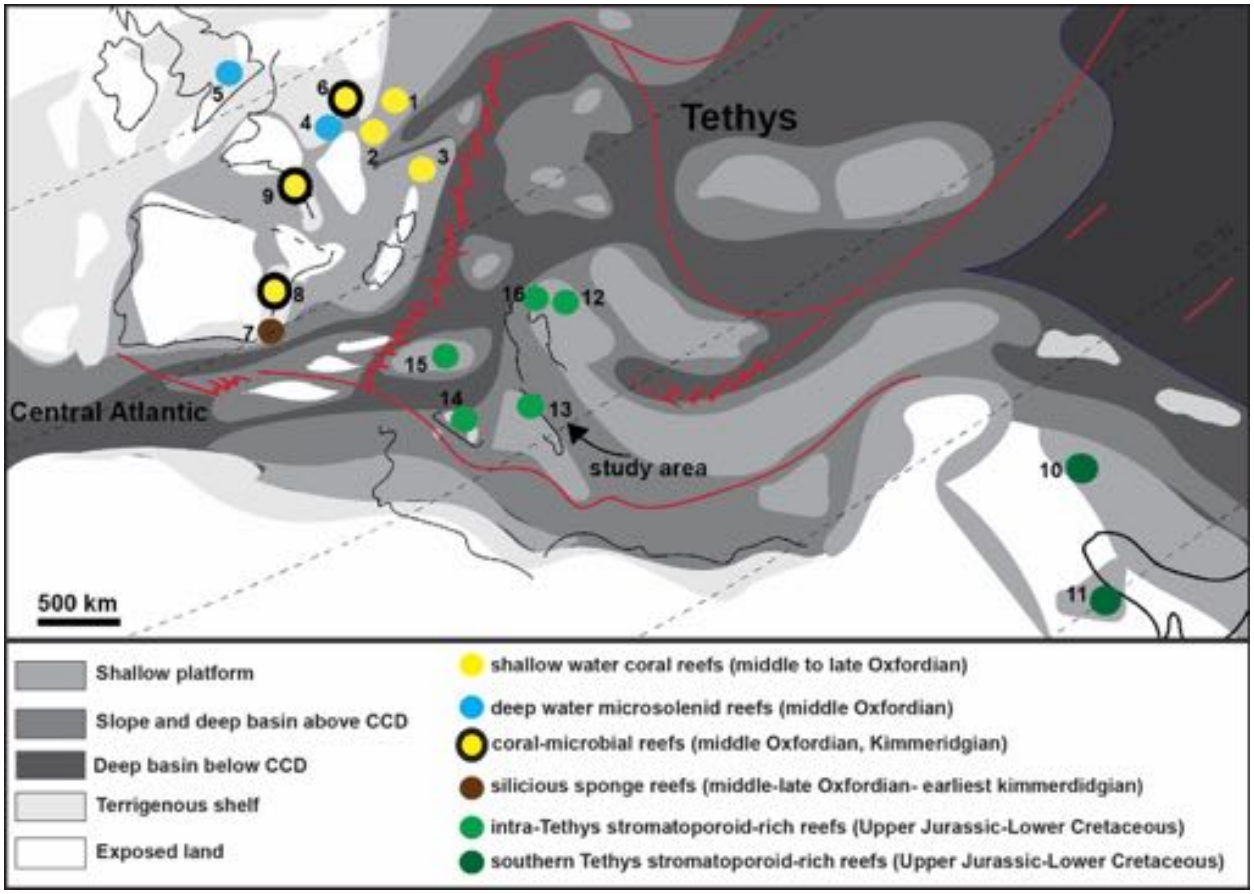

Figure. 2-1- Schematic paleogeographic map of Tethys during the Late Jurassic (modified from Dercourt et al., 2000), showing the distribution of different type of reefs. 1- Jura Platform, 2- France Lorraine, 3- Switzerland and northern Germany, 4- England (Yorkshire), 5- France Burgundy, 6- Pagny-sur-Meuse, 7-8- Iberian basin, 9- La Rochelle

platform, 10- Zagros basin, 11- Khurais basin, 12- Dinaric carbonate platform? 13- Apulia carbonate platform (this study, black arrow), 14- Sicily, 15- Apennines carbonate platform, 16- Friuli. The data extracted from various researches (Turnšek et al., 1981; Morsilli and Bosellini, 1997; Insalaco et al., 1997, 1999; Olóriz et al., 2003; Lathuilière et al., 2005; Leinfelder et al., 2005; Kano et al., 2007; Olivier et al., 2008; Rusciadelli et al., 2011; Al-Awwad and Pomar, 2015; Basilone and Sulli, 2016a; San Miguel et al., 2017).

On the other hand, in the southern Tethys and intra- Tethys, the main reefs were made generally by debris-rich stromatoporoid-coral, without main variation from the Oxfordian to the Tithonian (Leinfelder et al., 2002) (Fig.2-1). In the southern Tethys, different type of stromatoporoids associated with corals have been developed along the shallow shelf of the Arabian plate and the Zagros Basin during the Kimmeridgian and Tithonian (Kano et al., 2007; Al-Awwad and Pomar, 2015; El- Sabbagh et al., 2017) (Fig.2-1).

Reef growth is controlled by several factors, including light penetration, energy level, sedimentation rate, substrate, nutrient, and salinity, among others (e.g. Hallock, 2015), and their complex interaction. The concept of the tropical carbonate factory is associated with the carbonate production that occurs in oligotrophic, warm and well- illuminated waters of the tropics and subtropics (Schlager, 2000, 2003; Hallock, 2005). In this condition, the light penetration is one of the fundamental factor controlling loci, amount and type of carbonate production, and can be used as a useful tool to reconstruct different zone in the rock record (Bosscher and Schlager, 1992; Pomar, 2001; Wilson and Vecsei, 2005; Morsilli et al., 2012; Pomar et al., 2015; Michel et al., 2018). These zones are named “euphotic”, “oligophotic” or “mesophotic”, and “aphotic”. The bathymetric position of these light zones is variable and depends on water transparency and latitude, and they associate with the development of some autotrophic organisms. The range of modern seagrasses and, non-dasyclad green algae can be used to define the euphotic zone, and the deepest occurrence of *in-situ* red algae define the lower limit of the oligophotic zone (Pomar, 2001; Morsilli et al., 2012). In addition to light, nutrient availability also plays a major factor in controlling carbonate production and define as oligotrophic, mesotrophic, and eutrophic conditions (Hallock, 1987; 2015). Dupraz and Strasser (2002) discussed three main nutritional modes for Oxfordian coral- microbialite reefs of Swiss Jura (northern Tethys): phototrophic (light-dependent) associations which prevail in oligotrophic and pure carbonate settings, balanced photo-heterotrophic, and heterotrophic-dominated occur in association with siliciclastics input. According to some authors, the Upper Jurassic shallow coral buildups from northern Tethys were

a phototrophic-dominated system, deposited in clear water with good light availability (Dupraz and Strasser, 2002; Martin-Garin et al., 2012). In contrast, microsolenid biostromes, associated with heterotrophic micro and macrofauna, developed in eutrophic condition (Insalaco, 1999), where the light penetration is usually low (meso-oligophotic zone). Stromatoporoids, the main bioconstructor of southern and intra- Tethys reefs during the Upper Jurassic, are considered to develop in shallow, high energy settings with strong to moderate oligotrophy conditions (Leinfelder et al., 2005). The stromatoporoid and mix stromatoporoid-coral buildups in the intra-Tethys show a high degree of debris production related to turbulence events. This reflects the importance of energy level and hydrodynamic processes in the formation of this kind of buildups. The origin of turbulence in these systems has usually been related to storm events generated by surface waves. Recently, another source of turbulence has been highlighted in sedimentary systems linked to the internal waves and tides (Pomar et al., 2012; Shanmugam, 2013). Internal waves (IWs) are perturbations propagating along a pycnocline (e.g. Munk, 1981; Apel, 2002) and their breaking along continental margin and slopes creates episodic high- turbulence events which can remobilize the sediment and carry nutrients at the depth where the pycnocline intersects the sea floor (Leichter et al., 2003; Lamb, 2014; Arthur and Fringer, 2016; Woodson, 2018). However, the impact of internal waves in the sedimentary record and their effect on fossil communities has remained largely unrecognized. In carbonate systems, internal waves can provide two important factors for carbonate buildups to grow: food resources and water motion (Pomar et al., 2017). Furthermore, internal waves can resulted in deposition of high-energy facies associated with carbonate buildups dominated in low-energy settings (Pomar et al., 2012).

The debris-rich stromatoporoid facies were developed during the Late Jurassic-Early Cretaceous along the platform margin of Apulia Carbonate Platform (ACP). During this time, ACP was an isolated carbonate domain located in the eastern part of south Tethys (Figs.2-2A). The previous studies of stromatoporoid-rich facies in ACP were mostly focused on sedimentological characteristics (Morsilli and Bosellini, 1997, Morsilli, 1998) and taxonomical interpretation (Russo and Morsilli, 2007). However, the factors controlling the development of these stromatoporoid buildups have been poorly studied. According to Russo and Morsilli, 2007, the stromatoporoids are mostly represented by *Ellipsactinia* sp. and *Sphaeractinia* sp. and they were developed along the external margin and proximal slope environments (Morsilli and Bosellini, 1997).

The platform margin of the ACP crops out in the Gargano Promontory and displays several units of marginal facies (Morsilli and Bosellini, 1997; Morsilli et al., 2017). The aims of this study are: 1- to analyse the facies distribution and lateral change of Upper Jurassic- Lower Cretaceous Monte Sacro Limestones (MSL), in order to reconstruct a depositional model for these stromatoporoid-rich units and, 2- to study the factors controlling the developments of the stromatoporoid buildups in MSL, including the potential role of internal waves as a possible source of episodic turbulence, resulted in extensive reef debris production.

2-2- Paleogeography of the ACP

The Apulia Carbonate Platform (ACP), one of the peri-Adriatic carbonate banks, was a major paleogeographic element of the southern margin of the Mesozoic Tethys Ocean (Fig.2- 2A). The ACP extended from the southeastern Abruzzi region across Apulia and the Strait of Otranto to the Greek islands of Cephalonia and Zante (Bosellini, 2002). This carbonate platform is the foreland of both the Apennine and the Dinaric thrust and fold belts (Bernoulli, 2001). It is bounded on both sides by basinal deposits. The western margin of the platform is downfaulted and buried underneath terrigenous sediments of the Apennine foredeep and the adjacent Apennine chain. Instead, the eastern margin of the platform lies 20–30 km offshore from the present Apulia Coastline in the Adriatic Sea (Bosellini et al., 1999; Borgomano, 2000; Morsilli et al., 2017). The ACP mainly consists of Upper Jurassic to Eocene shallow-marine carbonates, and in the Gargano Promontory and the Maiella Mountain also by the coeval slope to basin facies (Bosellini et al., 1999; Borgomano, 2000; Bernoulli, 2001). The studied outcrops correspond to the Upper Jurassic-Lower Cretaceous Monte Sacro Limestones (MSL) (Fig.2-2B) and they are located along the platform margin belt of the ACP, cropping out in the Gargano Promontory (Monte di Mezzo, Torre Mileto and Masseria Prencipe, Fig.2- 2C). The MSL in studied outcrops is characterized by massive limestones with stromatoporoids such as *Ellipsactinia* sp. and *Sphaeractinia* sp. (Morsilli and Bosellini, 1997; Russo and Morsilli, 2007). The outcropping Monte Sacro succession is about 300 m in the type section (Monte Sacro mountain) and has a stratigraphic distribution from Oxfordian to Berriasian (Pavan and Pirini, 1966; Luperto Sinni and Masse, 1994) and probably reaches the early Valanginian (Morsilli, 1998). Duo to the lack of biostratigraphic data from MSL successions in the studied intervals, the exact stratigraphic age range cannot be identified. However, the occurrence of *Calpionella* sp. near the top of the studied stratigraphic section

(section A) can suggest an age interval between Tithonian to Berriasian (Bosellini and Morsilli, 1997).

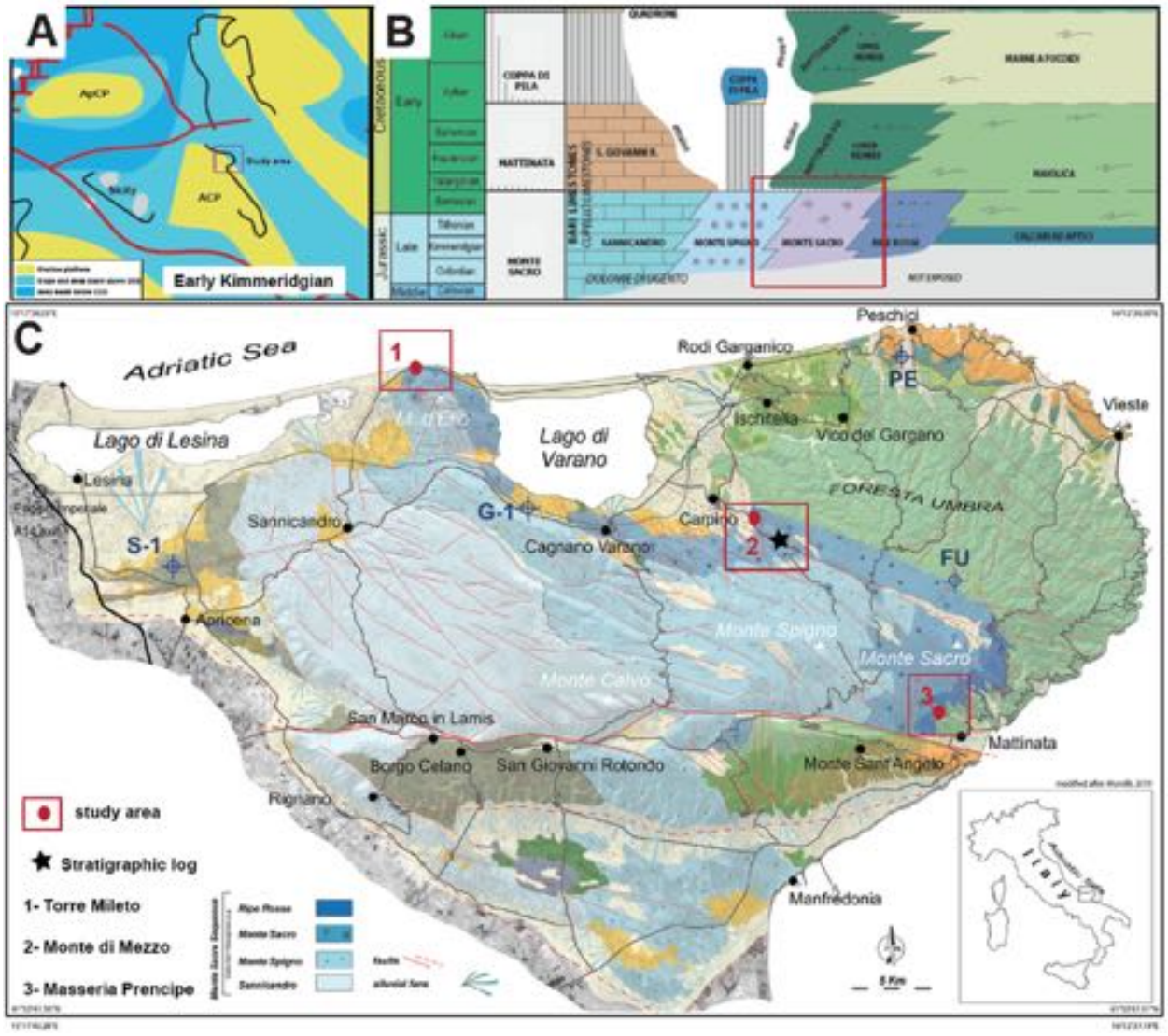

Figure. 2-2- A: Schematic palaeogeographic map showing the location of studied area (Gargano Promontory) along the platform margin of ACP (modified from Dercourt et al., 2000). B: Stratigraphic framework of the Gargano area during the Late Jurassic and Early Cretaceous succession. The studied interval belongs to Monte Sacro Limestones (red square) (modified from Morsilli, 2016). C: Simplified geological map of the Gargano Promontory showing different facies zones and study areas of this paper (modified after Morsilli, 2011). Coordinates: top left corner (41°589 6.340 N; 15°179 26.930 E); bottom right corner (41°329 57.660 N; 16°129 25.560 E). Study areas: 1- Torre Mileto 2- Monte di Mezzo 3- Masseria Prencipe. The external margin deposits are representing by Monte Sacro Limestones.

2-3- Methods

The studied MSL outcrops are exposed along the platform margin belt of ACP in the Gargano area (Fig. 2-2C). Despite the limitation imposed by highly weathered outcrops of MSL in Gargano area, the interpretation of facies is possible along the surface of some outcrops where the quality of exposure surface allowed the study of distribution, organization, the shape of main biotas and characteristics of different facies. The Monte Sacro Limestones are well exposed in Monte di Mezzo section in the area of ~1.6 km long with a stratigraphic thickness of ~ 100 m. For investigation of lateral changes of facies, seven outcrops surfaces have been selected. The outcrops are characterized by m-thick massive limestone with no visible bedding surfaces and geometry. For vertical facies changes, one stratigraphic log has been measured and described. Sampling along the stratigraphic log (average one sample in every 5 m) complemented with sampling from the adjusted outcrops. In the other areas (Torre Mileto and Masseria Prencipe) the MSL are partially exposed as small outcrop windows. The described outcrop surfaces in Torre Mileto and Masseria Prencipe are arranged in cm to m-thick massive limestones (~ 2 m^2). The stromatoporoid lithofacies were recognized based on field description of stromatoporoids and corals with the identification of their growth forms. In order to study the internal sediments, a total number of 90 samples have been collected. All samples have been prepared for thin section analysis in order to study the textural characterization of internal sediments and identification of skeletal components. Components abundance was estimated based on point counting using the JMicroVision program and grouped in five categories: rare (less than 1%), present (2%–25%), common (26%–50%), abundant (51%–75%) and very abundant (76%–100%). The facies were identified according to Dunham (1962) and Embry and Klovan (1971). Light zonation of depositional environments (oligophotic, mesophotic and euophotic) and their relative boundaries has been defined following Pomar (2001) and Morsilli et al. (2012).

2-4-Stratigraphy and facies analysis

2-4-1- Monte di Mezzo section

In Monte di Mezzo section, a total number of 7 outcrops (Fig. 2-3) and one stratigraphic section (Fig.2-4) have been described. MSL in this section is extended in area of ~ 2 km long and 100 m thick (Fig.2-3) All outcrops arranged in m-thick massive limestones. The main characteristics of studied outcrops is the presence of stromatoporoids, corals, stromatolite-like organism, sponges and echinoids. The organization of organisms in all studied sections showing the cluster fabric

(*sensu* Riding, 2002). Figures 2-5 to 2-27 showing the studied field data, their related schemes, dominant organisms internal sediments of each outcrops along the Monte di Mezzo road. The internal sediments of buildups showing different textures: wackestone, fine-grained packstone, packstone and grainstone.

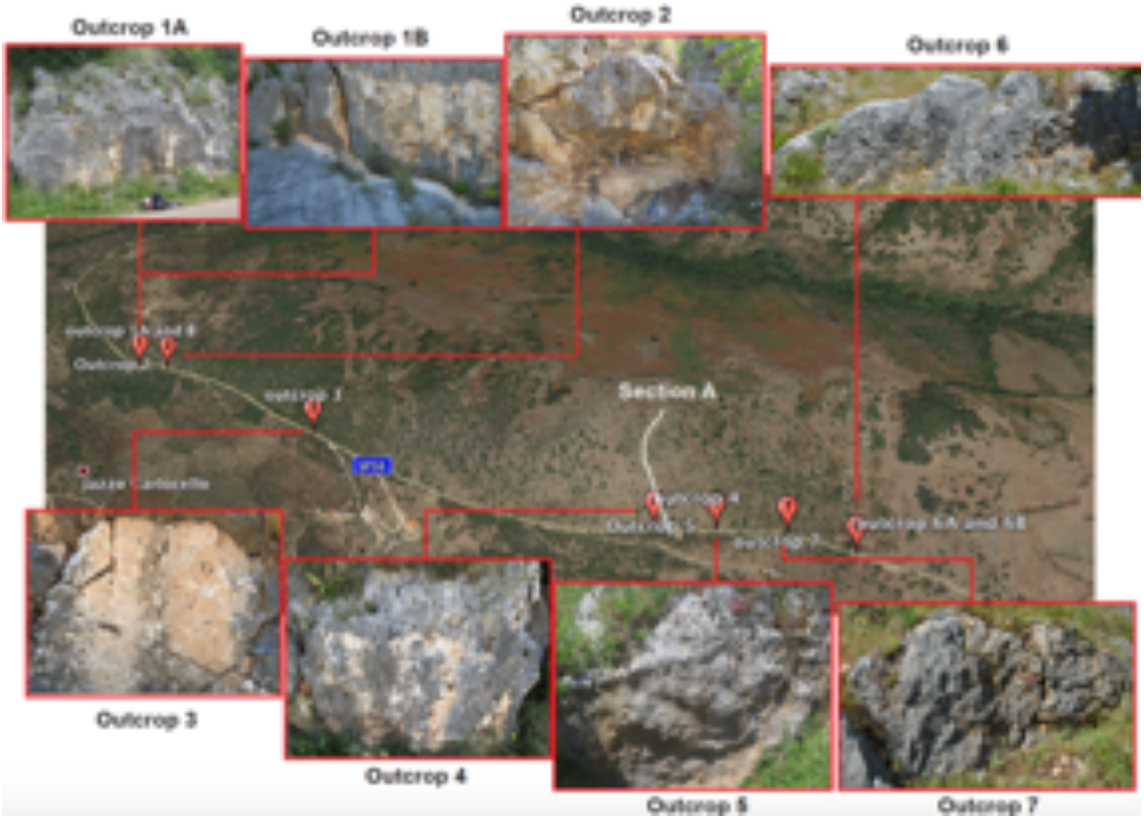

Figur. 2-3- Studied MSL outcrops along the Monte di Mezzo section. All of the outcrops are m-thick and arranged in massive limestones. Outcrop 1A: is represent by LF3: Stromatoporoid-microbial facies. Outcrop 1 B: is dominated by LF2 lithofacies, stromatoporoid-coral facies. Outcrop 2: represents by LF2 lithofacies, stromatoporoid-coral facies. Outcrop 3 to outcrop 7: belongs to stromatoporoid-rich facies (LF1). Section A is represent by about 100 meters thick, and the dominant facies is stromatoporoid-rich facies (LF1).

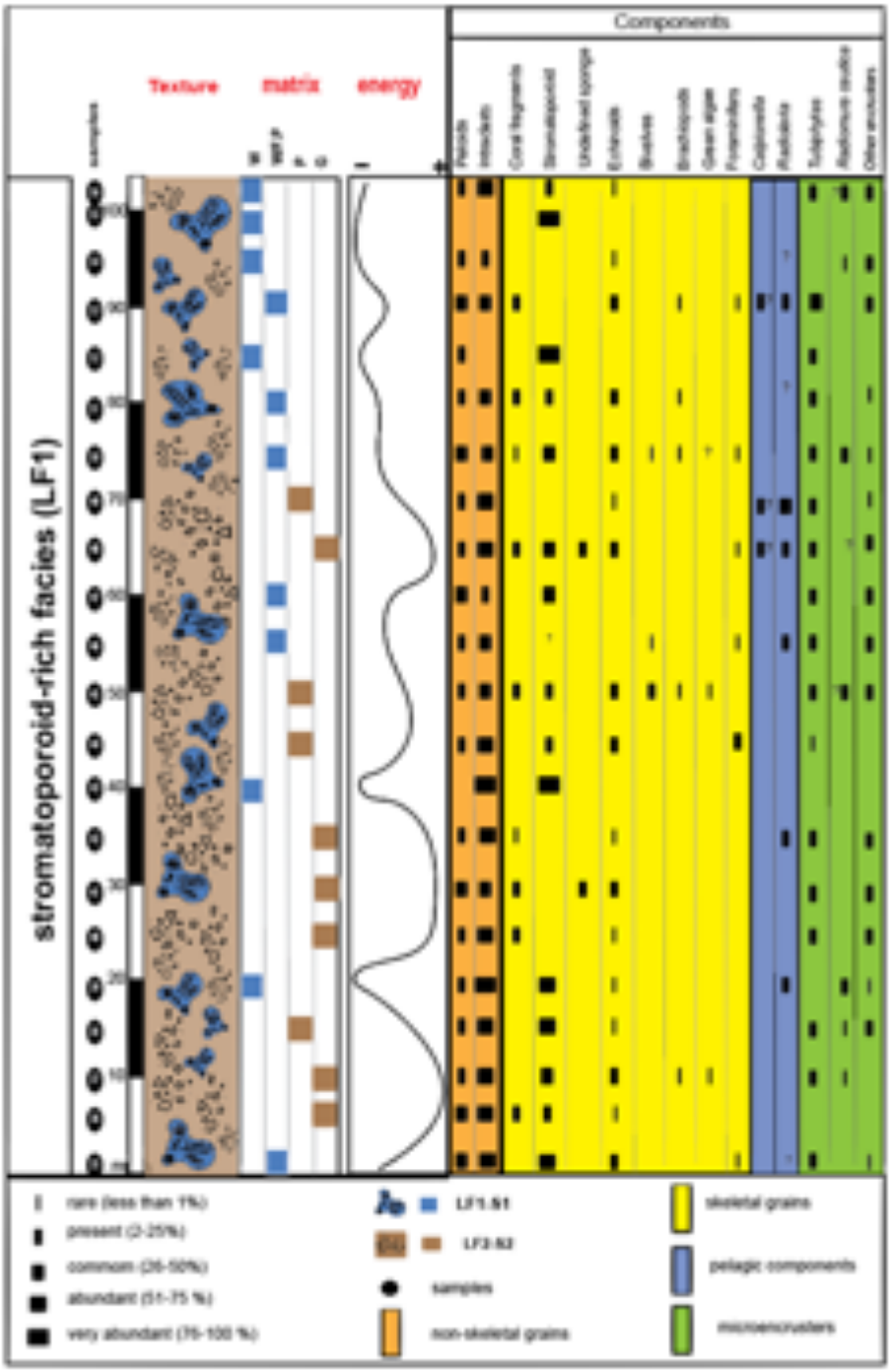

Figure.2-4- Stratigraphic section of Monte Sacro Limestones in Monte di Mezzo, showing main textures and relative abundance of skeletal and non-skeletal components along the measured log.

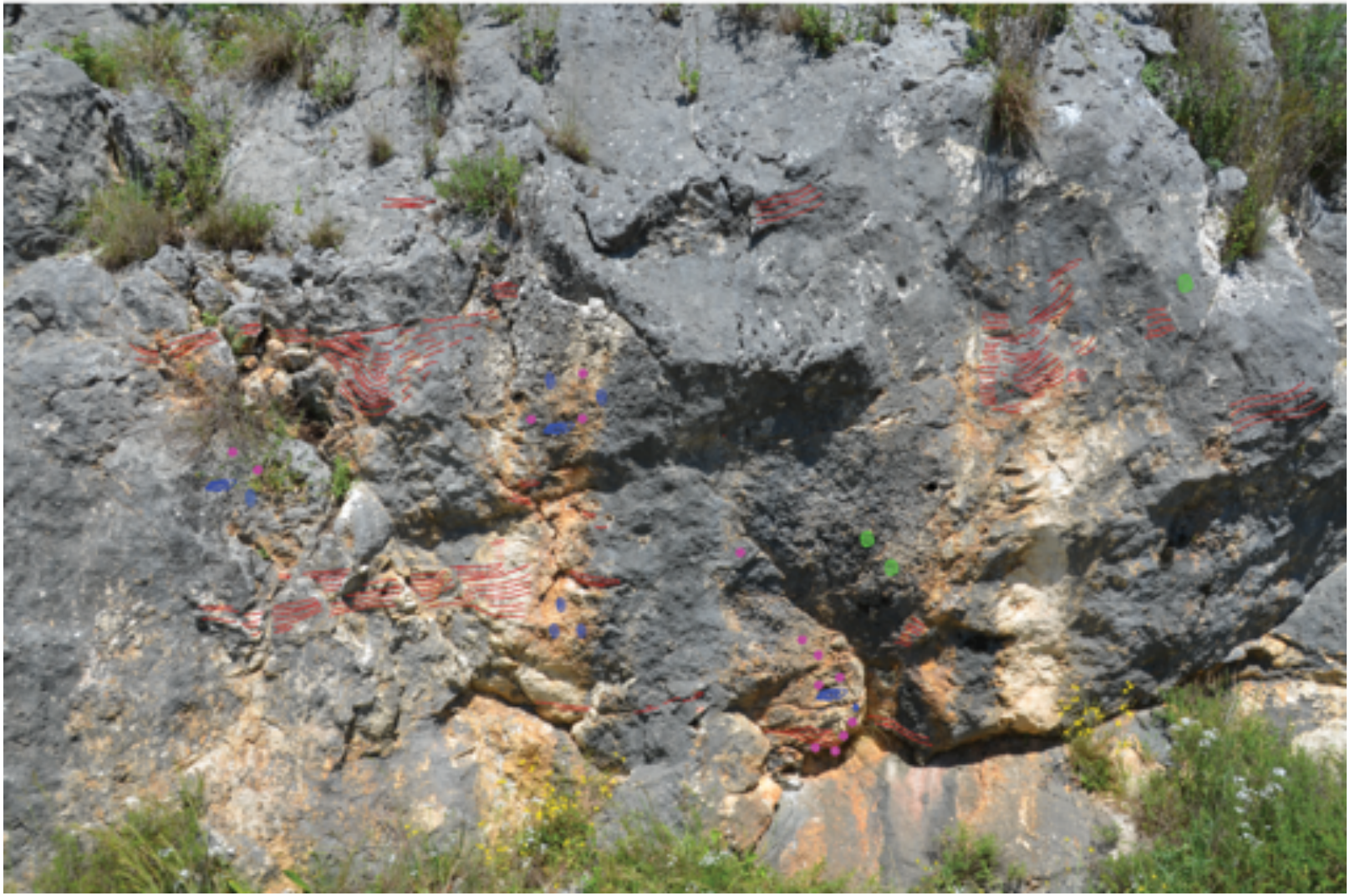

Figure.2-5- outcrop1A represent by ocuurance of stromatoporoids, stromatolite like structures, sponges and

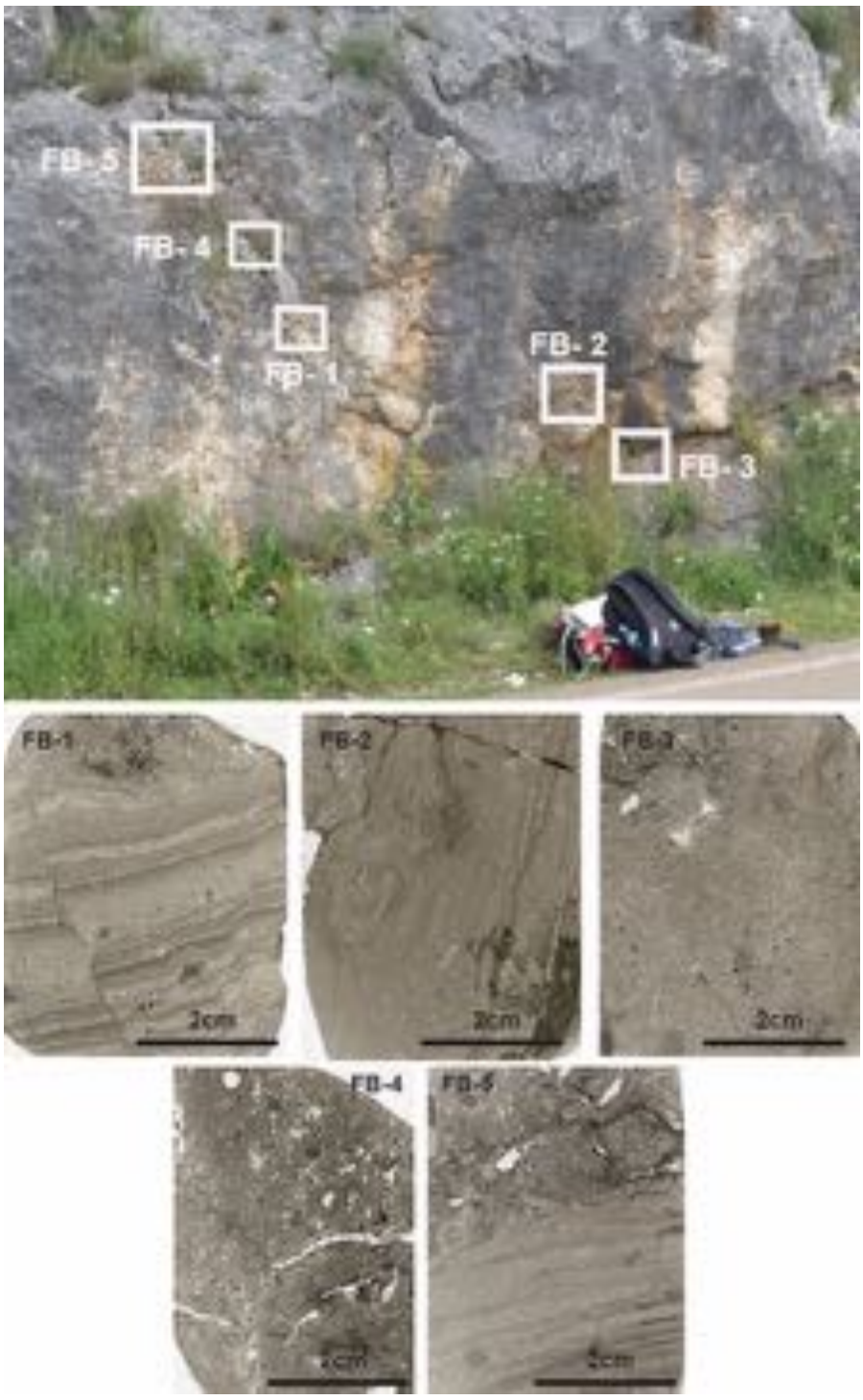

Figure. 2-6- photomicrographs of internal sediments of collected samples in outcrop 1a showing different textures: FB-1: wackestone with visibale lamination of stromatolite-like mats, FB-2-mudstone to wackestone with some irregular stromatolite-like mats, FB-3- wackestone, FB-4: packstone with peloids and micritic skeletal grains, FB-5: wackestone with stromatolite-like lamination at the bottoma and to packstone texture on top. This outcrop belongs to Stromatoporoid-microbial facies (LF3).

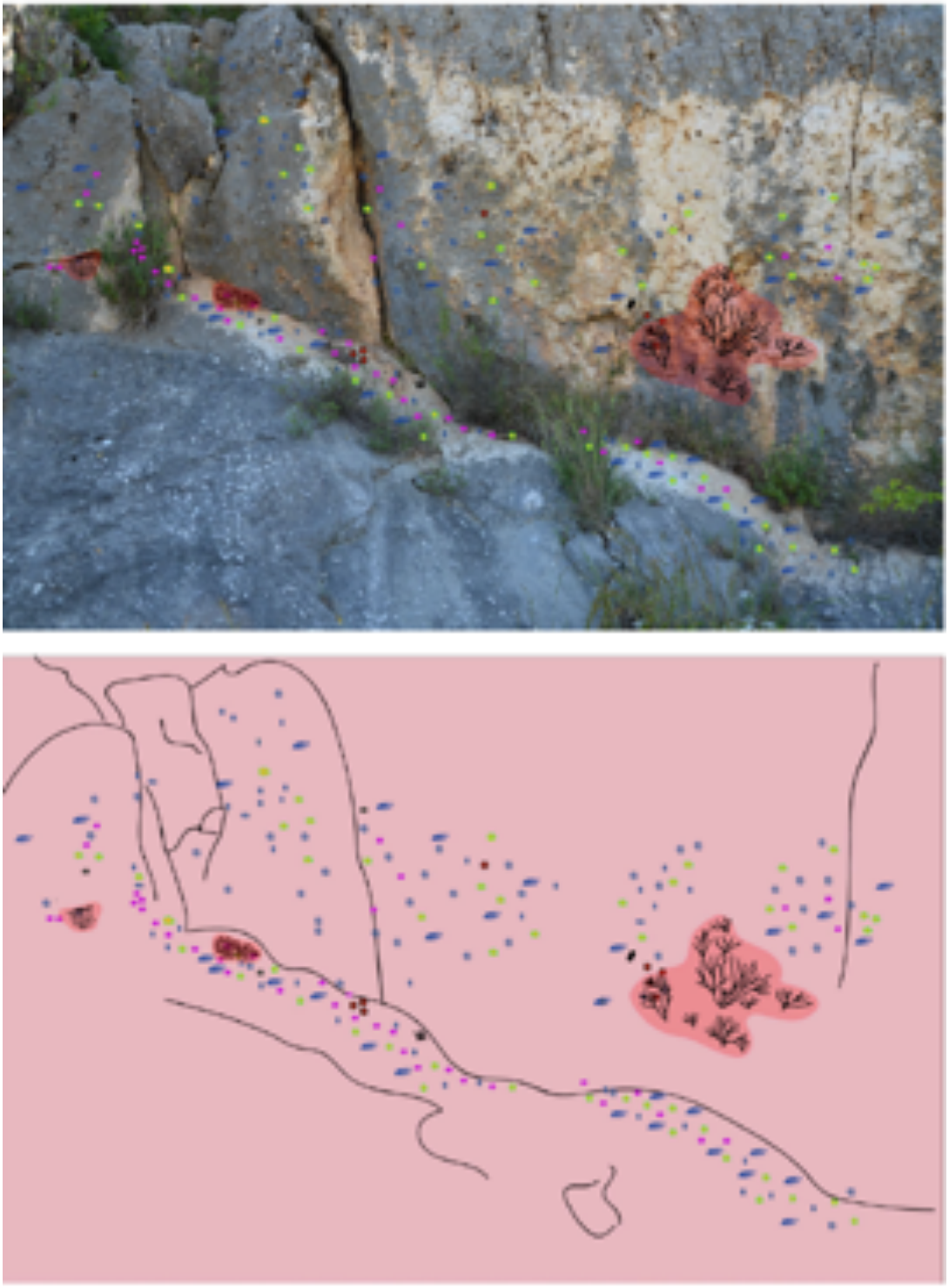

Figure. 2-7- Top: Scheme shows the field description of outcrop 1B, with stromatoporoids, corals and echinoid spines. Bottom: Simplified photo showing the organization and position of corals and stromatoporoids in outcrop 1B. This outcrops is represented by stromatoporoid-coral facies (LF2).

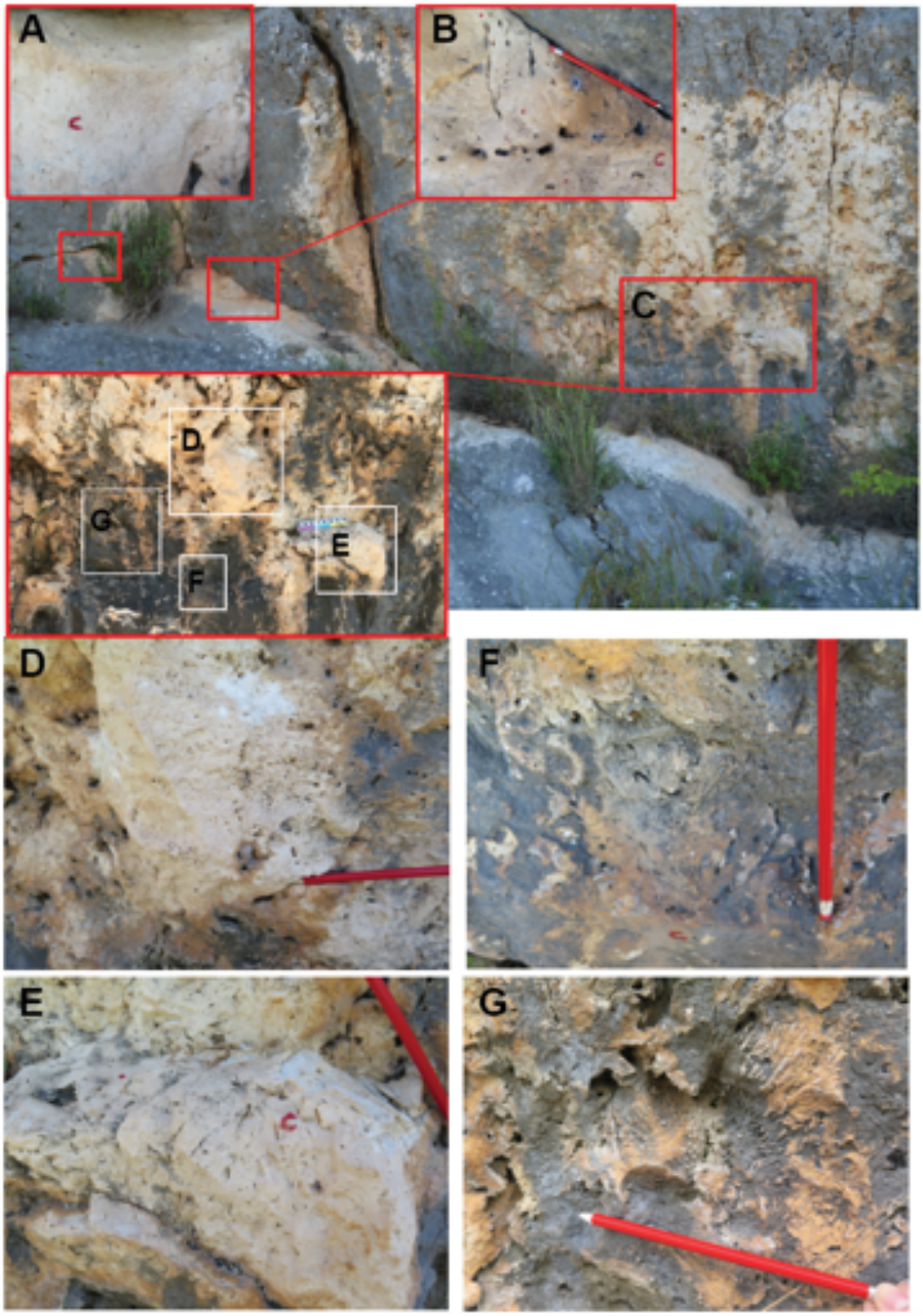

Figure. 2-8- Figure shows the branching corals developed along the outcrop1B. A: dm-sized pheceloid coral colony in growth position, B: thich branches dm-sized coral colony, C: the position of coral colonies distributed on outcrop, D: dm-sized coral coliny with branching morphology. The branches are close and in attach to eachothers. F: dm-sized

coral colony with branching morphology. E: dm-sized coral colony with in-attached branches. G: dm-sized coral colony. The branches are not compacted and there is space between them. This outcrop is representing by stromatoporoid-coral facies (LF2).

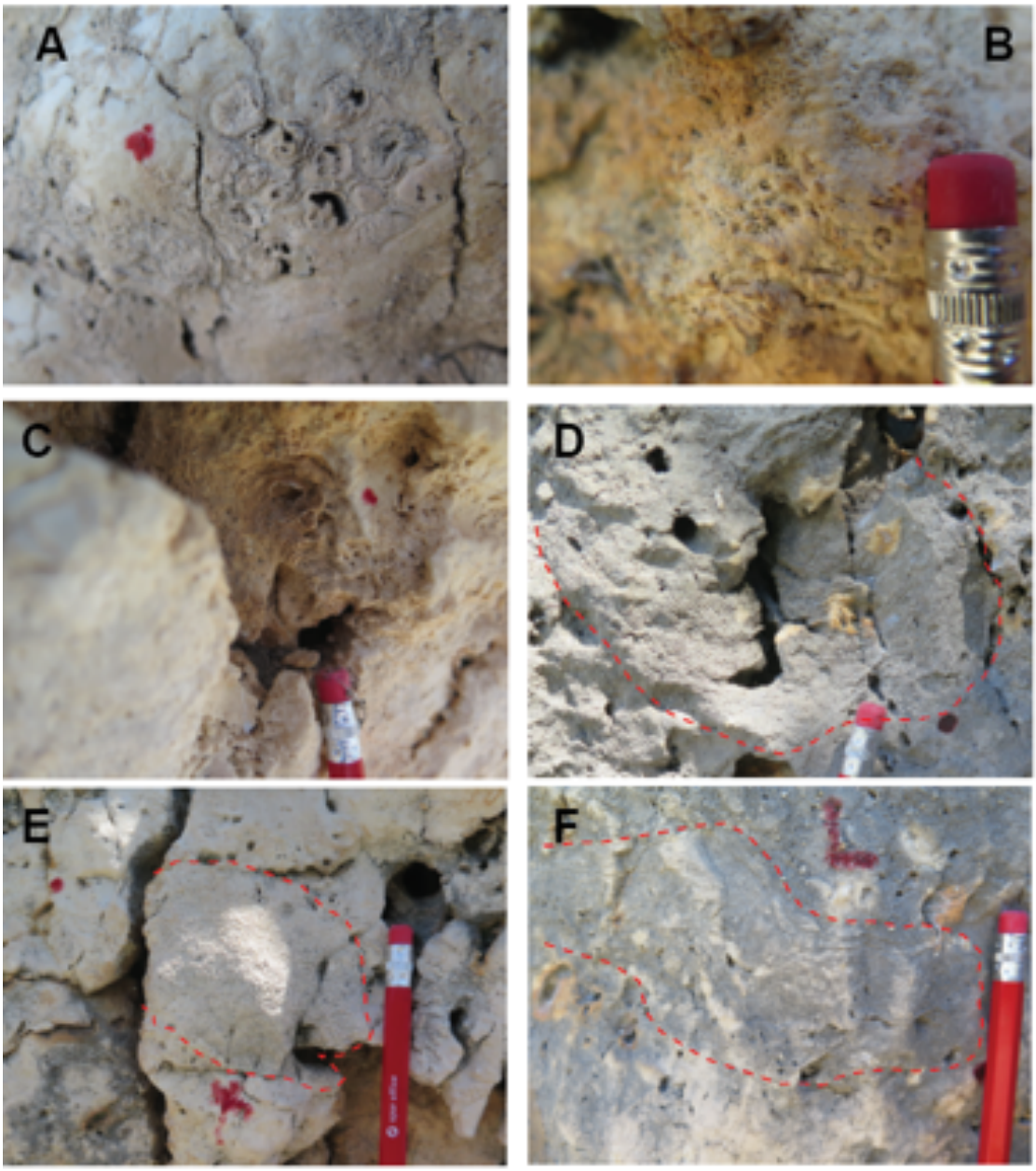

Figure. 2-9- Figues show the different skeletal biota associated with outcrop 1B. A: small phaceloid form corals, B: cm-sized coral in branching form, C: *Ellipsactinia* sp. (*in-situ*), D: *Ellipsactinia* sp. in growth position. F: un-defined sponge, G: stromatoporoid in growth position with associated lamination.

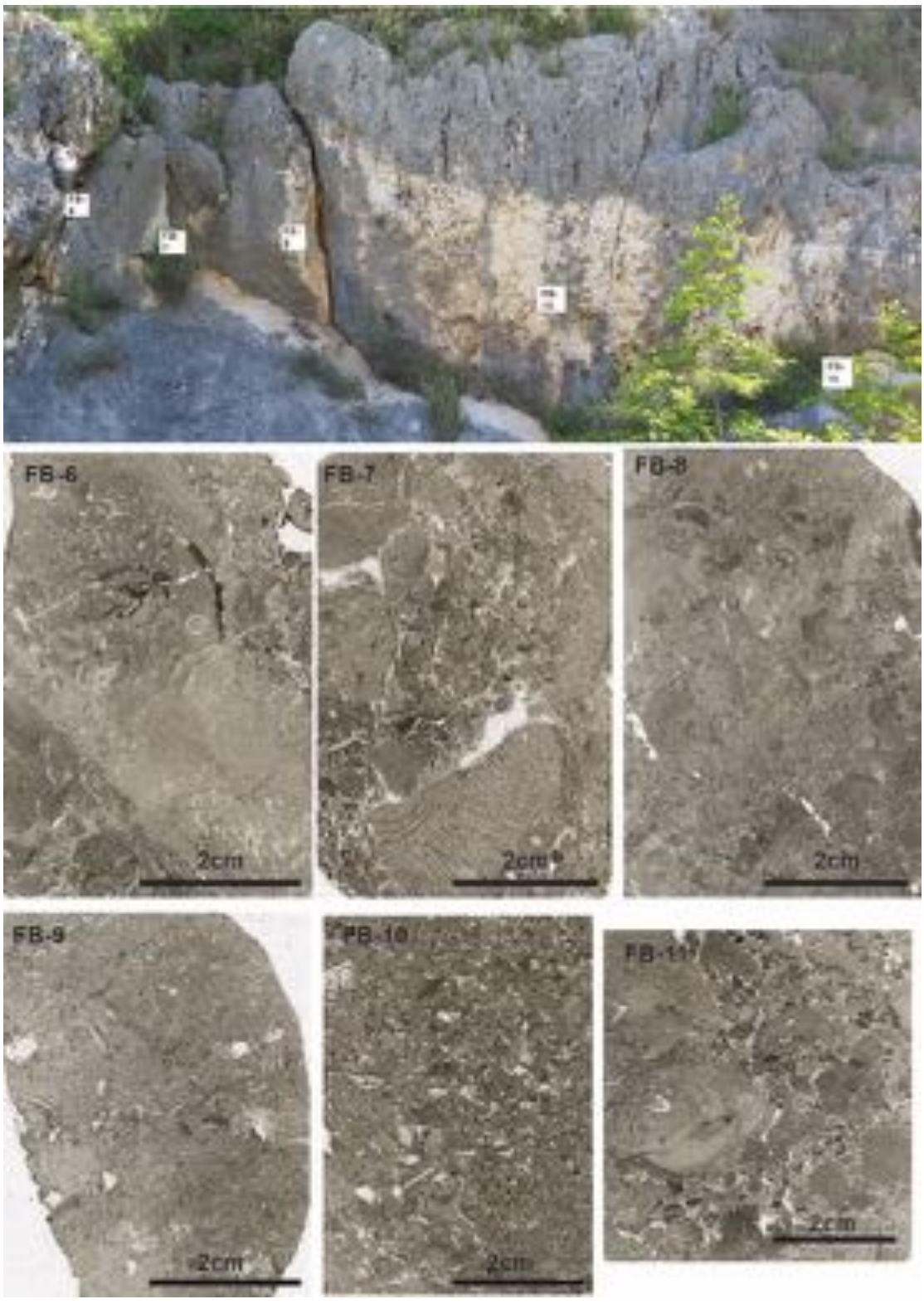

Figure. 2-10- Internal sediments of collected samples from outcrop 1B. FB-6: wackestone to packstone matrix with intraclast, FB-7- intraclastic packstone to grainstone with cm-sized clasts of stromatoporoids, FB-8: wackestone to very fine-grained packstone, FB-9: wackestone to fine-grained packstone, FB-10: packstone matrix with skeletal

grains and *Tubiphytes*, FB-11: intraclastic packstone with cm clasts of stromatoporoids and other types of clasts with *Tubiphytes* grains. This outcrop and the thin sections are representing by stromatoporoid-coral facies (LF2).

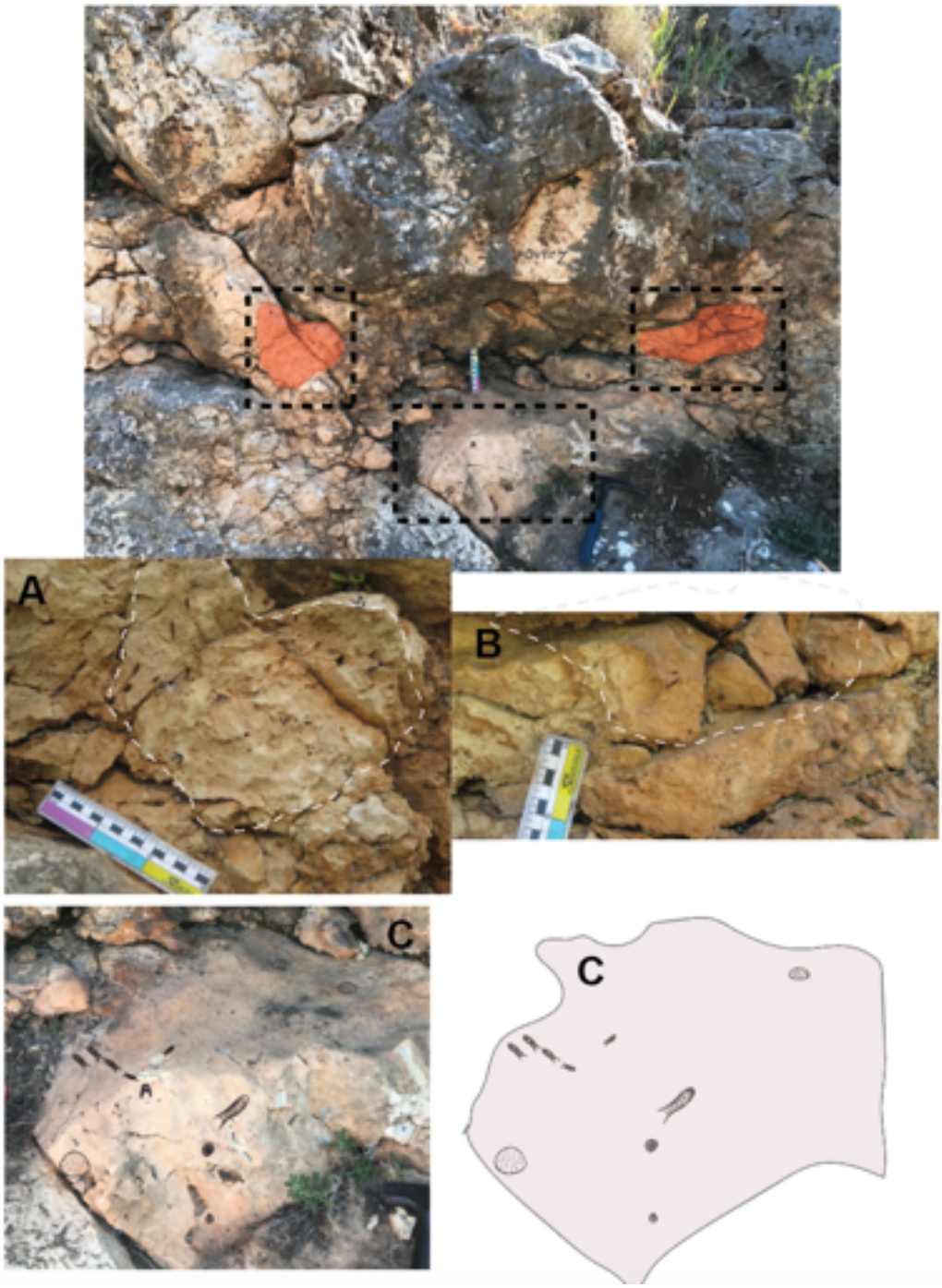

Figure. 2-11- The figure shows the position of coral colonies associated with stromatoporoids in outcrop 2. A: dm-sized coral colony. B: dm-sized coral colony with in-attached branching morphology. C: The figure show the distribution of stromatoporoids in the outcrop (with simplified scheme at the right). This outcrop is representing by stromatoporoid-coral facies (LF2).

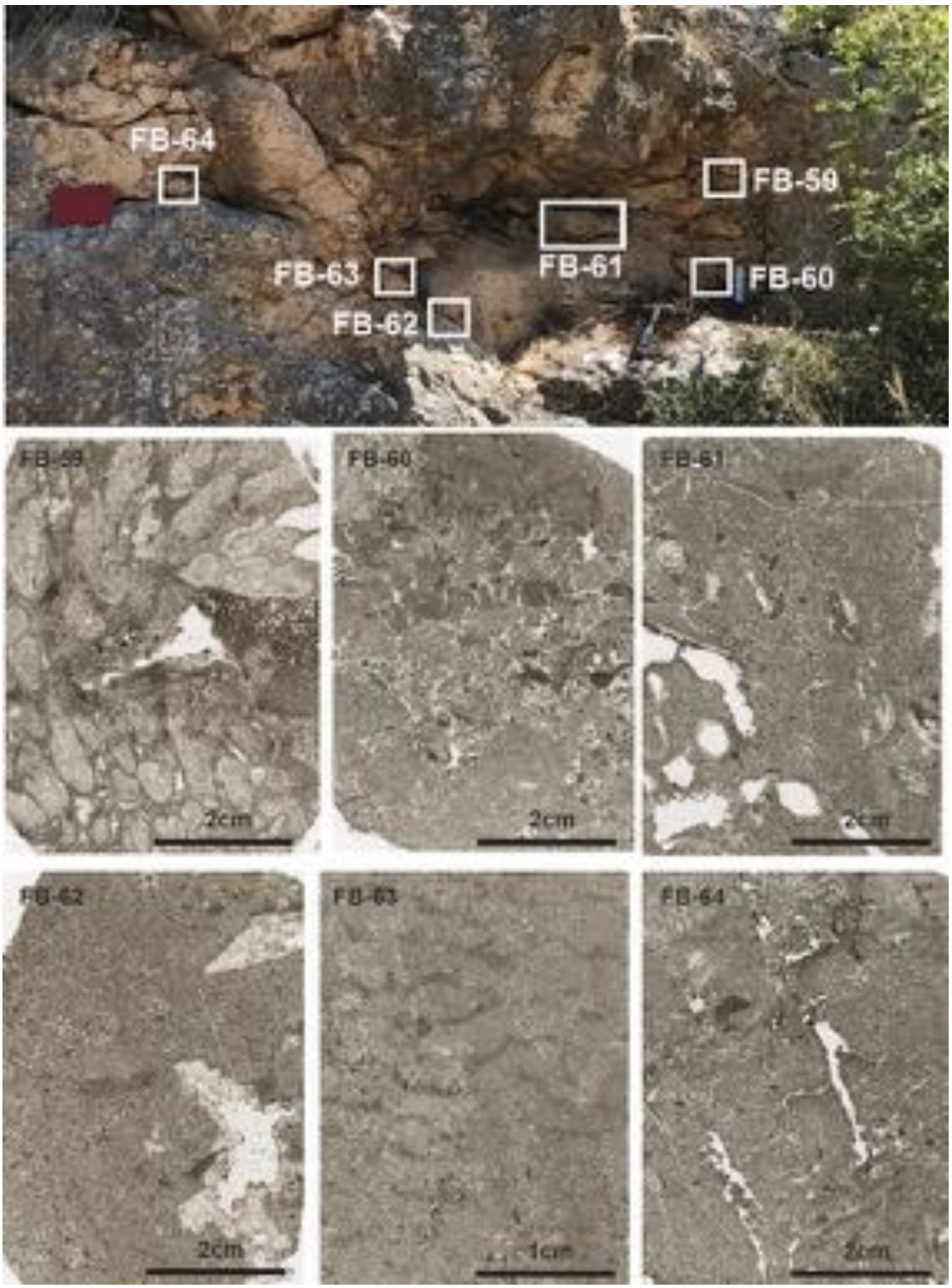

Figure. 2-12- Internal sediments between corals and stromatoporoids from collected samples along the outcrop 2. FB-59: branching coral boundstone with wackestone matrix, FB-60: intraclastic packstone, FB- 61: fine-grained packstone, FB-62- fine-grained packstone, FB-63- wackestone with fragments of *Saccocoma* sp., FB-64: packstone with *Tubiphytes* grain. The dominant facies is LF2 (Stromatoporoid-coral facies)

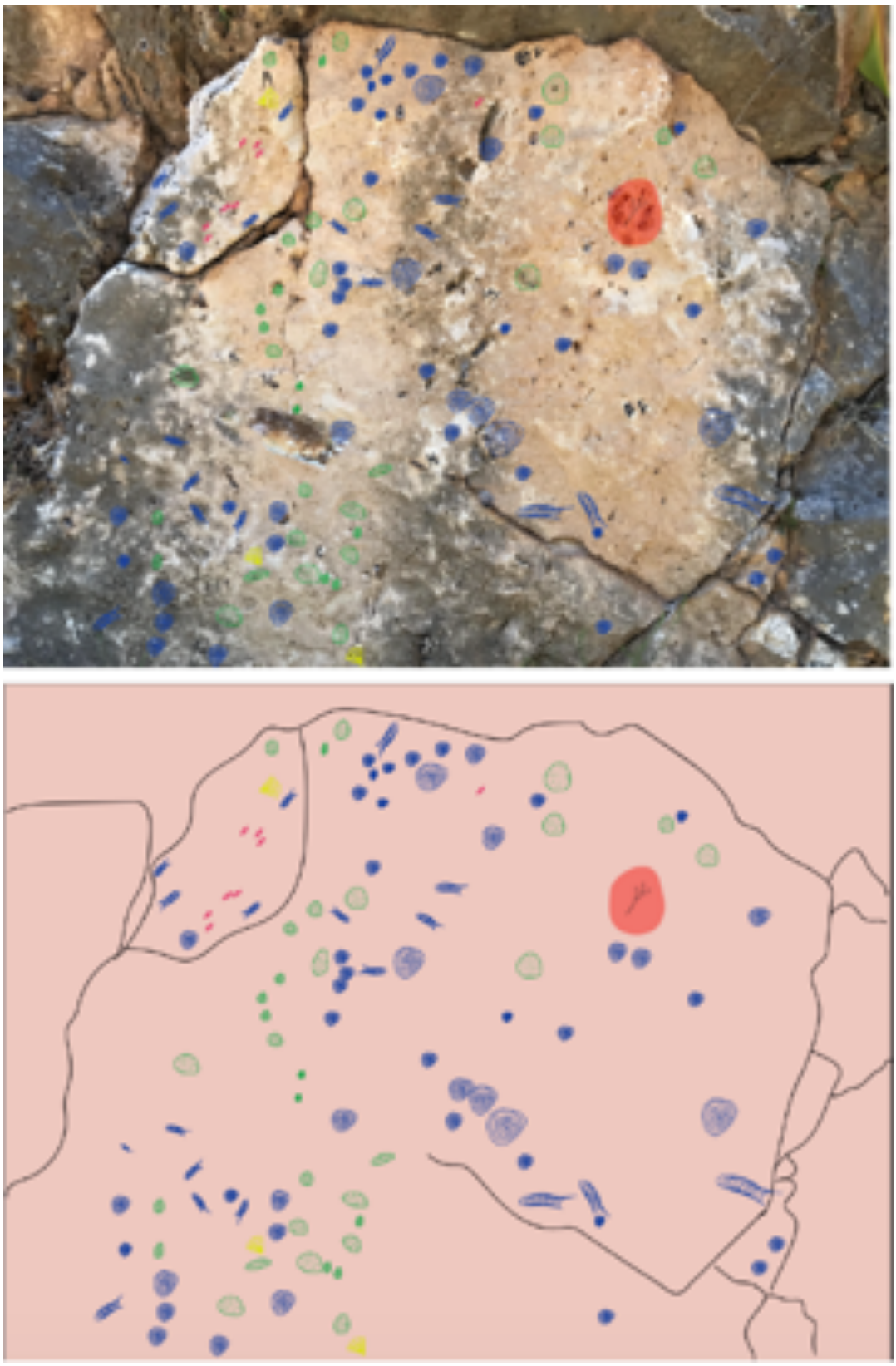

Figure. 2-13- Field description and associated scheme of outcrops 3, showing the distribution and organization of different biotic components along the surface of outcrop. The biota are mainly stromatoporoids, sponges, echinoid

spines and small corals. The bottom figure shows the simplified outcrop image. The outcrop belongs to stromatoporoid-rich facies (LF1).

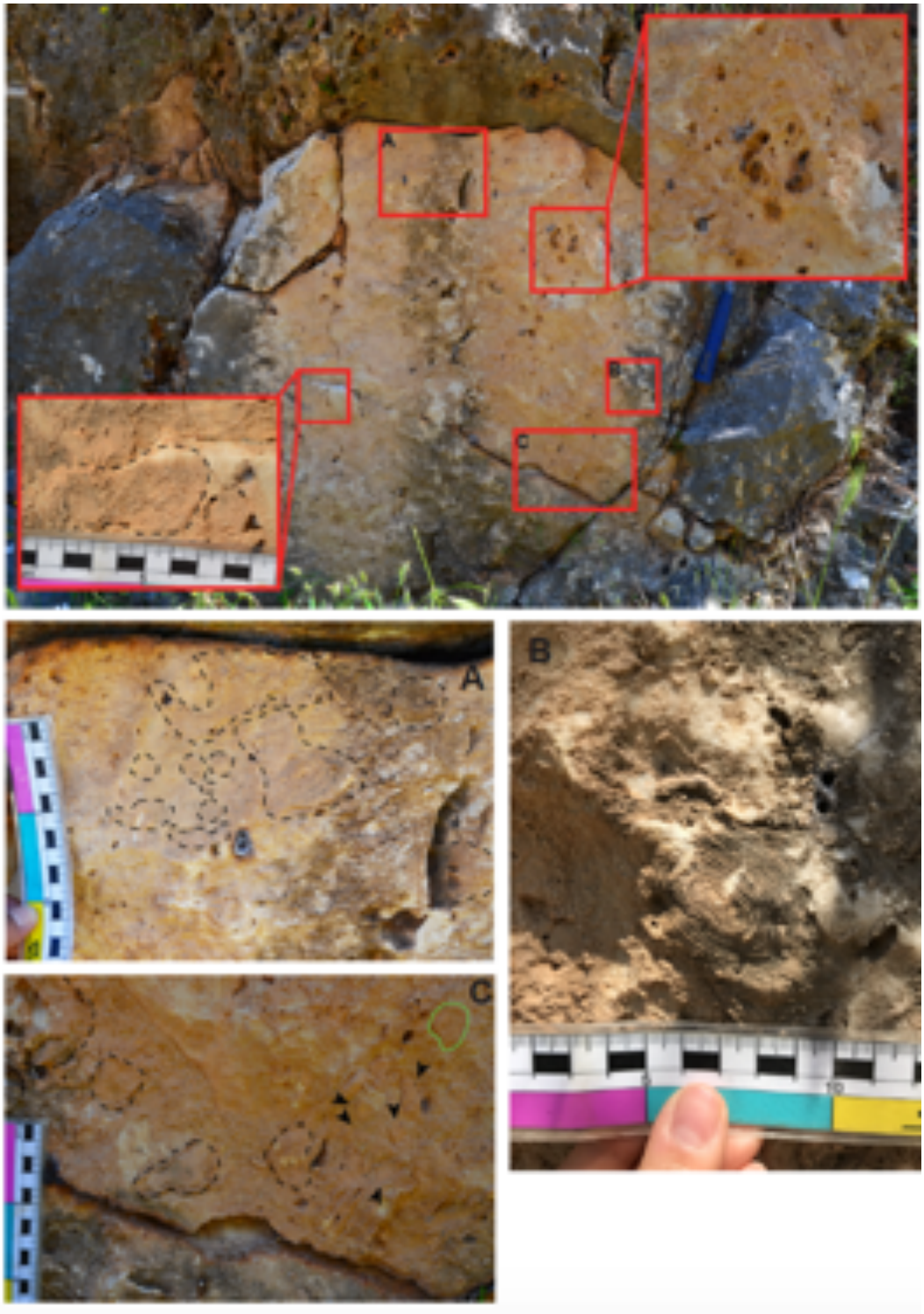

Figure. 2-14- The main components associated with outcrops 3. A: *in-situ* stromatoporoids in fine-grained matrix. B: cm-sized *Ellipsactinia* sp. showing bulbous growth form. C: stromatoporoids in growth position (*Ellipsactinia* sp. and

Sphaeractinia sp.). The dominat facies here is stromatoporoid-rich facies (LF1) with presence of two subfacies (LF1-S1, LF2-S2).

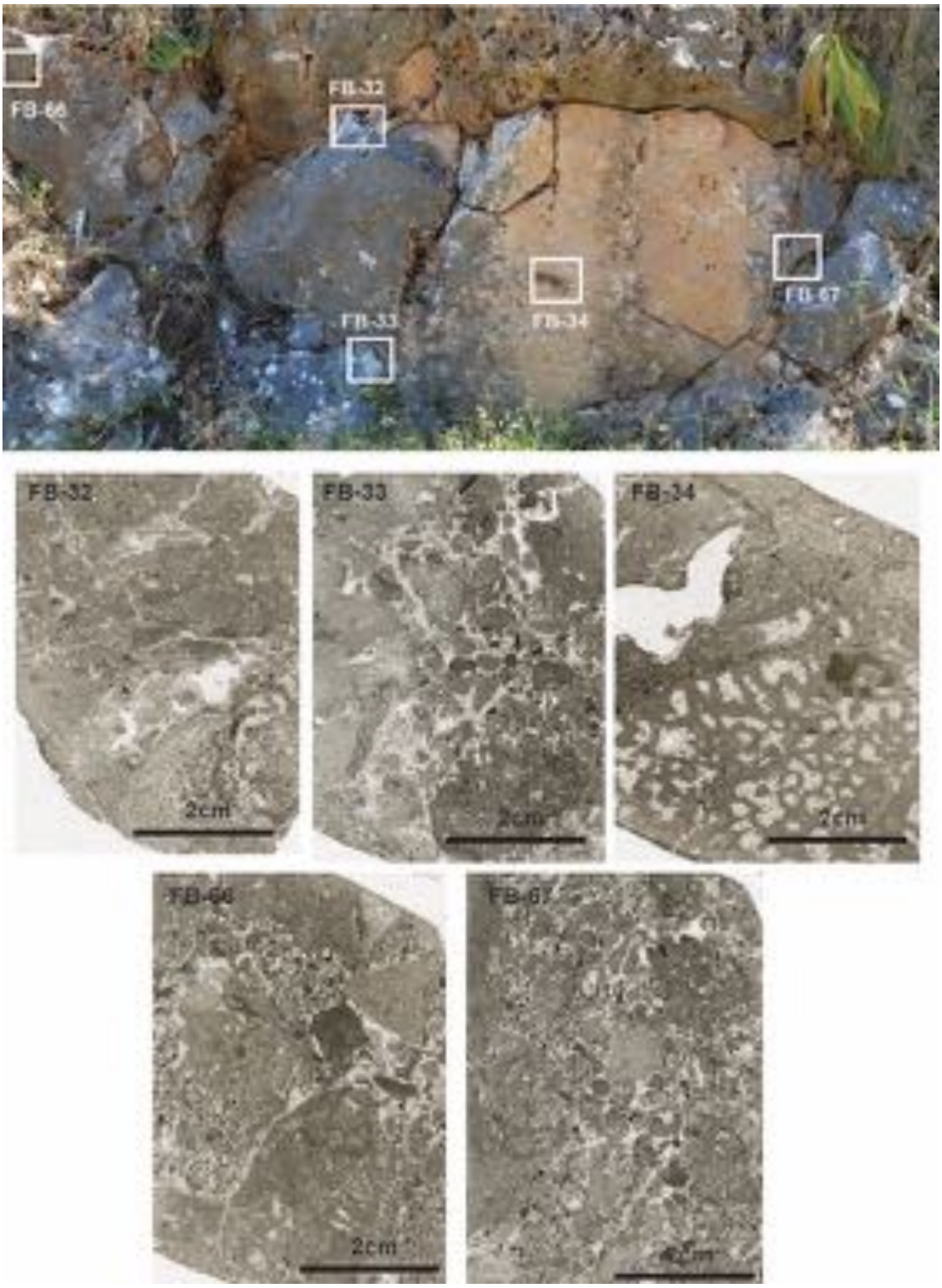

Figure. 2-15- Internal sediments which surrounded the stromatoporoids in outcrop 3. FB-32: fine-grained packstone, FB-33: intraclastic grainstone, FB-34: stromatoporoid clast associated with fine-grained packstone, FB-66: intraclastic

packstone to grainstone, FB-67: intraclastic packstone to grainstone. Thin sections refer to LF1 (Stromatoporoid-rich facies).

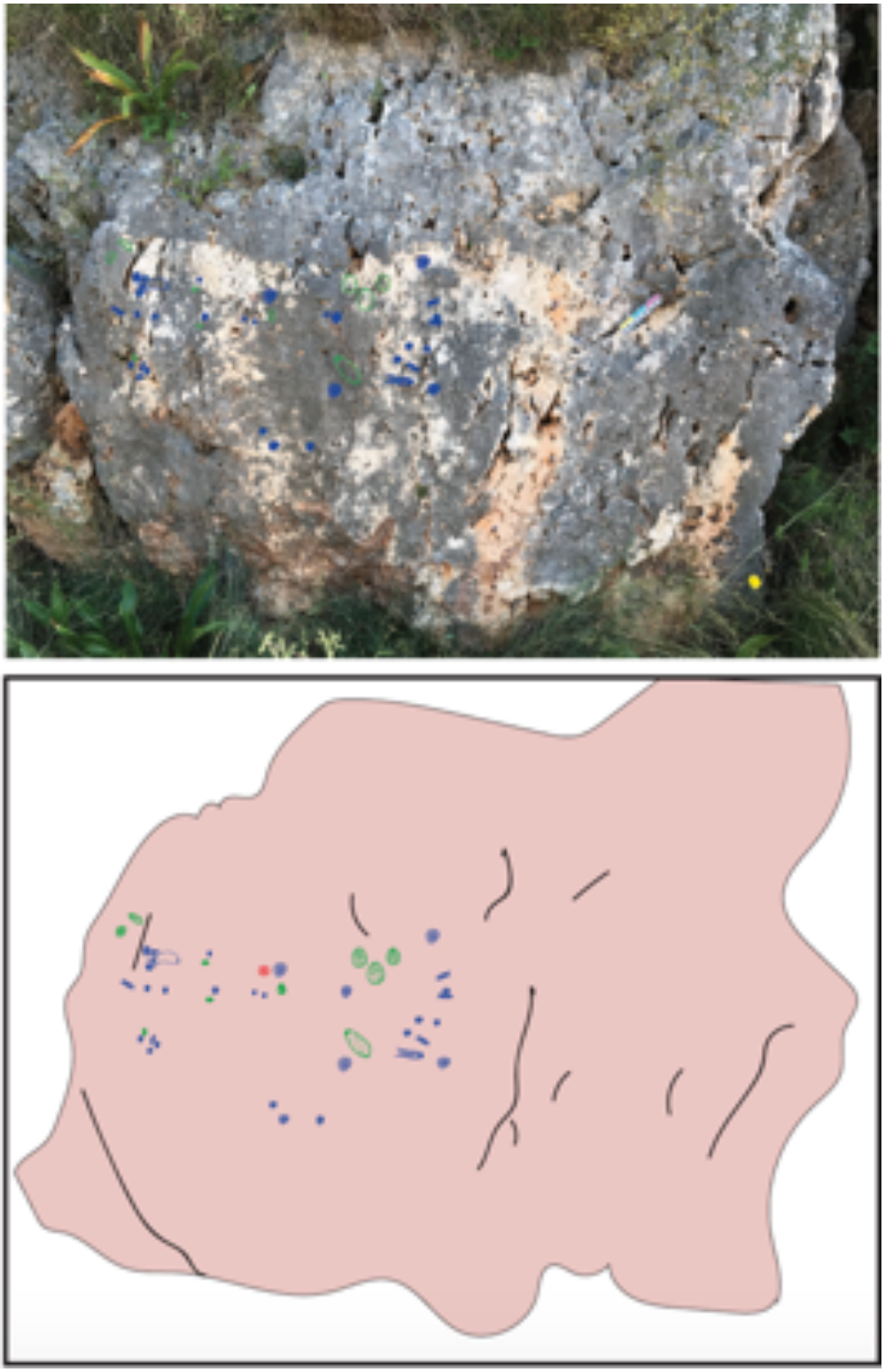

Figure. 2-16- Field description of outcrop 4 and its associated scheme showing the distribution of biota on the surface

of outcrop. Bottom image showing the simplified scheme of outcrop 4.

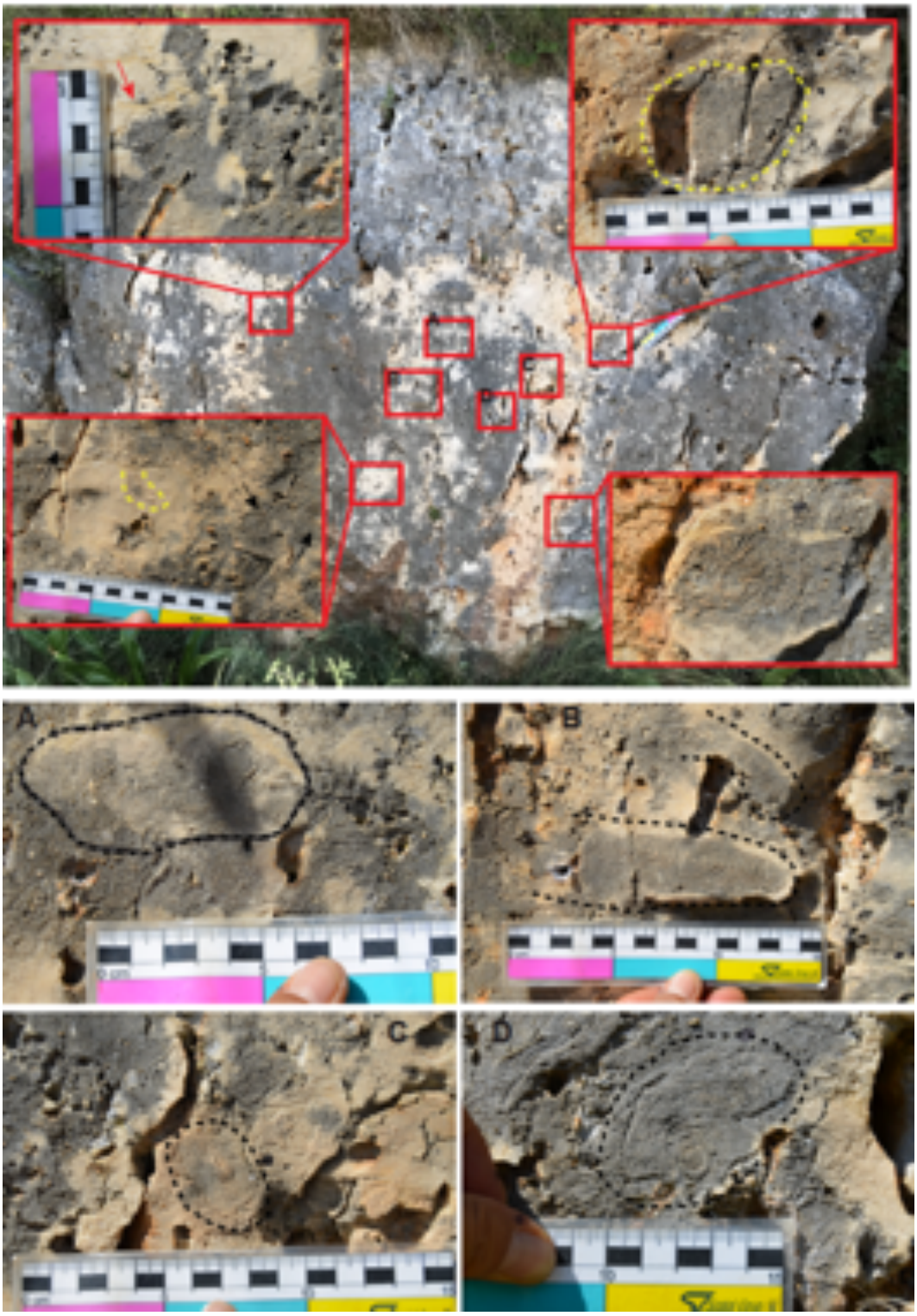

Figure. 2-17- Figures of different skeletal components (mainly stromatoporoid) associated with outcrop 4. A: Bulbouse shape *in-situ* stromatoporoid (*Sphaeractinia* sp.) B: *In-situ* columnar growth shape of *Sphaeractinia* sp. C

and D: cm-sized stromatoporoids (*Sphaeractinia* sp.). The main facies in this outcrop is stromatoporoid-rich facies (LF1).

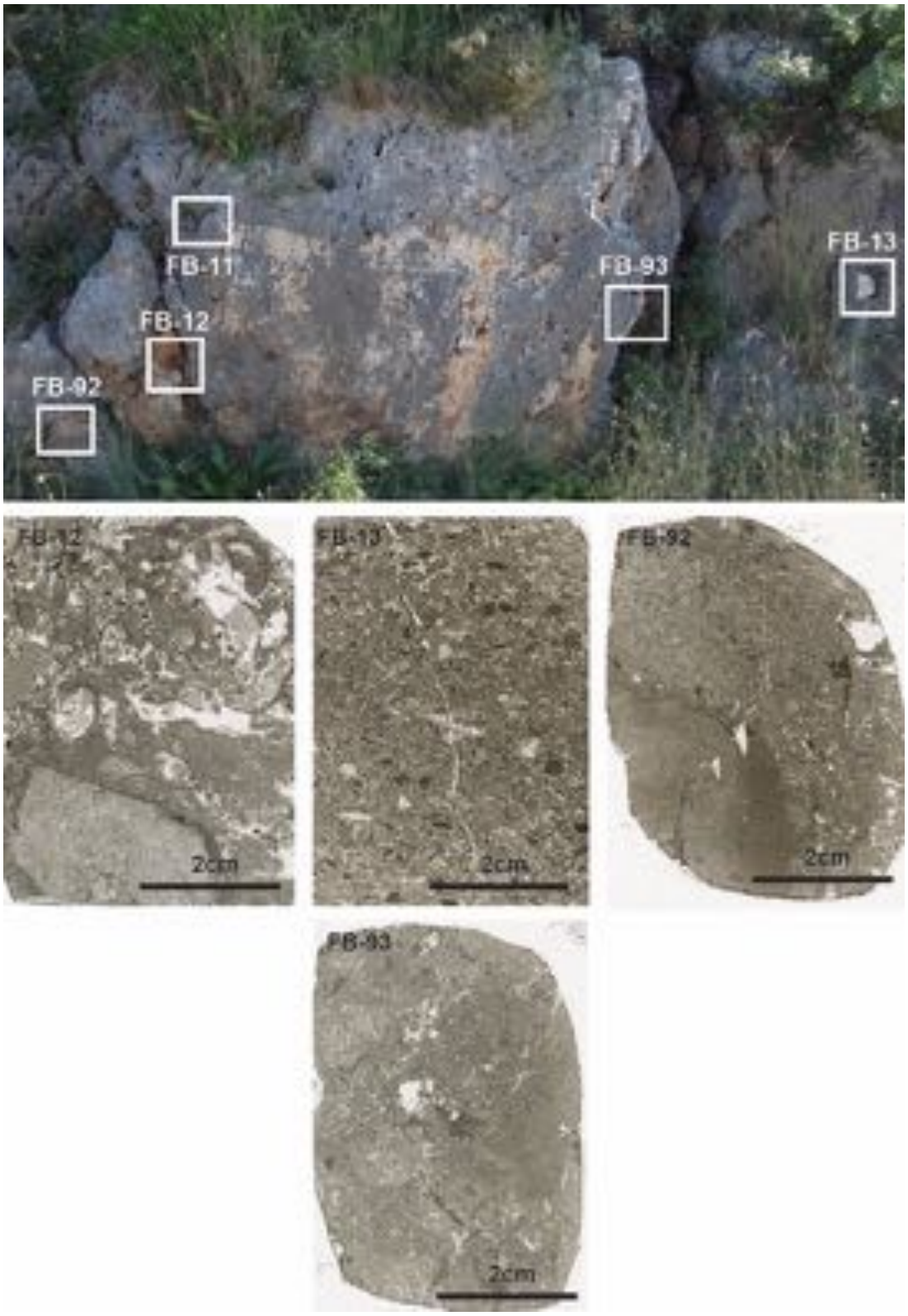

Figure. 2-18- Internal sediments which surrounded the skeletal components in outcrop 4. FB-12: intraclastic packstone

with cm-sized stromatoporoid clasts, FB-13: packstone with *Tubiphytes* grains, FB-92: wackestone to fine-grained packstone, FB-93: wackestone to fine-grained packstone.

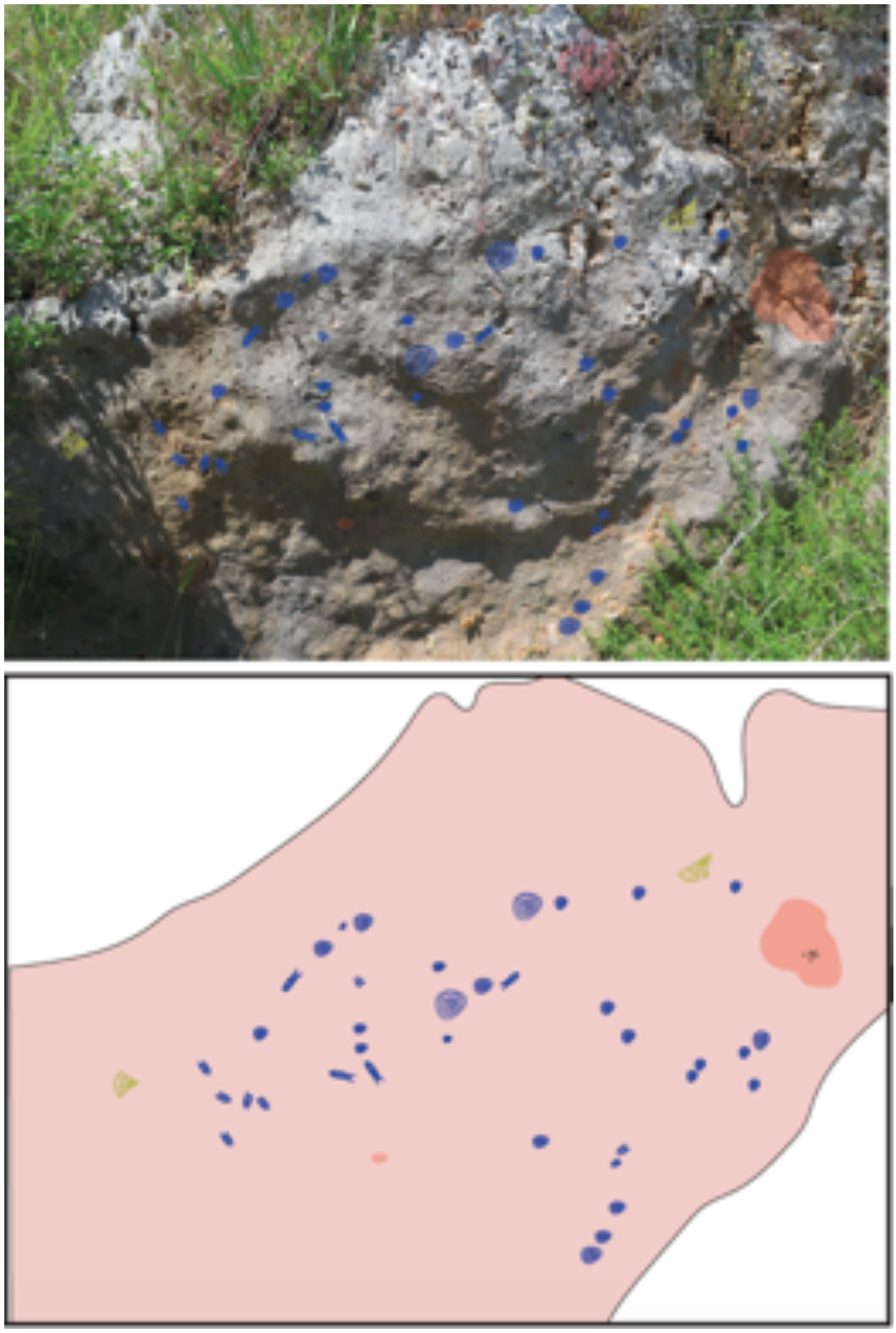

Figure. 2-19- Field description of outcrop 5 and its associated scheme showing the distribution of biota on the surface

of outcrop.

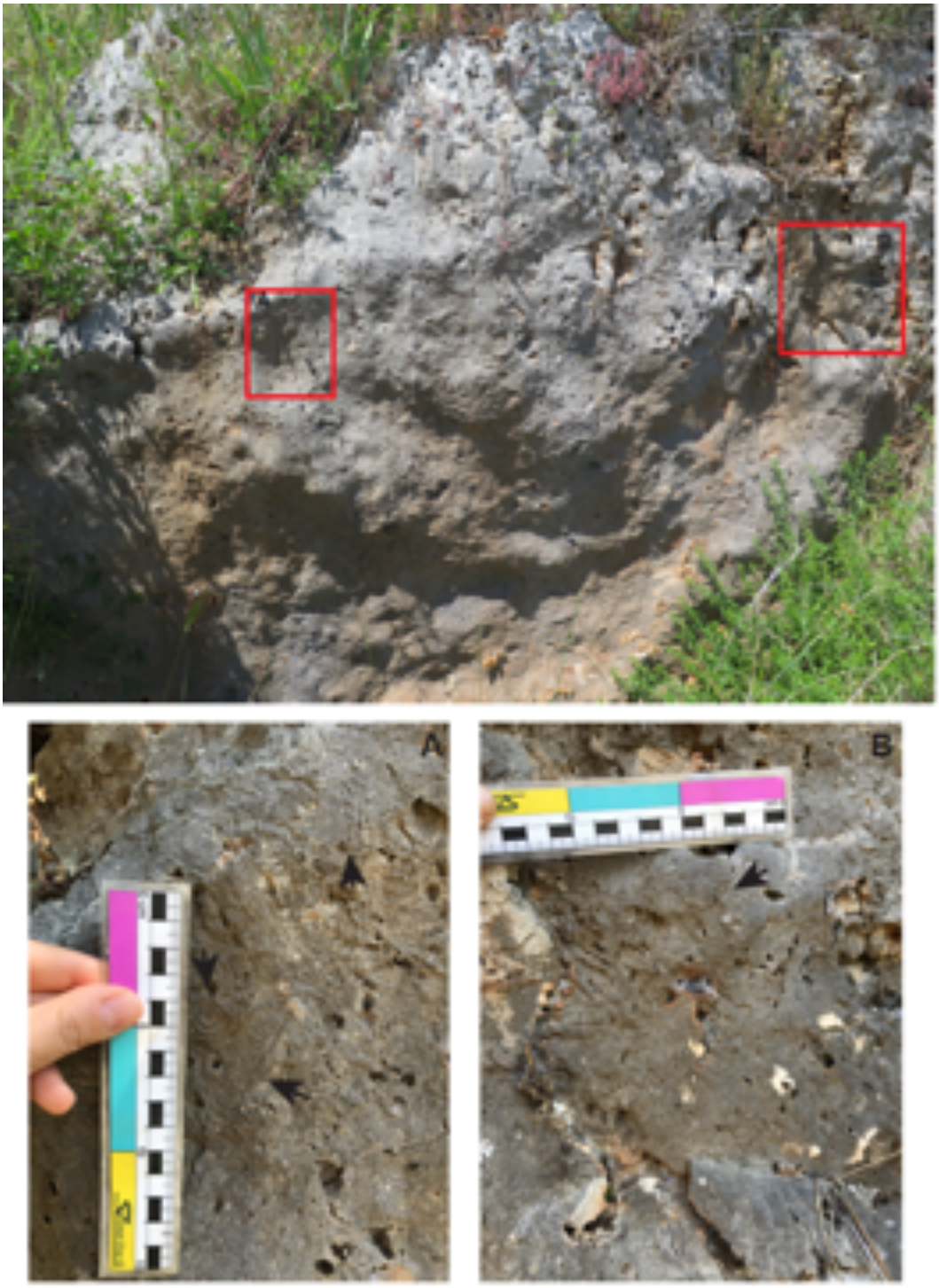

Figure. 2-20- Figures of different skeletal components associated with outcrop 5. A: a stromatoporoid in growth position (*Ellipsactinia* sp.), B: cm-sized coral colony

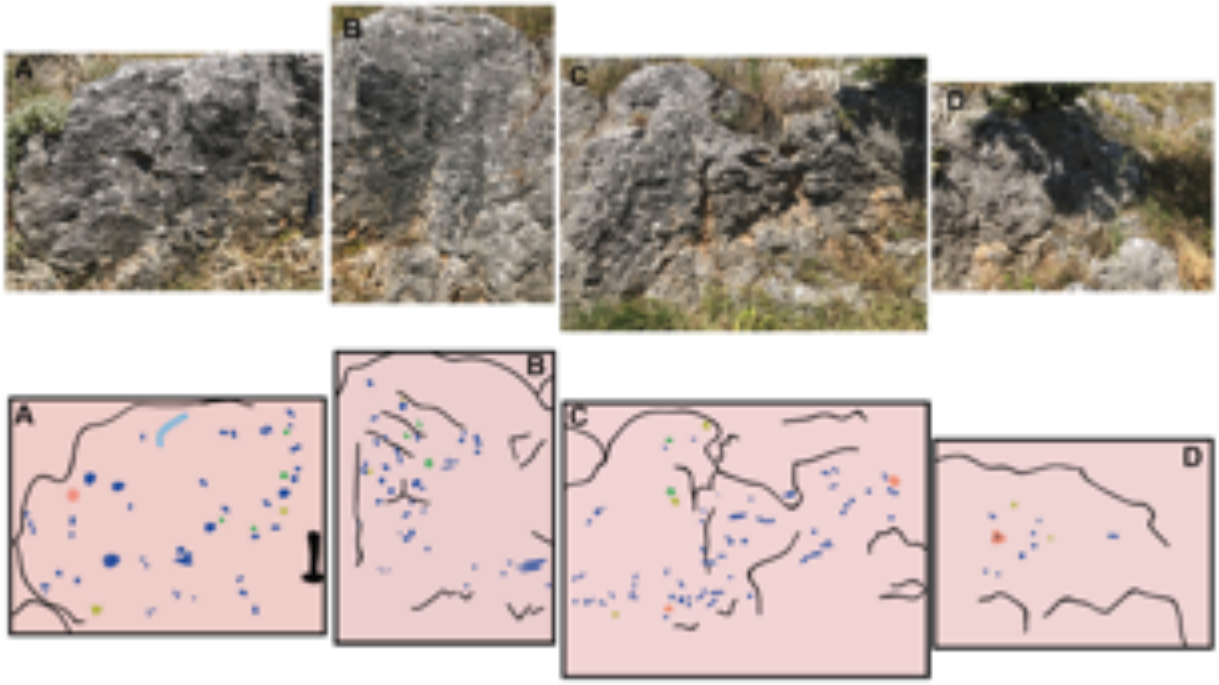

Figure. 2-21- Field description and related schemes of outcrop 6 and its associated scheme showing the distribution of biota on the surface of outcrop. The organism are mainly stromatoporoids, sponges and scatter small corals.

Figure. 2-22- Figures of different skeletal components associated with outcrop 6. A: stromatoporoid in growth position (bulbous form), B: un-defined skeletal components associated with other organisms, C: *Ellipsactinia* sp. The diameter of stromatoporoid reaches to 40 cm, D: cm-sized *in-situ* coral colony. The facies is associated with LF1 (stromatoporoid-rich facies).

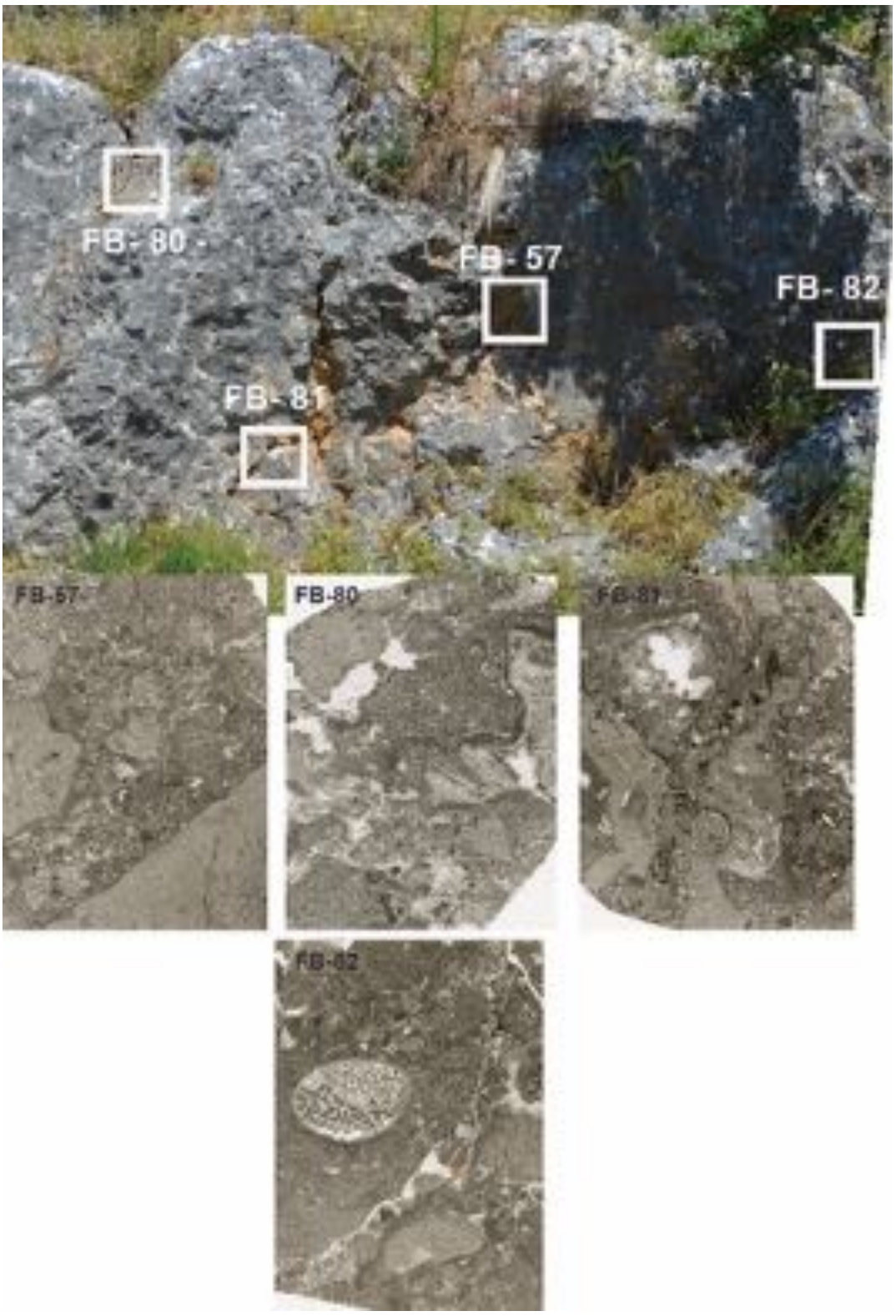

Figure. 2-23- - Internal sediments texture surrounded the skeletal components in outcrop 6. FB-57: intraclastic packstone with cm-sized clasts, FB-80: intraclastic packstone, FB-80: a packstone with abundant encrusting organisms inside the matrix. FB-82: stromatoporoid surrounded by intraclastic packstone. The thin sections are representing the

LF1 facies (stromatoporoid-rich facies).

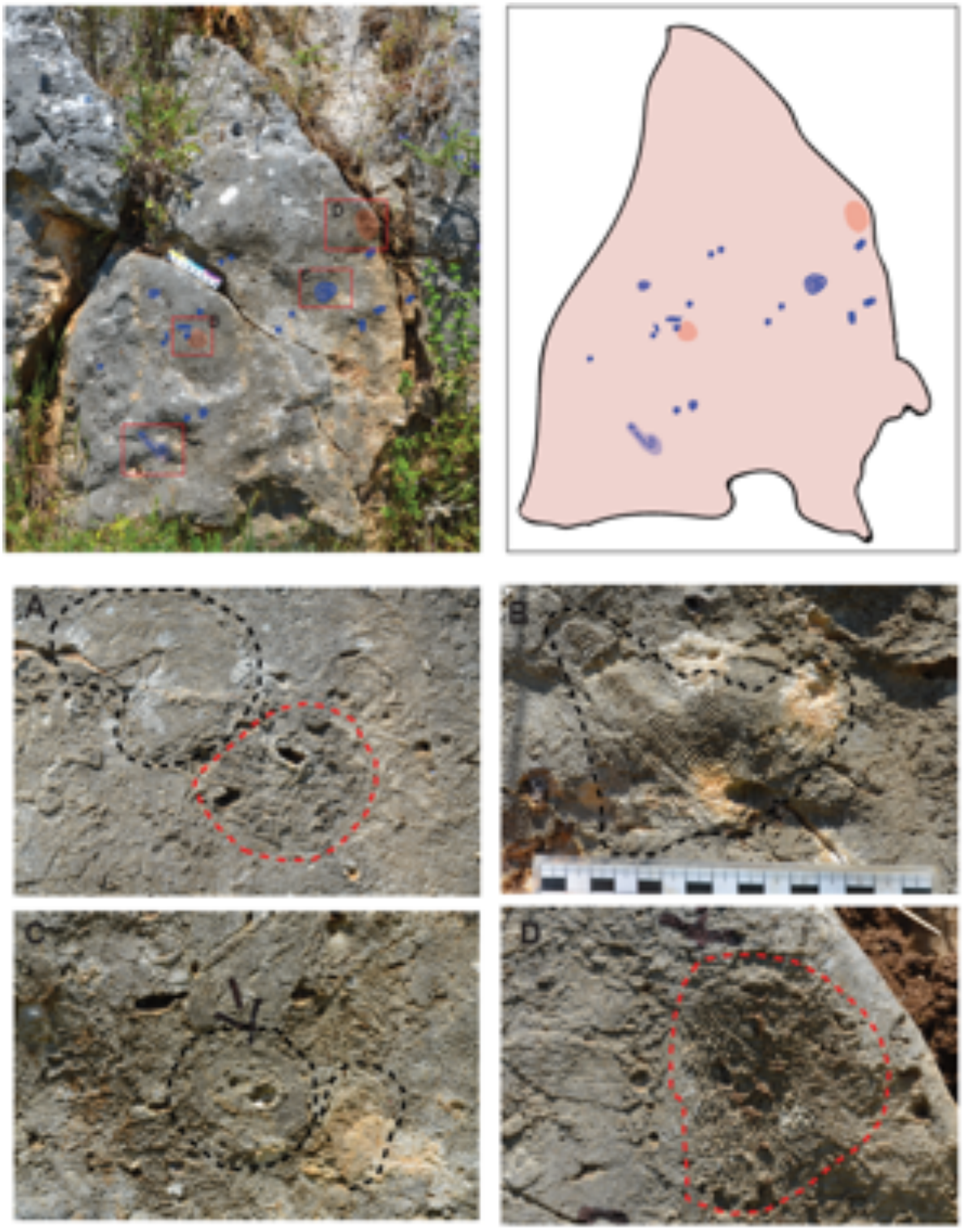

Figure. 2-24- Field description and related scheme of outcrop 6a showing the distribution of biota on the surface of outcrop. A-C: Different skeletal components associated with outcrop 6a. A: *Sphaeractinia* sp. in growth position. B: *Ellipsactinia* sp. showing thick branching morphology. C: un-defined organisms (stromatoporoids?). D: branching

stromatoporoid ? or Chaetetids?

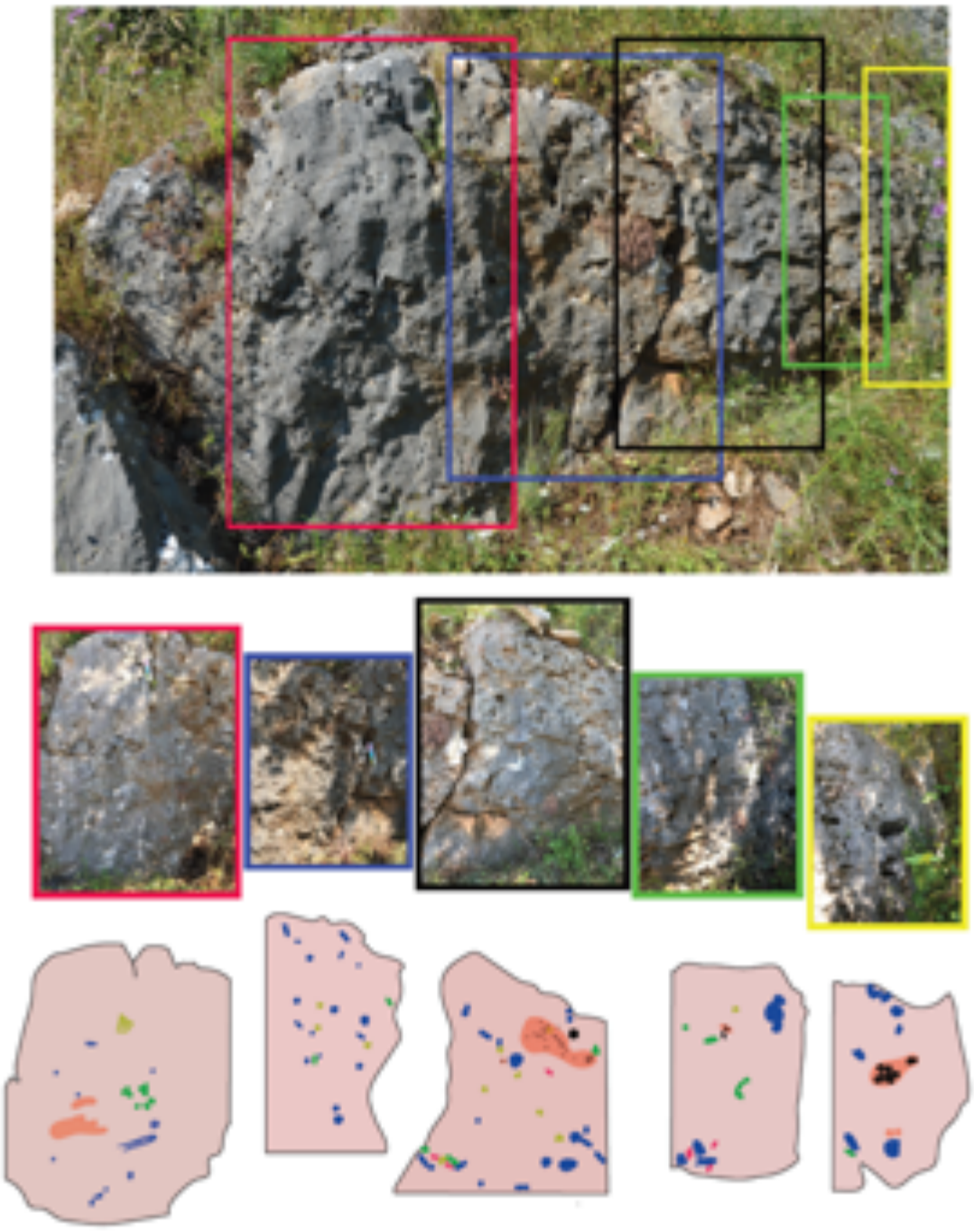

Figure. 2-25- Field description and related schemes of outcrop 7 showing the distribution of biota on the surface of outcrop. The organism are mainly stromatoporoids, sponges, echinoids and scatter small corals.

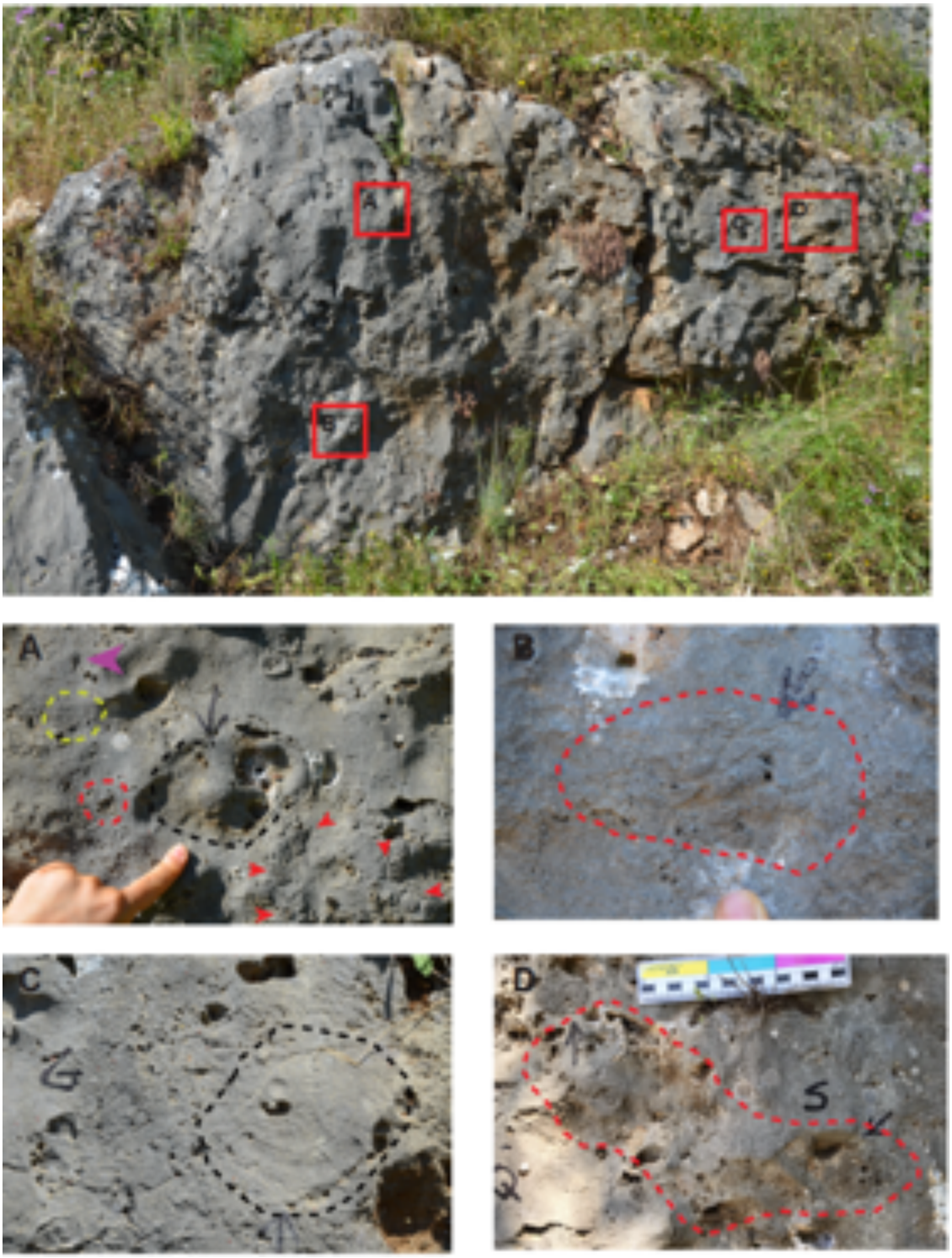

Figure. 2-26- Different skeletal components associated with outcrop 7. A, B, D: cm-sized coral colonies assosoated with stroamtoporoids. C: stromatoporoid (*Sphaeractinia* sp.) fragment.

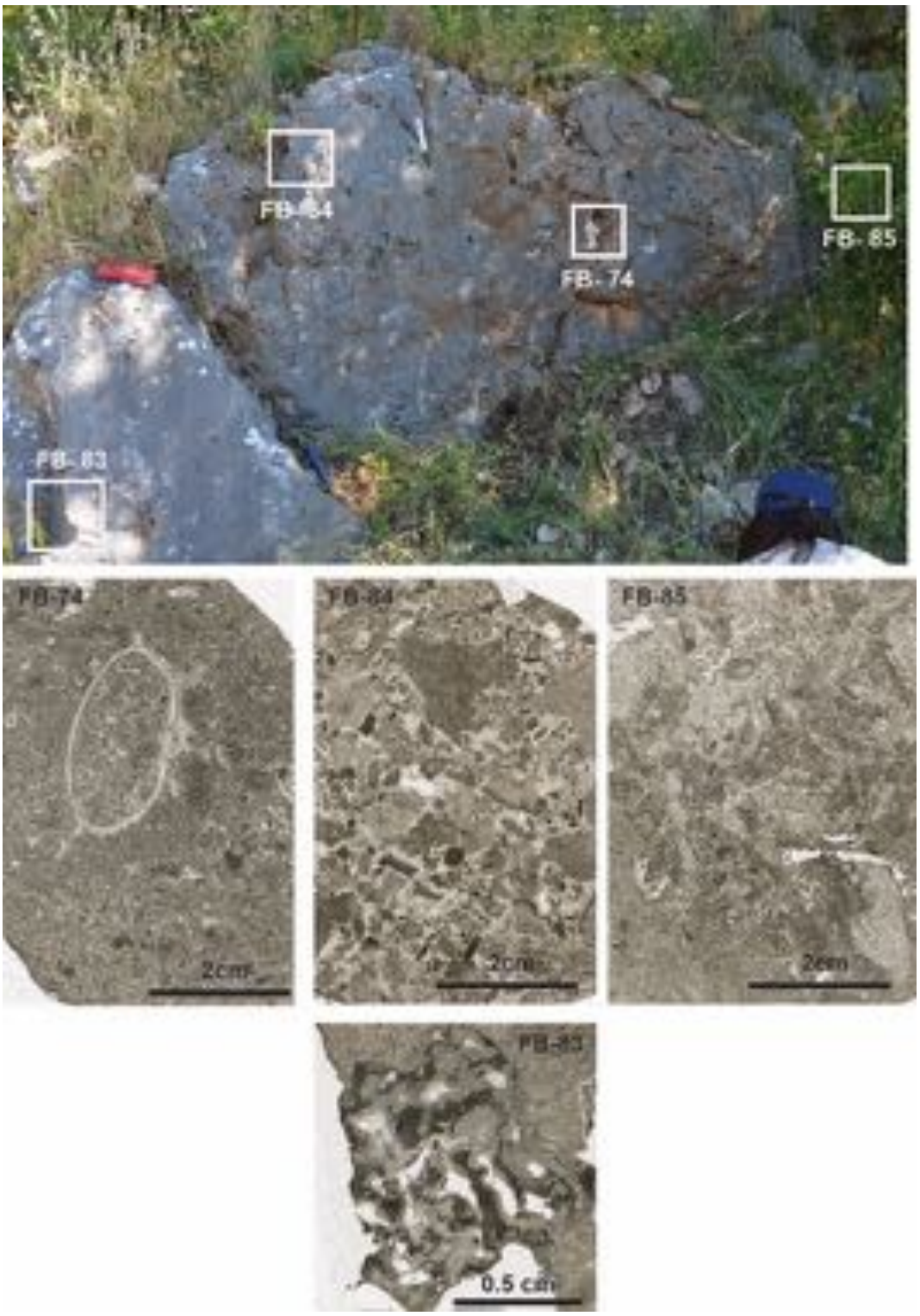

Figure. 2-27- Internal sediments texture surrounded the skeletal components in outcrop 7. FB-74: skeletal packstone, FB-84: intraclastic grainstone, FB-85: intraclastic packstone, FB-83: wackestone matri with stromatoporoid associated with *Tubiphytes* sp.

2-4-2-Torre Mileto and Monte d'Ellio section

Two outcrop have been studied in sea-cliff and road-cut located in Torre Mileto area and Monte d'Ellio section (Fig.2-28). These outcrops characterized by small massive outcrops (~ 2 m^2) and composed of stromatoporoids, sponges and echinoids distributed in matrix. Figure 2-29 showing the main components distributed on surface of outcrops 10 (Torre Mileto) and their internal sediments are shown in figure 2-30. The figures 2-31 and 2-32 is related to the MSL outcop exposed in Monte d'Ellio section.

Figure. 2-28- Studied MSL outcrops along in Torre Mileto and Monte d'Ellio sections. The outcrops are arranged in massive limestones and they are characterized by stromatoporoid-rich facies. Outcrop 10 and outcrop 13 consist of stromatoporoid-rich facies (LF2).

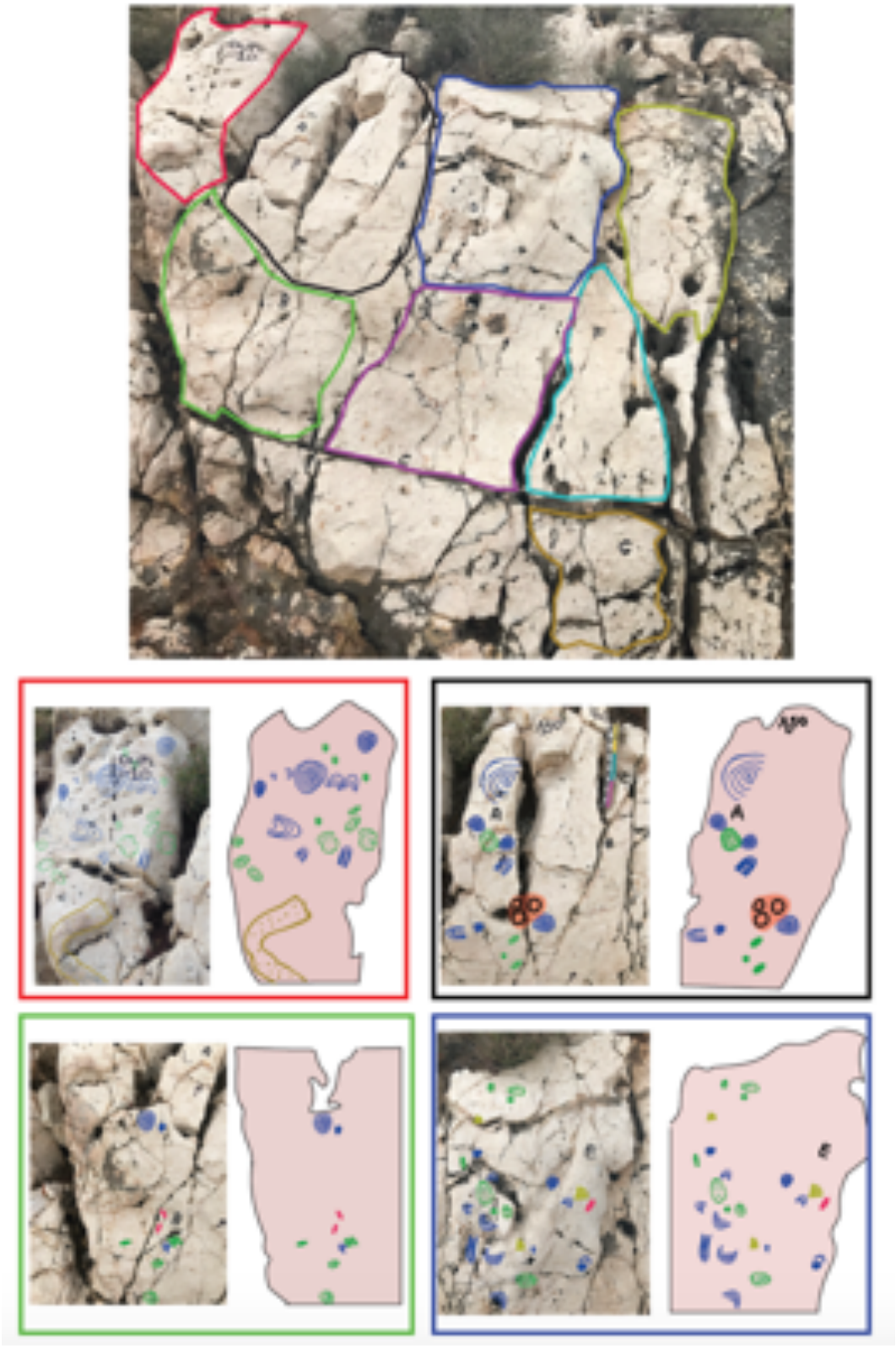

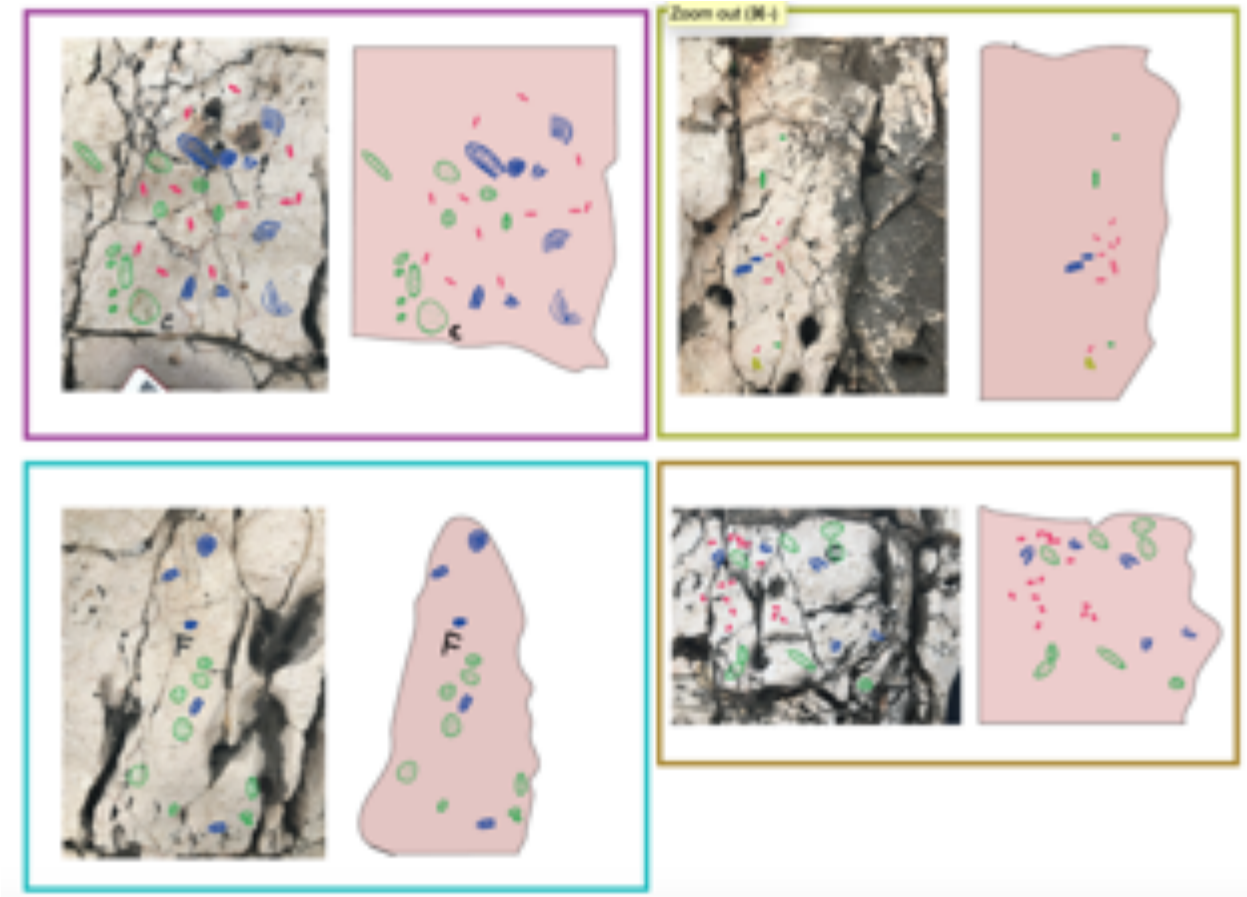

Figure. 2-29- Field description and related schemes of outcrop 10 (Torre Mileto) showing the distribution of biota on the surface of outcrop. The organism are mainly stromatoporoids, sponges, echinoids and scatter small corals.

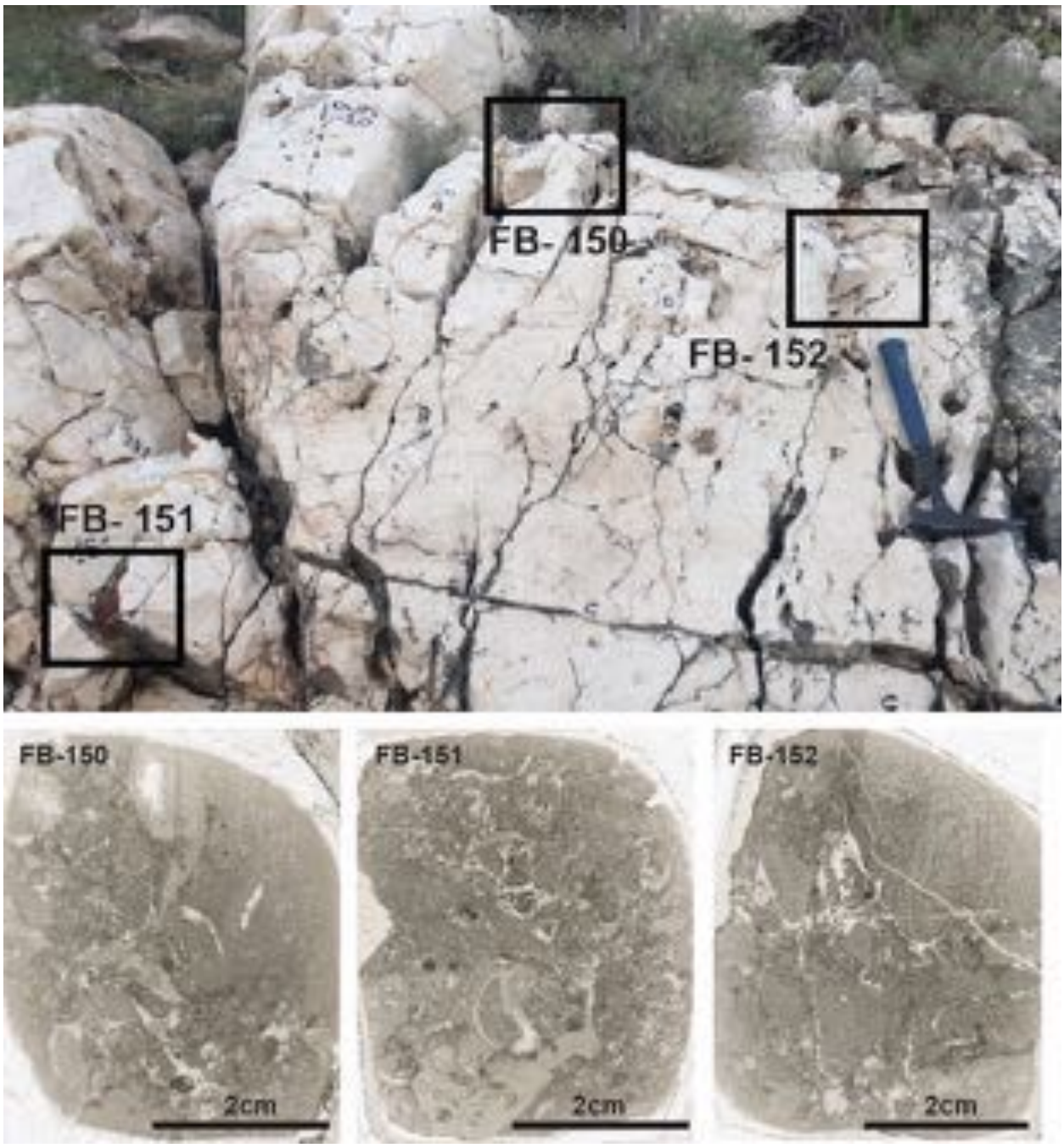

Figure. 2-30- Internal sediments texture surrounded the skeletal components in outcrop 10. FB-150: intraclastic packstone, FB-151: intraclastic packstone, FB-152: intraclastic-bioclastic packstone with cm-sized stromatoporoid clast. The thin sections are representing by LF2 (stromatoporoid-rich facies).

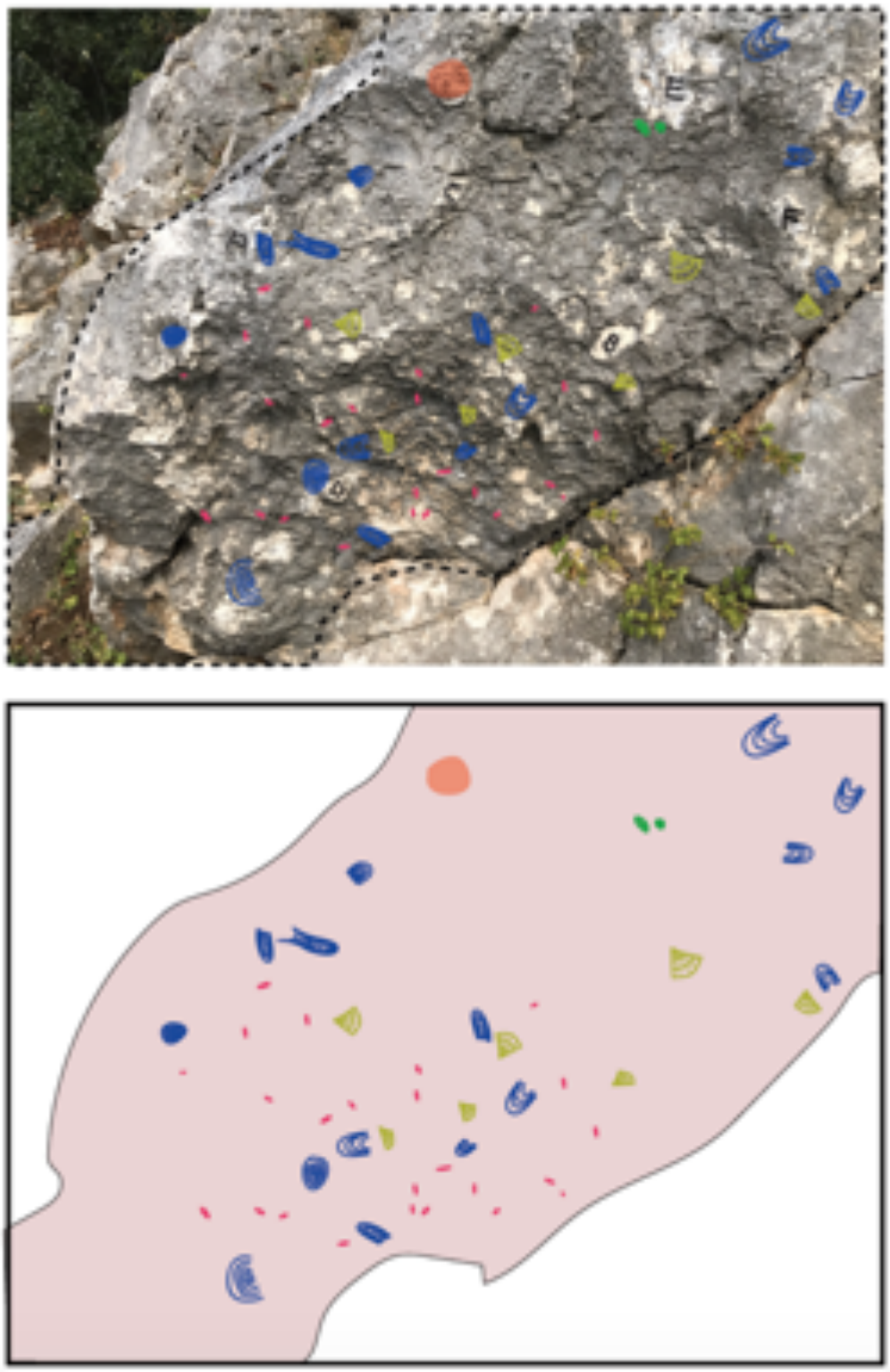

Figure. 2-31- Field description of outcrop 13 (Monte d'Ellio) and its associated scheme showing the distribution of biota on the surface of outcrop. The organisms are mainly composed of stromatoporoids, sponges and echinoid spines.

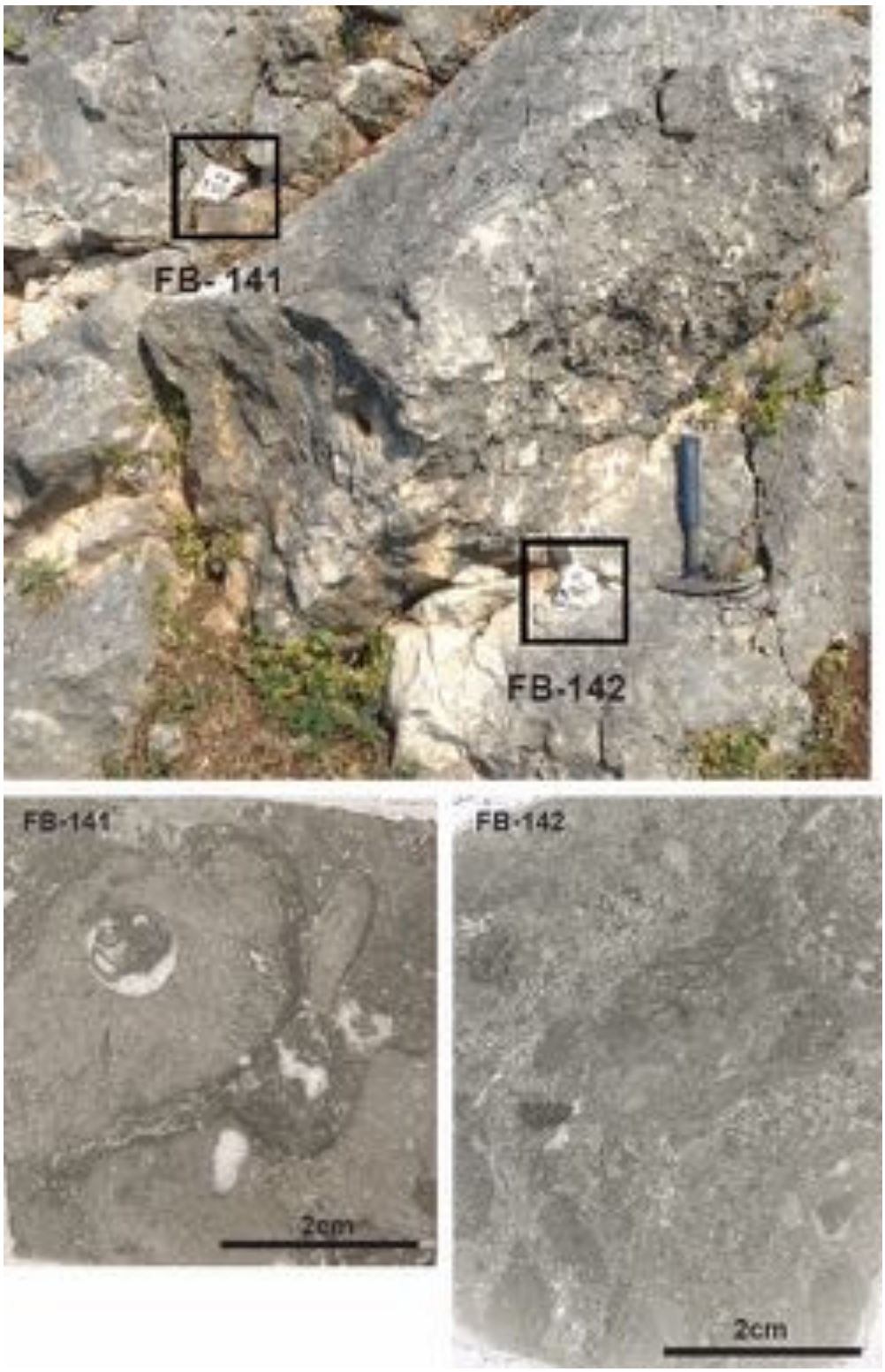

Figure. 2-32- Internal sediments texture surrounded the skeletal components in outcrop 13. FB-141: corals fragments distributed in wackestone to fine-grained packstone matrix, the corals are encrusted by *Tubiphytes* sp. and associated by bioerosion traces. FB-142: intraclastic packstone.

2-4-3- Masseria Prencipe

Small-sized outcrops from MSL exposed in Masseria Prencipe area of Gargano. These outcrops has been studied and sampled in order to describe the skeletal biota and lithofacies (Fig. 2-33). In the lower part of Masseria Prencipe three outcrops have been studied (Figs. 2-35 until 2-39). The studied outcrops are characterized by tabular form stromatoporoids associated with corals. The stromatoporoids in outcrop 17 shows *in-situ* form (Fig. 2-40).

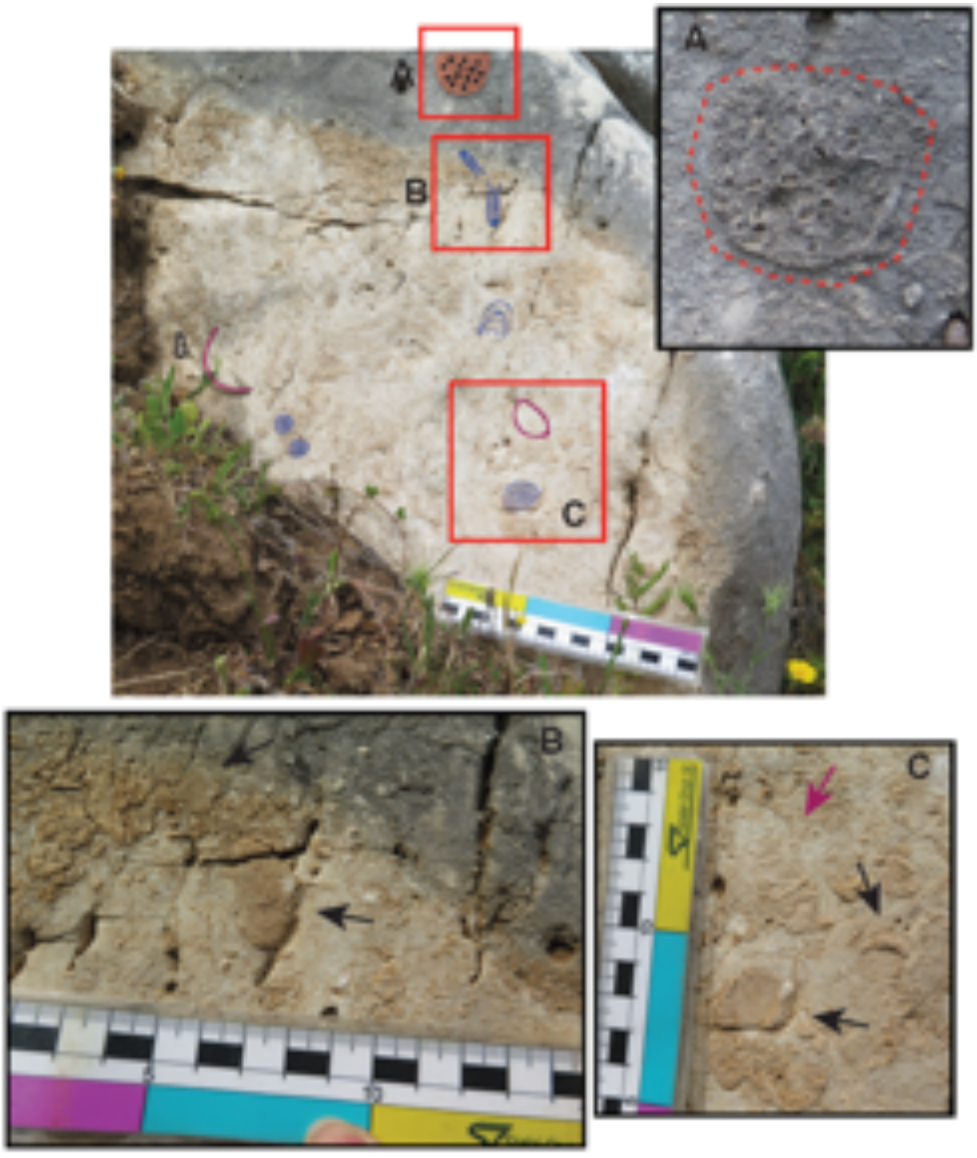

Figure. 33-2- - Different skeletal components associated with outcrop 18. The main components are stromatoporoids, bivalves and small corals. A: small-sized coral colony? B: cm-sized stromatoporid (*Ellipsactinia* sp.) black arrow. C: fragments of bivalve shell (purple arrow).

Figure. 2-34- Studied MSL outcrops along in Masseria Prencipe sections. The outcrops are arranged in massive limestones and they are characterized by tabular stromatoporoids associated with corals.

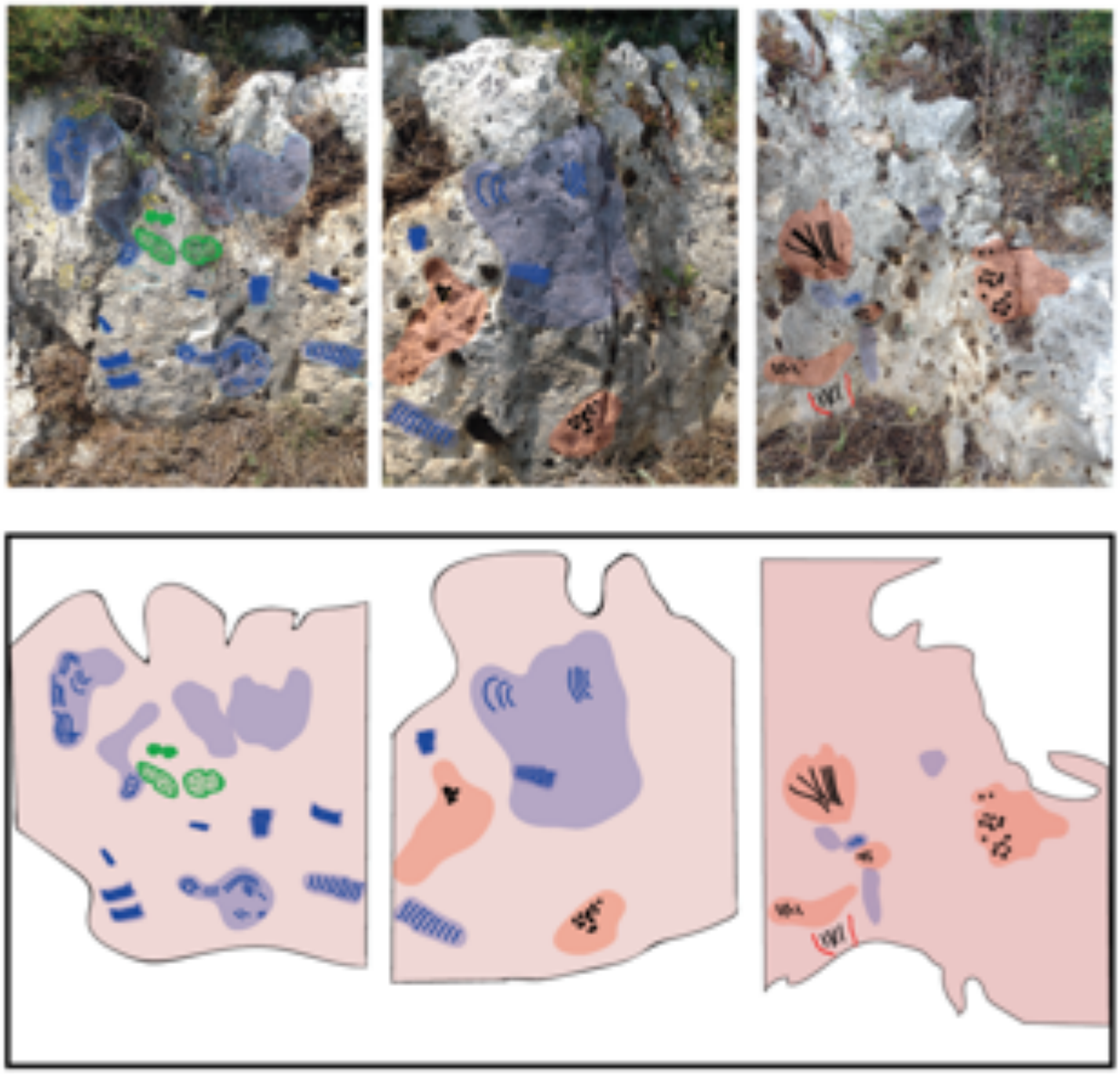

Figure.2-35- Field description and related schemes of outcrop 16 (Masseria Prencipe) showing the distribution of biota on the surface of outcrop. The organism are mainly fragments of tabular stromatoporoids, sponges, echinoids and small isolated corals colonies.

Figure. 2-36- Different skeletal components associated with outcrop 16. A: fragments of tabular stromatoporoids, B: fragments of tabular stromatoporoids, C: small coral colony associated with stromatoporoids.

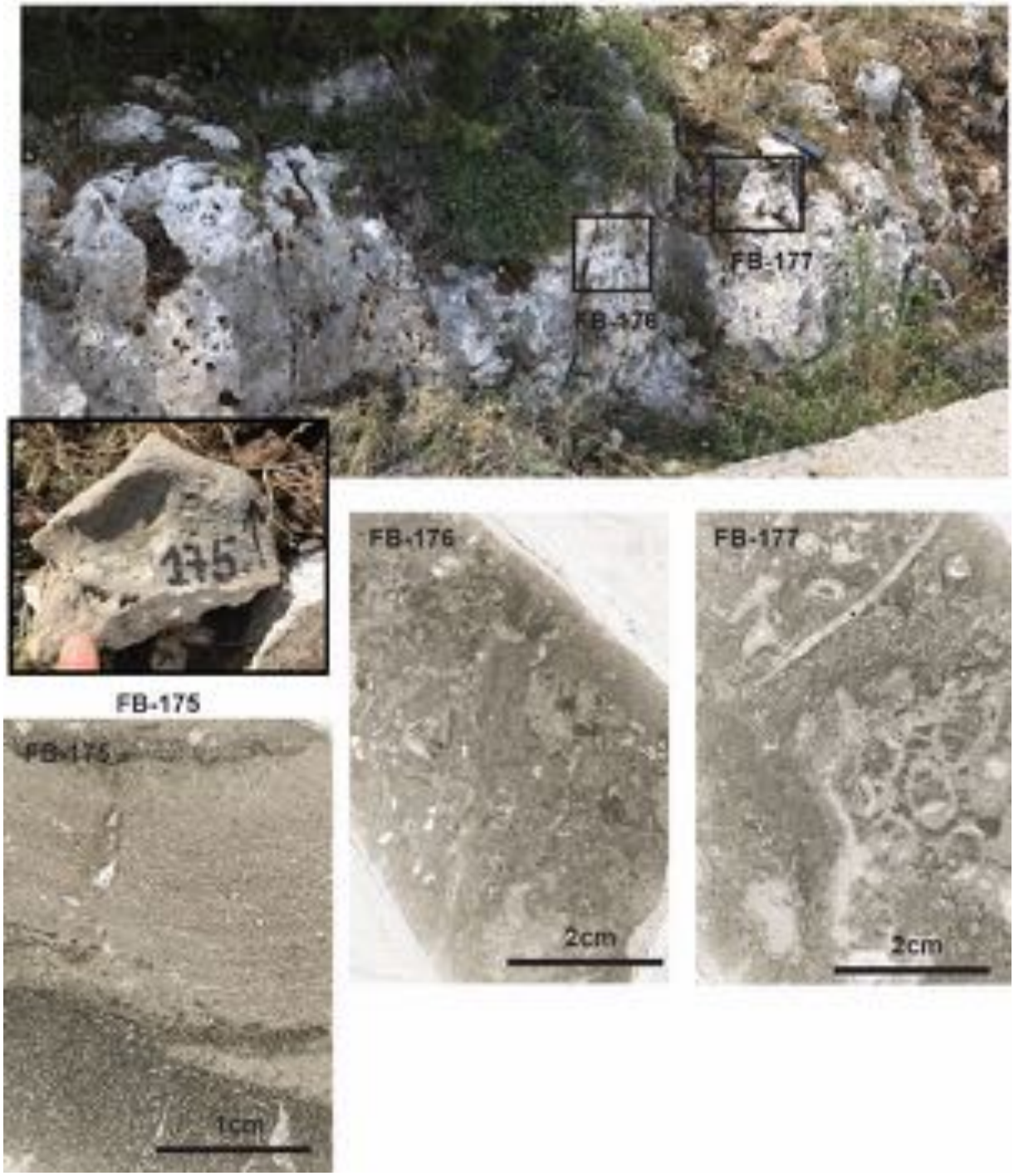

Figure. 2-37- Internal sediments texture surrounded the tabular stromatoporoids and corals in outcrop 16. FB-175: tabular stromatoporoid associated with a wackestone matrix rich in radiolarian. FB-176: wackestone to fine-grained packstone matrix, FB-177: un-defined sponge surrounded by fine-grained packstone matrix.

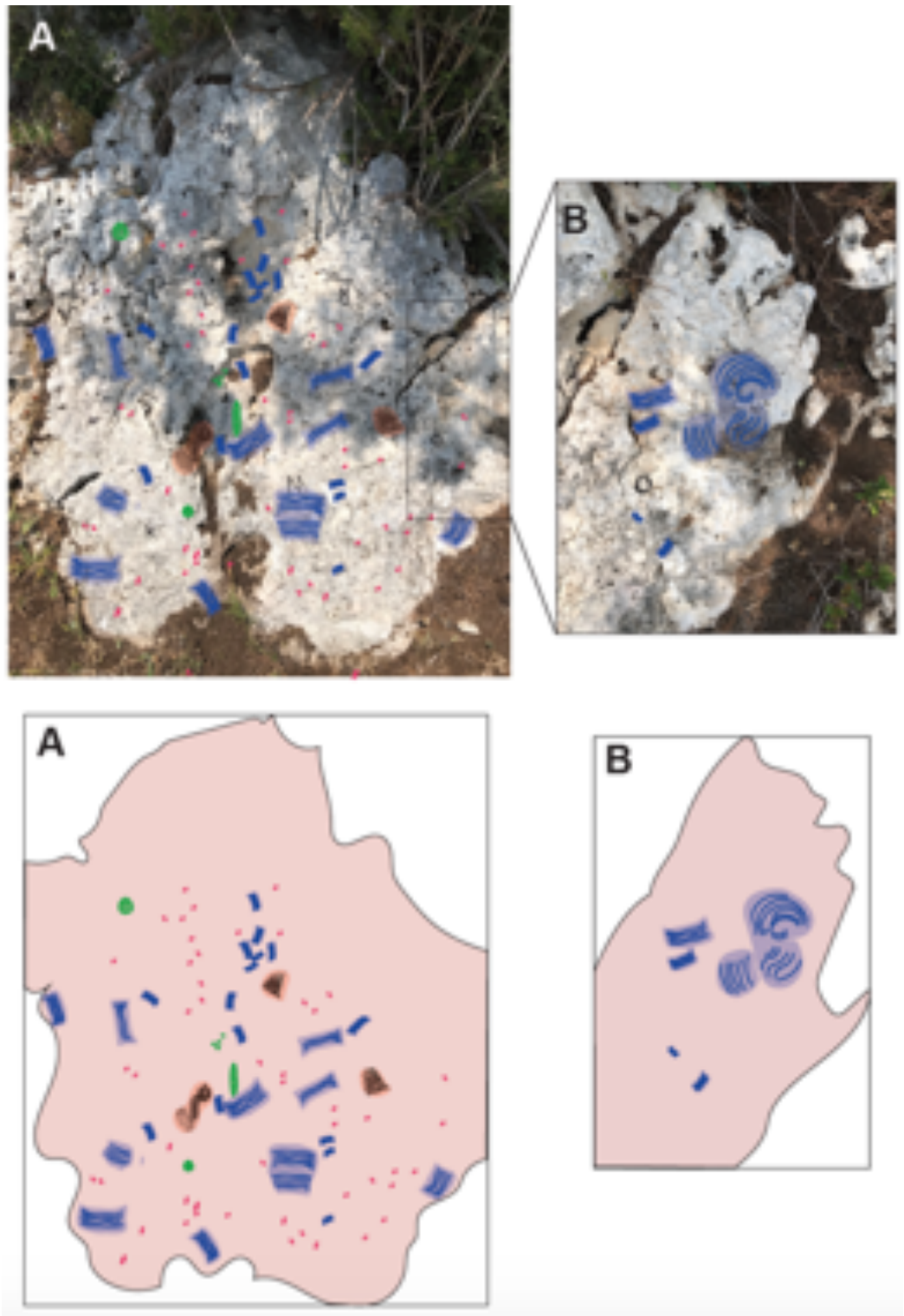

Figure. 2-38- Field description and related schemes of outcrop 16 (Masseria Prencipe) showing the distribution of biota on the surface of outcrop. The organism are mainly fragments of tabular stromatoporoids, sponges, echinoids and small isolated corals colonies.

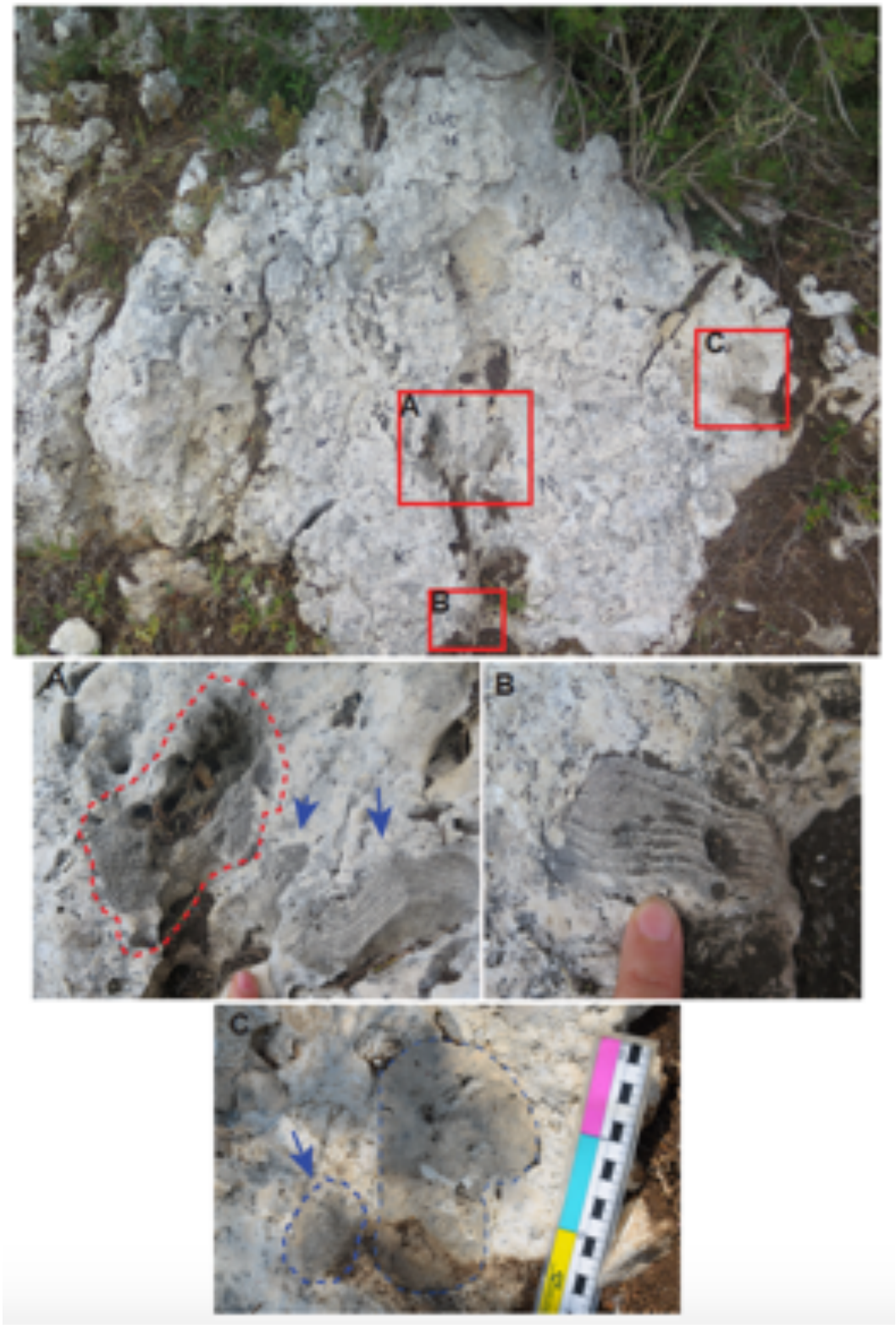

Figure. 2-39- Different skeletal components associated with outcrop 15. A: fragment of coral (red circle) associated with fragments of tabular stromatoporoid (blue arrows), B: fragment of tabular stromatoporoid, C: cm-sized fragment of tabular stromatoporoids (blue arrows).

Figure. 2-40- Tabular stroamtoporoid colony in life position (with related scheme) showing laminar growth form (outcrop 17).

2-5- Results and interpretation

2-5-1- Facies description

On the basis of the lithology, rock texture, and components, three main lithofacies and four subfacies have been distinguished (Table2-1): LF1- stromatoporoid-rich facies (LF1-S1: floatstone with wackestone to fine-grained packstone, LF1-S2: rudstone to floatstone with intraclastic- bioclastic packstone-grainstone matrix), LF2- stromatoporoid- coral facies (LF2-S1: floatstone with wackestone to packstone matrix, LF2-S2: tabular stromatoporoids and coral with wackestone matrix), and 3- stromatoporoid- microbial facies (LF3). All lithofacies (LF1, LF2, LF3) can be recognized in Monte di Mezzo section where the lateral facies changes are visible (Fig. 2-41A). LF1 are the most exposed lithofacies (~ 1.2 km long) passes gradually to LF2 and basin-ward to LF3. Vertically, the stromatoporoid-rich facies (LF1) is the only lithofacies observed along the stratigraphic log (Fig. 2-41B). The LF1 is also recognized in small outcrops (~ 2 m^2) in Torre Mileto. The distribution of subfacies LF1-S1 and LF1-S2 on the surface of outcrops show a chaotic organization with sharp boundaries (Fig. 2-41C, D). In the vertical position, the LF1-S2 represented by rudstone- floatstone with intraclastic packstone to grainstone matrix, is developed at the base of the section while floatstone with wackestone to fine-grained packestone (LF1-S1) associated

with *in-situ* stromatoporoids is more abundant at the top of section (Fig. 2-41B). stromatoporoid-coral facies (LF2) composed of cm to m- thick massive limestones exposed in Monte di Mezzo (LF2-S1) (Fig. 2-42A) and Masseria Prencipe (LF2-S2) (Fig. 2-42B). Stromatoporoid-microbial facies (LF3) recognized only in Monte di Mezzo section and characterized by m- thick massive limestones (Fig. 2-42C). The distribution of different lithofacies along the studied area shows that LF1 is the most abundant lithofacies (87.2%) followed by LF2 (11%) and LF1 (1.8 %) (Fig. 2-43A). In LF1, the debris-rich rudstone-floatstone (LF1-S2) is more frequent (62.7 %) than LF1-S1 (37.3 %) (Fig. 2-43B).

Table. 2-1- Summary of facies associations, with texture and main components, and environmental interpretation of each lithofacies.

Facies	Main component	Minor components	interpretation	locality
Stromatoporoid-rich facies (LF1)	stromatoporoids, minor corals, sponge-like organisms, chaetetids? and echinoid spines		Mix of low and high-energy facies	Monte di Mezzo, Torre Mileto,
stromatoporoid floatstone with wackestone to fine-grained packstone matrix (LF1-S1)	*In-situ* stromatoporoids (*Sphaeractinia* sp. and *Ellipsactinia* sp.)	rare intraclasts as well as rare skeletal grains including bivalves, bryozoans and echinoids, *Tubiphytes-Crescentiella*	Low-energy	Monte di Mezzo, Torre Mileto
rudstone to floatstone with intraclastic-bioclastic packstone to grainstone matrix (LF1-S2)	cm to dm-sized intraclasts and fragments of stromatoporoids (*Sphaeractinia* sp. and *Ellipsactinia* sp.) and corals (phaceloid corals) encrusted by *Tubiphytes-Crescentiella)*	bivalves, brachiopods, benthic foraminifersand echinoids fragments of micro-encrusters such as *Tubiphytes-Crescentiella*, *Radiomura cautica*, *Uvanella*?	High-energy	Monte di Mezzo, Torre Mileto
Stromatoporoid-coral facies (LF2)	Stromatoporoids and corals			Monte di Mezzo, Masseria Prencipe
Stromatoporoid and coral floated in a wackestone to packstone matrix (LF2-S1)	In-situ stromatoporoids (*Sphaeractinia* sp. and *Ellipsactinia* sp.) and phaceloid	debris of echinoids, bivalves and gastropods and some pelagic components such as *Saccocoma* sp. fragments of *Tubiphytes-Crescentiella*	Low to moderate energy	Monte di Mezzo

	corals in growth position, *Tubiphytes-Crescentiella*			
Tabular stromatoporoids and corals associated with wackestone matrix (LF2-S2)	*In-situ* tabular stromatoporoids and cm-sized *In-situ* phaceloid corals	Radiolarians in matrix	Low-energy	Masseria Prencipe
Stromatoporoid-microbial facies (LF3)	*in-situ* stromatoporoids (*Sphaeractinia* sp. and *Ellipsactinia* sp. *Cylicopsis* sp. ?) dm-sized of stromatolite-like organism sponge-like organisms and echinoid spines	Fragment of gastropods, foraminifers and micro-encrusters such as *Tubiphytes-Crescentiella* and *Radiomura cautica*	Low-energy	Monte di Mezzo

2-5-1-1- Stromatoporoid-rich facies (LF1)

In this facies the main biota and skeletal debris are represented by abundant cm to dm-sized stromatoporoids, minor corals, sponge-like organisms, chaetetids? and echinoid spines (Fig. 2-41 C). Two subfacies have been recognized (Fig. 2-44A, B, C): LF1-S1: stromatoporoid floatstone with wackestone to fine-grained packstone matrix (Fig. 2-44D), and LF1-S2- rudstone to floatstone with intraclastic-bioclastic packstone to grainstone matrix (Figs. 2-44 E, F). The LF1-S1 and LF1-S2 are co-existing within the stromatoporoid-rich facies (LF1), and they are separated by a sharp boundary (Fig. 2-44A, B, C). In LF1-S1, the dominant stromatoporoids taxa are

Sphaeractinia sp. and *Ellipsactinia* sp. and they occur mostly in growth position (Figs. 2-45A, B, C). *In-situ* stromatoporoids show different growth forms as bulbous (Fig. 2-45A) columnar (Fig. 2-45B) and dendroid with robust branching (Fig. 2-45C). in some parts, the stromatoporoids with columnar shape can reach to 40 cm in diameter. The *Ellipsactinia* sp. has thicker lamellae and thinner inter-lamellar spaces compared with *Sphaeractinia* sp. where lamellae are thinner than inter-lamellar spaces or show the same size (Figs. 2-45C, D). The wackestone to packstone matrix composed of fine-grained peloids, very rare intraclasts as well as rare skeletal grains including bivavles, bryozoans and echinoids (Fig. 2-44D). The micro-encrusters such as *Tubiphytes-Crescentiella* are very common within the matrix and they mostly grew in association with stromatoporoids (Fig. 2-45F) or they developed in a nodule shape.

Subfacies LF1-S2 is characterized by cm to dm-sized intraclasts and fragments of stromatoporoids and corals distributed in a poorly-sorted packstone to grainstone matrix (Fig. 2-44D, E). The stromatoporoid clasts comprise mostly of *Sphaeractinia* sp. and *Ellipsactinia* sp. fragments. Other bioclasts including corals are characterized by fragments of phaceloid corals and predominantly enveloped by micro-encrusters such as *Tubiphytes- Crescentiella* (Fig. 2-44D). Other common bioclasts are fragments of micro-encrusters such as *Tubiphytes- Crescentiella, Radiomura cautica*, *Uvanella*?, and other undefined micro-encrusters. Rare components are bivalves, brachiopods, benthic foraminifers and echinoids. In the vertical position (section A) (Fig. 2-41 B), the number of debris rich LF1-S2, with abundant intraclast and bioclast components, decreases towards the top of the section where the mud-dominated LF1-S1 are commonly more developed.

2-5-1-2- Stromatoporoid- coral facies (LF2)

This Lithofacies is characterized by stromatoporoids (*Sphaeractinia* sp. and *Ellipsactinia* sp) and corals floated in a wackestone to packstone matrix (LF2-S1), and tabular stromatoporoids and corals associated with wackestone matrix rich in radiolarians (LF2-S2) (Figs. 2-42A, B). In Monte di Mezzo section, the LF2-S1occurs as massive limestones with abundant fragments and *in-situ Ellipsactinia* sp., *Sphaeractinia* sp., other undefined stromatoporoids and corals colonies that mostly preserved in life position (Fig. 2-46). The dominant morphology of corals is branching (phaceloid), with coral colonies ranging from 10 up to 80 cm in diameter and up to 50 cm in height

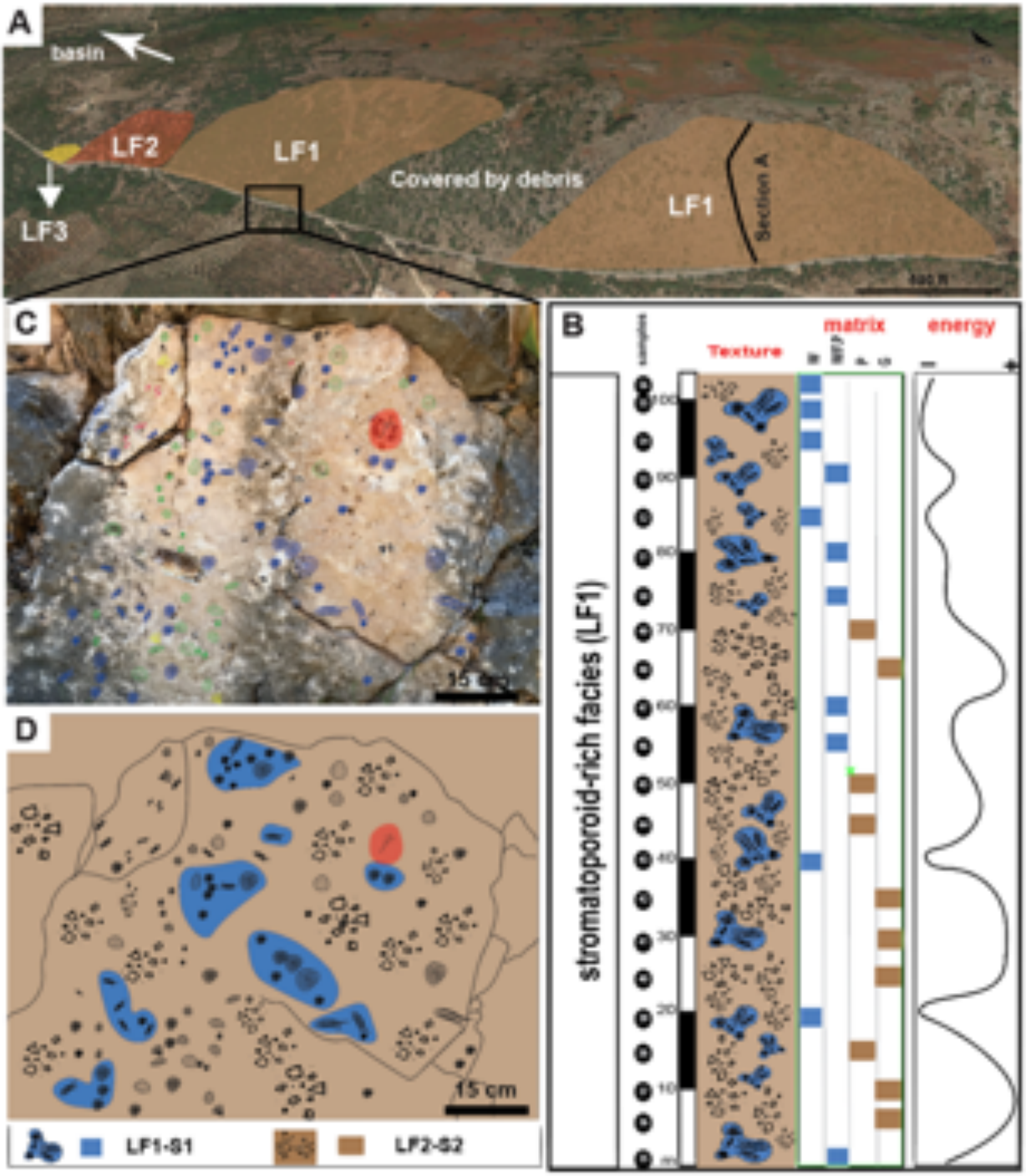

Figure. 2-41- A: Google map showing the position of studied lithofacies (LF1, LF2, LF3) and one stratigraphic log (section A) along the road of Monte di Mezzo section. LF1 is the more abundant lithofacies followed by LF2 and LF1. B: The stratigraphic log (section A) of stromatoporoid-rich facies showing the distribution of subfacies (LF1-S1 and LF2-2) and in a vertical position. The *in-situ* stromatoporoids (LF1-S1) are more concentrated towards the top of section when the energy is low. C: Figure shows the distribution of stromatoporoids on the surface of outcrop in Monte di Mezzo. The organization of biotic components show a cluster reef fabric (*sensu* Riding, 2002) D: The figure

indicates the organization of studied subfacies (LF1-S1 and LF2-2) on the surface of outcrop.

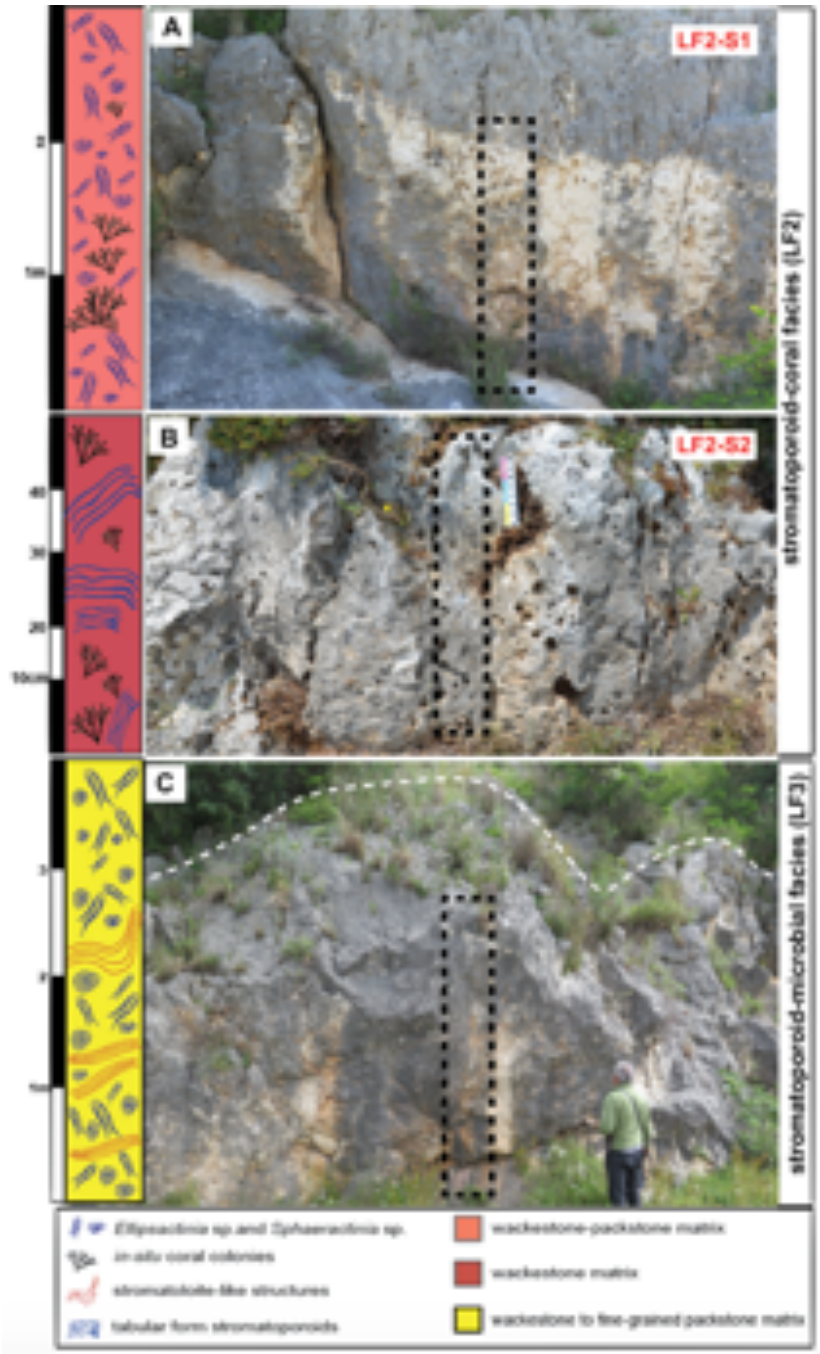

Figure. 2-42- Field observations of outcrops with their sketches show A: the distribution of *in-situ* corals and stromatoporoids (*Ellipsactinia* sp.and *Sphaeractinia* sp.) in LF2-S2 subfacies in Monte di Mezzo section. B: The LF2-S2 occur in cm- thick massive limestone and represented by tabular form stromatoporoids associated with *in-situ* coral colonies (Masseria Prencipe section). C: The LF3 is characterized by stromatolite-like structure followed by stromatoporoids (*Ellipsactinia* sp.and *Sphaeractinia* sp.) on the top (Monte di Mezzo section).

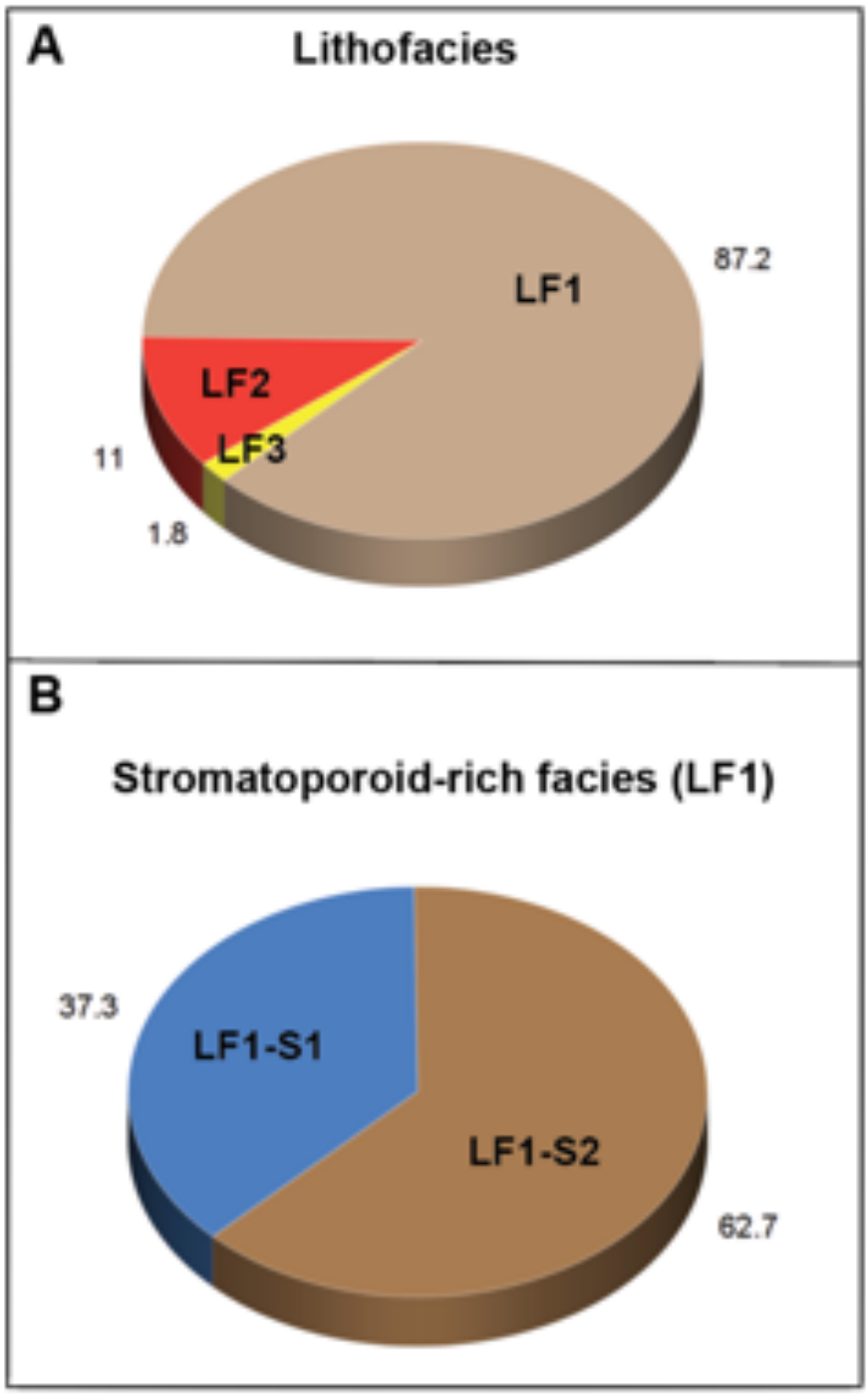

Figure. 2-43- A: Pie charts showing the distribution of lithofacies LF1, LF2, LF3 in studied area (in percentage). The Stromatoporoid-rich facies (LF1) is the main lithofacies followed by LF2 and LF3. B: The chart shows the percentage of subfacies LF1-S1 and LF1-S2 in stromatoporoid-rich facies. The subfacies LF1-S is more abundant compare with LF1-S2, showing the high percentage of debris contributed in formation of stromatoporoid-rich facies in MSL.

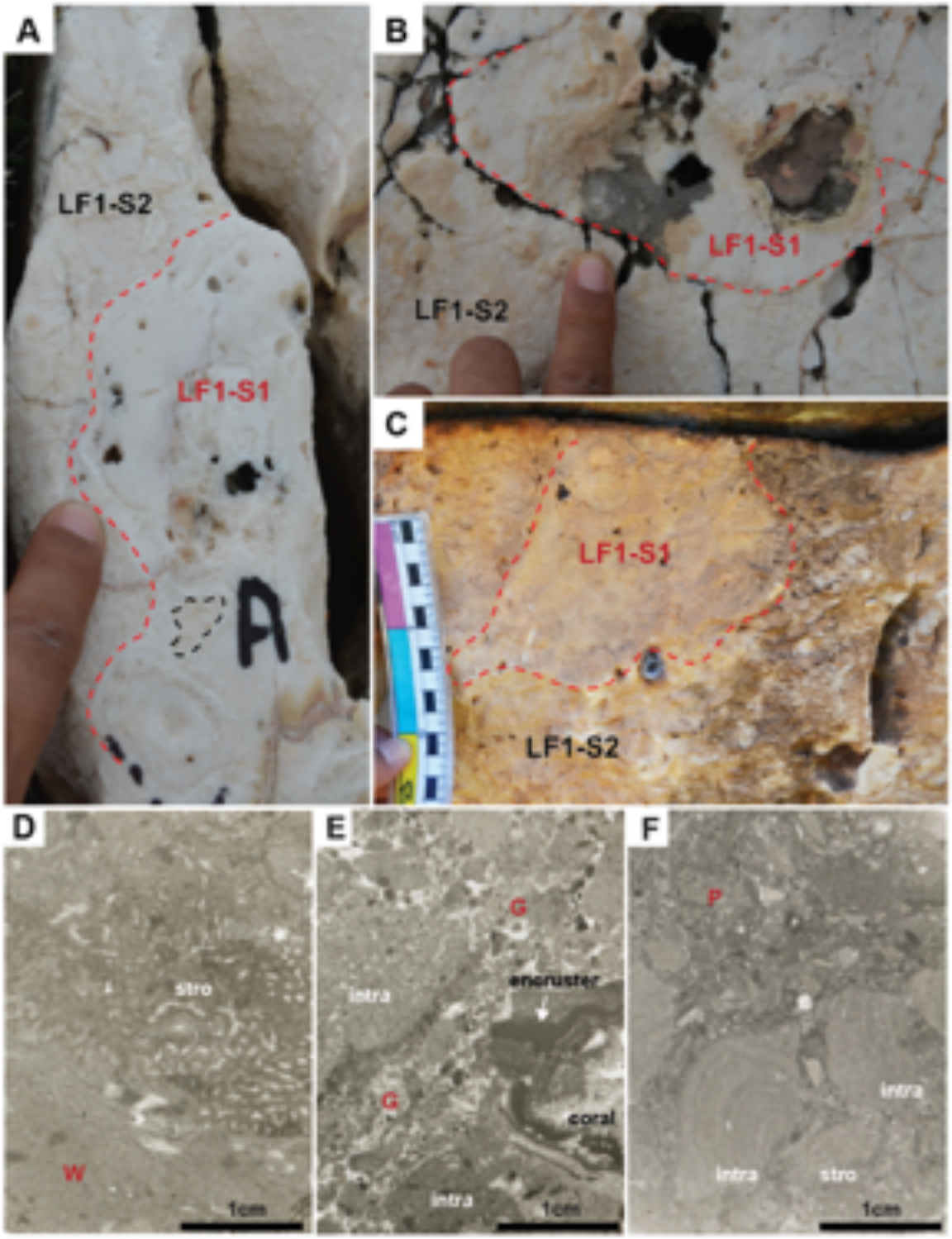

Figure. 2-44- Stromatoporoid-rich lithofacies (LF1). A, B: distribution of subfacies LF1-S1 and LF1-S2 on the surface of outcrop with their sharp boundaries (Torre Mileto section) and C: Monte di Mezzo section. D: Thin section image shows the stromatoporoid (stro) surrounded by a wackestone (W) matrix in (LF1-S1). E: The image shows the mm to

cm-sized intraclasts and bioclasts distributed in a grainstone matrix (LF1-S2). The micro-encrusters are developed around the coral fragments and represented mostly by *Tubiphytes* sp. G: The LF1-S2 in this image is characterized by mm to cm-sized intraclasts and bioclasts distributed in a packstone (P) matrix

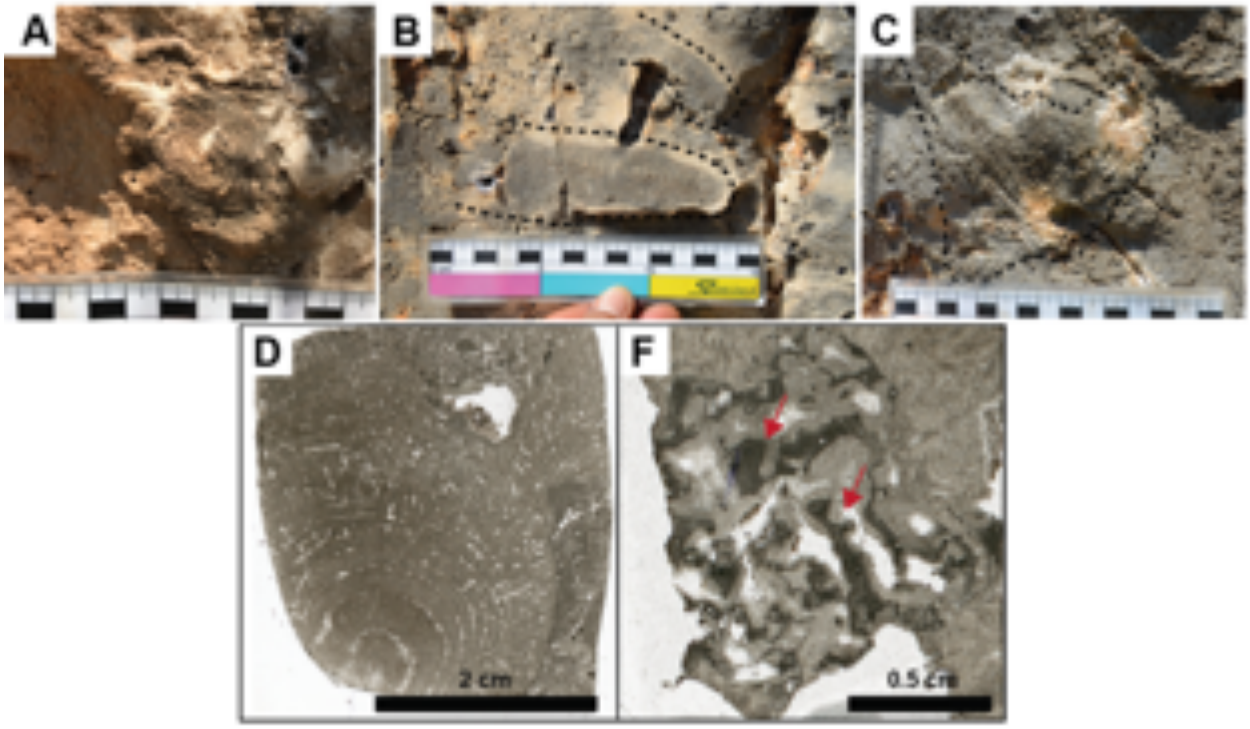

Figure. 2-45-Stromatoporoid-rich lithofacies (LF1) (continue). A: Figure shows the bulbous growth form of an *in-situ* *Ellipsactinia* sp. B: *Sphaeractinia* sp. stromatoporoid shows an *in-situ* columnar growth shape. Note the lamellae are thinner than inter-lamellar spaces or show the same size compare with *Ellipsactinia* sp. (Figs. 2-45A, C). C: An *Ellipsactinia* sp. shows an *in-situ* robust dendroid form. D: Thin section image of *Ellipsactinia* sp. with lamellae are thicker than inter-lamellar space. E: Thin section image shows *Tubiphytes* sp. (red arrows). growing in association with stromatoporoids.

(Fig. 2-46 A). The coral branches are mainly delicate, but the robust form is also present (Fig. 2-46B). The branches touched each other's, leaving a very thin space in between (Fig. 2-46 C, D, F). The internal sediments between stromatooroids and corals composed of mm-sized bioclasts distributed in a wackestone to packstone (Fig. 2-47A, B). The non-skeletal grains are peloids and rare amount intraclasts. The bioclasts are debris of echinoids, bivalves and gastropods and some pelagic components such as *Saccocoma* sp. (Fig. 2-47C).

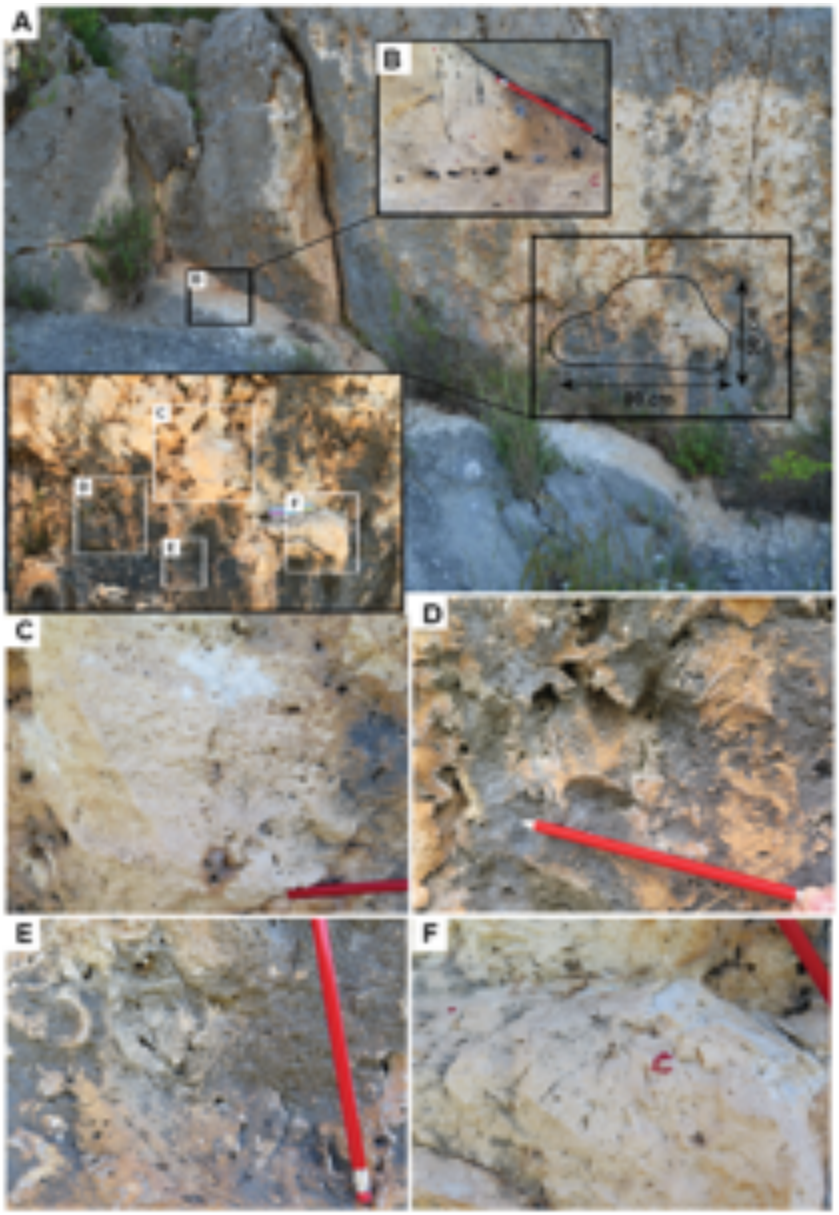

Figure. 2-46- Stromatoporoid- coral facies (LF2) (LF2-S1). A: Photo shows the position and size of coral colonies in outcrop. B: The coral shows a roboust branching. C, D, F: The field photos of coral colonies show growth form of *in-situ* colonies. Note that the corals show branching growth form with delicate branches that positioned in close to each other.

The skeletal debris are usually micritized or enveloped by micrites. The micro-encrusters are commonly represented by *Tubiphytes- Crescentiella* which occur mostly as nodules or in growth form by growing on other biotic components (Fig. 2-47D). The fragments of *Tubiphytes-Crescentiella* are also present.

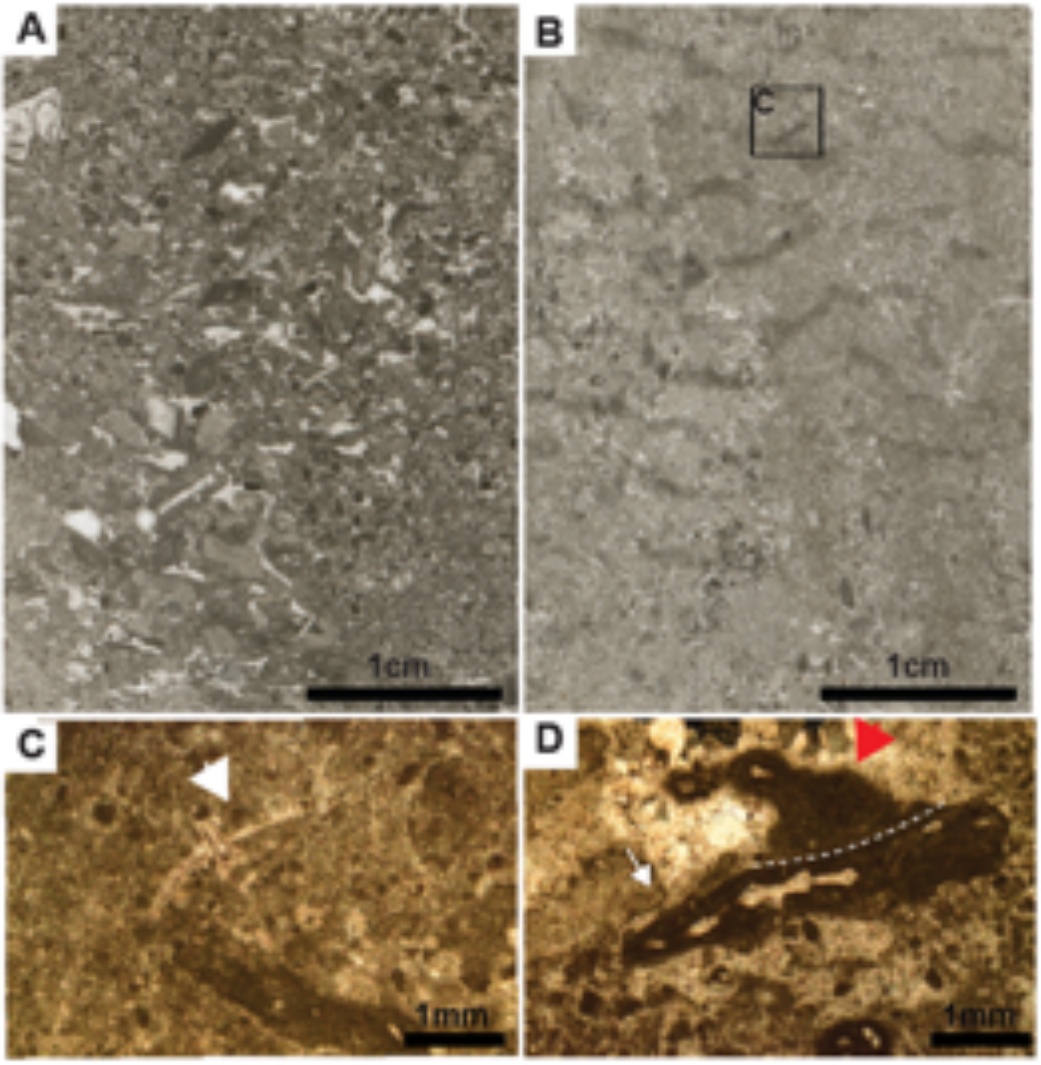

Figure. 2-47-A: Thin section photo of LF2-S1 shows a packstone matrix rich in peloids and *Tubiphytes* sp . nodules. B: Thin section photo of LF2-S1 subfacies showing h a wackestone matrix with *Saccocoma* sp. C: A close view of *Saccocoma* sp. (white arrow) distributed in wackestone matrix of LF2-S1. D: A photomicrograph shows a *Tubiphytes* sp. in growth position (red arrow) associated with other fragment of *Tubiphytes* sp.

In the lower part of Masseria Prencipe, the LF2-S2 shows different characteristics. *Ellipsactinia* sp. and *Sphaeractinia* sp. are completely absent in this area. Instead, *in-situ* and tabular form stromatoporoid colonies were developed in association with corals (Fig.2-42B). The stromatoporoid colonies reach 50 cm in height and up to 60 cm in diameter (Fig. 2-48 A), and characterized by thick and continuous lamellae which envelope each other's (Fig. 2-48 A). The stromatoporoid colonies are associated with cm-sized *in-situ* phaceloid coral colonies (Fig. 2-48B). The internal sediments are characterized by dark muddy wackestone matrix with main components

represent by radiolarians (Fig. 2-48C). The radiolarians are mostly dissolved and replaced by fine-grained dolomites. (Fig. 2-48C).

2-5-1-3- Stromatoporoid- microbial facies (LF3)

This lithofacies occur in massive limestone and crops out only in one outcrop in Monte di Mezzo section (Fig. 2-41A; 2-42C). The lithofacies is characterized by *in- situ* stromatoporoids surrounded by wackestone to fine-grained packstone and developed on the top of discontinuous dm-sized of *Ellipsactinia* sp. and *Sphaeractinia* sp. and *Cylicopsis* sp? (Fig. 2-49C). These biotic components are associated with fragments of sponge- like organisms and echinoid spine. The other components within the matrix are fragments of gastropods, foraminifers and micro-encrusters such as *Tubiphytes- Crescentiella* and *Radiomura cautica.* Under the microscope, the internal fabric of stromatolite-like structures can be distinguished from the stromatoporoids (Fig. 2-49 D, E). The stromatolite-like fabric is characterized by alternating micritic dark laminae and clear laminae composed of microgranular calcite cements (Fig. 2-49E). Geopetal fabrics are present in some cavities and characterized by fine-grained internal sediment fillings at the base and sparry calcite at the top of cavities.

2-5-2- Depositional environments interpretation

In the Gargano Promontory during the Late Jurassic, the Apulia Carbonate Platform (ACP) was a part of a carbonate bank passing downslope to the Adriatic Basin. The MSL represent deposition in the distal part of margin and it characterized by the development of stromatoporoid facies with some branching corals. The external margin passes gradually to clinostratified slope facies of Ripe Rosse Formation with breccia and calciturbidites, passing basinward to pelagic mudstone with chert of the Maiolica Formation (Morsilli and Bosellini, 1997). The model proposed by these Authors is a sort of a distally steepened ramp, with an inclination of 5-10 degree associated with the external part of margin (Fig. 2-50).

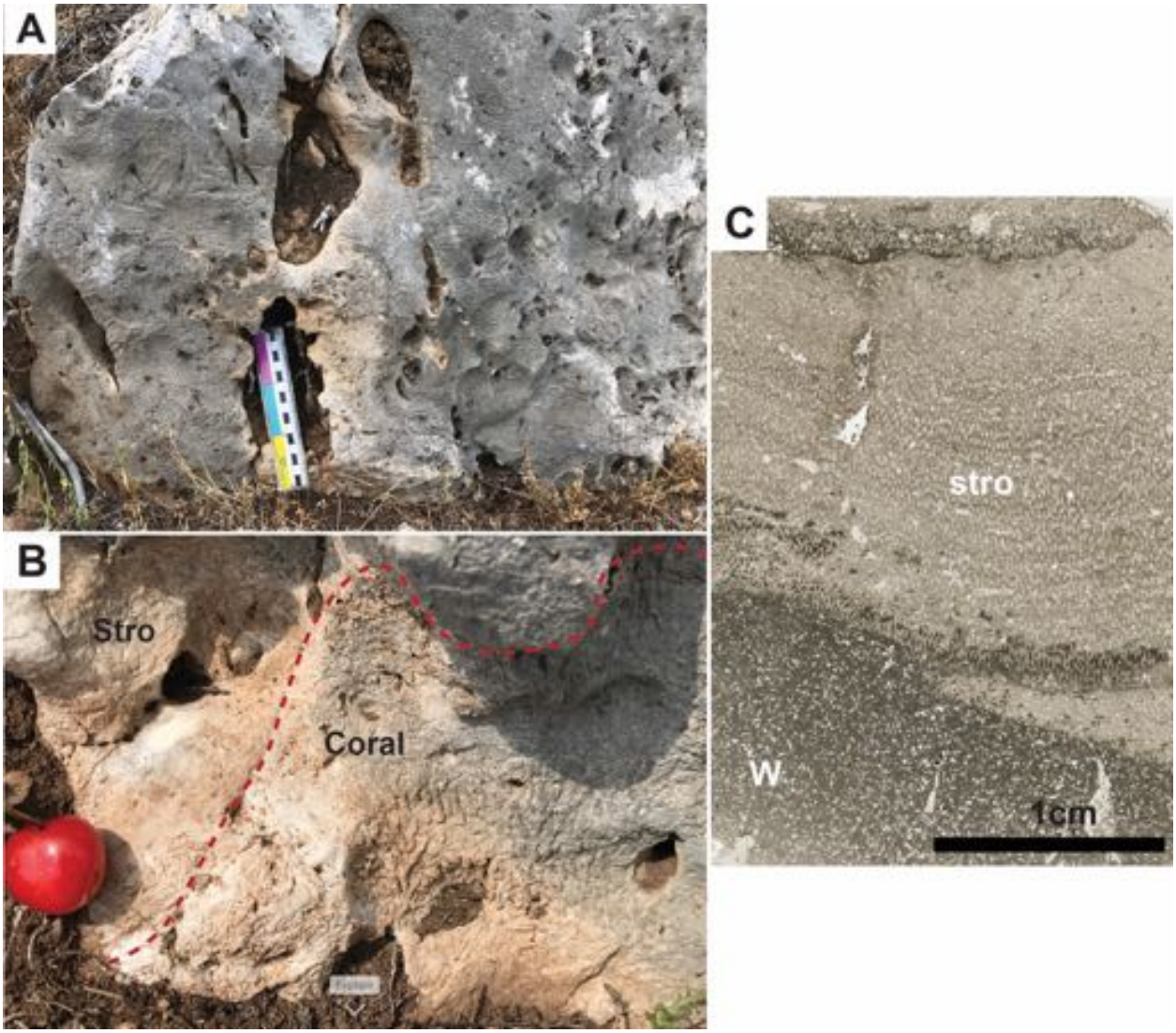

Figure. 2-48- Stromatoporoid- coral facies (LF2) (LF2-S2). A: Photo shows a tabular stromatoporoid colony developed in Masseria Prencipe area. B: Image shows the co-occurrence of *in-situ* phaceloid form coral colonies associated with tabular stromatoporoid (stro). C: Thin section photo of tabular stromatoporoids surrounded by a wackestone (W) matrix rich in radiolarians.

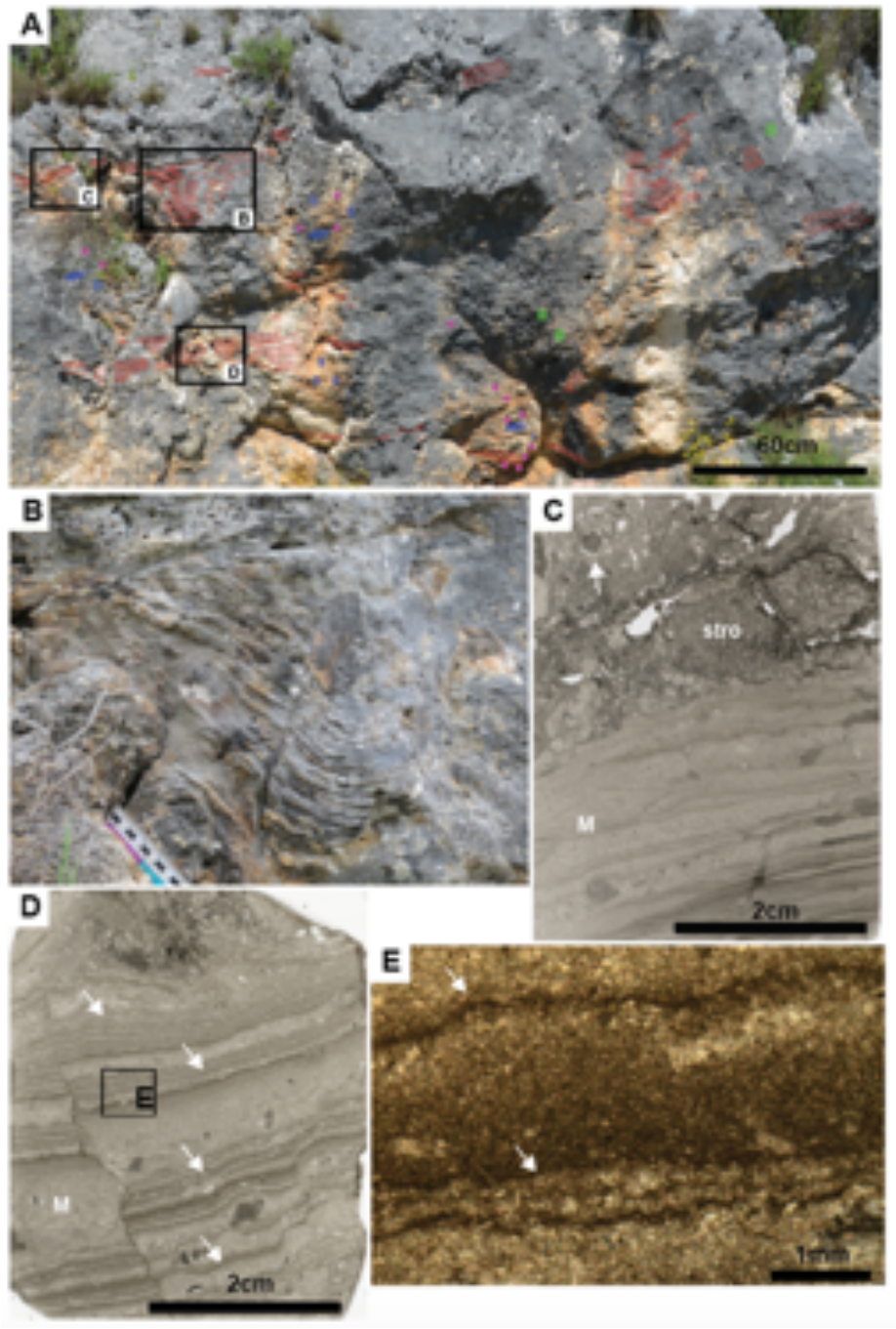

Figure. 2-49- Stromatoporoid- microbial facies (LF3). A: Field photo shows the distribution of stromatoporoids, spongy- like organisms and echinoids accompanied with stromatolite- like structures. B**:** A close view of stromatolite-like structures. C: Thin section photo shows the in-growth form of stromatoporoids (sto, white arrow) (*Cylicopsis* sp.?) surrounded by a wackestone to packstone matrix. D: Thin section photo of stromatolite-like structures shows the alternation of dark and clear laminae of stromatolites (white arrows). E: photomicrograph shows a microbial mat-like character (white arrows) of dark laminations alternating with clear laminae (Fig. 2-49D).

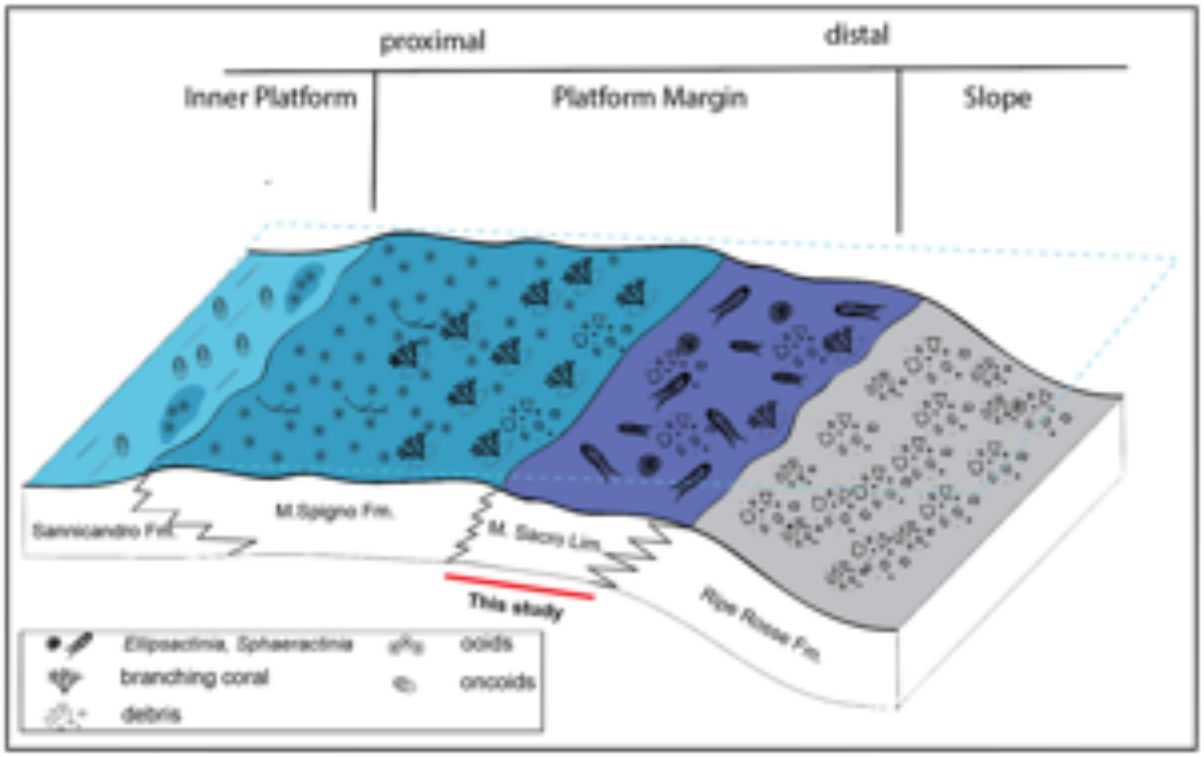

Figure. 2-50- Schematic depositional model of the Gargano margin during the Late Jurassic-Early Cretaceous (modified after Morsilli and Bosellini, 1997). The model shows the facies belts from inner platform, margin, slope to base-of-slope to basin.

According to this general model, the three main lithofacies here distinguished, stromatoporoid-rich facies, stromatoporoid- coral facies and stromatoporoid- microbial facies, represents the external margin from the proximal zone to the more distal part, respectively (Fig. 2-51). Despite the limitations imposed by the limited lateral continuity of the studied outcrops and lack of depositional geometry, the general interpretation of the lithofacies has been made on the basis of skeletal components and textures. The bathymetric position of lithofacies can be estimated by recognition of components adapted to different light zones (euphotic, mesophotic and oligophotic). Stromatoporoid-rich facies (LF1) mainly consists of stromatoporoids such as *Ellipsactinia*, *Sphaeractinia* with bulbous, dendroid, branching and columnar shape (Fig.2-51). The stromatoporoids are characterized by enveloping growth bands (Fig. 2-45A-C). Based on James and Bourque (1992), these growing form of stromatoporoids can adapt to quite to moderate water energy.

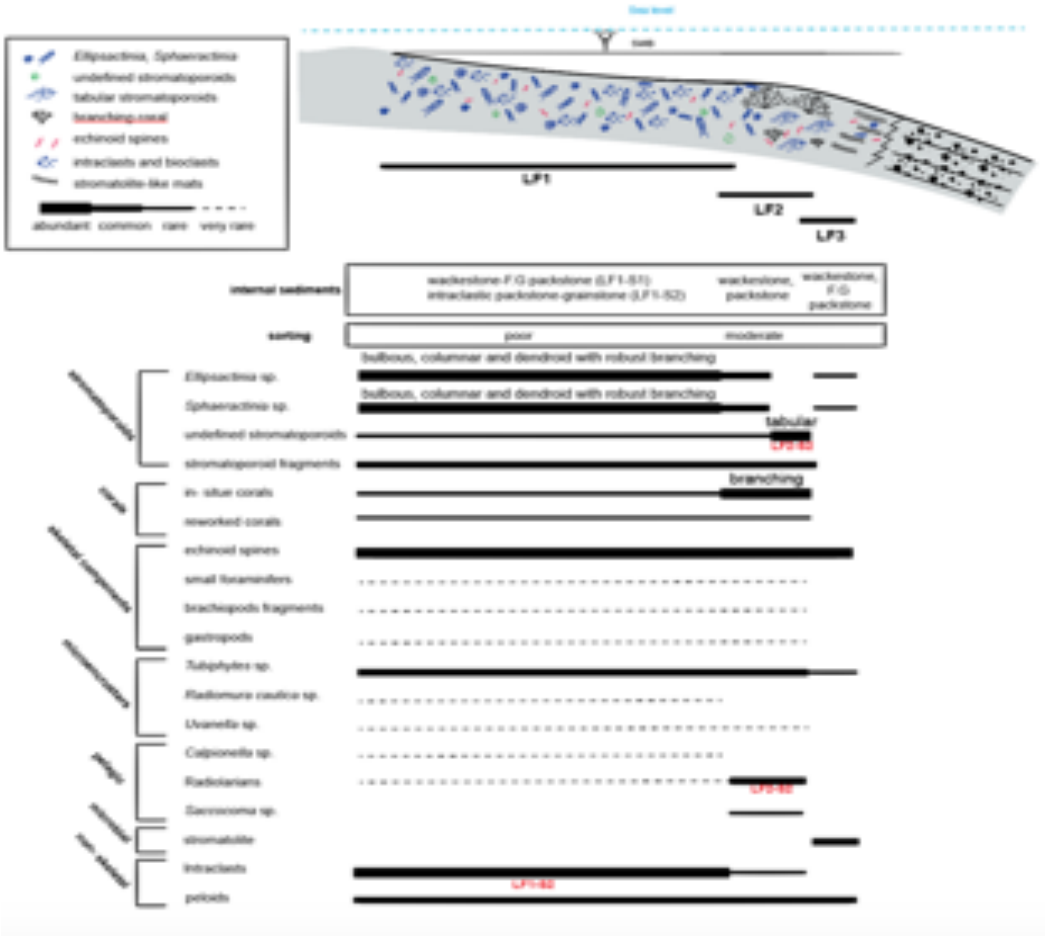

Figure. 2-51- Schematic cross section of external marginal facies of the Monte Sacro Limestones in Gargano area. Lateral distribution of lithofacies, internal sediment textures, and main carbonate particles of various lithofacies are shown.

In LF1, the *in-situ* stromatoporoids are close but not densely stacked nor in contact. So, they could not build a rigid framework reef (Fig. 2-41C). These characteristics fit the "close cluster" reef type of Riding (2002). These matrix-supported reefs are characterized by deposition in low-energy environments where they can develop large size and moderate relief buildups (Riding, 2002). This close cluster reefs, despite the deposition in quiet environments, are mainly prone to high-energy hydrodynamic events, but the close arrangement of skeletons may prevent the high-energy events to remove and sorting the internal sediments (Riding, 2002). The internal sediments in stromatoporoid-rich buildups are represented by wackestone to fine-grained packstone (LF1-S1) (Fig. 2-44D) and packstone to grainstone (LF1-S2) (Fig. 2-44E, F). This indicates that LF1 can be developed under different energy conditions. The wackestone to fine-grained packstone matrix

(LF1-S1) between *in-situ* stromatoporoids (Fig. 2-44D) shows that this kind of organisms grew in low-energy and quiet environments. Figure 2-41B shows that *in-situ* stromatoporoids associated with wackestone matrix (LF1-S1) are better developed at the top of Monte Sacro section (section A) where the hydrodynamic energy is low due to possible sea-level rise. *Tubiphytes* sp. is the dominant micro-encruster which directly developed on the surface of stromatoporoids (or other hard substrates) (Fig.2-45F). The absence of *in- situ* light-dependent micro-encrusters such as *Lithocodium- Bacinella* and development of heterotrophic micro-encrusters (*Tubiphytes* sp.) indicates that this subfacies can be developed in mesophotic conditions where the light is not enough for phototrophic micro-encrusters to grow. The LF1-S1 is in association with intraclastic-bioclastic packstone-grainstone (LF1-S2). In this subfacies, the occurrence of cm-sized angular intraclasts and bioclasts in a poorly-sorted packstone-grainstone (Fig. 2-44E, F) indicates that LF1-S2 were deposited under high-energy conditions. The intraclast and bioclast debris are only sourced from the current lithofacies (LF1) (clasts of stromatoporoids, corals and micro-encrusters). The angular intraclasts associated with poorly-sorted packstone-grainstone indicate that the hydrodynamic energy was not continuous enough to improve the roundness and sorting of the sediments. The characteristics and origin of internal sediments suggest that stromatoporoids were mainly developed in low-energy environments (LF1-S1) where the energy was not enough to build a rigid framework (close cluster fabric), then the buildups were affected by episodic high-energy events resulted in the accumulation of high-energy deposits (LF1-S2). This also can interpret the chaotic organization of LF1-S1 and LF1-S2 in stromatoporoid-rich facies in MSL (Fig. 2-44 A, B, C). This lithofacies were deposited in proximal zone of external margin (Fig.2-51).

In stromatoporoid-coral facies (LF2) the *in-situ* phaceloid corals are characterized by delicate branching shape, suggesting that these corals can be thrived in relative low- energy environments. Also, Dupraz and Strasser (2002) discussed that corals with phaceloid morphology could be adapted to soft substrates and thrived in high sedimentation rates and quiet environments. In LF2-S1, the stromatoporoids and corals are floated in a matrix without building a wave-resistance rigid framework. This fits the characteristics of "cluster reef" and indicates the deposition in relative quiet conditions (Riding, 2002). The internal sediments represent by bioclast wackestone and packstone matrix (LF2-S1) suggest that corals and stromatoporoids were developed in relative moderate to low-energy environments. Micritization of skeletal debris and rare amounts of intraclasts suggests low hydrodynamic conditions. Also, the absence of light-dependent organisms

such as *Lithocodium- Bacinella* and dasyclad green algae can indicate the deposition in limited-light conditions (mesophotic).

In LF2-S2, the stromatoporoids developed laminar to tabular shape morphology (Fig.2-48A). Compare with Devonian stromatoporoids, this kind of growth form can develop in deeper and quiet waters (Kershaw, 1998). The coral colonies are represented by phaceloid form, suggesting deposition in quite environments (Dupraz and Strasser, 2002). The internal sediments associated with stromatoporoids and corals in LF2-S2 are characterized by wackestone matrix rich in radiolarian. This indicates the deposition of this subfacies in more distal margin under low-energy conditions. This lithofacies were developed between proximal and distal part of external margin (Fig.2-51).

The stromatoporoid- microbial facies (LF 3) is characterized by stromatolite-like structures accompanied by stromatoporoids in growth position. Stromatolites are known to form in marginal marine, shallow and deep subtidal and basinal environments (Flügel, 2004). In the Upper Jurassic, the microbial-dominated reefs were mostly grown in deep and low energy environments where the sedimentation rate was very low (Leinfelder et al., 1996; Schmid, 1996). On the top of stromatolite-like laminae, the internal sediments between stromatoporoids are wackestone to fine-grained packstone showing that in this lithofacies the stromatoporoids were developed in relative low-energy environments. This lithofacies were deposited in the distal part of external margin (Fig.2-51).

2-6- Discussion

2-6-1- Other examples from South and intra-Tethys reefs

In the intra-Tethys and southern part of Tethys, Upper Jurassic reefs are quite common.

The sedimentological characteristics of this kind of reefs have been described in Italy: Central Apennines (Rusciadelli et al., 2011) and NW Sicily (Basilone and Sulli, 2016a), Slovenia (Turnšek et al., 1981), Austria: Northern Calcareous Alps (Schlagintweit and Gawlick, 2008); and in Czech Republic (Hoffmann et al., 2017). In Arabian Plate, the Upper Jurassic facies are reported from Saudi Arabia (Al-Awwad and Pomar, 2015, Rosales et al., 2018) and Iran (Kano et al., 2007).

In central Apennines of Italy, (Rusciadelli et al., 2011) have been studied the different reef units developed in Ellipsactinia Limestones. These units represent by coral and Chaetetids Unit (CCU), corals and stromatoporoids unit (CSU), and the stromatopores unit (SSU). These units were

deposited along three main reef zones 1- coral and Chaetetids Unit was deposited in an internal and protected deep back-reef- lagoon, 2- corals and stromatoporoids unit were developed in a reef flat, and 3- stromatopores unit which occur in an external and shallow zone. In

SSU unit of Ellipsactinia Limestones, the stromatoporoids are surrounded by bio-lithoclastic sediments. This shares similarity with LF1-S2 in MSL where debris-rich subfacies developed in association with stromatoporoid-rich facies (LF1). However, the stromatopores unit in Ellipsactinia Limestones described being deposited along the shallowest part of margin and with high energy conditions, while in MSL this facies placed in the deeper part of margin, in more quiet environments with an episodic source of high energy events.

In NW Sicily, Basilone and Sulli (2016a) described the upper Tithonian–Valanginian carbonate facies distribution along a tectonically controlled rimmed carbonate shelf. A reef complex is composed of inner reef flats which characterized by corals. The outer zone (reef wall) were dominated by *Ellipsactinia* sp. boundstone, and toward sea direction, the encrusters were well developed. In the deeper part of the platform (fore- reef), breccia and calcarenites were deposited as clinoforms passing deep-ward to calpionellids limestone. In *Ellipsactinia* boundstone facies the internal sediments are ranging from intraclastic breccia to bioclast packstone to grainstone. The *Ellipsactinia* sp. is characterized by densely packed clusters and quasi-rigid mound-shaped structures which suggest the deposition of this zone under high-energy hydrodynamic conditions (Basilone and Sulli, 2016a). The *Ellipsactina* sp. reefs are developed as matrix of the Upper Tithonian–Valanginian breccias described by Basilone et al. (2016b). The stromatoporoid-rich facies (LF1) of MSL is comparable with *Ellipsactinia* boundstone described here by Basilone and Sulli (2016a). In both examples, the main biotic components are stromatoporoids (*Ellipsactinia* sp.) surrounded by intraclastic rich sedimends (LF1-S2). However, in MSL the LF1 interpreted to be developed in low-energy environments hitting by episodic high-energy events.

The Upper Jurassic reefs represent by *Ellipsactinia* limestones have also been reported from Friuli Platform, southern Alps (Italy) by Cati et al. (1987) and Picotti and Cobianchi (2017). These studies are mostly focused on the stratigraphic interpretation of Upper Jurassic- Lower Cretaceous successions. In this area, the *Ellipsactinia* limestones considered to be real reef sequences, and they were grown along the margin of Friuli Platform.

Schlagintweit and Gawlick (2008) studied the Upper Jurassic- basal Cretaceous shallow-water carbonates in Northern Calcareous Alps, Austria, and described as the main reef body a micro-

encruster boundstones with a variable amount of cement crusts. This platform is characterized by a steep margin, and the reef facies occurs in a fore-reef slope environment, with coral-stromatoporoid patch-reefs and monotypic microsolenid floatstone. Instead, the *Ellipsactinia* wackestone facies is associated with platform margin and upper slope. In this example, *Ellipsactinia*-rich facies were associated with wackestone, showing the depositional of this facies in quiet and low energy conditions. The *Ellipsactinia* wackestone facies described by Schlagintweit and Gawlick (2008) can be comparable with stromatoporoid-rich facies (LF1) in MSL where the stromatoporoids are surrounded by wackestone to fine-grained packstone matrix (LF1-S1).

Turnšek et al. (1981) studied the Oxfordian- lower Kimmeridgian reef complex of north-western ex-Yugoslavia (Croatia). This reef complex is interpreted as a classical barrier reef, with all the typical sub-environments, from the lagoon to the basin. The main reef is subdivided into *Actinostromarid zone* which is dominated by stromatoporoids and a *Parastromatoporoid zone* which is characterized by coral- chaetetids facies. The back reef corresponded to a lagoon with patch reefs and defined as a *Cladocoropsis* zone. The stromatoporoid-rich facies (LF1) of MSL are comparable with *Actinostromarid zone* which located in the shallow central reef. The sediments between biocounstructors contain debris of breccia and calcarenite, which suggest this facies to develop in very high energy settings. However, in this zone, on the contrary with LF1 in MSL, the corals are well developed.

Hoffmann et al. (2017) studied the Tithonian–lower Berriasian of Štramberk reef complex, Czech Republic. These reefs were developed on an isolated intra- Tethys carbonate platform. Two main boundstone types have been recognized. A- Coral- microbial boundstone attributed to a low-energy setting and composed mostly of branching corals associated with light- dependent micro-encrusters (*Lithocodium- Bacinella*), and B- micro-encruster-cement boundstone that corresponds to the high-energy setting of an upper fore-reef slope environment. This facies is characterized by the presence of micro-encrusters accompanied by synsedimentary cements and absence of corals and light-dependent micro-encrusters like *Lithocodium- Bacinella.* In this research the corals considered to be the main metazoan reef builders outcompeted stromatoporoids. This can be an exception for reefs developed in intra-Tethys realms including MSL in Apulia Platform.

In the Arabian Plate, Al- Awwad and Pomar (2015) studied the origin of rudstone- floatstone beds in the Upper Jurassic Arab-D reservoir, instead Rosales et al. (2018) described the distribution of

microfacies along this carbonate ramp. The middle ramp setting is defined by a reef belt with microbial-stromatoporoid- coral buildups which are characterized by the presence of coral and stromatoporoids in a wackestone to grain-dominated packstone matrix. Microbial fabrics are mostly thrombolite and microbial filaments. In the Zagros Basin, Iran, Kano et al. (2007) reported stromatoporoid biostromes during Tithonian. The stromatoporoids are associated with corals and calcareous algae showing rudstone to floatstone texture. On the contrary respect to the Arab-D the interpreted depositional environment is as a back-reef lagoon. The last two examples from Saudi Arabia and Iran show that in this part of southern Tethys, stromatoporoid-rich buildups can be developed along the different part of a carbonate platform profile, while corals were less developed. This shares the similarity with other stromatoporoid-rich facies that occur in other south and intra-Tethys realms and partially the interpreted setting of the Apulia Platform. However, in intra-Tethys area stromatoporoids are represented by *Ellipsactinia* sp. and *Shpaeractinia* sp., as in MSL.

2-6-2- Factors controlling the MSL reef development

Development of carbonate buildups is strongly related to different factors including nutrient and light availability, hydrodynamic energy and sedimentation rate (Mutti and Hallock, 2003; Pomar et al., 2012, 2017). Among these factors, the nutrient source and light availability was the most important factor which resulted in the formation of different buildups in Upper Jurassic. The comparison of the factors controlling the development of MSL reefs with northern Tethys reefs is shown in figure 2-52.

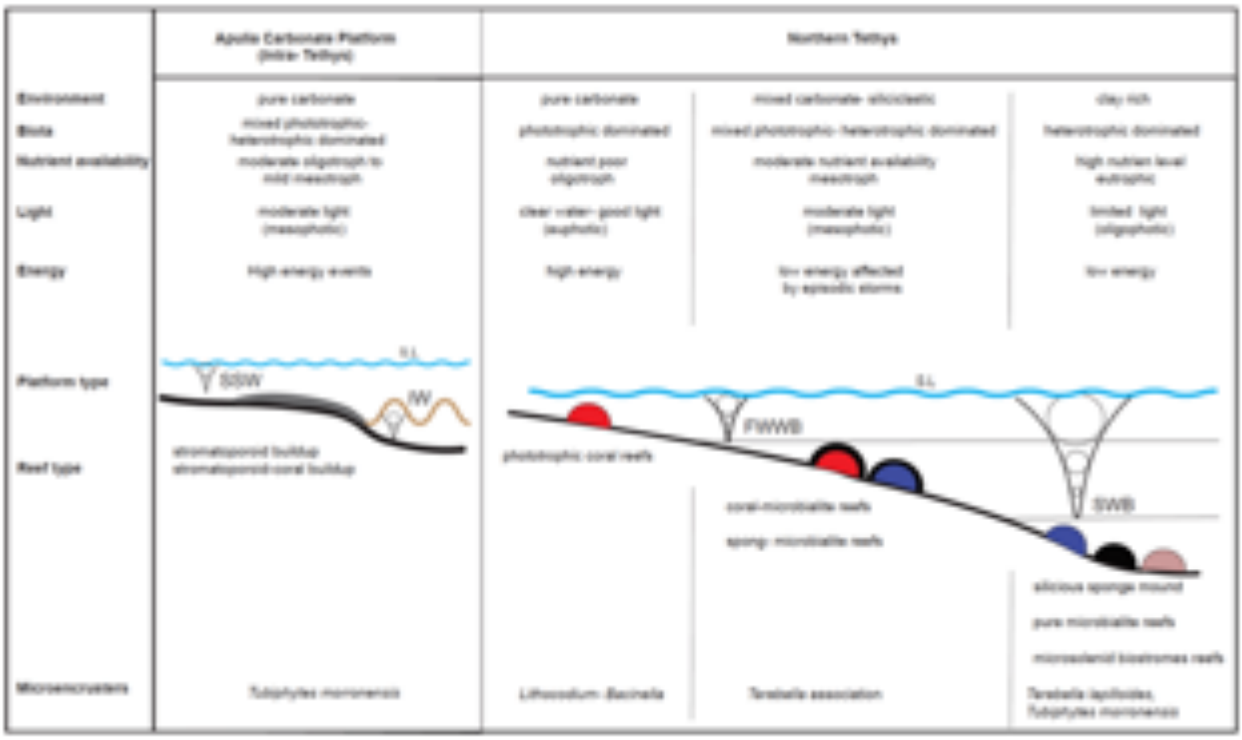

Figure. 2-52- A general schematic diagram showing the major control factors on the growth, dominated biota groups and distribution of Upper Jurassic reefs of northern Tethys on a carbonate platform (modified from Leinfelder et al., 2002) and stromatoporoid-rich buildups in Apulia Carbonate Platform (ACP). The information used in this figure are extracted from Insalaco, 1996; Dupraz and Strasser, 2002; Olóriz et al., 2003; Olivier et al., 2007, 2011). (SSW: surface storm waves, IW: internal waves, FWWB: fair weather wave base, SWB: storm wave base, S.L: sea level)

Dupraz and Strasser (2002) discussed the nutritional modes required for Oxfordian coral-microbialite reefs growth in Swiss Jura. Reefs with light-dependent, phototrophic-dominated fauna were developed in nutrient-poor, pure carbonate environments. Balanced phototrophic-heterotrophic reefs fauna were prevalent in mixed siliciclastic-carbonate environments. In this condition the development of light-dependent micro-encrusters such as *Lithocodium- Bacinella* is limited. With the increase of terrigenous input, the water alkalinity will enhance and together with nutrients, an ideal condition for the growth of microbialites can be occurred favouring the condition for the development of the heterotrophic-dominated type reefs (Fig.2-52).

In the Apulia Platform all the stromatoporoid-rich facies are developed in a carbonate environment without evidence of terrigenous input (Fig.2-52). The phototrophic-dominated faunas are represented by the presence of corals in stromatoporoid- coral facies. However, the abundant presence of organisms such as echinoids in all studied facies (LF1, LF2, LF3), the absence of light-

dependent micro-encrusters (e.g. *Lithocodium- Bacinella*) on the surface of organisms, and the developments of microbial facies in LF3, make these buildups fall within the phototrophic-heterotrophic reefs (*sensu* Dupraz and Strasser, 2002) (Fig.2-52).

Olivier et al. (2004) studied the middle and late Oxfordian coral-microbialite reefs of northeastern France and argued that microbialites mostly grow in mesotrophic conditions in mixed siliciclastic-carbonate environments. In this setting, the light-dependent micro-encrusters (e.g. *Lithocodium*) were rare showing the poor light availability favoured by this kind of organisms. In pure carbonate environments, a low microbialite amount can be developed on phototrophic coral communities in oligo- mesotrophic conditions (Olivier et al., 2007). Also, San Miguel et al. (2017) studied the Kimmeridgian metazoan to microbial-dominated buildups in the shallow ramp of the Iberian basin, Spain. The author discussed the formation of microbial buildups under high nutrient levels. In MSL, the microbialites grown in a pure carbonate environment and they have not strongly developed in the studied facies. As a result, they may be assumed to be formed in an oligo-mesotrophic conditions as discussed by Olivier et al. (2007). While an increase of nutrient level can act as a factor limiting penetration of light, the stromatoporoids buildups associated with microbialites can be adapted to mesophotic environments. In the Upper Jurassic reefs, siliceous sponge mound, pure microbialites and microsolenid biostromes reefs we adapted to high nutrient levels (eutrophic) and poor light (oligophotic) (Insalaco, 1996; Olóriz et al., 2003; Leinfelder et al., 2002). There is no evidence of formation of this kind of organisms in MSL. The other important factor in Upper Jurassic reef development is hydrodynamic energy. The coral reefs in northern Tethys can expand in high energy condition, and they are mostly associated with high energy facies (e.g. rudstone- floatstone) (Dupraz and Strasser, 2002). In mid-ramp setting, Olivier et al. (2011) reported coral- microbialite reefs developed under low energy conditions. These coral-microbialite reefs influenced by episodic high energy events evidenced by coarse bioclastic interbeds. This can be a case for MSL, where the *in-situ* stromatoporoids developed in quiet conditions (LF1-S1) and hit by episodic high-energy events resulting in the formation of debris rich facies (LF1-S2).

Unlike Late Jurassic stromatoporoids, paleoecological and morphological characteristics of Palaeozoic stromatoporoids received more attention in literatures (e.g., Kershaw, 1998; Da Silva et al., 2011a, b; Corlett and Jones, 2011; Kershaw et al., 2013; Kershaw and Mõtus, 2016; Jakubowicz et al., 2018). Based on Kershaw (1998), in low-nutrient and oligotrophic conditions,

the stromatoporoids can develop large bioherms and biostromes while in mesotrophic conditions the small bioherms are more likely to be developed. In the case of MSL the stromatoporoids did not build a high relief buildups or rigid framework (Fig. 2-41C). This indicates that stromatoporoid-rich buildups in MSL could be developed under the mesotrophic conditions.

In MSL, stromatoporoid- coral facies (LF2) indicates grow of stromatoporoids and corals in a similar setting. This kind of stromatoporoid- coral intergrowths is also reported from Devonian stromatoporoid- coral buildups. Corlett and Jones (2011) studied the Devonian stromatoporoid-dominated and coral-dominated reefs in the Mackenzie Basin, Canada, and they argued that coral-stromatoporoid intergrowth is adapted to a transitional ecological zone between two main buildups. Da Silva et al. (2011a) demonstrated that stromatoporoid and corals could grow into an association without any negative impact on each other growth. Corals can be also grown on the dead part of stromatoporoids and *vice versa*. In MSL, the *in-situ* growth of branching form corals associated with stromatoporoids suggests that this form of corals can generate in ecological conditions close to the stromatoporoids. This zone can be equivalent to transitional zone argued by Leinfelder et al. (2005), for environmental ranges of Upper Jurassic stromatoporoids and corals, which placed the stromatoporoid- corals intergrowths in moderate oligotrophy conditions which can be reached to mild mesotrophy in the case of MSL (Fig. 2-52).

2-6-3- Origin of turbulence event- the impact of internal waves

High energy reefs, rich in debris and poor in micrite, were developed during the Late Jurassic time in north and southern part of Tethys (Leinfelder et al., 2002). In MSL, the stromatoporoid-rich facies (LF1) consist of low-energy deposits associated with stromatoporoids (LF1-S1). These low-energy facies are embedded with poorly sorted rudstone to floatstone with intraclastic-bioclastic packstone-grainstone debris (LF1-S2). This indicates that stromatoproid-rich buildups in MSL were affected by range of episodic high-energy events, interpreted as storm-events (Morsilli and Bosellini, 1997). The key point is to explain the source of episodic high energy turbulence in a context of relatively deep water. In the literature, generally the high energy events are explained as the effect of surface storm waves. This storm waves generate turbulence (Ager, 1974) and occur in the shallow part of shelf and coastal zone and they can move the eroded sediments in the direction of the wind, causing erosion, and down-dip transport, and re-deposition of sediments known as tempestites (Immenhauser, 2009). However, the characteristics of intraclastic- bioclastic

rudstone- floatstone debris (LF1-S2) in the MSL do not fit in the context of surface storm waves deposits because 1- the most components and clasts are related to the same depositional setting (e.g., clasts of stromatoporoids, corals, and microbialites), and 2- there are no shallow water components or clasts associated with debris.

In this context, internal waves can be a good candidate for the possible source of episodic storms in stromatoporoid buildups of MSL. Internal waves (IWs) are waves perturbations propagating along the interface of two density-stratified fluids (Pycnocline) (e.g., Munk, 1981; Apel, 2002 among others). The depth of pycnocline commonly occur at the mid-shelf setting when it related to seasonal thermocline (shallow pycnocline), or it can occur at deeper depths when it is associated with permanent thermocline (Butman et al., 2006; Pomar et al., 2012) (Fig.2-53).

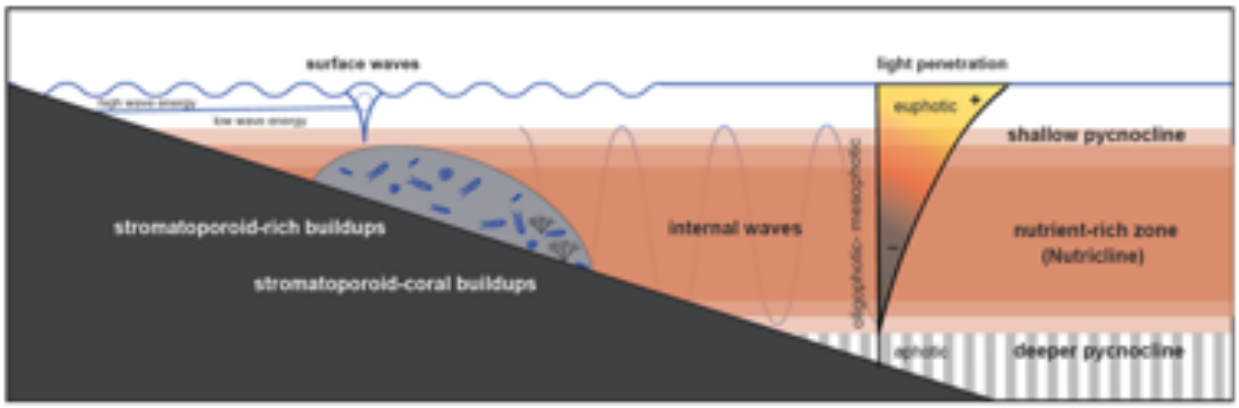

Figure. 2-53- Stromatoporoid-rich facies and stromatoporoid- coral facies developed in the mesophotic zone, below the surface storm wave action; in this environments, episodic strong turbulence events hitting the buildups provided the energy to produce intraclast- bioclast rudstone to floatstone debris between bioconstructors.

Internal waves can cause episodic high turbulence events at any depth where pycnocline intersect the sea floor. As a result, these IWs can remobilize, rework and re-deposited the sediments in both down-dip and up-dip direction (Pomar et al., 2012; Morsilli and Pomar, 2012; Bádenas et al., 2012).

In carbonate systems, internal waves are also an important mechanism for distribution of nutrients, planktons and larvae associated with thermal variation as a result of vertical movement of the thermocline (Pomar et al., 2012). Pycnocline is associated with the zone of internal wave propagation and high nutrient availability (Fig.2-53), and therefore suspension-feeder metazoans can produce buildups at this depth (Pomar et al., 2017). This can be an explanation for the reason

that most Phanerozoic buildups developed in the mid-shelf setting.

As discussed before the *in-situ* stromatoporoid buildups (LF1-S1) in MSL can be developed under mesophotic conditions in low-energy ambients (Fig. 2-53). In these quiet environments, the generation of debris-rich stromatoporoids facies (LF1) in MSL can be summarized as the following stages (Fig. 2-54).

Stage A) growth of the stromatopotoids (LF1-S1): in this stage the stromatoporoids can grow on a mud-dominated substrate under low-energy and mesophotic conditions (Fig. 2-54A).

Stage B) development of debris-rich facies of LF1-S2: during this period, high energy internal waves hit the stromatoporoid buildups developed in the stage A (Fig. 2-54B). The debris of stromatoporoids, corals, and other biota can be generated as a result of high-energy event produced by internal waves (intraclastic-bioclastic packstone-grainstone). These debris can be placed between the big fragments of LF1-S1 and resulted in chaotic arrangement of LF1-S1 and LF1-S2 in stromatoporoid-rich facies (LF1) (Fig. 2-41C, D). During this step, the internal waves can also bring nutrient-rich waters to the buildups.

Stage C) re-generation of stromatoporoids (LF1-S1) in this phase, the quiet condition between two high-energy events allowing precipitation of mud again (Fig. 2-54C). The amount of nutrients provided by internal waves during stage B, is sufficient for stromatoporoids to re-generate again under low-energy condition of this stage before hitting by internal waves in the next stage (stage B).

The effect of internal waves on the formation of high energy rudstone- floatstone facies has also been reported from other parts of Tethys (Alnazghah et al., 2013; Al-Awwad and Pomar, 2015). Alnazghah et al. (2013) reported the development of high energy intraclastic–bioclastic rudstone-floatstone facies associated with flank facies of pinnacles in carbonate ramp of Iberian basin, Spain (western Tethys). These pinnacles were occurred in mud-dominated settings, below the wave- base level. In this case, the occurrence of high energy, coarse-grained flank facies in a context of low-energy ambient conditions reported as a paradox that solved by interpretation of the internal waves as a possible source of turbulence to explain the origin of the flank facies.

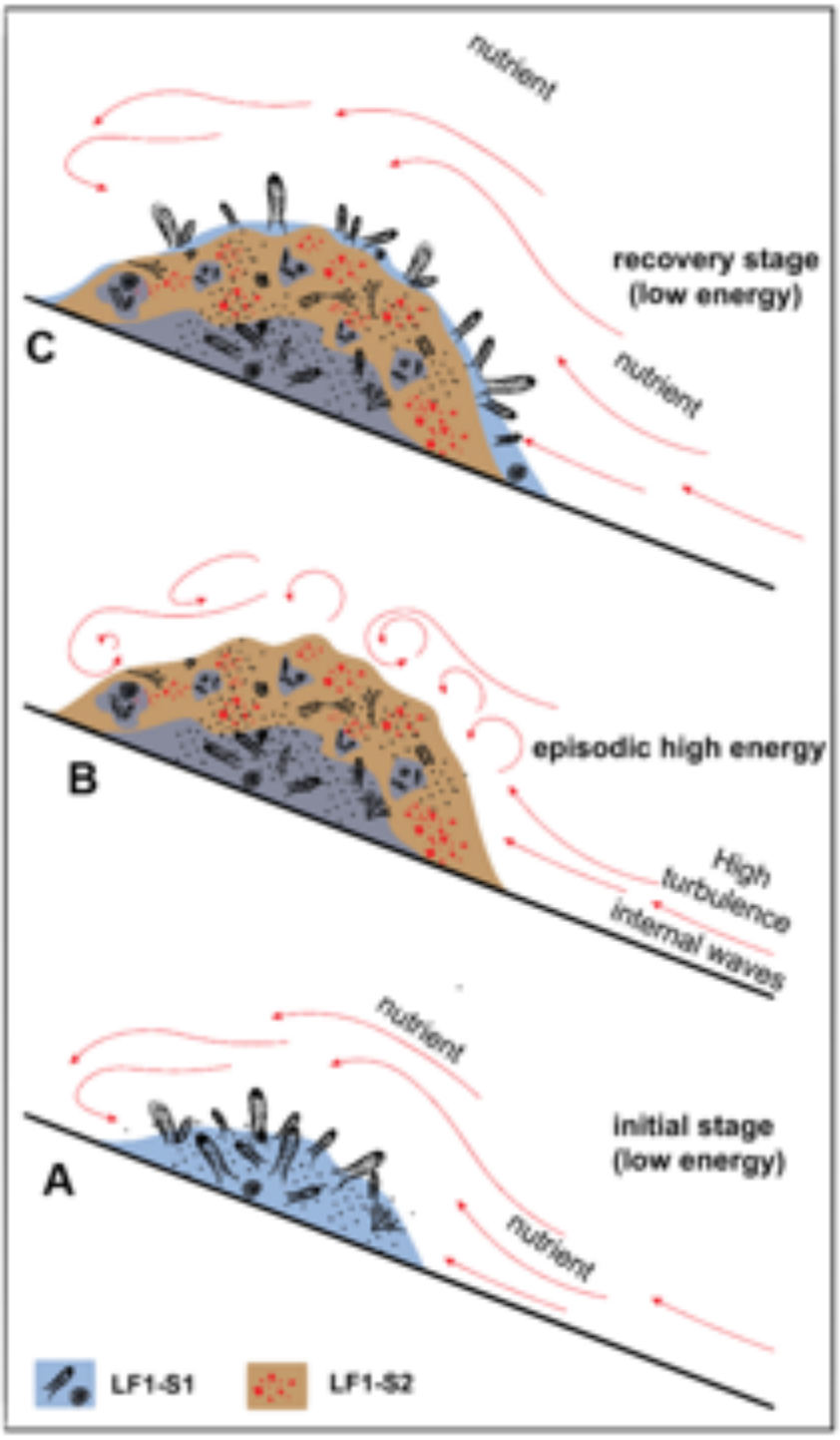

Figure. 2- 54- Figure illustrating the different growth stages of stromatoporoid-rich facies (LF1) in Monte Sacro Limestone. (A) the stromatoporoids developed in a quiet environment and mud- dominated substrates (LF1-S1). (B) Internal waves provide a high energy turbulence event hitting the buildups and result in the production of debris rich facies in buildups (LF1-S2). Apart from hydrodynamic energy, Internal waves can also provide nutrients to the buildups. (C) The stromatoporoids can regenerate again (LF1-S1) due to nutrient availability provided by internal

waves in a calm environment before hitting by episodic high-energy events again.

Comparing with MSL, the main difference is the type of metazoans which in MSL the biota are represented by stromatoporoids but in Iberian basin the corals are the main mezatoans. However, this example shares similarities with the MSL. 1- In Monte Sacro limestones, the *in-situ* stromatoporoids are mostly surrounded by wackestone to fine-grained packstone (LF1-S1) which is comparable with the Iberian basin where the metazoans are distributed a mud-dominated matrix. 2- The occurrence of high energy intraclastic- bioclastic rudstone- floatstone facies (LF1-S2) in low-energy environments in MSL is comparable with Iberian basin where the high-energy flank facies occurred in a quiet environment, which in both cases can be interpreted as a result of internal waves. Al- Awwad and Pomar (2015), studied the origin of the rudstone- floatstone beds in Upper Jurassic Arab- D Formation, Saudi Arabia. The authors proposed a ramp depositional settings where the outer ramp was dominated by deposition of muds, interbedded with high energy rudstone- floatstone deposits. In this case, the generation of these high-energy beds in a context of low energy ambient interpreted to be a result of internal waves. This is compatible with the condition of occurrence of intraclastic-bioclastic debris (LF1-S1) in the case of MSL. However, in this example, the rudstone- floatstone beds were deposited in deeper part of the ramp where no associated buildups reported.

2-7- Conclusion

1- Along the deeper part of upper Jurassic- lower Cretaceous marginal facies of Monte Sacro Limestone, Gargano Promontory (southern Italy), three main lithofacies have been distinguished: LF1- stromatoporoid-rich facies, LF2- stromatoporoid-coral facies, and LF3- stromatoporoid- microbial facies. Stromatoporoid-rich facies (LF) are characterized by abundant growth of *Ellipsactinia* sp. and *Sphaeractinia* sp. in a low-energy mud-dominated matrix (wackestone to fine-grained packstone) (LF1-S1) with embedded rudstone-floatstone within higher energy intraclastic-bioclastic packstone-grainstone (LF1-S2). The organization of stromatoporoids, matrix-dominated fabric and lack of rigid framework share the characteristics of cluster reefs. Toward basin, a range of branching coral colonies is associated with stromatoporoids mainly *Ellipsactinia* sp. and *Sphaeractinia* sp. (LF2) distributed in wackestone to packstone matrix (LF2-S1) and

tabular form stromatoporoids and corals occur within a wackestone matrix rich in radiolarian (LF2-S2). In the deeper part of margin, the stromatoporoids accompanied with stromatolite-like mats (stromatoporoid- microbial facies) and surrounded by wackestone to fine-grained packstone.

2- Nutrients and light availability as well as hydrodynamic energy, are the most important factors controlling the development of this type of buildups during the Late Jurassic. In Monte Sacro Limestones, a mild oligotrophy to moderate mesotrophy condition is proposed for stromatoporoid-rich buildups. The lack of light-dependent components in studies facies shows that the light penetration was not enough and the stromatoporoid-rich buildups were developed in pure carbonate environments in a mesophotic settings.

3- In Monte Sacro Limestone, as well as other intra-Tethys stromatoporoid-dominated facies, the high amount of debris-rich facies indicates that these buildups were prone to a range of episodic high-energy events. While no evidence of surface storm waves has been seen (lack of shallow depth components), the turbulence events can be related to internal waves. Internal waves affected the buildups in two main ways: producing the debris-rich facies of LF1-S2 and pumping the nutrients needed by metazoans (mainly stromatoporoids) to grow (LF1-S1). These effects can be also found in other carbonate systems developed during other geological time intervals.

The most part of chapter 2 text and Figures: 2-1, 2-2, 2-41 to 2-54 are extracted from the published work:

Harchegani, F.K., Morsilli, M., 2019. Internal waves as controlling factor in the development of stromatoporoid-rich facies of the Apulia Platform margin (Upper Jurassic-Lower Cretaceous, Gargano Promontory, Italy). Sediment. Geol. 380, 1–20. https://doi.org/https://doi.org/10.1016/j.sedgeo.2018.11.011

Chapter 3

Case study 2

Late Oligocene (Chattian): Grotta San Michele Limestones, Gargano, Italy and Asmari Formation, Zagros Basin, Iran

3-1- Introduction

Mesophotic corals are light- dependent corals communities occur in the deepest part of the photic zone, ranging from 40 m to more than 150 m depths in tropical and sub-tropical regions (Kahng et al., 2014; 2017). In the last decades, the shallow coral reefs (> 40 m) have suffered extreme degradation due to anthropogenic factors that negatively impact the growth of these shallow-water reef communities. Therefore, the study of modern deep- water mesophotic corals have been received an increased interest by ecologists (Lesser et al., 2009; Kahng et al., 2010; Bongaerts et al., 2011; Kahng et al., 2014; Papastamatiou et al., 2015; Kahng et al., 2017; Feldman et al., 2018; Rocha et al., 2018). However, the mesophotic corals have been poorly documented from sedimentary records during the geological periods (Morsilli et al., 2012.

Based on bathymetric position of modern light-dependent carbonate communities, mesophotic zone has been defined to be located below the normal wave base where the light is sufficient for coral growth (Liebau, 1984, Pomar et al., 2012, Pomar et al., 2017). Mesophotic zone is positioned between euphotic zone in shallow part and oligophotic and aphotic zone in the deepest part. The depth range of euphotic zone (very good light and with high wave energy) is defined by the presence of modern seagrasses and non-dasyclad green algae. The lower limit of *in-situ* green algae is corresponded to lower limit of eupotic zone and defined by chlorocline (sensu Liebau, 1984). While, the base of oligophotic (sufficient light for coralline red algal growth), is identified by the deepest occurrence of *in-situ* coralline red algae, rhodocline (sensu Liebau, 1984).

The similar ecological demands between modern coral reefs and Cenozoic corals (Pomar et al., 2017) can enhance our knowledge about the palaeoecological conditions favoured by ancient mesophotic coral communities to grow. *Zooxanthellate* corals and larger benthic foraminifers (LBF) considered to have mixotrophy nutrition strategies. They host symbiontic microalgae which can obtain trophic resources by both photosynthesizing and feeding (Hallock, 1981, 2001). Most scleractinian–zooxanthellae communities tend to thrive in warm and shallow (highly illuminated) water in tropics/ subtropics (Hallock & Schlager, 1986; Schlager, 2000, 2003; Hallock, 2005). Pomar et al., 2017 discussed that food source and water turbulence are the main two factors for *zooxanthellate* corals buildups to grow.

Recently, the role of internal waves, as a source of water turbulence, has been considered as a useful tool in interpretation of mesophotic carbonate communities (Morsilli et al., 2012). Internal waves are waves that propagate at the depth of pycnocline (Pomar et al., 2012; Shanmugam, 2013),

a boundary layer between two different density water masses (e.g. Munk, 1981; Apel, 2002). The breaking of internal waves along continental margin and slopes creates high energy turbulence carry nutrients at the depth where the pycnocline meets the sea floor (Leichter et al., 2003; Lamb, 2014; Arthur and Fringer, 2016; Woodson, 2017). The upper part of pycnocline is typically coincides with high plankton concentration zone (trophic recourse) and high turbulence internal waves (e.g., White and Dorschel, 2010; Hernández-Molina et al., 2011). The top of pycnocline also coincides with nutricline, which represent a pick in chlorophyll and phaeophytin (degrading chlorophyll) concentrations (Hallock et al.,1991). The presence of internal waves can be associated with high concentration of phytoplankton and zooplankton (Leichter et al., 1998) as well as vertical exchange of nutrients and heat, which can enhance the biological productivity (Alford et al., 2015). As a results, suspension-feeder metazoans such as corals tend to produce buildups at the bathymetry of pycnocline where the trophic source and turbulence can be both supplied by internal waves (Pomar et al., 2017).

Extensive coral buildups were developed in central Tethys realms during the four time intervals of Cenozoic time, Danian, Bartonian–Priabonian, early Chattian, and late Tortonian–early Messinian (Pomar et al., 2017).

After a warm period during the Eocene, the Oligocene time was characterized by a significant global cooling trend followed again by a warmer climate during the Miocene (Pomar et al., 2014). The larger benthic foraminifers (LBF) were noticeably dominated in the warm Eocene accompanied by high diversities scleractinian corals, while the dramatic cooling trend during the Oligocene allowed extensive coral buildups to flourish, particularly during the Late Oligocene (Budd, 2000; Perrin, 2002; Perrin and Bosellini, 2012). During the Early Oligocene, the levels of carbon dioxide (CO_2) in the atmosphere increasingly dropped, but through the Late Oligocene the atmospheric CO_2 reached to pre-industrial level (Pagani et al., 2005). Hallock (1996) discussed that the dramatic drop of atmospheric CO_2 concentration during the Oligocene can be a possible role to in rapid development of reef- builders compare with the Eocene. As well as corals, Coralline-red algae and larger benthic foraminifers (LBF) were also among the main carbonate-producing biotas during the Oligocene (Aguirre et al., 2000; Pomar and Hallock, 2008). However, Coralline-red algae became globally the main wide separated carbonate communities during the Early to Middle Miocene period (Halfar and Mutti, 2005).

During the Late Oligocene, the extensive coral reefs were developed along the Tethys realms (Frost, 1977; Frost et al., 1983) as well as in the Caribbean and the Indo-Pacific regions (Budd, 2000; Wilson, 2008). In the Mediterranean Tethys, a range of mesophotic corals were spread during the Oligocene time and have been reported by several authors (Bassi and Nebelsick, 2010; Nebelsick et al., 2013; Pomar et al., 2014; Van Buchem et al., 2010; Shabafrooz et al., 2014, Dill et al., 2018).

The Late Oligocene (Chattian) coral-rich facies cropped out in the Gargano promontory (Apulia Carbonate Platform), Italy, known as San Michele Limestones. Also, in the central Tethys, the Oligocene-Miocene Asmari Formation were deposited along the most part of Zagros Basin (Lurestan, Izeh, Dezful Embayment, Fars, High Zagros), SW Iran. The Asmari Formation also host one of the biggest oil reservoirs in the Middle east, and it considers as one of the most important subject for exploration sedimentologists to study. The visible depositional geometries and well-preserved stratigraphic architectures of Oligo-Miocene Asmari Formation in Izeh zone, make it an ideal case study in order to study the position of Chattian Coral buildups along depositional profile. The aim of this chapter is to 1-to describe the vertical and lateral distribution of the Late Oligocene coral-rich facies in the both Gargano, Italy and Zagros Basin, Iran, and 2-to test the potential role of internal waves on formation of studied coral-rich facies in Gargano and Zagros area.

3-2- Asmari Formation (Zagros Basin, Iran)

Geological setting and stratigraphy: Iranian plate has been divided to eight structural basins: Zagros, Sanandaj Sirjan, Uromiyah Dokhtar, Central Iran, Alborz, Kopeh dagh, Lut and Makran (Alavi, 1991, 2004; Heydari, 2008). The Zagros basin is located along the North-Eastern margin of the Arabian plate with the main NW–SE trend extended from Turkey to Hormuz strait in the Persian Gulf and it subdivided into 5 tectono-stratigraphic zones including Izeh, High Zagros, Fars (Interior and Costal Fars), Lurestan and Dezful Embayment (Heydari, 2008; Farzipour- Saein et al., 2009). The Izeh zone is situated in a simply folded zone of Zagros and numerous Asmari Formation outcrops are located in this part (Van Buchem et al., 2010). The studied outcrops of this paper are located in the eastern part of Izeh zone (Fig.3-1).

The creation of NW–SE trending foreland basin during the Late Cretaceous compression phase was an important stage as it controlled the major sedimentation of Arabian Plate during

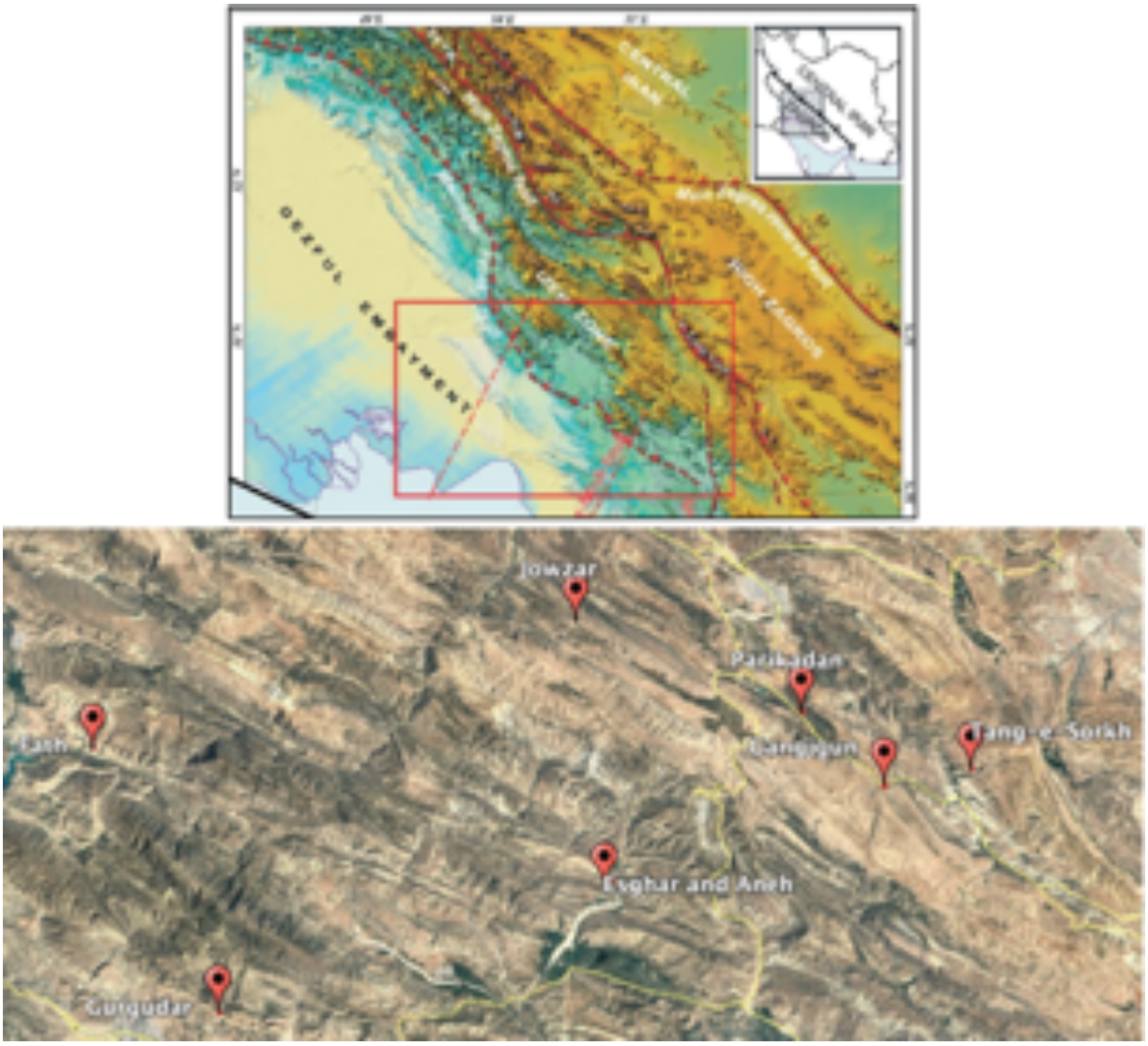

Figure. 3-1- The figure shows the position of the studied area located in the Izeh zone of Zagros basin, SW Iran.

Paleogene (James&Wynd, 1965; Motiei 1993; Sherkati & Letouzey, 2004 Van Buchem et al., 2010). The Paleocene-Eocene platform was initially developed and prograding along the margin of the Arabian Plate while the Oligocene-Miocene Asmari carbonate platform continued to be deposited until the final stage of the closing of the NeoTethys Ocean and following collision phase during the late Miocene (Homke, 2004; Van Buchem et al., 2010).

In the Izeh zone, the lower boundary of the Asmari Formation is in contact with the Pabdeh Formation which is of Paleocene-Oligocene age (Fig. 3-2), but in central Lurestan this formation overlies the Late Eocene Shahbazan Formation and in Interior Fars it shows a paraconformable

contact with the Jahrum Formation (Eocene) (Fig. 3-2). In certain areas, as in the Izeh zone, the Asmari Formation is covered by anhydrites of the Gachsaran Formation, Early Miocene in age, and in interior Fars the Asmari Formation is covered by Razak Formation of Early Miocene and Jahrum Formation in Tang-e- Abolhayat section. The base of the Asmari Formation is Lower Oligocene (Rupelian) in some area and younger (Chattian) in other parts, also the top has a different stratigraphic distribution from upper Chattian to Lower Miocene (Aquitanian-Burdigalian). In the Fars zone, Asmari Formation is Rupelian to Chattian, instead in Izeh and Dezful embayment, the age of Asmari Formation is Rupelian to early Burdigalian. In Lureztan zone (Lali section), the Asmari Formation is Chattian to Burdigalian (Motiei, 1993; Vaziri-Moghaddam et al, 2006; Sadeghi et al, 2011; Shabafrooz et al., 2015).

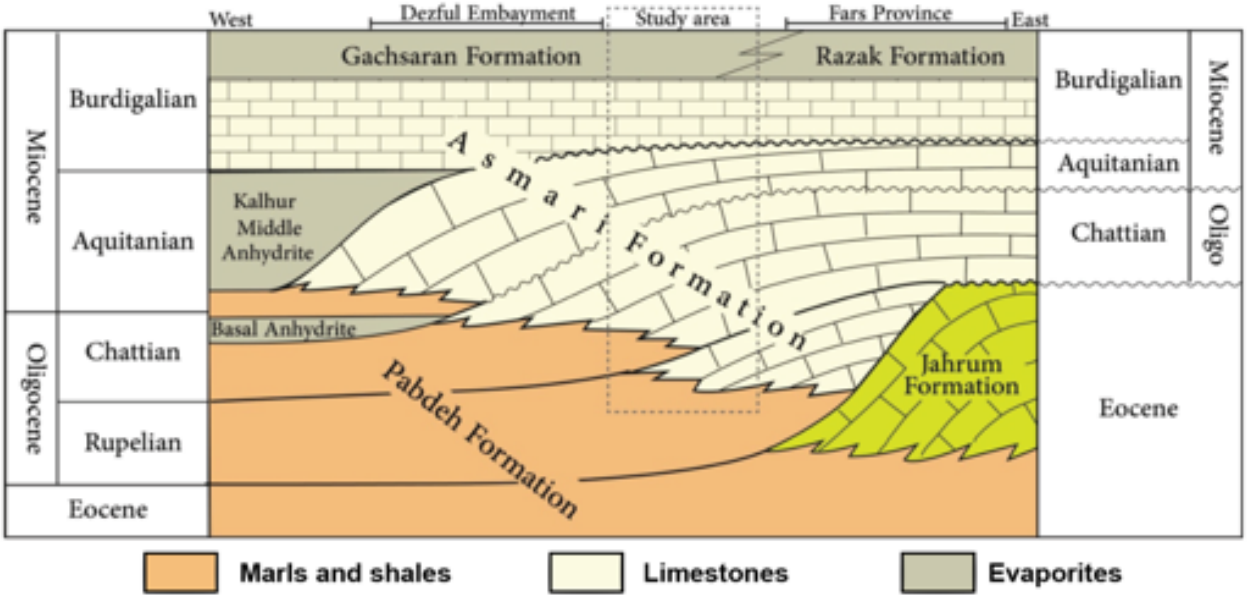

Figure. 3-2- The stratigraphic framework of Asmari Formation and their boundaries with Pabdeh Fm in different zone of Zagros basin (from Shabafrooz et al., 2015). The studied area is shown by black square.

In the Izeh zone, the depositional system (interpreted as a carbonate ramp) was dominated by Nummulites- rich facies (NU unit) during the Rupelian and by Lepidocyclinid and nummulitids rich facies (UN unit) during the Rupelian/Chattian. During the Chattian, the system was dominated by coral buildups and red algae (CB unit) and during the Early Miocene time, the platform was characterized by porcellaneous foraminifers and coralline red algae (BF unit) (Van Buchem et al., 2010; Shabafrooz et al., 2015) (Fig.3-3).

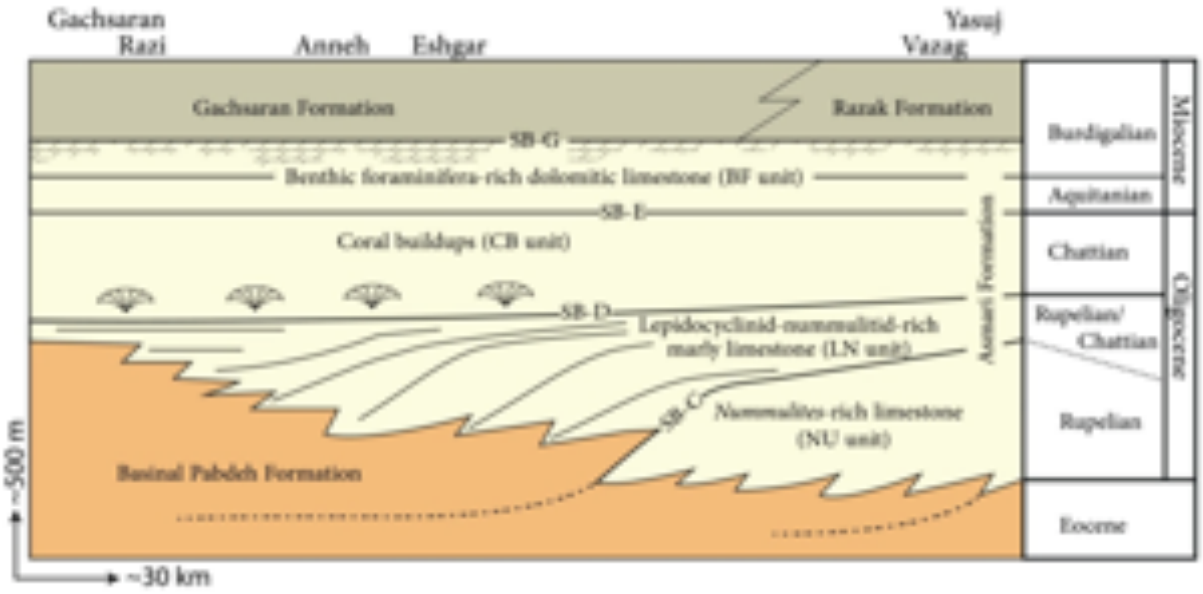

Figure. 3-3- The figure illustrates the different stratigraphic units of Asmari Formation and their lateral changes (from Shabafrooz et al., 2015).

3-3- Methods

Sea-cliffs, road-cuts with three logged stratigraphic section allowed analysing facies distribution of the Grotta San Michele Limestones in the two stadied areas: Ferrovia section and Grotta S. Michele. In Asmari Formation, the excellent visible depositional geometry allowed to describe the vertical and lateral changes of facies and determine the position of Chattian coral buildups along the depositional profile. We select three locations where the coral buildupas geometry showing excellent preservation. A total number of 88 samples for thin sections has been collected for textural characterization and identification of skeletal components from both Gargano area and Zagros basin. In Gargano the sampling took placed along the dip direction. Each samples collected based on lateral and vertical change of facies. In Asmari formation, the samples were mostrly collected from the Chattian coral buildups, in order to describe the different type of components associated with corals matrix. Components abundance has been estimated and grouped in five categories: rare (Less than 1%), present (2%–25%), common (26%–50%), abundant (51%–75%) and very abundant (76%- 100%). Carbonate facies were classified according to the Dunham (1962) and Embry and Klovan (1971). Light zonation of depositional environments (oligophotic, mesophotic and euophotic) and their relative boundaries has been defined following Pomar (2001) and Morsilli et al. (2012).

3-4- Stratigraphic sections and facies

3-4-1- Asmari Formation

3-4-1-1- Chattian coral buildups unit

The lower boundary of Chattian Coral buildups unit in Asmari Formation is characterized by diminish of Lepidocyclinid rich unit (LN) especially *Eulepidina* sp. and increasing of different species of *Archaias* sp. and *Miogypsina* sp. This unit is equivalent to Chattian according to Shabafrooz et al. (2015) and Van Buchem et al. (2010). The Coral buildups unit is also characterized by important changes of carbonate producer's communities. A notable decrease of large hyaline foraminifers to large increase of corals and red algae which they arranged in thick-bedded to massive limestones. These kind of changes in carbonate communities resulted in development of unique and complex depositional geometries in Asmari Formation successions. These coral buildups are mainly develop on the LN unit. The coral buildups are well exposed in Eshgar, Aneh and Gorgoda section.

3-4-1-1-1- Eshgar section

In this section, the Asmari Formation overlain the inter-bedded limestone and marl Pabdeh Formation. The Chattian succession in this area is characterized by development of thick coral buildus with 100-150 meters in diameters and about 60 meters' height (Fig.3-5). These buildups composed of thick-bedded to massive limestone with isolated coral colonies and small coral patches along with red algae. The thickness of coral buildups decrees upward and gradually they pass to m- thick bedded. These coral buildups are mainly developed on the the Lepidocylinid-rich under layer unit (UN). This section is also characterized by development of thick-bedded flank facies (70-80 meters) with 15º dip to SW. Toward the basin (Figs. 3-6).

Figure. 3-4- Partial stratigraphic logs from the studied area in Zagros basin showing the lateral changes of different facies along the section. See the legend for description.

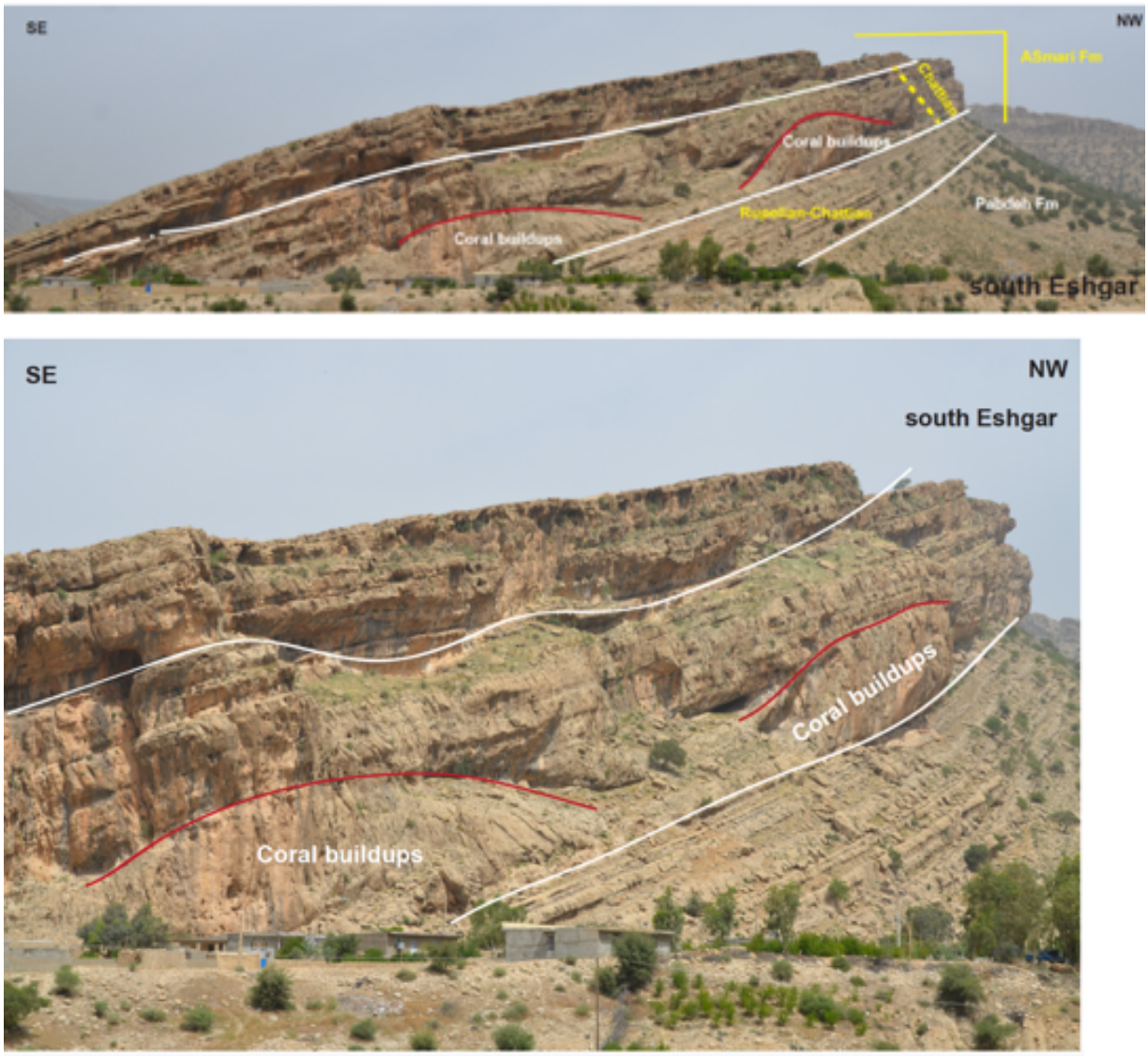

Figure-.3-5- Depositional geometry and position of coral buildups is Eshgar anticline.

3-4-1-1-2- Aneh section

In this area, the boundary between Asmari Formation and Pabdeh Formation is gradual. The coral builups unit is developed in 70-80 meters in diameter and 70 meters height downlaping the under layer unit. This coral buildups unit is characterized by thick-bedded to massive limestone associated with isolated coral colonies and small coral patches. Coral occur in growth position, with domal, irregular massive or branching form. coral buildups arranged coral floatstone with a fine-grained packstone matrix. Most abundant components are non-articulated red algae, small benthic foraminifers and small fragments of LBF. These coral buildups architectures show alternating episodes of aggradation and aggradation/progradation.

Aggradation occurs mostly in the lower part, while toward the top, the sediments deposited on the flank of the coral buildups display progradation geometries and toplap at their top (Fig.3-7).

Figure. 3-6- The figure shows the complex depositional geometry of Asmari Fm in Eshgar anticline and the position of coral buildups. The buildups show aggradation as result of different growth phase.

3-4-1-1-3- Gorgoda section

In this area, Asmari Formation covered Pabdeh Formation and characterized by thick-bedded clinoforms (90 m) with 15º dip toward NE-SW (Fig.3-8). These clinoforms are also reported from Van Buchem et al. (2010) and Shabafrooz et al. (2015). The clinoforms are represented by argillceous- marly limestones with planner bedding. On the clinoforms unit, coral buildups are developed as 80- 100 m thick-bedded to massive limestones. They are characterized by the occurrence of isolated coral colonies and small coral patches (Fig.3-9). The internal sediments mostly consist of coral floatstone with a fine-grained packstone matrix. Most abundant components are red algae and small benthic foraminifers.

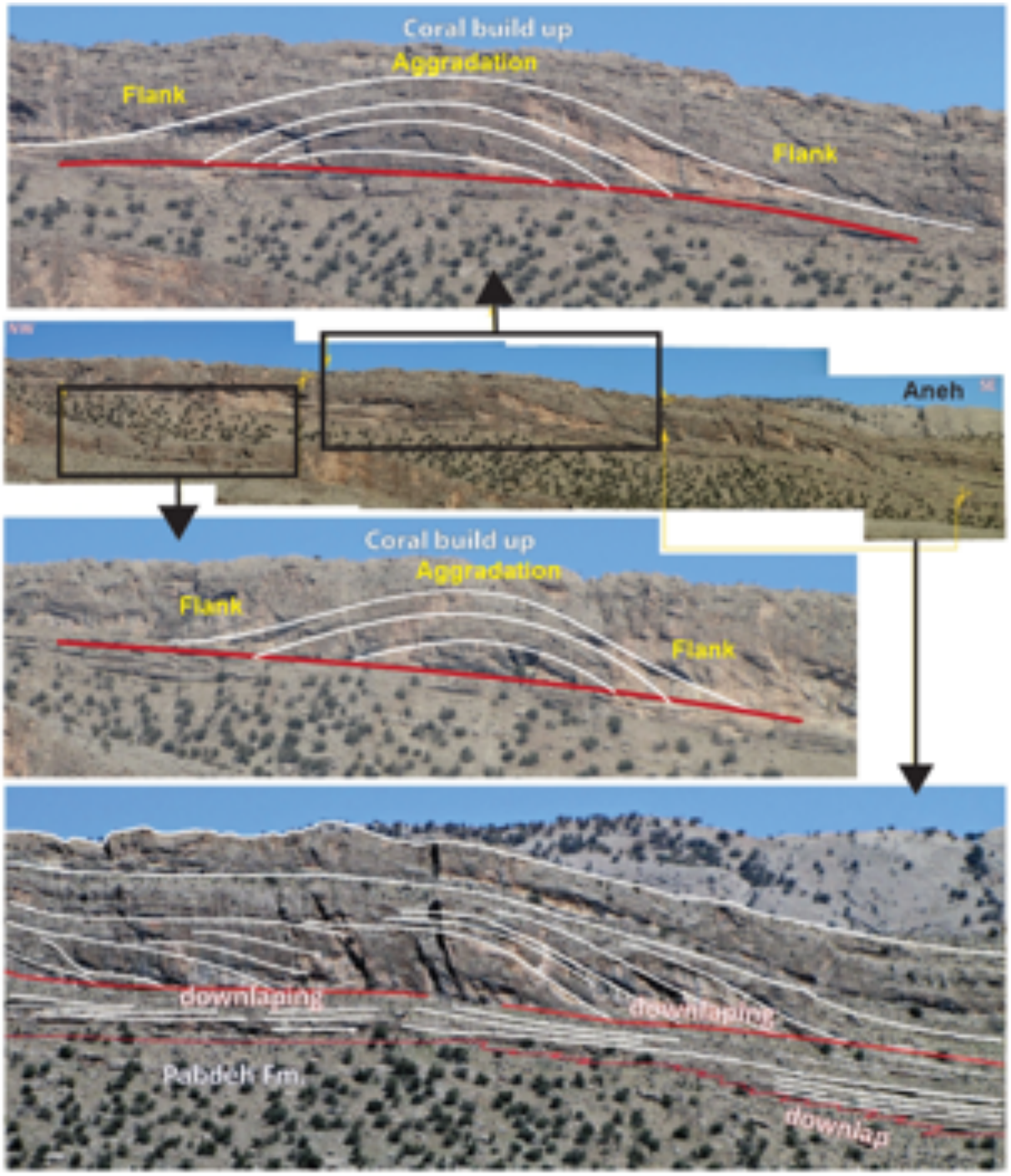

Figure. 3-7- The complex depositional geometry of Asmari Fm in Aneh anticline showing the aggradation of coral buildups and how they developed the previous units. The last figure indicates the geometry of flank facies (slightly modified from Shabafrooz et al., 2015).

Figure. 3-8- The geometry and position of coral buildups in Tange-Gorgoda section

3-4-1-2- Facies description

Coral buildups (CB) were mainly developed during the Chattian in Asmari Formation. In this unit, the corals show different growth forms such as branching and domal morphology (Fig.3-10A-D). The coral colonies, where they found, are mostly in growth position (Fig.3-10) or slightly displaced but still *in-situ* form. Sparsely distribution of corals in a mud-dominated matrix and the lack of rigid framework fits these coral builups to cluster type fabric (*sensu* Riding 2002). The inter-coral sediments are wackestone to fine-grained packstone. Red algae are abundant in this facies and they occur mainly the non-articulate form, but articulate form is also seen as a minor type of red algae. the corals in this facies are strongly encrusted by red algae (Fig.3-11). The rare to present foraminifers are miliolids, *Lepidocyclina*, *Heterostegina*, *Amphistegina* as well as encrusting foraminifers such as *Planorbulina*. Ostracods, bivalves, bryozoan and echinoids are also present.

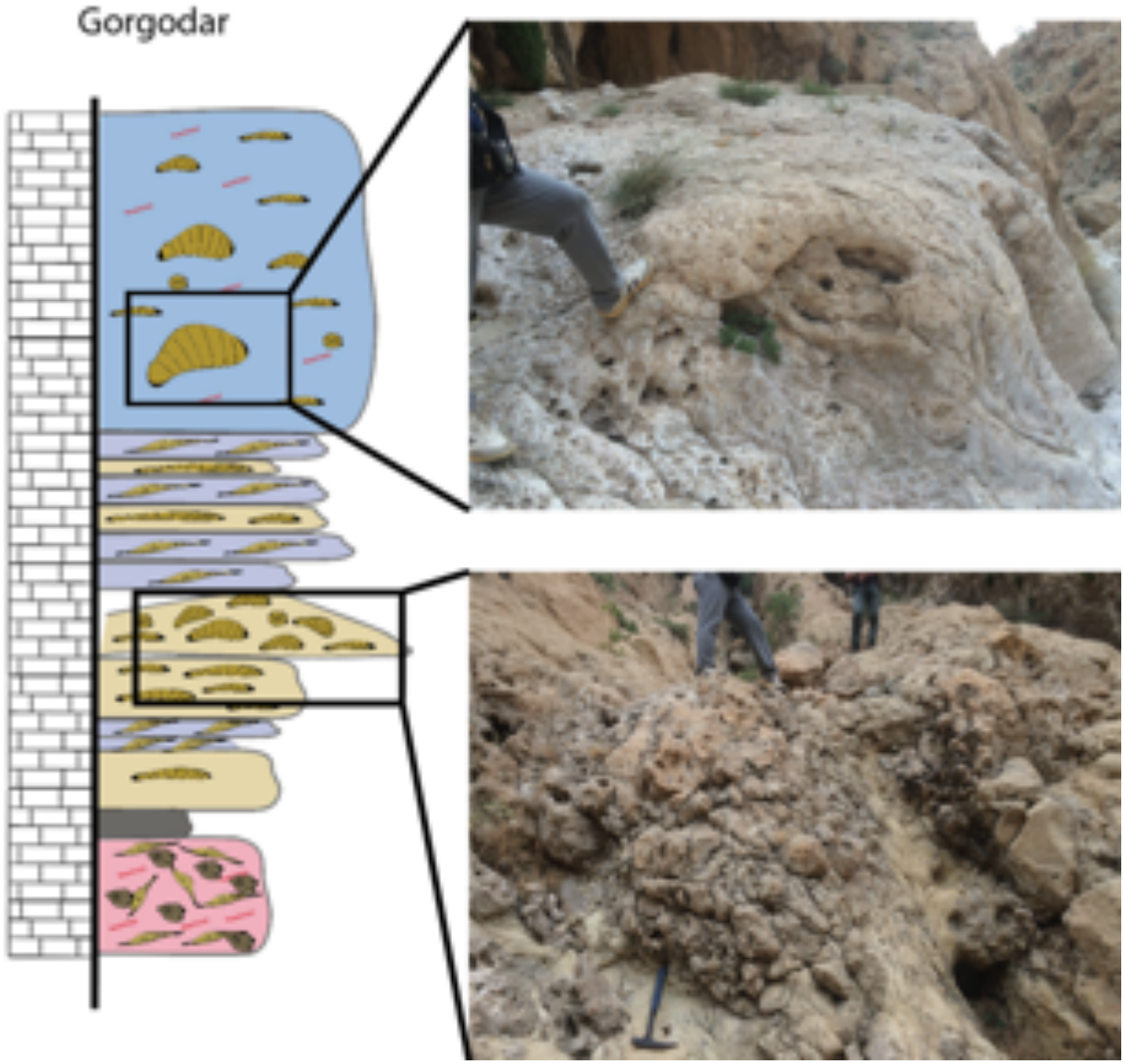

Figure.3-9- Isolated coral colonies developed in CB unit in Tange Gorgod. Corals developed in mud-dominated matrix (upper image). Very packed coral mound interval developed at the base of Asmari Fm (lower image)

Chattian coral facies associations displays two subfacies: 1- coral-coralline red algae boundstone/framestone and 2- coral-coralline red algae rudstone/floatstone. coral-coralline red algae boundstone/framestone facies is characterized by presence of *in-situ* coral colonies showing branching, platy and domal morphologies. The red algae are common and they mostly encrusting corals and benthic foraminifers and sometimes they occur as Rhodolith. Inside the muddy matrix between the corals, the larger benthic foraminifers such as rotaliid and *Amphistegina* and porcelanous foraminifers like miliolids, *Archaias* and *Borelis* are distributed. The second facies

(coral-coralline red algae boundstone/framestone) composed of large fragments (about 1.5 cm and it can reach to 10 cm) of corals and red algae as well as larger benthic foraminifers like *Amphistegina* and *Operculina.* The components are distributed in a muddy matrix that is contains rare amount of gastropod, echinoid, *Archaias*, Miliolids and Rotaliids.

In more distal part, Allahkarampoor et al, 2018 defined the coralgal floatstone-rudstone/ boundstone facies and he described two subfacies: 1- Non- articulate red algae floatstone-rudstone which were deposited during Rupelian to early Chattian and composed of fragments of corals as well as in situ form of coral colonies with coarse-grained packstone to wackestone matrix. The secondary present foraminifers are *Neorotalia, Miogypsinoids, Nephrolipidina, Heterostegina and Spiroclypeus*. The second subfacies is 2- coral boundstone (Chattian age). In this facies the corals show different growth types such as platy, domal and branching. (subfacies 2 is buildup body and 1 is flank). The muddy matrix between corals, cluster fabrics of buildups as well as occurrence abundant non-articulated red algae indicate that these buildups were developed under oligo-mesophotic condition.

3-4-1-3-Depositional environment

The depositional environments of Oligo-Miocene Asmari Formation in Izeh zone (Zagros Basin) has been studied in details by Shabafrooz et al., 2015 (Fig.3-12). According to the author, during the Chattian, the coral boundstone (CB unit) were developed in a ramp setting. The inner ramp was characterized by benthic carbonate community of seagrass factory within euphotic zone. The middle ramp coral colonies were mainly preserved in life position as well as some overturned colonies. The corals are floated in a matrix and they were not developed a rigid framework (cluster reef *sensu* Riding 2002). As a result, beddings can be recognized in this units. The flank of coral buildups is characterized by small coral debris in a coarse- to medium-grained facies composed of mesophotic components such as abundant fragments of large rotaliids (such as *Neorotalia* and *Nephrolepidina*) and coralline algae. The Mud dominated matrix indicates deposition in a quiet environment below wave action zone. Between the corals, the sediments composed of inner ramp components. Two depositional stages have been suggested, 1- coral buildups developed in

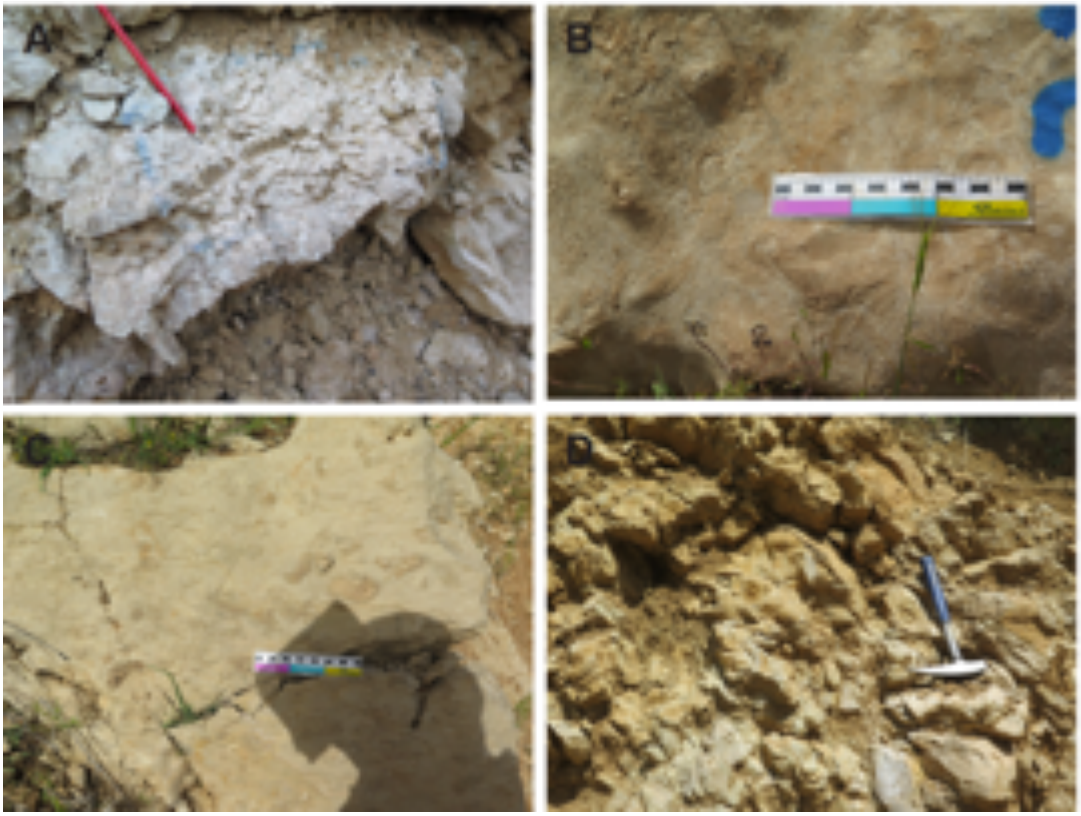

Figure.3-10- Figures show the different morphology of *in-situ* corals in Asmari Fm: A: phacheloid, B,C: massive and D: domal form

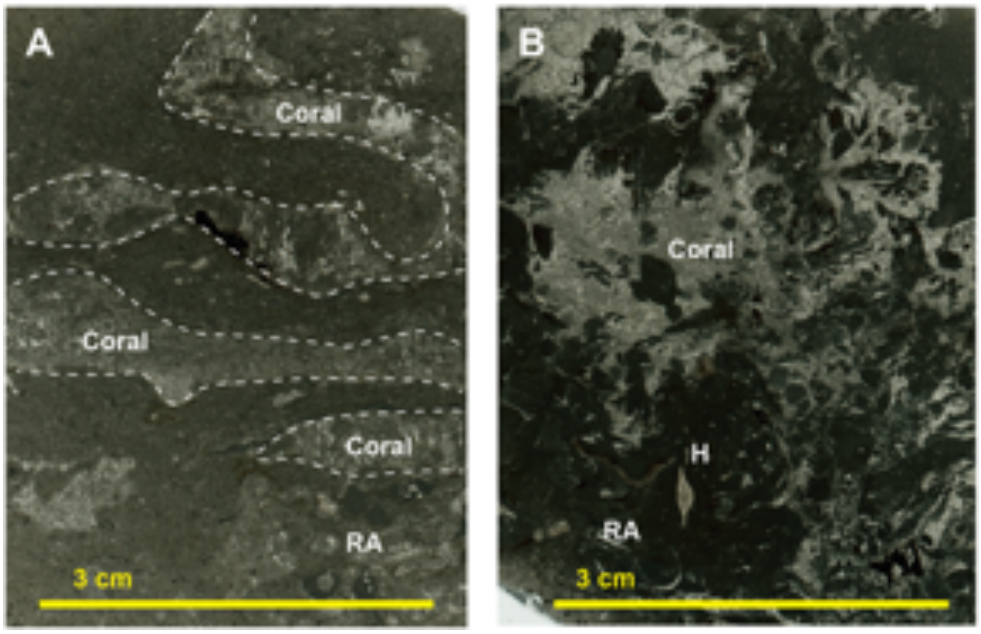

Figure. 3-11- Thin section images of coral-rich facies in Asmari Fm. A: corals distributed in muddy matrix. B: corals accompanied with non-articulate red algae (RA) and *Heterostegina* (H).

mesophotic condition in middle ramp setting and 2- the falling sea level allows euphotic seagrass components of inner ramp to be deposited between the corals. Toward the basin, the coral buildups pinched out with mud- dominated packstone to wackestone facies with local interbedded small coral colonies and mounds and marls with planktonic foraminifers (Fig.3-12). Figure 3-13 shows the distribution of marine carbonate producers during the Chattian Asmari Fm.

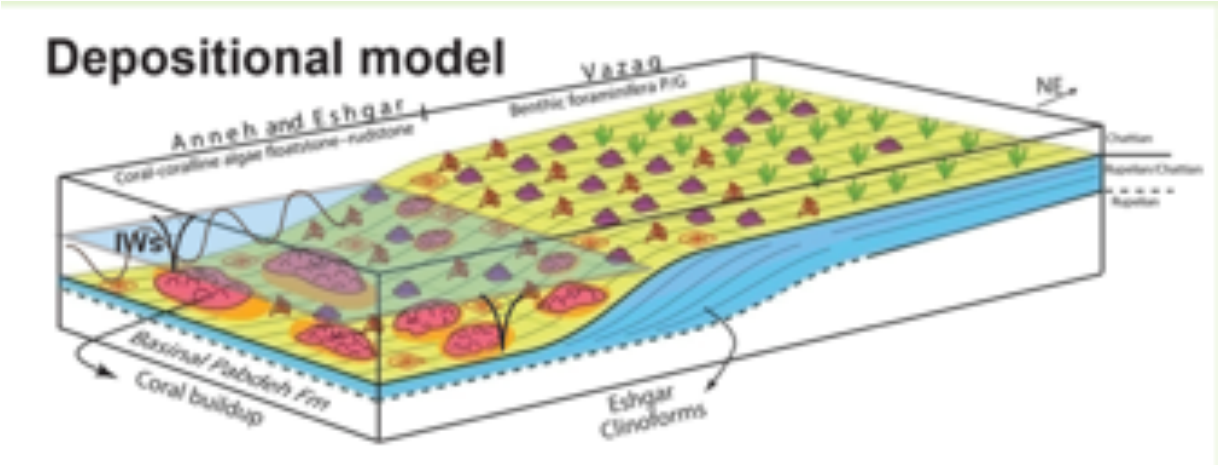

Figure. 3-12- Depositional model for Chattian coral buildups unit in Eshgar and Aneh section. The internal waves can propogate at the depth pf pycnocline and result of development of coral buildups in studied section. (slitly modified from Shabafrooz et al., 2015).

3-4-2-Grotta San Michele Limestones (GSML)

Geological setting and stratigraphy: The studied outcrops of GSML is located along the margin of ACP exposed in Gargano area. ACP extended from the southeastern Abruzzi region across Apulia and the Strait of Otranto to the Greek islands of Cephalonia and Zante (Bosellini, 2002). This carbonate platform is the foreland of both the Apennine and the Dinaric thrust and fold belts (Bernoulli, 2001). It is bounded on both sides by basinal deposits. The western margin of the platform is downfaulted and buried underneath terrigenous sediments of the Apennine foredeep and the adjacent Apennine chain. Instead, the eastern margin of the platform lies 20–30 km offshore from the present Apulia Coastline in the Adriatic Sea (Bosellini et al., 1999; Borgomano, 2000; Morsilli et al., 2017). The ACP mainly consists of Upper Jurassic to Eocene shallow-marine carbonates, and in the Gargano Promontory and the Maiella Mountain also by the coeval slope to basin facies (Bosellini et al., 1999; Borgomano, 2000; Bernoulli, 2001). The Grotta San Michele

Limestones have been recognized by Morsilli et al. (2005), and crops out along the northern border of the Gargano Promontory in some scattered outcrops of limited extension (Fig. 3-14, B), and lie unconformably over various Mesozoic unit, mostly Late Jurassic in age (Fig.3-15).

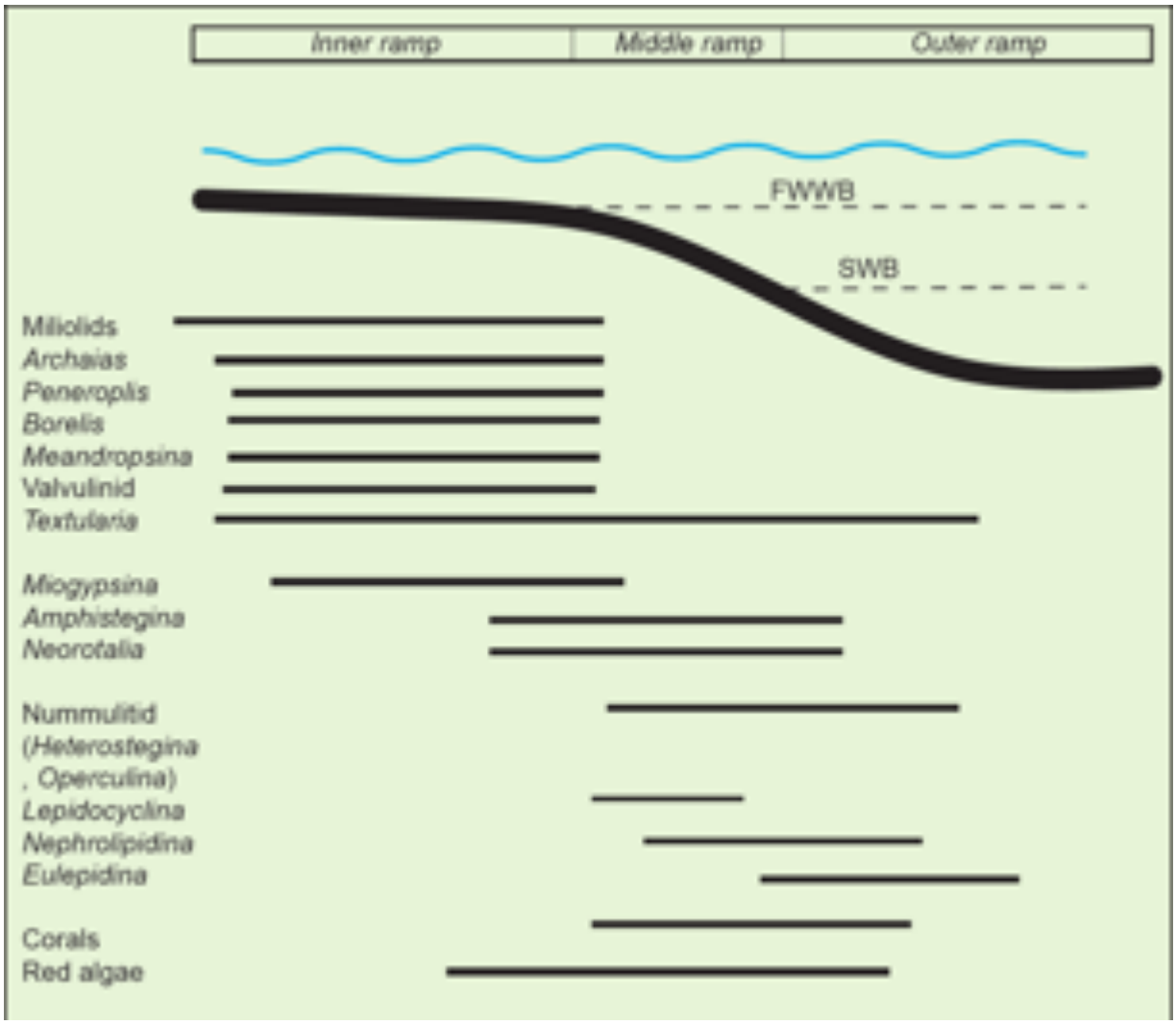

Figure. 3-13- Depositional profile and distribution of marine carbonate producers during the Chattian Asmari Fm,

This stratigraphic unit, about 28 m thick, mainly consits of white to pink wackestone to packstone, with thick beds rich in corals and red algae. The lower part of this unit (about 15 m thick) consist of an alternation of packstone to packstone/wackestone with abundant corals (*Porites* sp., *Stylophora* sp.) and various red algae genera (*Sporolithon* sp., *Lithoporella* sp., *Titanoderma* sp.), bryozoan, large benthic foraminifera (*Austrotrillina* cf. *asmariensis*, *Nephrolepidina* sp., *Lepidocyclina* sp., *Alveolina* sp., *Miogypsinoides* sp.), miliolids (*Quinqueloculina* sp., *Pyrgo* sp.), rotalids (*Planorbulina* sp., *Acervulina* sp., *Amphistegina* sp., *Cibicides* sp., *Ammonia* sp., *Elphidium* sp.), as well as textularids, peneroplids, soritids (*Sorites* sp., *Dendritina* sp.), some bivalvs, small gastropods and echinoids fragments. The upper part (about 13 m) consists mostly of wackestone with some red algae, bryozoan, rare coral fragments and some planctonic foraminifera as globigerinoids and globoratalids.

The presence of *Nephrolepidina* sp., *Austrotrillina* cf. *asmariensis* e *Miogypsinoides* sp. permits to assign a stratigraphic range between Chattian and Aquitanian p.p.

3-4-2-1- Ferrovia section

This area in located along the S-E trend of Ferrovia road cut of in the northern margin of Apulia Carbonate platform exposed in Gargano area (Fig.3-14). The lithology is represented by about 18 meters pinkish white to red color limestone with visible bedding with dip direction toward the east. The main lithofacies is characterized by coral floatstone distributed in muddy matrix. The corals not heavily stacked and not build a rigid framework which can fit the characteristics of cluster reef (*sensu* Riding, 2002). The corals are mainly developed as rubble of thin to thick branches, with some cm-sized coral colonies found in growth position (Fig. 3-17). The other components are bivalves and gastropods and red algae toward the end of the section. Figure 3-16 showing the main textures and relative abundance of skeletal and non-skeletal components and main facies along the Ferrovia section.

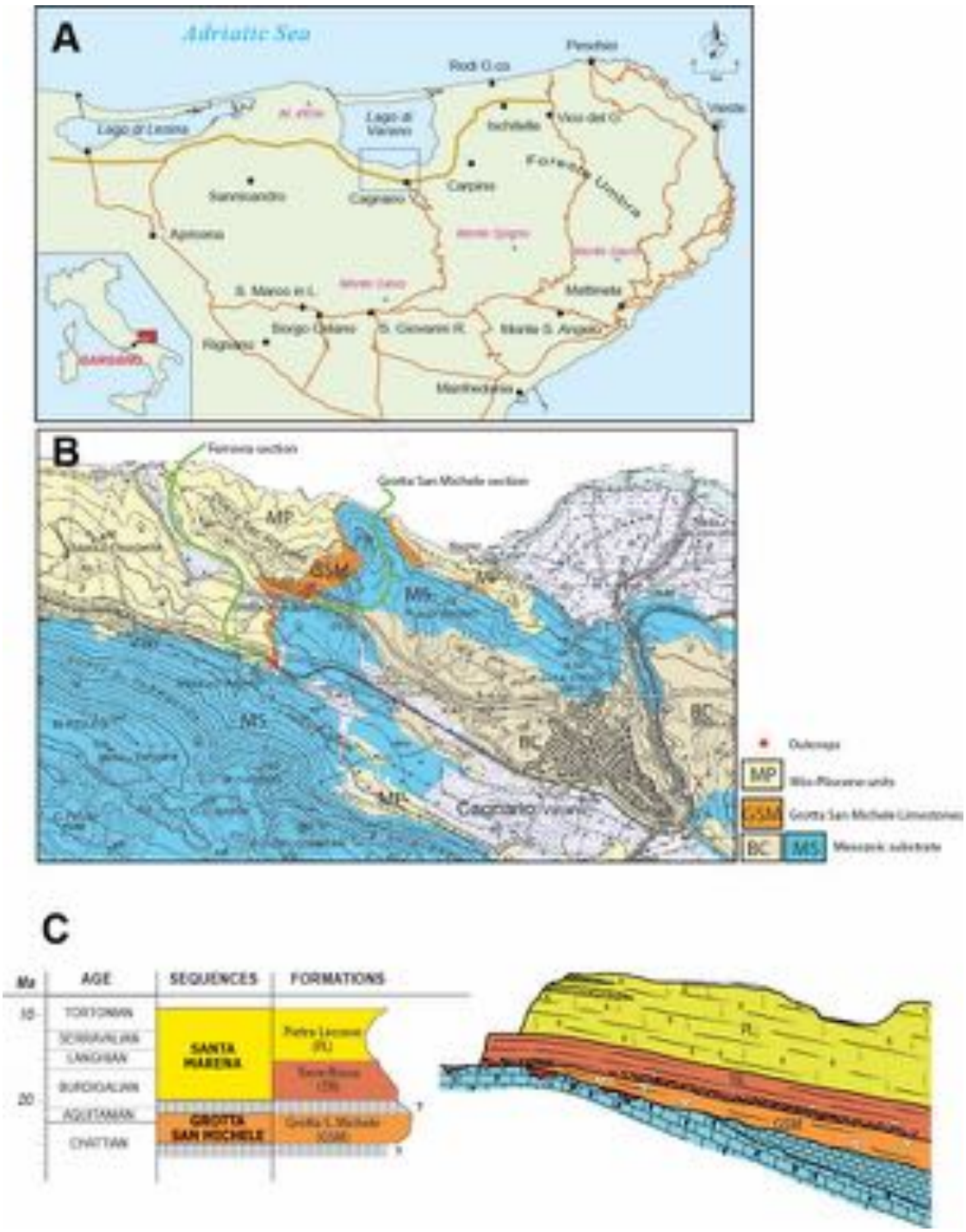

Figure. 3-14- A: Figure shows the position of studied area in Gargano promontory (black square), B: geological map of Gargano area showing the position of GSM outcrops (red stars), C: stratigraphic framework of Gargano area during the Oligocene and Miocene showing the GSM age from Chattian to Aquitanian.

Figure. 3-15- Field image shows the Late Oligocene GSM lie unconformably over Late Jurassic sequences

3-4-2-2- Grotta S. Michele section

This area is located Grotta S.Michele in GarganoVarano area in northern part of Gargano (Fig. 3-14). In this area The late Chattian sequences overlain the Upper Jurassic successions by an unconformity. The GSML is represented here by 11 meters white to pinkish white m-dm to cm-thick massive to bedded limestones. The corals are mainly ruble and reworked and distributed in muddy matrix and categorized as cluster reef (*sensu* Riding, 2002).

The corals are mostly show phaceloid morphology (Fig. 3-20) but massive form is also present. Some corals are arranged as dm-sized *in-situ* colonies but the majority of corals are organized as single form (Fig. 3-19). In this section, red algae are associated with corals. Other components are bivalves and gastropods. Two sections have been measured: GSM1 (Fig. 3-18) and GSM2 (Fig.3-19)

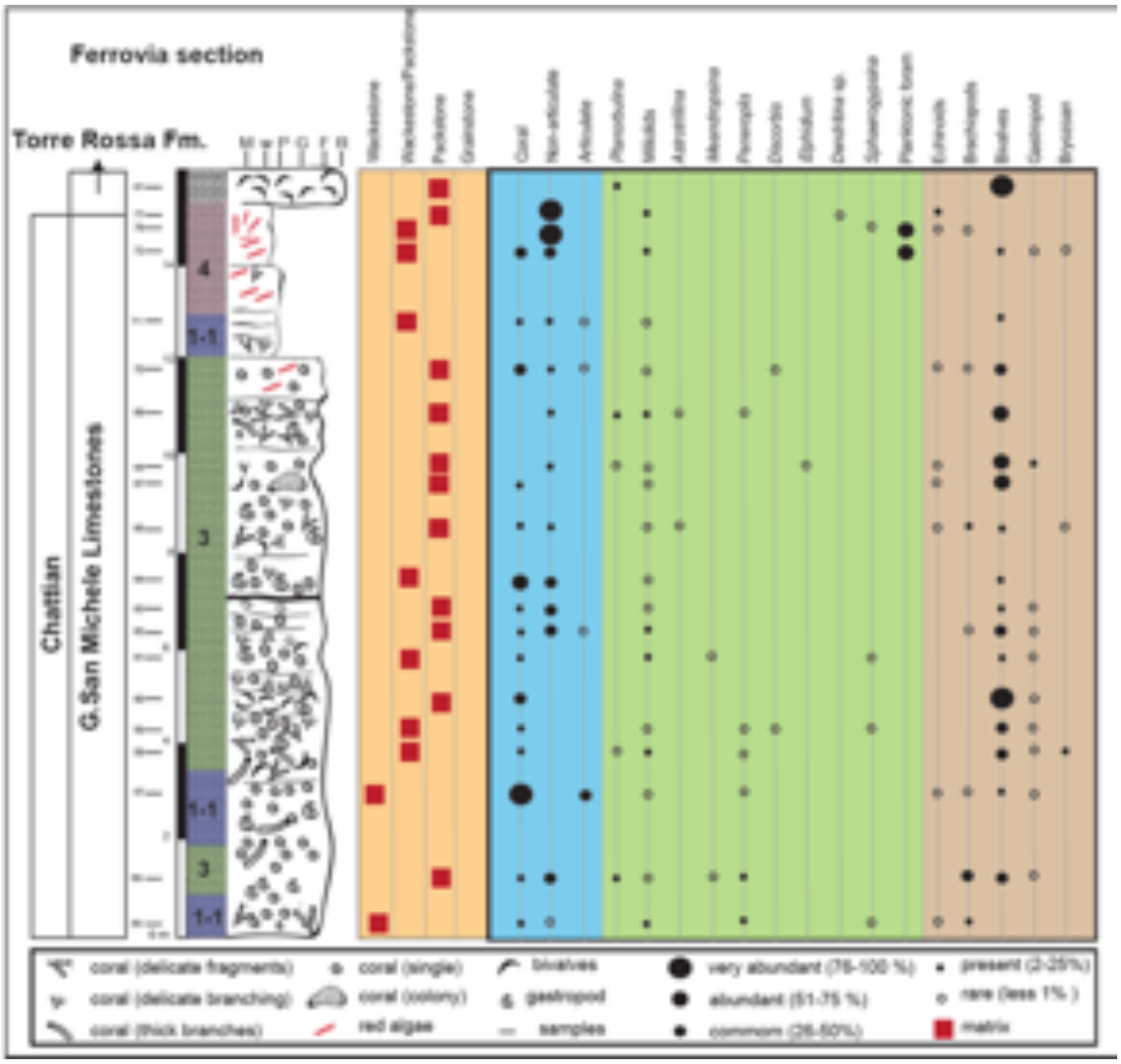

Figure. 3-16- Stratigraphic section of GSML in Ferrovia section, showing main textures and relative abundance of skeletal and non-skeletal components along the measured log.

Figure. 3-17- Field images of coral- rich facies in Ferrovia section: A: *in-situ* coral colonies in phaceloid form. B,C,D: Delicate and thick branches fragments of corals distributed in muddy matrix. E: Gastropods associated with corals. F: Bivalves associated with phaceloid form corals

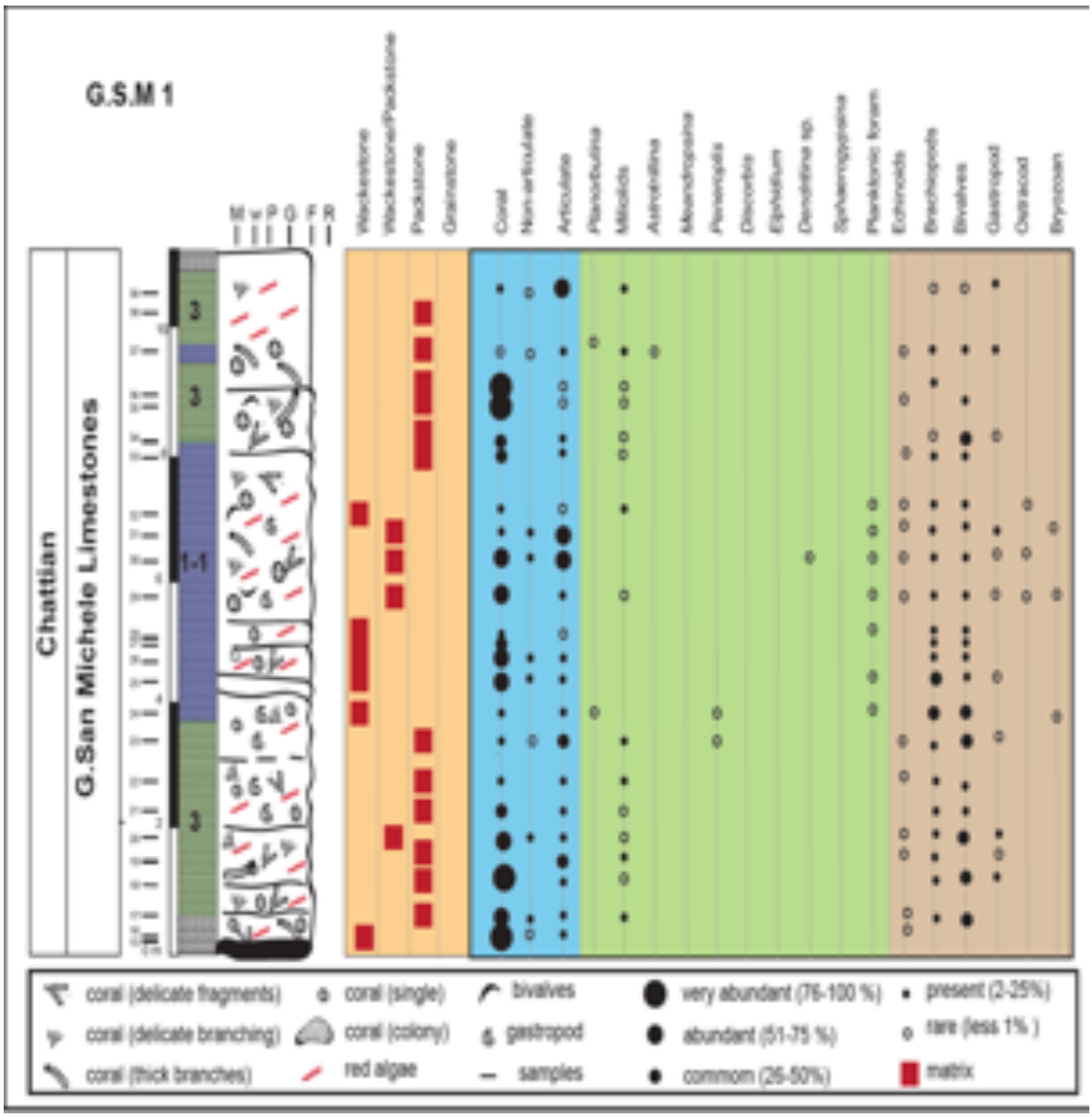

Figure. 3-18- Stratigraphic section of GSML in GSM 1 section, showing main textures and relative abundance of skeletal and non-skeletal components along the measured log.

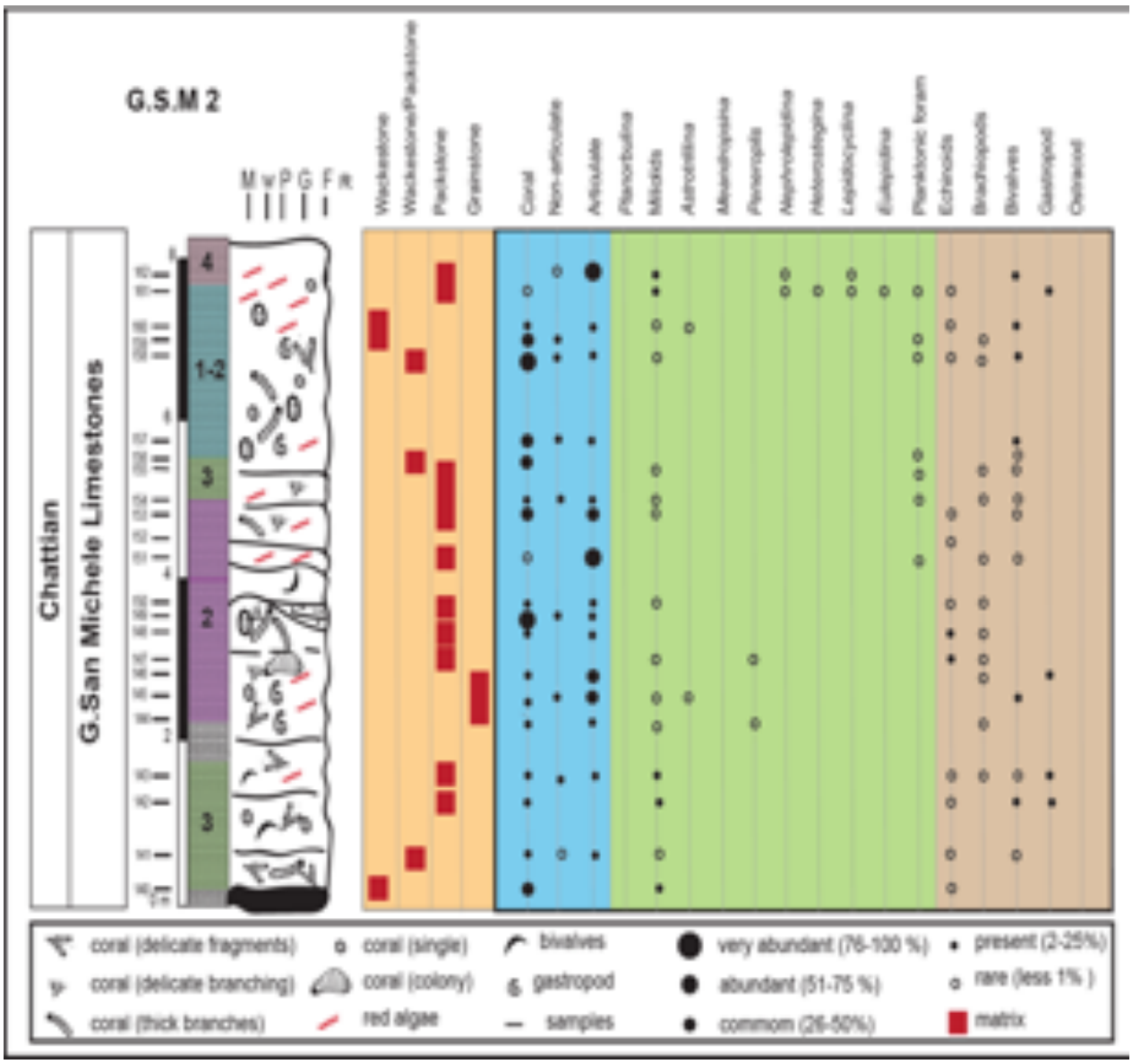

Figure. 3-19- Stratigraphic section of GSML in GSM 2 section, showing main textures and relative abundance of skeletal and non-skeletal components along the measured log.

3-4-2-3- Facies description

Based on texture and components four main facies have been described:

3-4-2-3-1- Coral wackestone to packstone facies: (C w-p)

This facies is characterized by dm to m-sized light pinkish to white limestone. In this facies, corals, mainly branching (*Actinacis*, *Goniopora*?, *Acropora*?) and phaceloid forms are distributed in a mud dominated wackestone to packstone matrix. Based on texture and components, two subfacies have been recognized:

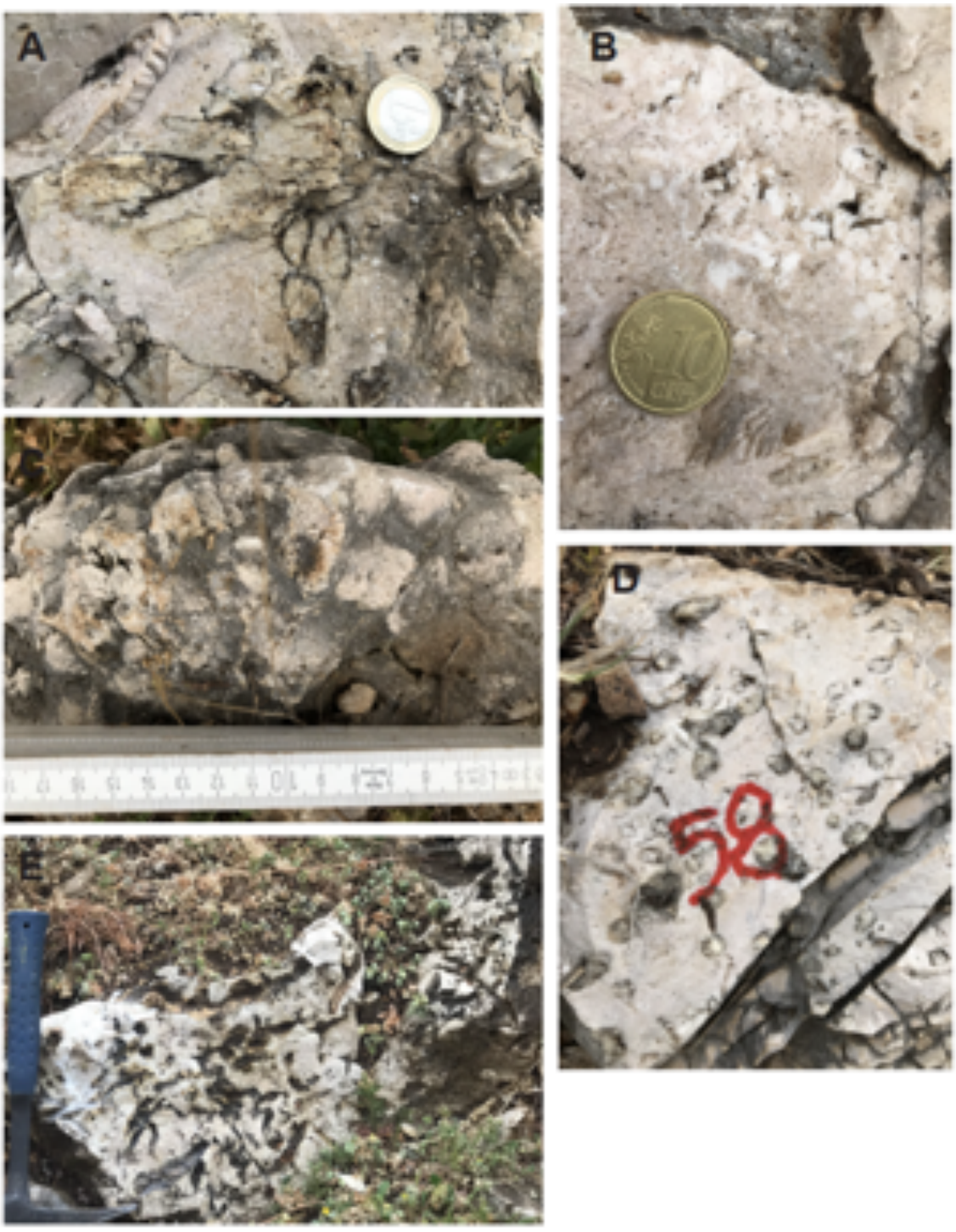

Figure. 3-20- Field images of coral- rich facies in GSM 2 section:A: phaceloid form corals distributed in muddy matrix. B: Fragments of red algae associated with corals. C: coral colony in branching form D: phaceloid form corals distributed in muddy matrix. E: Corals colony with thick branches.

Subfacies 1-1: Bioclast rich coral wackestone to fine-grained packstone: (B-C w-p)

In this facies, the dominant components are delicate branching corals and bioclast grains (Fig.3-21). The coralline red algae are mostly non-articulated form, although they are not abundant in this facies. The red algae mostly consist of fragments of rhodoliths, nodules and crusts with rare amount of articulated form. The corals are rarely encrusted by thin layer of red algae. The *Polystrata alba* is also present among the red algae. The other components are common to abundant thin shell bivalves, gastropods, echinoids, brachiopods, ostracods and bryozoans. Among other components, foraminifers are rarely present (miliolids and *Sphaerogypsina*).

The size and preservation of bioclasts change from wackestone to packstone. The most components are fine-grained and well preserved in the wackestone, while the skeletal grains are coarser (bivalves, gastropods) and show more fragmentation in the packestone texture. Bioerosion is rarely present associated with coral fragments. This facies has been identified in G.S.M section 1 and Ferrovia.

Interpretation: The abundance of fine-grained muddy matrix (wackestone to fine-grained packstone) indicates that this facies has been deposited below the wave action zone, where the environment is quiet. However, in packestone matrix, the presence of slightly fragmantated skeletal components shows the effect of some higher energy event. The presence of non-articulated red algae, rhodoliths and red algae nodules as well as *Polystrata alba* suggests occurrence of this facies in meso-oligophotic zone. The very rare amounts of miliolids and *Sphaerogypsina* and other shallow water and euphotic components such as articulated red algae in this facies display could also support the occurrence under oligo-mesophotic condition.

subfacies 1-2: Red algal rich coral packstone: (R-C p)

The dominant components in this facies are corals (branching and phaceloids) and red algae (Fig. 3-22). The common to abundant red algae are characterized by mixed articulate and non- articulate fragments. Rhodoliths (with coral nuclei), red algae nodules and fragment of crusts are also present. The secondary components are fragments of thin shell bivalves, gastropods, echinoids. The foraminifers are represented by rare amount miliolids and encrusting foraminifers. The components are mostly broken in this facies but the well-preserved skeletal grains are also present. Some of corals are affected by bioerosion and re-infill of sediments. This facies has been occurred in G.S.M 2.

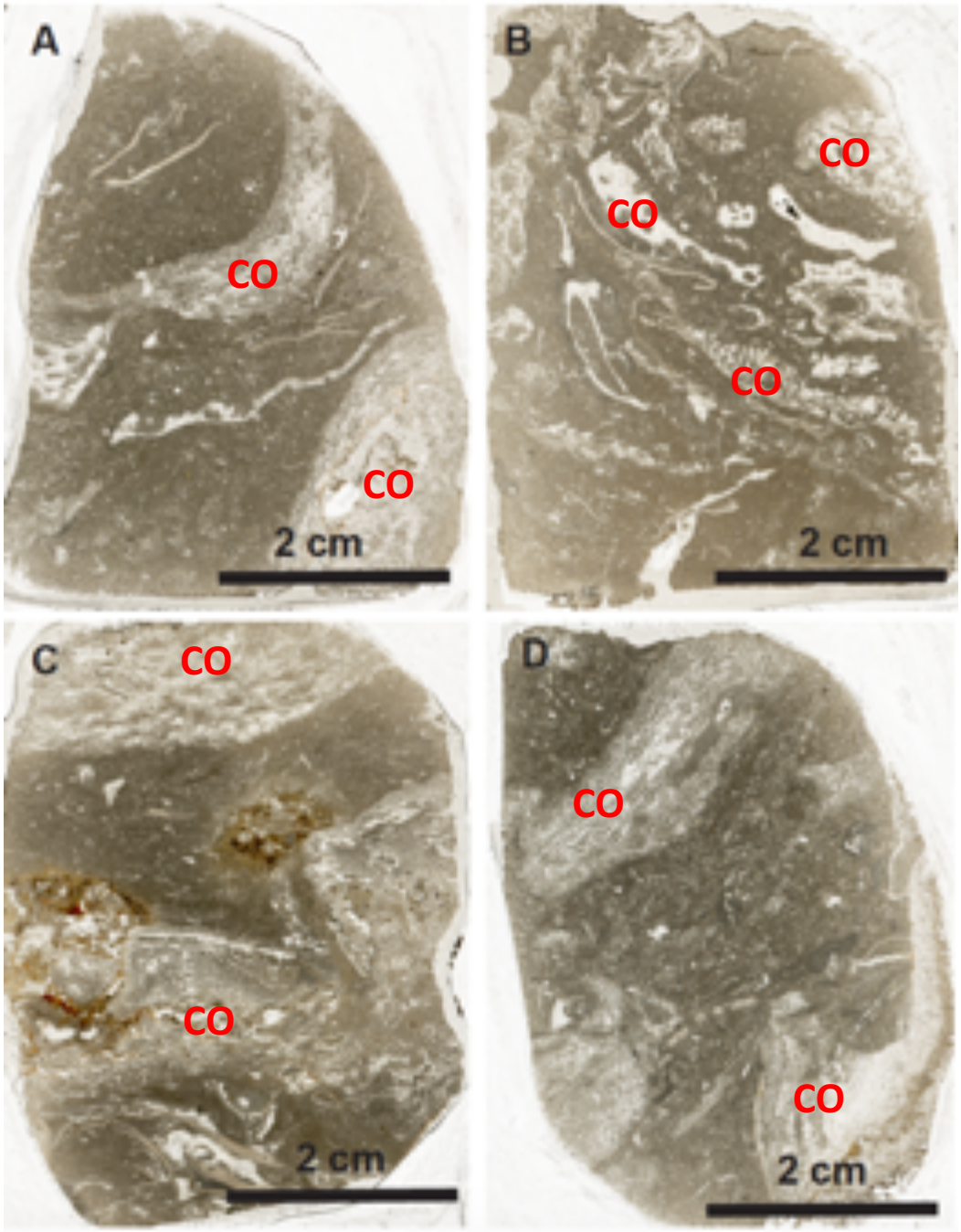

Figure. 3-21- Subfacies 1-1: Bioclast rich coral wackestone to fine-grained packstone. A-D: different coral genera distributed in wackestone to fine-grained packstone

Interpretation: more fragmentation of components and the packstone matrix indicates that this facies developed in higher energy settings compare with B-C w-p facies. The mixture of euphotic components (articulated red algae and rare miliolids) with meso-oligophotic components (non-

articulated red algae) in this facies can be explained by 3 scenarios: 1- the euphotic components transported from the shallow depth to deeper parts of mesophotic factory by some storm events (eg. storm waves) 2- This mixture can be also explained by sea-level rise and reworking and mixture of the components during the sea-level fall.

3-4-2-3-2- Coral-red algal rich packstone to grainstone facies: (CR p-g)

This facies is characterized by m-thick bedded limestone with fragments of corals and red algae as main components. Corals are showing branching (*Stylophora, Acropora*) and phaceloid or massive (*Alveopora*) form (Fig.3-23). The coralline red algae fragments are common to abundant in this facies. Red algae are represented by both articulate and non- articulated forms. The articulated red algae show hooked shape in some samples. The rhodoliths and encrusted form of red algae is common and they are mostly coated the coral and bryozoan fragments. Among other red algae, the nodules forms are also present. Rare fragments of *Polystrata alba* is also occur. The secondary components are bivalves, echinoids, brachiopods and gastropods. The foraminifers are mainly rare to present porcellaneous such as miliolids, *Peneroplis, Austrotrillina* and textulariids. The base of this facies is mainly represent by grainstone texture and toward the top the mud contents increase. The skeletal components in grainstone texture tend to more fragmentation. Also, porcellaneous foraminifers are more present at the base of this facies in the grainstones. Bioerosion is seen associated with coral fragments. This facies is distributed in G.S.M section 2.

Interpretation: The grainstone to packestone matrix and fragmentation of skeletal components show that this facies prone to some high energy events. The presence of some porcellaneous foraminifers indicates the deposition reworking of these components from seagrass meadow to the deeper settings. However, this facies is not represents a classical shallow water and euphotic duo to presence of meso-oligophotic components such as non-articulated red algae and rhodoliths and rare *Polystrata alba*. In the middle ramp settings, the occurrence of rhodoliths started from 10-20 meters and below (Brandano et al., 2005). On the other hand, the articulated red algae developed in euphotic zone. Hooked form red algae is usually occurring in seagrass meadow and its growth forms adapted to the contour line of the seagrass leaf (Beavington-Penney et al., 2004). This facies can be represent occurrence in euphotic to mesophotic condition.

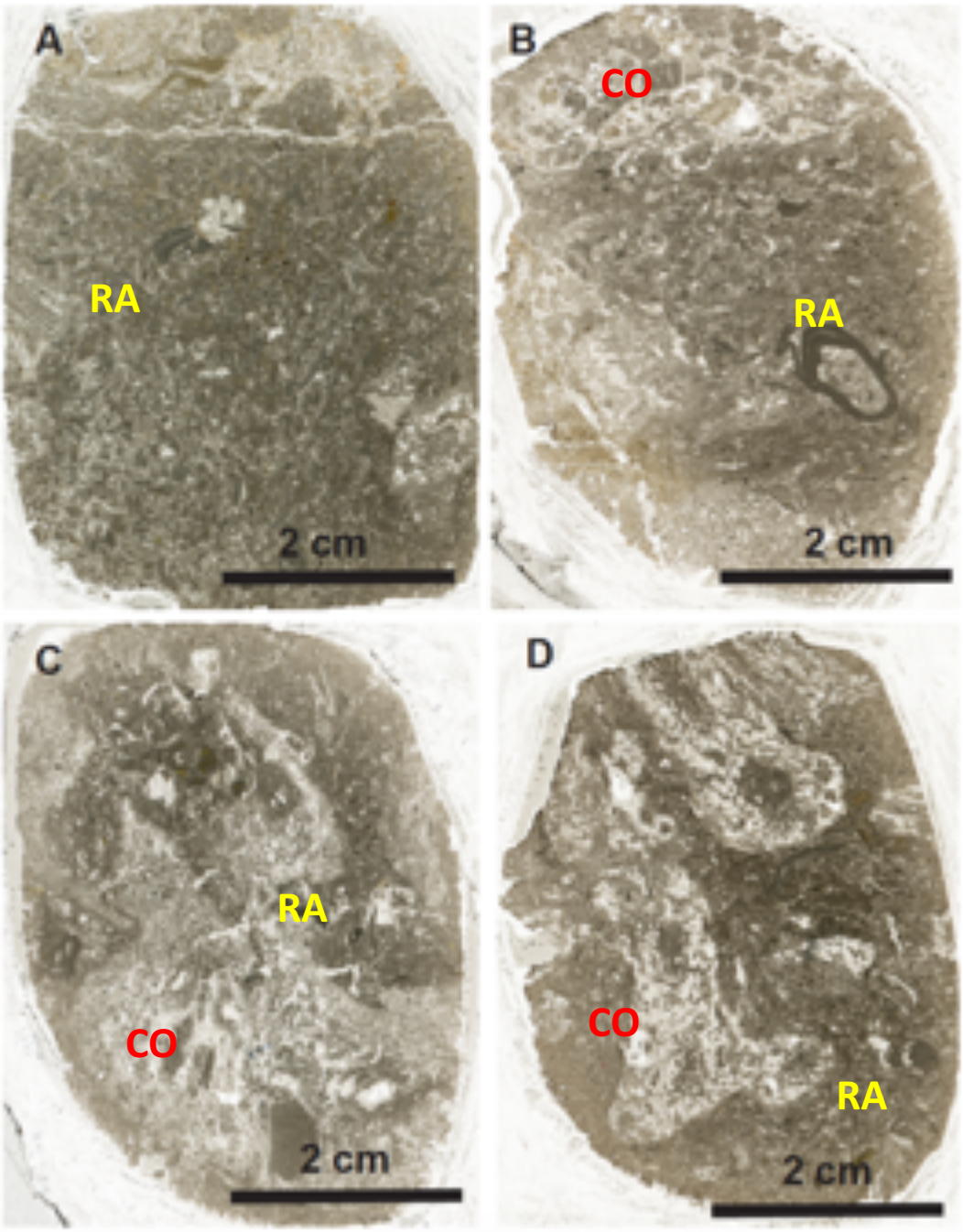

Figure. 3-22- Subfacies 1-2: Red algal rich coral packstone. A-D: different coral genera distributed in packstone matrix rich in red algae. The red algae are mixed of non-articulate and articulate form.

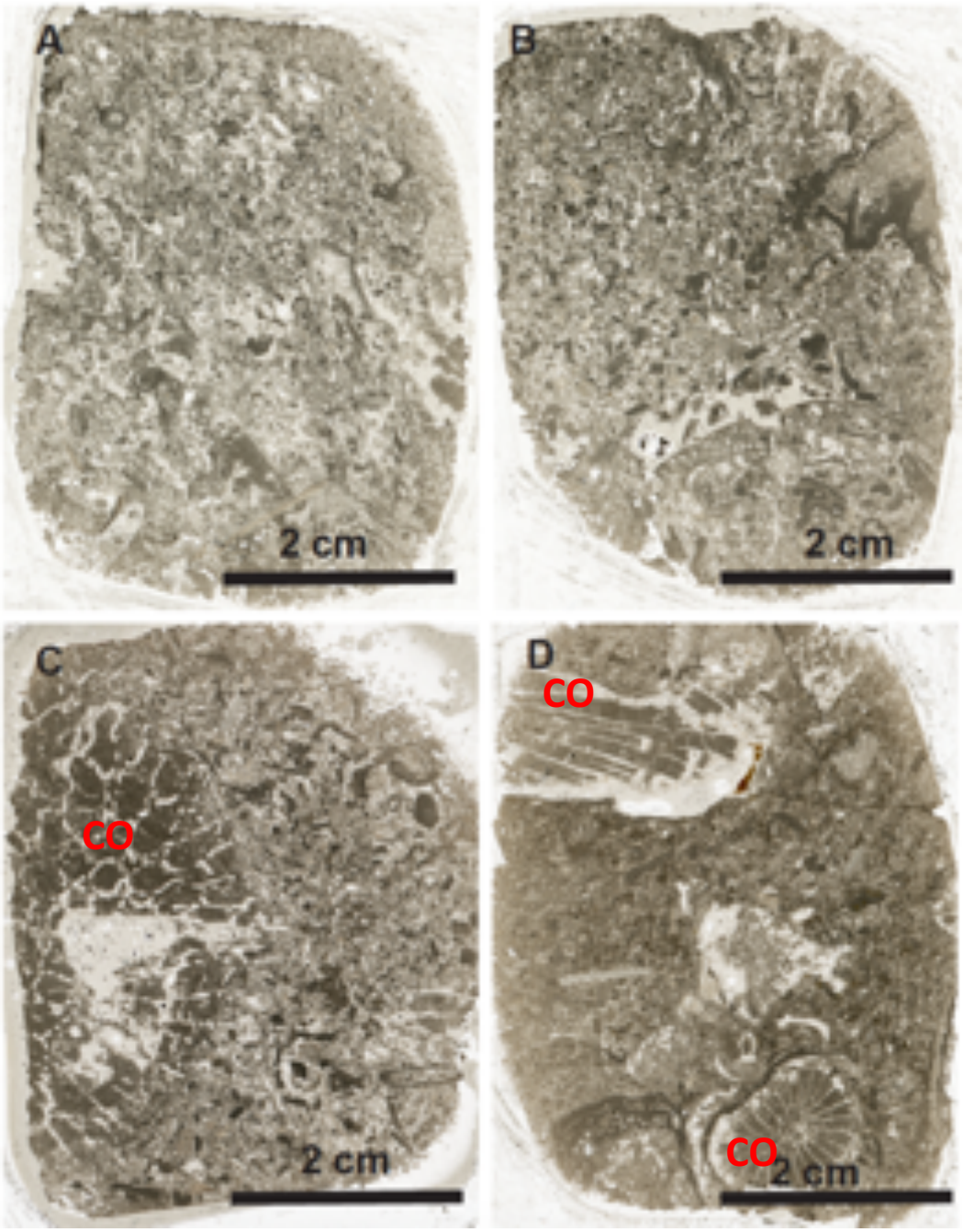

Figure. 3-23- facies 2: Coral-red algal rich packstone to grainstone facies. A: Red algae distributed in grainstone matrix. B: red algae distributed in packstone to grainstone matrix. C: A massive coral accompanied with red algae and surrounded by pack-grainstone matrix. D: Phaceloid corals encrusted by thin layer of red algae distributed in packstone matrix.

3-4-2-3-3- Coral- Bivalve rich packstone to rudstone facies: (CB p-r)

This facies consists of light pinkish limestones with dominant components of corals, bivalves and gastropods. Fragment of corals are abundantly distributed in matrix and they are mostly showing branching and phaceloid morphology. The corals are mostly delicate branching of *Stylophora* and thicker branches of *Acropora* (Fig.3-24). In some layers, the number of cm sizes of bivalves are very abundant, represented by bivalve rich bed with rudstone texture. The bivalves are distortionary arranged inside the layers. Under microscope, the bivalve shells are completely dissolved but they preserved their original shape, although some of them show broken form (Fig. 3-24A). These bivalves are distributed in a packstone matrix with abundant amount of broken and thin shell bivalves and gastropods. Red algae are also present, although they are not abundant. The present to common coralline red algae are mixing of articulate and non-articulate fragments. Some corals are encrusted by thin layer of red algae. also the red algae nodules are present. Among red algae, the fragments of *Polystrata alba* algae are also rarely recognized. The other present to rare subordinate components are bryozoans, echinoids and brachiopods. The foraminifers are mostly represented by rare to present miliolids, *Peneroplis, Austrotrillina, Meandropsina, Elphidium* sp., and *Dendritina*. Bioerosion is common in this facies and the most important borings are bivalves (lithophaga) on poritid corals (Fig.3-24 B). The holes resulted by bioerosion are re-infilled by sediments again. This facies has been in Ferrovia section, G.S.M 1, 2 and Ferrovia.

Interpretation: the grain dominated texture (packstone to rudstone) and high fragmentation of components, indicates that this facies were deposited in high-energy condition, however, the presence of mud between the components displays that the energy was not as high as enough to remove the muds. In this facies, the number of meso-oligophotic components such as non-articulated red algae are decreased while the number of euphotic components (porcellaneous and epiphytic foraminifers and articulated red algae) show that this facie can be deposited close to euphotic factory. The common bioerosion associated with corals displays the presence of high trophic sources (Hallock, 1988).

3-4-2-3-4- Red algal- wackestone to packstone with larger benthic foraminifers: (RL w-p)

Red algal- wackestone to packstone facies is identified by dark pinkish color limestones. This facies is characterized by abundant to very abundant red algae with rare corals fragments (Fig.3-25). The red algae consist of abundant articulated form with present red algae nodules and non-articulated fragments. This facies is characterized by presence of larger benthic foraminifers such

as: *Heterostegina* and *Nephrolepidina*, although they are not very common. Other rare foraminifers are miliolids, *Dendritina* sp., *Rupertia* sp.. Other minor components are bivalves, echinoids, brachiopods, *Ditrupa* sp., gastropods and bryozoan. This facies occur at the top of G.S.M limestones in both Ferrovia and G.S.M section 2.

Interpretation: the mud dominated wackestone to packstone matrix displays the deposition in quite environments. The abundant articulated red algae indicate that this facies can be deposited under euphotic condition. The presence of well-preserved mesophotic large rotalids such as *Nephrolepidina* in this facies suggests that this facies can be deposited under euphotic-mesophotic condition.

3-4-2-4- Depositional environments

The limitation imposed by lack of lateral continuity of outcrops as well as lack of depositional geometry in studied outcrops, depositional model for Grotta San Michele Limestones has been not defined in this research. Moreover, In the studied facies, except in facies B-C w-p, the mixing of euphotic and meso-oligophotic components prevents distinguish between the different depositional environments based on light penetration zone (euphotic, mesophotic and oligophotic). Based on carbonate components and facies distribution, Grotta San Michele limestones in Ferrovia section indicates formation of corals rubbles associated with shallower components. The more presence of porcellaneous foraminifers in Ferrovia section confirms that sedimments can deposited more close to shallow environments. However, in Ferrovia section, the corals are distributed mainly in a mud dominated matrix (wackestone to packstone) with lack of high energy sedimentary structures, which indicates that deposition was in quiet environments. Although, the fragmentation of some skeletal components can be resulted by some high-energy events. In Grotta San Michele section 1 and 2, less amount of seagrass components, shows that G.S.M.L in this area can be characterized by more distal settings. The general depositional trends in Grotta San Michele section 1 and 2 characterized by a higher energy facies in the bottom of section passing to more deepening and fine grained facies toward the top. In all studied section the rubbles of coral are floated in a mud dominated matrix and they were not able to build a rigid framework up to sea level. As a results, their characteristics fits to cluster reef (*sensu* Riding 2002).

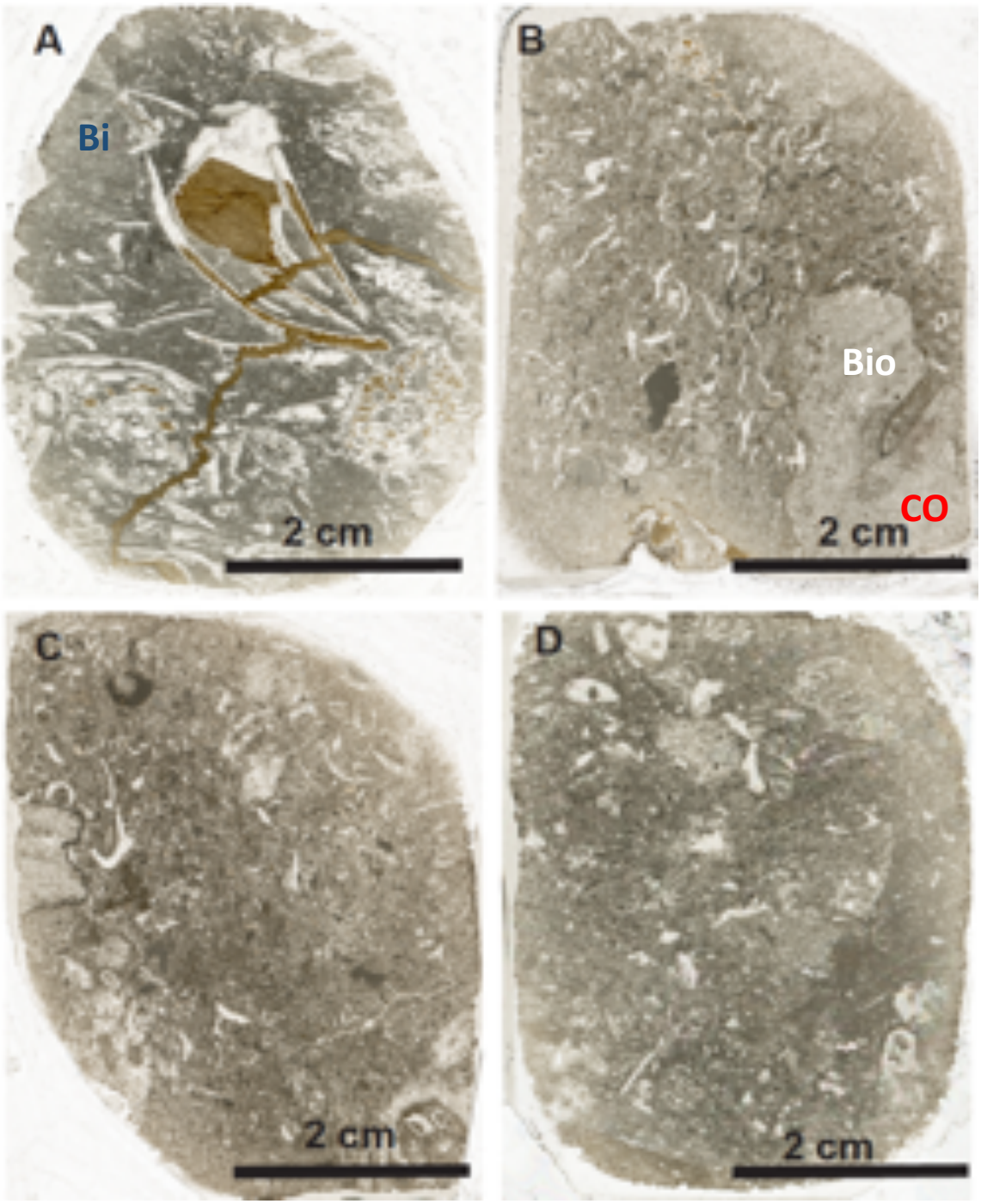

Figure. 3-24- facies 3: Coral- Bivalve rich packstone to rudstone facies. A: bivalve rudstone with packsstone matrix. Bivalves (Bi) B: Coral fragments with visibile bioerosion trace (bio) in packstone matrix. C-D: The bivalve rich packestone with fragments of red algae

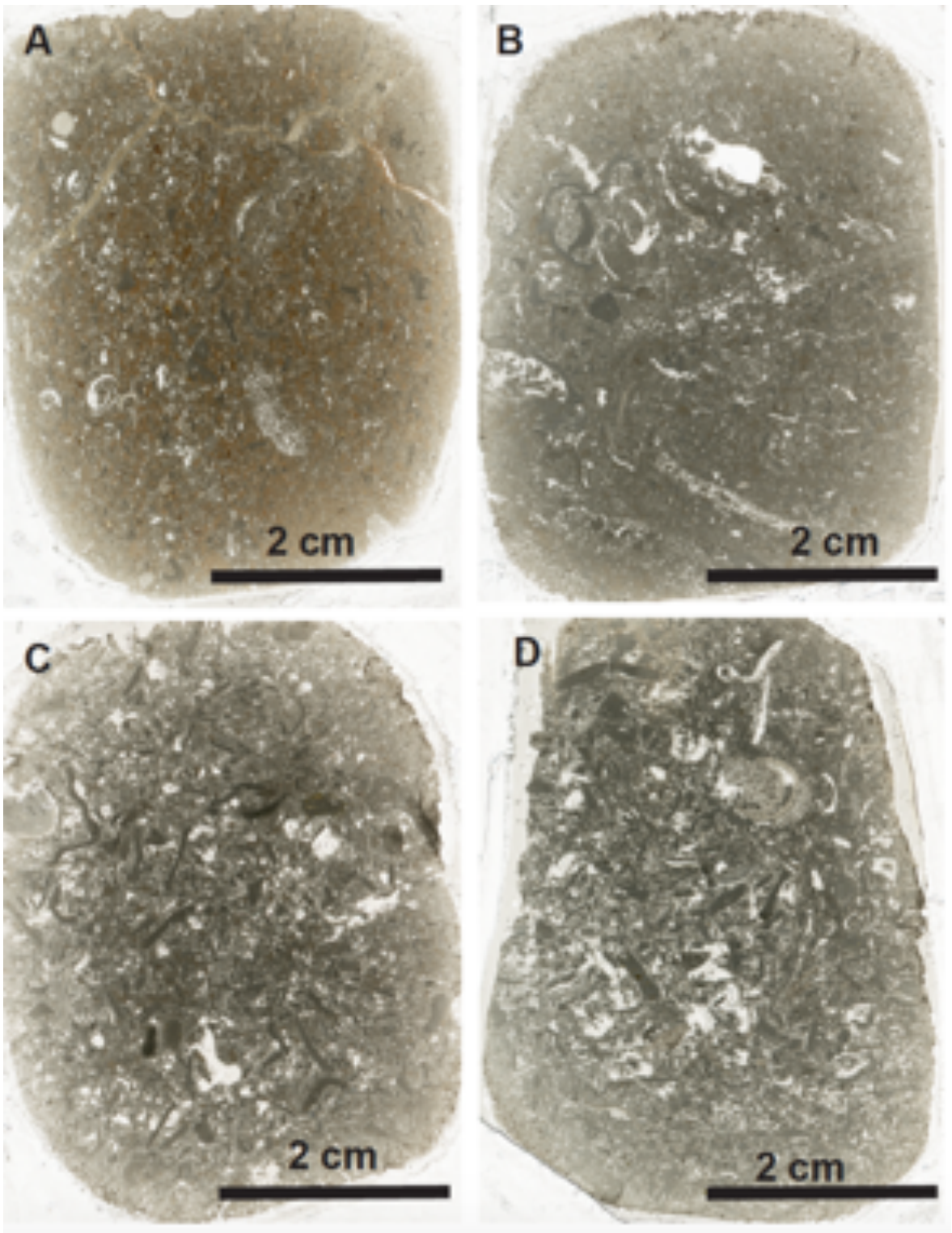

Figure. 3-25- facies 4: Red algal- wackestone to packstone. A-D: Abundant non-articulate red algae in wackestone to packstone matrix.

According to Riding, 2002 this kind of reefs are developed in quit waters and the may prone episodically to some high energy storms. According to Pomar et al., 2017, the most reported coral buildups from Oligocene fit to the cluster reef type and they were deposited in middle to outer part of a low angle ramps along the mesophotic zone (Geister and Ungaro, 1977; Bassi and Nebelsick, 2010; Van Buchem et al., 2010; Nebelsick et al., 2013, Pomar et al., 2014; Shabafrooz et al., 2014). During the Early Miocene (Burdigalian), the most dominated reef builders were red algae and corals showing the cluster type reef and they were deposited in inner to middle low angle ramps with light zone from euphotic to mesophotic (seagrass canopy) (Brandano and Corda, 2002; Brandano, 2003; Pomar et al., 2004; Benisek et al., 2009; Benisek et al., 2010; Pomar et al., 2012). In G.S.M.L, the mixing of euphotic represented mainly by articulated red algae and meso-oligophotic components such as non-articulated red algae, can be related to deposition of cluster coral facies in light zone from euphotic to mesophotic factory.

3-5- Discussion

3-5-1- Coral- rich facies in Grotta San Michele Limestones vs Asmari Formation

Coral-rich facies in Asmari Formation and G.S.M.L shares some similarities in term of depositional fabric and energy level. In both Asmari Fm and G.S.M.L the corals in buildups did not densely packed and they did not build a wave resistant rigid framework. They are both matrix-supported and the matrix in both examples characterized by a mud-dominated matrix. As results they are both show the characteristic of cluster reefs (*sensu* Riding, 2002). However, there are several difference between these two examples and they are mostly related to type of biota and components accompanied the coral buildups. In Asmari Formation, the non-articulate form of red algae is the main components accompanied the corals. Also, the corals are strongly encrusted by red algae. In G.S.M.L, the articulated red algae are the main type of red algae accompanied corals. Moreover, the corals are not strongly encrusted by red algae as in case of Asmari Fm. Also, LBF such as *Nephrolipidina, Heterostegina, Neorotalia*, are well documented in Asmari Fm while the number of LBF in G.S.M.L is very rare. Brandano et al., 2009 discussed that during the Late Oligocene, the less development of LBF allowed the expansion of red algae into the shallower environments. In the other hand, the LBF development declined by the cooling of the climate in the higher latitudes by the end of Eocene and Oligocene when the thermohaline circulation intensified (Hottinger, 1998; Zachos et al., 2001; Pearson et al., 2008).

On the other hand, in Asmari Fm corals developed as large thick-bedded buildups and the coral colonies are mostly preserved in life position while in G.S.M.L corals are not mainly developed in a life position. Although in both cases the facies are developed in mud-dominated matrix, the coral buildups in Asmari Formation tend to developed in deeper setting compare with G.S.M.L. This interpretation is based on the carbonate components accompanied the corals in both examples. While in Asmari Formation the components are more characterized by mesophotic to oligophotic (e.g. non-articulate red algae, *Nephrolipidina, Heterostegina, Neorotalia*), in G.S.M.L the biota are mainly represented by euphotic (e.g. articulate red algae) to mesophotic (e.g. rhodolith) components.

3-5-2- Impact of internal waves

During the cooling earth in Eocene and Oligocene, accelerating thermohaline circulation resulted in strong bathymetric and latitudinal gradients and therefore strong high latitude storms that generate stronger surface waves and pycnocline and as a result high energetic internal waves. (Pomar et al., 2017). This can be led to more effective turbulence for delivery of nutrients to the catcher and pumpers. According to De Carlo et al. (2015) internal waves can effect modern reefs in three ways: 1) internal waves elevate plankton flux and increase coral heterotrophy, 2) heterotrophy enhances coral growth rates, and 3) calcification is also enhanced by water motion. Moreover, metazoan mounds need a high turbulence because the vertical accretion of a bioherm increases impinging efficiency of nutrient-rich current which favoring the suspension feeders (Pomar and Hallock, 2008; Pomar et al., 2012). Suspension-feeder metazoan such as corals can build buildups at the depth of pycnocline where the internal waves are a good candidate to carry nutrient-rich water to this depth (Pomar et al., 2012) (Fig.3-26).

In Asmari Formation, m-thick coral buildups developed showing an aggradation respect to sea-level. These large coral buildups were developed in oligophotic to mesophotic zone at the depth of pycnocline. In this depth, internal waves are a good candidate to pump the nutrient-rich water needed by buildups to grow. Moreover, the associated high-energy flank facies is interpreted to develop in a mesophotic and low-energy ambient. The paradox here the source of hydrodynamic in order to produce such high energy flank facies in a relative quiet environment. Again, interval waves can be a good candidate to explain the source of turbulence in order to generate the high-energy flank facies in a low-energy context.

Alnazghah et al. (2002), described such facies in Upper Jurassic ramp. In this setting, the coral-microbial buildups were developed in low-energy mud-dominated matrix. The author explained the internal waves as possible source of high-energy event in order to create the high-energy flank facies in low-energy ambient. In GSML, the corals are distributed in mud-dominated matrix which indicates the occurrence of these facies in relative low-energy environments. The grainstone facies may represent the part of buildups prone to high-energy events. However, the corals are not developed here as large and distinct buildups such as Asmari Formation. The corals are mostly well preserved fragments with some *in-situ* coral colonies. The shallow euphotic fragments such as articulated red algae can transported here as result of some currents. The role of internal waves in formation of these coral facies is not very evident as in Asmari Formation. The mixing of shallow water euphotic with mesophotic components imposed the limitation to introduce the internal waves as main source for hydrodynamic energy independent from the surface waves. However, internal waves can still 1- provide turbulence for some *in-situ* isolated coral mounds to grow, 2- shed down carbonate components produced along the ramp and, 3- provide necessary energy for rhodoliths to turnover from the original buildups. Other scenario is that the coral buildups in GSML which developed in a low-energy mesophotic condition were affected by internal waves and produced a coral debris and shifted them basinward. During the sea-level fall the euphotic shallow components can mix with deeper mesophotic factory. However, the lack of depositional geometry cannot prove this scenario.

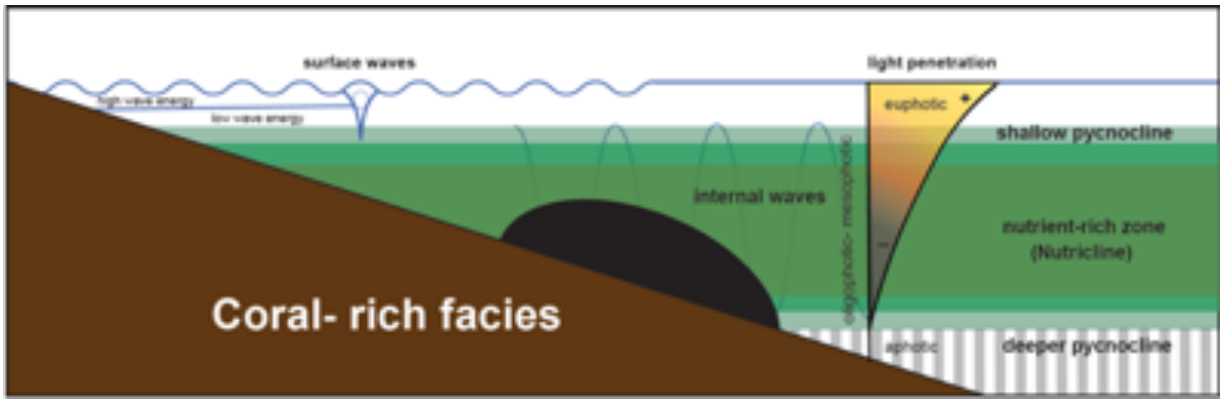

Figure. 2-26- Coral-rich buildups developed in the mesophotic zone, below the surface storm wave action; in this environments, internal waves associated with pycnocline can bring nutrient rich waters needed by coral buildups to develop (*sensu* Pomar et al., 2012, Kiani Harchegani and Morsilli, 2019).

3-5-3- Comparison with other Late Oligocene system

While the most interpretations of Late Oligocene coral buildups are based on the modern Caribbean barrier-reef shelf-lagoon complex model (e.g.: Frost, 1981; Bosellini and Perrin, 1994; Bosellini, 2006) some other studies considered the different light zone factories (euphotic, mesophotic, oligophotic) in order to describe the position of coral buildups and distribution of carbonate facies: in Italy (Lessini Shelf and Venetian foreland basin: Bassi et al., 2007; Bassi and Nebelsick, 2010, Salento, southern Italy: Pomar et al., 2014, Central Apennines, Italy (Brandano et al., 2016) and in Malta (Brandano et al., 2009).

Bassi and Nebelsick, 2010 studied the Chattian mixed carbonate–siliciclastic sequences in northern Italy (Lessini Shelf and Venetian foreland basin). The authors described well-developed inner to middle ramp facies deposited in an homoclinal ramp. The major factors controlling sedimentary facies were local hydrodynamic conditions and water turbidity. Cross- bedded sandstones were deposited in the Inner-ramp setting and basinward passes into LBF and miliolid packstones as a transition of inner/middle ramp, and then into rhodolithic rudstone were deposited in proximal middle ramp setting and subsequently into Lepidocyclinid packstone of the distal middle ramp. The majority of carbonate production occured in distal inner- and proximal middle ramp as a result of development of Chattian larger foraminiferal and rhodolith facies.

In southern Italy, (Salento), Pomar et al., 2014 studied two stratigraphic units: the lower Chattian Castro Limestone and the upper Chattian Porto Badisco Calcarenite. The Castro Limestone characterized by of coral-bearing limestones, with abundant and different coral faunas associated with red algae as subordinate components. This unit was classically interpreted as a fringing reefs (Bosellini and Russo, 1992; Bosellini and Perrin, 1994) while in the new study by Pomar et al., 2014 the Castro Limestone interpreted to be deposited in a distally steepened ramp with a distal talus induced by the basal paleo-escarpment (Fig. 3-27).

The seagrass meadows were characterized by abundant Epiphytic biota and sediment dweller organisms representing the deposition in a shallow-water euphotic zone. In mesophotic zone large rotalid foraminifers were dominants components. The corals built isolated mounds near the edge of the escarpment in mesophotic zone. These corals were not developed wave-resistant growth fabrics (cluster reef). Toward the basin, clinobeds with 25° to 30° dipping composed of rudstone/floatstone textures resulted from downfall of corals debris and sediments.

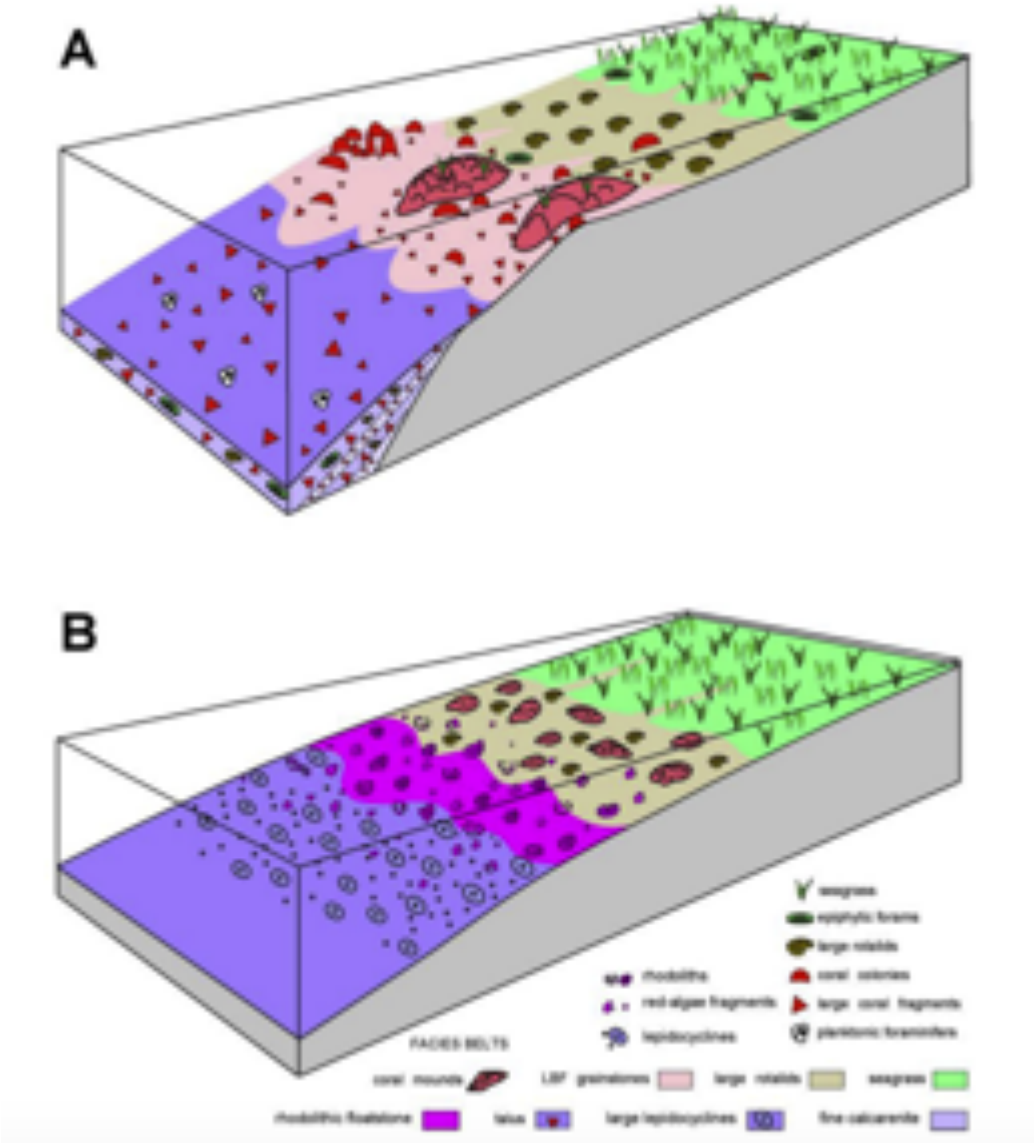

Figure. 27-3- A: Depositional model for the lower Chattian Castro Limestone: a distally steepened ramp induced by a substrate paleo-escarpment. B: Depositional model for the Porto Badisco Calcarenite (from Pomar et al., 2014).

The Porto Badisco Calcarenite (upper Chattian) interpreted to be deposited in a homoclinal ramp (Fig.3-27) and dominated by packstone texture. The inner ramp is characterized by extensive occurrence of seagrass meadows biota in euphotic zone. Mesophotic zone is characterized by development large rotalid packstone and small coral mounds and rhodolithic floatstone/ rudstone facies and large lepidocyclinid packstone were deposited in the deeper oligophotic zone. Aphotic

zone is a zone of deposition of skeletal debris. In the meso-oligophotic zone the source of hydrodynamic can be explained by breaking of internal waves.

In the Central Apennines, Italy, Brandano et al., 2016 studied the Oligocene- Miocene Bolognano Fm in Majella carbonate platform. Five lithofacies interpreted to be deposited in a homoclinal ramp that developed in a warm, subtropical environment: Lepidocyclina calcarenites, cherty marly limestone, bryozon calcarenites, hemipelagic marls and marly limestone, and Lithothamnion limestone.

In Malta, Brandano et al., 2009 studied the Late Oligocene Attard Member of the Lower Coralline Limestone Formation in order to describe the facies, palaeoenvironments and factors controlling the evolution of Late Oligocene platform. The authors defined four facies deposited along the inner and middle ramp settings. The shallow water high-energy inner ramp passed downslope to inner ramp characterized by seagrass and interfingering scattered corals. The middle ramp facies composed of in situ production and sediments carried from the shallower inner ramp by currents and they were deposited in the oligophotic zone.

The authors discussed that the characteristics and facies distribution of studied carbonate units are more similar to Miocene ramp. This similarity may be related to the extensive development of seagrass factory in euphotic zone. This extensive development may also result to less occurrence of larger benthic foraminifers facies. The main similarity between Late Oligocene facies of Attard Member and G.S.M.L is the reduce number of LBF in both carbonate units.

3- 6- Conclusion

1- The coral- rich Late Oligocene (Chattian) units are well exposed in Gargano promontory, southern Italy. These units are known as Grotta San Michele Limestones.

In Zagros Basin, Iran, the Chattian sequences of Asmari Formation are exposed in Izeh zone with well preservation of depositional geometry. The Chattian of Asmari Formation characterized by development of coral buildups (CB unit) and flank facies of these coral buildups

2- In GSML, the main facies are: 1- coral wackestone to packstone facies (C w-p) with two subfacies 1- bioclast rich coral wackestone to fine-grained packstone (B-C w-p) and 2- Red algal rich coral packstone (R-C p) 2- Coral-red algal rich packstone to grainstone facies (CR p-g) 3- Coral- Bivalve rich packstone to rudstone facies (CB p-r) and 4- Red algal-

wackestone to packstone with larger benthic foraminifers (RL w-p). In Asmari Formation, the CB units represent by 2 main facies: 1- coral-coralline red algae boundstone/framestone and 2- coral-coralline red algae rudstone/floatstone.

3- Based on components and texture, the GSML is interpreted to develop in meso-oligophotic to euphotic zone. The lack of depositional geometry is a key limitation to reconstruct a depositional model for GSML.Instead the well exposed depositional geometry of Asmari Formation in Zagros Basin suggest the deposition of Chattian coral buildups along the Ramp setting in mesophotic zone.

4- The coral facies in both studied areas show cluster fabric and they deposited in quiet environments. interval waves can be good candidate to explain the source of hydrodynamic energy to provide the necessary nutrient for corals in order to grow. Also, internal waves can be a potential source for high-energy flank facies to develop in the low-energy mesophotic setting.

Chapter 4

General conclusion

1- The internal waves are waves propagating along two different density water (pycnocline) and their impact on sedimentary records remain largely unrecognized. In carbonate system these waves can act as a fundamental mechanism for carrying the nutrients as well as displace the nutrient- rich waters from the deeper parts to the shallower depths and to create high energy and turbulence in settings also located under the storm wave base. Recently, the role of internal waves on development of mesophotic carbonate communities has been highlighted. Based on bathymetric position of modern light-dependent carbonate communities, mesophotic zone has been defined to be located below the normal wave base where the light is sufficient for coral growth. Mesophotic zone is positioned between euphotic zone in shallow part and oligophotic and aphotic zone in the deepest part. The depth range of euphotic zone (very good light and with high wave energy) is defined by the presence of modern seagrasses and non-dasyclad green algae. The lower limit of in situ green algae is corresponded to lower limit of euphotic zone and defined by chlorocline. While, the base of oligophotic (sufficient light for coralline red algal growth), is identified by the deepest occurrence of in situ coralline red algae, rhodocline.

2- During the geological time, extensive reefs were developed in the Late Jurassic time in both northern and southern Tethys. Also, the Late Oligocene (Chattian) was characterized by developments of Coral buildups in Mediterranean Tethys. In this research, two carbonate systems have been investigated in order to evaluate the role of internal waves on developments of these systems: 1- Upper Jurassic- Lower Cretaceous stromatoporoid-rich facies (Gargano, Italy) and 2- Late Oligocene (Chattian) coral-rich facies from Gargano, Italy and Chattian facies of Asmari Formation in Zagros Basin, Iran.

3- The Upper Jurassic- Lower Cretaceous Monte Sacro Limestones are characterized by development of the stromatoporoid-rich buildups and isolated coral colonies as secondary organisms. The stromatoporoid buildups in MSL are characterized by high percentage of high-energy debris-rich facies associated with low-energy facies. The origin of these high-energy facies are still matter of debates.

4- The study of the Monte Sacro Limestones (MSL) in the Gargano Promontory (Apulia), in various localities (Monte di Mezzo, Monte d'Elio, Torre Mileto and Masseria Prencipe), revealed three main lithofacies: LF1- stromatoporoid-rich facies, LF2- stromatoporoid-coral facies and, LF3- stromatoporoid-microbial facies. LF1- stromatoporoid-rich facies characterized by abundant growth of stromatoporoids (*Ellipsactinia* Sp. and *Sphaeractinia* sp.) surrounded by a wackestone to fine-grained packstone matrix (LF1-S1). This subfacies is associated with rudstone-floatstone with intraclastic-bioclastic packstone-grainstone matrix (LF1-S2). The organization and growth form of stromatoporoids fits to the cluster fabric. Basinward, isolated branching coral colonies is associated with stromatoporoids (LF-2- stromatoporoid-coral facies). In this facies, stromatoporoids (mainly (*Ellipsactinia* Sp. and *Sphaeractinia* sp.) are distributed in a wackestone to packstone matrix (LF2-S1) and tabular stromatoporoid-corals surrounded by wackestone matrix (LF2-S2). In the deeper part of margin, the number of stromatoporoids decreased and accompanied with stromatolite-like mats (LF3- stromatoporoid- microbial facies). These facies were interpreted to be deposited along the middle part of a distally steepened ramp.

5- The stromatoporoid-rich buildups of MSL are characterized by presence of phototrophic-heterotrophic reefs generated in a pure carbonate environment. The abundant development of light-independent micro-encrusters such as *Tubiphytes morronensis*, and the lack of light-dependent microencrusters (*Lithocodium- Bacinella*) in the MSL facies can be considered as a result of limit light penetration and occurrence in a mesophotic to oligophotic condition. In this low-energy setting, close to nutricline, internal waves can be a good candidate for provide a nutrient-rich waters needed by stromatoporoids to grow (LF1-S1). Also, the IWs can produce the episodic turbulences in this depth and resulted to high production of debris-rich facies (LF1-S2).

6- The Late Oligocene (Chattian) coral-rich facies are well exposed in both Zagros Basin (Asmari Formation) and Gargano promontory (Grotta San Michele Limestones). Asmari Formation is characterized by development of coral buildups (CB unit) and flank facies of these coral buildups with well-preserved depositional geometry allowing study the position of coral buildups along the depositional profile. These buildups considered to be developed

in mesophotic to oligophotic conditions. While the modern mesophotic corals are well studied by ecologist, their characteristics in ancient geological records still poorly documented.

7- The main facies in Grotta San Michele Limestones (GSML) are: 1-1 coral wackestone to packstone facies with two subfacies a- bioclastic rich coral wackestone to fine-grained packstone, and 1-2- Red algal rich coral packstone. 2- coral-red algal rich packstone to grainstone facies, 3- coral- bivalve rich packstone to rudstone facies, and 4- red algal-wackestone to packstone with larger benthic foraminifers. The lack of depositional geometry imposed limitation to propose a depositional model. In the Asmari Formation, the CB (coral buildups) units represent by two main facies: 1- coral-coralline red algae boundstone/ framestone and 2- coral-coralline red algae rudstone/floatstone.

8- The corals in GSML, are associated with meso-oligophotic components such as non-articulate red algae, rhodolith and *Polystrata alba*. However, the euphotic components such as articulated red-algae, and rare miliolids are associated with corals buildups. The coral-rich facies in GSLM interpret to be deposited in euphotic to meso-oligophotic condition based on components and texture. In the Asmari Formation, the corals are strongly encrusted by red algae and also associated with meso-oligophotic components such as non-articulated red algae, *Neorotalia* and *Nephrolepidina* suggesting mesophotic conditions. These coral builups were developed along the middle ramp setting under a low-energy condition.

9- In both GSML and Asmari Formation, coral-rich facies were developed in quiet and low-energy environments and they did not develop a rigid framework (cluster fabric). In this environments dominated under mesophotic condition, internal waves are good candidate to provide the nutrient resources to buildups in order to grow. Moreover, the internal waves can provide necessary hydrodynamic energy and turbulence to the buildups. The formation of high energy flank facies of coral buildups in Asmari Formation in a context of low-energy condition cab be also explained by the effect of internal waves in these settings.

10- While internal waves can play an important role on development of the Upper Jurassic-Lower Cretaceous stromatoporoid-rich and the Late Oligocene coral-rich facies, other factors can also be considered such as light, trophic level and the level of hydrodynamic energy. The stromatoporoid-rich facies of the Upper Jurassic –Lower Cretaceous Monte Sacro Limestone, are mostly characterized by the lack of the presence of *in-situ* light-dependent organisms such as Dasyclad green algae and *Lithocodium-Bacinella*, and the high development of light-independent micro-encrusters (*Tubiphytes morronensis*) which indicate that light penetration was confined (mesophotic condition). The coral-rich facies in the Late Oligocene of Asmari Formation are characterized by highly presented meso-oligophotic organisms such as non-articulated red algae as well as rhodoliths and LBF (*Nephrolipidina, Heterostegina, Neorotalia*) which confirms that this succession was developed in low-light conditions. In the Late Oligocene coral-rich facies of GSML, the presence of light-dependent organisms such as articulated red algae associated with light-independent non-articulated red algae and rhodoliths may indicates the development of this formation in good to moderate level of light condition (euphotic- mesophotic). Nutrient availability is the other factors which can affect the buildup development in the studied successions. The Upper Jurassic – Lower Cretaceous MSL are developed in moderate oligotrophic to mild mesotrophic condition. In the Late Oligocene coral-rich facies, some of the corals are strongly affected by macrobioerosion which could be result of high-nutrient condition. in general, and in both example of studied buildups, the presence of nutrient was critical for buildups to grow. The level of hydrodynamic energy is one of the key factor which controls the development of stromatoporoid-rich buildups in the Upper Jurassic –Lower Cretaceous MSL as well as Late Oligocene coral-rich facies in both GSML and Asmari Formation. In MSL, the debris-rich intraclastic grainstone to packstone subfacies is the main contributor of stromatoporoid-rich buildups characterized by high-energy condition. In the Late Oligocene GSML, the high percentage of coral rubbles and the fragmentation degree of skeletal grains in packstone to grainstone facies, indicates that these successions were developed under high hydrodynamic energy. In Asmari Formation, the coral buildups developed in mud dominated matrix which indicates the growth phase in a low-energy condition. However, the high energy flank facies is associated with high hydrodynamic energy.

11- In summury, the internal waves can be considered to play an effective role in carbonate buildups development during both Upper Jurassic and Late Oligocene carbonate systems. In the Upper Jurassic-Lower Cretaceous carbonate systems, with the high percentage of debris, contributed in stromatoporoid-rich buildups, the role of internal waves can be defined as a potential source of episodic high energy events which hit the buildups and produce high energy intraclastic-bioclastic rich facies. In the Oligocene carbonate system, with extensive development of corals in low energy mesophotic settings, internal waves can be an important factor to provide the nutrient-rich source and water motion for coral buildups to grow. Also, the internal waves can be a good candidate to explain the presence of high energy flank facies along the various coral buildups.

Chapter 5

References

Ager, D. V, 1974. Storm deposits in the Jurassic of the Moroccan High Atlas. Palaeogeography, Palaeoclimatology, Palaeoecology 15, 83–93. https://doi.org/https://doi.org/10.1016/0031-0182(74)90026-1.

Aguirre, J., Riding, R., Braga, J.C., 2000. Diversity of coralline red algae: origination and extinction patterns from the Early Cretaceous to the Pleistocene. Paleobiology 26, 651-667.

Al-Awwad, S.F.A., Pomar, L., 2015. Origin of the rudstone–floatstone beds in the Upper Jurassic Arab-D reservoir, Khurais Complex, Saudi Arabia. Marine and Petroleum Geology 67, 743–768. https://doi.org/10.1016/j.marpetgeo.2015.05.014

Allahkarampour, M., Vaziri-moghaddam, H., Seyra, A., Behdad, A., 2018. Oligo-Miocene carbonate platform evolution in the northern margin of the Asmari intra-shelf basin, SW Iran 92, 437–461. https://doi.org/10.1016/j.marpetgeo.2017.11.008

Alnazghah, M.H., Bádenas, B., Pomar, L., Aurell, M., Morsilli, M., 2013. Facies heterogeneity at interwell-scale in a carbonate ramp, Upper Jurassic, NE Spain. Marine and Petroleum Geology 44, 140–163. https://doi.org/10.1016/j.marpetgeo.2013.03.004

Apel, J.R., 2002. Oceanic internal waves and solitons. In: Jackson, C.R. (Ed.), An Atlas of Oceanic Internal Solitary Waves. Global Ocean Associates. Prepared for Office of Naval Research - Code 322 PO, Alexandria, VA, pp. 1–40

Arthur, R.S., Fringer, O.B., 2016. Transport by breaking internal gravity waves on slopes. Journal of Fluid Mechanics 789, 93-126. doi:10.1017/jfm.2015.723

Bádenas, B., Aurell, M., 2010. Facies models of a shallow-water carbonate ramp based on distribution of non-skeletal grains (Kimmeridgian, Spain). Facies 56, 89–110. https://doi.org/10.1007/s10347-009-0199-z

Bádenas, B., Pomar, L., Aurell, M., Morsilli, M., 2012. A facies model for internalites (internal wave deposits) on a gently sloping carbonate ramp (Upper Jurassic, Ricla, NE Spain). Sedimentary Geology 271–272, 44–57. https://doi.org/10.1016/j.sedgeo.2012.05.020

Basilone, L., Sulli, A., 2016a. A facies distribution model controlled by a tectonically inherited sea bottom topography in the carbonate rimmed shelf of the Upper Tithonian–Valanginian Southern Tethyan continental margin (NW Sicily, Italy). Sedimentary Geololgy 342, 91–105. https://doi.org/10.1016/j.sedgeo.2016.06.013

Basilone, L., Sulli, A., Gasparo Morticelli, M., 2016b. Integrating facies and structural analyses with subsidence history in a Jurassic–Cretaceous intraplatform basin: Outcome for paleogeography of the Panormide Southern Tethyan margin (NW Sicily, Italy). Sedimentary Geology 339, 258–272. doi:10.1016/j.sedgeo.2016.03.017

Bassi, D., Hottinger, L., Nebelsick, J.H., 2007. Larger foraminifera from the Upper Oligocene of the Venetian area, north-east Italy. Palaeontology 50 (4), 845–868. http://dx.doi. org/10.1111/j.1475-4983.2007.00677.x

Bassi, D., Hottinger, L., Nebelsick, J.H., 2007. Larger foraminifera from the Upper Oligocene of the Venetian area, north-east Italy. Palaeontology 50 (4), 845–868. http://dx.doi. org/10.1111/j.1475-4983.2007.00677.x

Bassi, D., Nebelsick, J.H., 2010. Components, facies and ramps: redefining Upper Oligocene shallow water carbonates using coralline red algae and larger foraminifera (Venetian area, northeast Italy). Palaeogeogr. Palaeoclimatol. Palaeoecol. 295, 258-280. http://dx.doi.org/10.1016/j.palaeo.2010.06.003.

Benisek, M.-F., Marcano, G., Betzler, C., Mutti, M., 2010. Facies and stratigraphic architecture of a Miocene warm-temperate to tropical Fault-block carbonate platform, Sardinia (Central Mediterranean Sea). In: Mutti, M., Piller, W., Betzler, C. (Eds.), Carbonate Systems during the OligoceneeMiocene Climatic Transition. Wiley-Blackwell, pp. 129-148.

Benisek, M.F., Betzler, C., Marcano, G., Mutti, M., 2009. Coralline-algal assemblages of a Burdigalian platform slope: implications for carbonate platform reconstruction (northern Sardinia, western Mediterranean Sea). Facies 55, 375-386. http://dx.doi.org/10.1007/BF02536947.

Bernoulli, D., 2001. Mesozoic-Tertiary carbonate platforms, slopes and basins of the external Apennines and Sicily, In: Vai, G.B., Martini, I.P. (Eds.), Anatomy of an Orogen: The Apennines and Adjacent Mediterranean Basins. Springer Netherlands, Dordrecht, pp. 307–325. https://doi.org/10.1007/978-94-015-9829-3_18

Boegman, L., Ivey, G.N., 2009. Flow separation and resuspension beneath shoaling nonlinear internal waves. Journal of Geophysical Research 114, C02018.
Boegman, L., Ivey, G.N., Imberger, J. 2005. The degeneration ofinternal waves in lakes with sloping topography. Limnology and Oceanography. 50, 1620–37.

Boegman, L., Stastna, M., 2019. Sediment Resuspension and Transport by Internal Solitary Waves. Annual Review of Fluid Mechanics 51, 129–154.
Bongaerts, P., Bridge, T.C.L., Kline, D.I., Muir, P.R., Wallace, C.C., Beaman, R.J., Hoegh-Guldberg, O., 2011. Mesophotic coral ecosystems on the walls of Coral Sea atolls. Coral Reefs 30, 335-335. https://doi.org/10.1007/s00338-011-0725-7

Borgomano, J.R.F., 2000. The Upper Cretaceous Carbonates of the Gargano-Murge Region, Southern Italy: A Model of Platform-To-Basin Transition. American Association of Petroleum Geologists Bulletin 84, 1561. https://doi.org/10.1306/8626BF01-173B-11D7-8645000102C1865D

Bosellini, A., 2002. Dinosaurs “re-write” the geodynamics of the eastern Mediterranean and the paleogeography of the Apulia Platform. Earth-Science Reviews 59, 211–234. https://doi.org/10.1016/S0012-8252(02)00075-2

Bosellini, A., Morsilli, M., 1997. A Lower Cretaceous drowning unconformity on the eastern flank of the Apulia Platform (Gargano Promontory, southern Italy). Cretaceous Research. 18, 51–61. https://doi.org/https://doi.org/10.1006/cres.1996.0049

Bosellini, A., Morsilli, M., Neri, C., 1999. Long-Term Event Stratigraphy of the Apulia Platform Margin (Upper Jurassic To Eocene, Gargano, Southern Italy). Journal of Sedimentary Research 69, 1241–1252. https://doi.org/10.2110/jsr.69.1241

Bosellini, F., Perrin, C., 1994. The coral fauna of Vitigliano: qualitative and quantitative analysis in a back reef environment (Castro Limestone, Late Oligocene, Salento Peninsula, southern Italy). B. Soc. Paleontol. Ital. 33, 171-181.

Bosellini, F.R., 2006. Biotic changes and their control on Oligocene–Miocene reefs: a case study from the Apulia Platform margin (southern Italy). Palaeogeogr. Palaeoclimatol. Palaeoecol. 241, 393–409. http://dx.doi.org/10.1016/j.palaeo.2006.04.001

Bosellini, F.R., 2006. Biotic changes and their control on Oligocene–Miocene reefs: a case study from the Apulia Platform margin (southern Italy). Palaeogeogr. Palaeoclimatol. Palaeoecol. 241, 393–409. http://dx.doi.org/10.1016/j.palaeo.2006.04.001

Bosellini, F.R., 2006. Biotic changes and their control on Oligocene–Miocene reefs: a case study from the Apulia Platform margin (southern Italy). Palaeogeogr. Palaeoclimatol. Palaeoecol. 241, 393–409. http://dx.doi.org/10.1016/j.palaeo.2006.04.001

Bosence, D., 2005. A genetic classification of carbonate platforms based on their basinal and tectonic settings in the Cenozoic. Sedimentary Geology 175, 49 – 72.

Bosscher, H., Schlager, W., 1992. Computer simulation of reef growth. Sedimentology 39, 503–512.

Brandano, M., 2003. Tropical/Subtropical Inner Ramp Facies in Lower Miocene “Calcari a Briozoi e Litotamni” of the Monte Lungo Area (Cassino Plain, Central Apennines, Italy). Boll. Soc. Geol. It. 122, 85-98.

Brandano, M., 2016. Oligocene Rhodolith beds in the Central Mediterranean area. In: Riosmena-Rodríguez, R., et al. (Eds.), Rhodolith/Maerl Beds: A Global Perspective. Coastal Research Library, vol. 15, pp. 195-219. http://dx.doi.org/10.1007/ 978-3-319-29315-8_8.

Brandano, M., Corda, L., 2002. Nutrients, sea level and tectonics: constrains for the facies architecture of a Miocene carbonate ramp in central Italy. Terra Nova 14, 257-262.

Brandano, M., Frezza, V., Tomassetti, L., Pedley, M., Matteucci, R., 2009. Facies analysis and palaeoenvironmental interpretation of the late Oligocene attard member (lower coralline limestone formation), Malta. Sedimentology 56, 1138-1158. http://dx.doi.org/10.1111/j.1365 3091.2008.01023.x.

Brown, J., Colling, A., Park, D., Phillips, J., Rothery, D., Wright, J.D., 1989. Seawater: Its Composition, Properties and Behavior. Pergamon Press and The Open University, Oxford. (238 pp.).

Budd, A.F., 2000. Diversity and extinction in the Cenozoic history of Caribbean reefs. Coral Reefs 19, 25-35.

Burchette, T.P., Wright, V.P., 1992. Carbonate ramp depositional systems. Sediment Geology 79,3–57.

Burgess, P.M., 2010. Measuring and modelling carbonate strata: Patterns and prediction from platforms to beds. Conference Abstract, British Sedimentological Research Group.

Burgess, P.M., Wright, V.P., 2005. The carbonate factory continuum, facies mosaics and microfacies: an appraisal of some of the key concepts underpinning carbonate sedimentology Facies 51, 17–23.

Butman, B., Alexander, P.S., Scotti, A., Beardsley, R.C., Anderson, S.P., 2006. Large internal waves in Massachusetts Bay transport sediments offshore. Continental Shelf Research 26, 2029–2049.

Catalano, R., D'Argenio, B., 1981. Paleogeographic evaluation of a continental margin in Sicily. Guidebook, Penrose Conference, Controls of Carbonate Platform Evolution, Palermo, Italy. p. 142.

Carter, G.S., Gregg, M.C., Lien R.C., 2005. Internal waves, solitary-like waves, and mixing on the Monterey Bay shelf. Continental Shelf Research. 25,1499–520.

Cati, A., Sartorio, D., Venturini, S., 1989. Carbonate platforms in the subsurface of the northern Adriatic Sea. Memorie della Società Geologica Italiana 40, 295–308.

Cecca, F., Martin Garin, B., Marchand, D., Lathuiliere, B., Bartolini, A., 2005. Paleoclimatic control of biogeographic and sedimentary events in Tethyan and peri-Tethyan areas during the Oxfordian (Late Jurassic). Palaeogeography, Palaeoclimatology, Palaeoecology 222, 10–32. https://doi.org/10.1016/j.palaeo.2005.03.009

Corlett, H., Jones, B., 2011. Ecological controls on Devonian stromatoporoid-dominated and coral-dominated reef growth in the Mackenzie Basin, Northwest Territories, Canada. Canadian Journal of Earth Sciences 48, 1543–1560. https://doi.org/10.1139/e11-056

Da Silva, A.C., Kershaw, S., Boulvain, F., 2011a. Sedimentology and stromatoporoid palaeoecology of Frasnian (upper Devonian) carbonate mounds in southern Belgium. Lethaia 44, 255–274. https://doi.org/10.1111/j.1502-3931.2010.00240.x

Da Silva, A.C., Kershaw, S., Boulvain, F., 2011b. Stromatoporoid palaeoecology in the Frasnian (Upper Devonian) Belgian platform, and its applications in interpretation of carbonate platform environments. Palaeontology 54, 883–905. https://doi.org/10.1111/j.1475-4983.2011.01037.x

DeCarlo, T.M., Karnauskas, K.B., Davis, K.A., Wong, G.T.F., 2015. Climate modulates internal wave activity in the Northern South China Sea. Geophys. Res. Lett. 42, 831-838. http://dx.doi.org/10.1002/2014GL062522

Dercourt, J., Gaetani, M., Vrielynck, B., Barrier, E., Biju, Duval B., Brunet, M.F., Cadet, J.P., Crasquin, S., Sandulescu, M., 2000. Atlas Peri-Tethys, Paleogeographical Maps. CCGM/CGMW, Paris, pp. 1–269.

Dromart, G., Gaillard, C., Jansa, L.F., 1994. Deep-Marine Microbial Structures in the Upper Jurassic of Western Tethys, in: Bertrand-Sarfati, J., Monty, C. (Eds.), Phanerozoic Stromatolites II. Springer Netherlands, Dordrecht, pp. 295–318. https://doi.org/10.1007/978-94-011-1124-9_12

Dunham, R.J., 1962. Classification of carbonate rocks according to depositional texture. In: Ham, W.E. (Ed.), Classification of Carbonate Rocks. American Association of Petroleum Geologists Memoir vol. 1, pp. 108–121.

Dupraz, C., Strasser, A., 1999. Microbialites and micro-encrusters in shallow coral bioherms (Middle to Late Oxfordian, Swiss Jura mountains). Facies 40, 101–129. https://doi.org/10.1007/BF02537471

Dupraz, C., Strasser, A., 2002. Nutritional modes in coral-microbialite reefs (Jurassic, Oxfordian, Switzerland): Evolution of trophic structure as a response to environmental change. Palaios 17, 449–471. https://doi.org/10.1669/0883-1351

El-sabbagh, A.M., El-hedeny, M.M., Mansour, A.S., 2017. Paleoecology and Paleoenvironment of the Middle – Upper Jurassic sedimentary succession, central Saudi Arabia. Proceedings of the Geologists' Association 128, 340–359. https://doi.org/10.1016/j.pgeola.2017.02.001

Embry, A.F., Klovan, J.E., 1971. A Late Devonian reef tract on northeastern Banks Island, NWT. Bulletin of Canadian Petroleum Geology 19, 730–781. https://doi.org/10.5072/PRISM/22817

Farzipour-Saein, A., Yassaghi, A., Sherkati, S., Koyi, H., 2009. Basin evolution of the Lurestan region in the Zagros fold-and-thrust belt, Iran. J Pet Geol 32, 5–19.

Feldman, B., Shlesinger, T., Loya, Y., 2018. Mesophotic coral-reef environments depress the reproduction of the coral Paramontastraea peresi in the Red Sea. Coral Reefs 37, 201–214. https://doi.org/10.1007/s00338-017-1648-8.

Flügel, E., 2004. Microfacies of Carbonate Rocks: Analysis, Interpretation and Application. 976 pp. Springer-Verlag, Berlin Heidelberg. https://doi.org/10.1007/978-3-642-03796-2

Frieder, C.A., Nam, S.H., Martz, T.R., Levin, L.A., 2012. High temporal and spatial variability of dissolved oxygen and pH in a nearshore California kelp forest. Biogeosciences 9,3917–30.

Frost, S.H., 1977. Oligocene Reef Coral Biogeography Caribbean and Western Tethys. Mem. B.R.G.M., Paris, pp. 342-352.

Frost, S.H., 1981. Oligocene reef coral biofacies of the Vicentin, northeast Italy. In: Toomey, D.F. (Ed.), European Fossil Reef Models. SEPM Spec. Publ., pp. 483-539.

Frost, S.H., Harbour, J.L., Realini, M.J., Harris, P.M., 1983. Oligocene reef tract development, southwestern Puerto Rico. Sedimenta 9, 141 pp.

Garrett, C., Munk, W., 1979. Internal waves in the ocean. Annual Review of Fluid Mechanic 11, 339–69.

Garrett, C., Kunze, E., 2007. Internal tide generation in the deep ocean. Annu. Rev. Fluid Mech. 39, 57–87.

Geister, J., Ungaro, S., 1977. The Oligocene coral formations of the Colli Berici. Eclogae Geol. Helv. 70, 811-23.

Ginsburg, R.N., James, N. P., 1974. Holocene carbonate sediments of continental shelves. Continental Margins. Berlin, Springer-Verlag: 137-154.

Guo, L., Vincent, S.J., Lavrishchev, V., 2011. Upper Jurassic Reefs from the Russian Western Caucasus: Implications for the Eastern Black Sea. Turkish Journal of Earth Sciences 20, 629–653. https://doi.org/10.3906/yer-1012-5

Halfar, J., Mutti, M., 2005. Global dominance of coralline red-algal facies: a response to Miocene oceanographic events. Geology 33, 481-484. http://dx.doi.org/ 10.1130/G21462.

Hallock, P., 1981. Algal symbiosis: a mathematical analysis. Marine Biology. 62, 249-255.

Hallock, P., 1987. Fluctuations in the trophic resource continuum: a factor in global diversity cycles?. Paleoceanography and Paleoclimatology 2, 457-471.

Hallock, P., 2001. Coral reefs, carbonate sedimentation, nutrients, and global change. In: Stanley Jr., G.D. (Ed.), The history and sedimentology of ancient reef systems. Kluwer Academic/ Plenum Publishers, New York, Topics in Geobiology, 17, 387-427.

Hallock, P., 2005. Global change and modern coral reefs: new opportunities to understand shallow-water carbonate depositional processes. Sedimentary Geology. 175, 19–33. http://dx.doi. org/10.1016/j.sedgeo.2004.12.027

Hallock, P., 2015. Changing influences between life and limestones in earth history. In: Birkeland, C. (Ed.), Coral Reefs in the Anthropocene. Springer, Dordrecht, pp. 17–42. http://dx.doi.org/10.1007/978-94-017-7249-5.

Hallock, P., Premoli-Silva, I., Boersma, A., 1991. Similarities between planktonic and larger foraminiferal evolutionary trends through Paleogene paleoceanographic changes. Palaeogeography, Palaeoclimatology, Palaeoecology 83, 49–64.

Hallock, P., Schlager, W., 1986. Nutrient excess and the demise of coral reefs and carbonate platforms. Palaios 1, 389-398.

Handford, C.R., Loucks, R. G., 1993. Carbonate depositional sequences and systems tracts: responses of carbonate platforms to relative sea-level changes. Carbonate Sequence Stratigraphy: Recent Developments and Applications. B. Loucks and R. J. Sarg, American Association of Petroleum Geologists Bulletin. 57, 3-41.

Handford, C.R., Loucks, R.G., 1993. Carbonate depositional sequences and systems tracts: responses of carbonate platforms to relative sea-level changes. Carbonate Sequence Stratigraphy:

Recent Developments and Applications. B. Loucks and R. J. Sarg, American Association of Petroleum Geologists Bulletin. 57, 3-41.

Haq, B.U., 2018. Jurassic Sea-Level Variations: A Reappraisal. GSA Today 4–10. https://doi.org/10.1130/GSATG359A.1

Heydari, E., 2008. Tectonics versus eustatic control on supersequences of the Zagros Mountains of Iran. Tectonophysics 451,56–70.

Hine, A.C., 1983. Modern shallow water carbonate platform margins: Platform margin and deep water carbonates. USA, Lecture Notes for Short Course No. 12, Society of Economic Paleontologists and Mineralogists.: 3-100.

Hoffmann, M., Kołodziej, B., Skupien, P., 2017. Microencruster-microbial framework and synsedimentary cements in the Štramberk Limestone (Carpathians, Czech Republic): Insights into reef zonation. Annales Societatis Geologorum Poloniae 87, 325–347. https://doi.org/10.14241/asgp.2017.018

Holz, M., 2015. Mesozoic paleogeography and paleoclimates - A discussion of the diverse greenhouse and hothouse conditions of an alien world. Journal of South American Earth Sciences 61, 91–107. https://doi.org/10.1016/j.jsames.2015.01.001

Hosegood, P., Bonnin, J., van Haren, H., 2004. Solibore-induced sediment resuspension in the Faeroe-Shetland Channel. Geophysical Research Letter 31, L09301-4.

Hosegood, P., van Haren, H., 2004. Near-bed solibores over the continental slope in the Faeroe-Shetland Channel. Deep Sea Research II 51, 2943–71.

Hottinger, L., 1998. Shallow benthic foraminifera at the paleocene-Eocene boundary. Strata s_erie 1 (9), 6-64.In: Stanley, G.D. (Ed.), The History and Sedimentology of Ancient Reef Ecosystems. Kluwer Academic/Plenum Publishers, pp. 387-427.

Immenhauser, A., 2009. Estimating palaeo-water depth from the physical rock record. Earth-Science Reviews 96, 107–139. https://doi.org/10.1016/j.earscirev.2009.06.003

Insalaco, E., 1996. Upper Jurassic microsolenid biostromes of northern and central of northern and central. Europe: Facies and depositional environment. Palaeogeography, Palaeoclimatology, Palaeoecology. 121, 169-194.

Insalaco, E., 1999. Facies and Palaeoecology of Upper Jurassic (Middle Oxfordian) Coral Reefs in England. Facies 40, 81–99. https://doi.org/10.1007/BF02537470

Insalaco, E., Hallam, A., Rosen, B., 1997. Oxfordian (Upper Jurassic) coral reefs in Western Europe: reef types and conceptual depositional model. Sedimentology 44, 707–734. https://doi.org/10.1046/j.1365-3091.1997.d01-44.x

Jakubowicz, M., Król, J., Zapalski, M.K., Wrzołek, T., Wolniewicz, P., Berkowski, B., 2018. At the southern limits of the Devonian reef zone: Palaeoecology of the Aferdou el Mrakib reef (Givetian, eastern Anti-Atlas, Morocco). Geological Journal 1–29. https://doi.org/10.1002/gj.3152

James, G.A., Wynd, J.G., 1965. Stratigraphic nomenclature of Iranian Oil Consortium Agreement Area. AAPG Bull 49, 2182–2245.

James, N.P., Bourque, P.A., 1992. Reefs and mounds. In: Walker, R.G., James, N.P. (Eds.), Facies Models: Response to Sea Level Change. Geological Association of Canada, St. John's, Newfoundland, pp. 323–347.

Jones, B., Desrochers, A., 1992. Shallow Platform Carbonates. Facies Models. R. G. Walker and N. P. James. Newfoundland, Geological Association of Canada: 277-301.

Kahng, S., Copus, J.M., Wagner, D., 2017. Mesophotic Coral Ecosystems, in: Rossi, S., Bramanti, L., Gori, A., Covadonga, O. (Eds.), Marine Animal Forests: The Ecology of Benthic Biodiversity Hotspots. Springer International Publishing, Cham, pp. 185–206. https://doi.org/10.1007/978_3-319-21012-4_4

Kahng, S.E., Copus, J.M., Wagner, D., 2014. Recent advances in the ecology of mesophotic coral ecosystems (MCEs). Curr. Opin. Environ. Sustain. 7, 72–81. https://doi.org/10.1016/j.cosust.2013.11.019

Kahng, S.E., Garcia-Sais, J.R., Spalding, H.L., Brokovich, E., Wagner, D., Weil, E., Hinderstein, L., Toonen, R.J., 2010. Community ecology of mesophotic coral reef ecosystems. Coral Reefs 29, 255–275. https://doi.org/10.1007/s00338-010-0593-6

Kano, A., Wang, W., Matsumoto, R., 2007. Facies and depositional environment of the uppermost Jurassic stromatoporoid biostromes in the Zagros Mountains of Iran. Gff 129, 107–112. https://doi.org/10.1080/11035890701292107

Kershaw, S., 1998. The applications of stromatoporoid palaeobiology in palaeoenvironmental analysis. Palaeontology 41, 3, 509–544.

Kershaw, S., Min, L., Yuan, W., 2013. Palaeozoic stromatoporoid futures: A discussion of their taxonomy, mineralogy and applications in palaeoecology and palaeoenvironmental analysis. Journal of Palaeogeography 2, 163–182. https://doi.org/10.3724/SP.J.1261.2013.00024

Kershaw, S., Mõtus, M., 2016. Palaeoecology of corals and stromatoporoids in a late Silurian biostrome in Estonia. Acta Palaeontologica Polonica 61, 33–50. https://doi.org/10.4202/app.00094.2014

Kiessling, W., 2002. Secular variations in the Phanerozoic reef ecosystem. In: Kiessling, W., Flü gel, E., Golonka, J. (Eds.), Phanerozoic Reef Patterns, Society of Economic Paleontologists and Mineralogists. Special Publication 72, pp. 625 – 690. Tulsa

Kiessling, W., 2009. Geologic and Biologic Controls on the Evolution of Reefs. Annual Review of Ecology, Evolution, and Systematics 40, 173–192. https://doi.org/10.1146/annurev.ecolsys.110308.120251

Krajewski, M., Olchowy, P., Felisiak, I., 2016. Late Jurassic facies architecture of the Złoczew Graben: implications for evolution of the tectonic-controlled northern peri-Tethyan shelf (Upper

Oxfordian–Lower Kimmeridgian, Poland). Facies 62, 1–19. https://doi.org/10.1007/s10347-015-0455-3

Lamb, K.G., 2014. Internal Wave Breaking and Dissipation Mechanisms on the Continental Slope/Shelf. Annual Review of Fluid Mechanics 46, 231–254. https://doi.org/10.1146/annurev-fluid-011212-140701

Lathuilière, B., Gaillard, C., Habrant, N., Bodeur, Y., Boullier, A., Enay, R., Hanzo, M., Marchand, D., Thierry, J., Werner, W., 2005. Coral zonation of an Oxfordian reef tract in the northern French Jura. Facies 50, 545–559. https://doi.org/10.1007/s10347-004-0035-4

Leichter, J.J., Shellenbarger, G., Genovese, S.J., Wing, S.R., 1998. Breaking internal waves on a Florida (USA) coral reef: a plankton pump at work? Mar. Ecol. Prog. Ser. 166, 83-97.

Leichter, J.J., Stewart, H.L., Miller, S.L., 2003. Episodic nutrient transport to Florida coral reefs. Limnology and Oceanography 48, 1394–1407.

Leinfelder, R.R., 1993. Upper Jurassic reef types and controlling factors. A preliminary report. Profil 5, 1–45.

Leinfelder, R.R., Schlagintweit, F., Werner, W., Ebli, O., Nose, M., Schmid, D.U., Hughes, G.W., 2005. Significance of stromatoporoids in Jurassic reefs and carbonate platforms - Concepts and implications. Facies 51, 287–325. https://doi.org/10.1007/s10347-005-0055-8

Leinfelder, R.R., Schmid, D.U., Nose, M., Werner, W., 2002. Jurassic reef patterns. The expression of a changing globe. In: Kiessling, W., Flügel, E., Golonka, J. (Eds.), Phanerozoic Reef Patterns: SEPM Special Publication 72, 465–520.

Leinfelder, R.R., Werner, W., Nose, M., Schmid, D.U., Krautter, M., Laternser Tokacs, M., Hartmann, D., 1996. Paleoecology, growth parameters and dynamics of coral, sponge and

microbolite reefs from the Late Jurassic. Göttinger Arbeiten zur Geologie und Paläontologie 2, 227–248.

Lerczak, J.A., Hendershott, M.C., Winant, C.D., 2001. Observations and modeling ofcoastal internal waves driven by a diurnal sea breeze. Journal of Geophysical Research: Oceans 106,19715–29.

Lerczak, J.A., Winant, C.D., Hendershott, M.C., 2003. Observations of the semidiurnal internal tide on the southern California slope and shelf. Journal of Geophysical Research: Oceans 108, 30-68.

Lesser, M.P., Slattery, M., Leichter, J.J., 2009. Ecology of mesophotic coral reefs. J. Exp. Mar. Bio. Ecol. 375, 1–8. https://doi.org/10.1016/j.jembe.2009.05.009

Liebau, A., 1984. Grundlagen der €Okobathymetrie. Pal€aontol. Kursb. 2, 149-184.

Lim, K., Ivey, G.N., Jones, N.L., 2010. Experiments on the generation of internal waves over continental shelf topography. Journal of Fluid Mechanics 663, 385–400.

Lomando, A.J., Harris, P.M., 1991. SEPM Core Workshop: Mixed Carbonate-Siliciclastic Sequences. Tulsa, SEPM.

Longman, M.W., 1980. Carbonate diagenetic textures from near surface diagenetic environments. The American Association of Petroleum Geologists Bulletin 64, 461-487.

Luperto Sinni, E., Masse, J.P., 1994). Precisazioni micropaleontologiche sulle formazioni di piattaforma carbonatica del Giurassico superiore e del Cretaceo basale del massiccio del Gargano (Italia Meridionale) e implicazioni stratigrafiche. Paleopelagos 4, 243-266.

Mann, K.H., Lazier, J.R.N., 2006. Dynamics of Marine Ecosystems: Biological–Physical Interactions in the Oceans. Wiley-Blackwell. (496 pp.).

Martin-Garin, B., Lathuilière, B., Geister, J., 2012. The shifting biogeography of reef corals during the Oxfordian (Late Jurassic). A climatic control?. Palaeogeography, Palaeoclimatology, Palaeoecology 365–366, 136–153. https://doi.org/10.1016/j.palaeo.2012.09.022

Matyszkiewicz, J., Kochman, A., Duś, A., 2012. Influence of local sedimentary conditions on development of microbialites in the Oxfordian carbonate buildups from the southern part of the Kraków–Częstochowa Upland (South Poland). Sedimentary Geology 263–264, 109–132. https://doi.org/10.1016/j.sedgeo.2011.08.005

Michel, J., Borgomano, J., Reijmer, J.J.G., 2018. Heterozoan carbonates: When, where and why? A synthesis on parameters controlling carbonate production and occurrences. Earth-Science Reviews 182, 50–67. https://doi.org/10.1016/j.earscirev.2018.05.003

Morsilli, M., 1998. Stratigrafia e sedimentologia del margine della piattaforma Apula nel Gargano (Giurassico superiore - Cretaceo inferiore). PhD thesis. University of Bologna. 222 pp.

Morsilli, M., 2011. Introduzione alla geologia del Gargano, in M. Tarantini and A. Galiberti, eds., Le Miniere Di Selce Del Gargano, VI-III Millennio a.C. Alle Origini Della Storia Mineraria Europea: Florence, Italy, All'Insegna del Giglio, 17–27.

Morsilli, M., Bosellini, A., 1997. Carbonate facies zonation of the Upper Jurassic–Lower Cretaceous Apulia platform margin (Gargano Promontory, southern Italy). Rivista Italiana Paleontologia Stratigrafica 103, 193–206.

Morsilli, M., Bosellini, F.R., Pomar, L., Hallock, P., Aurell, M., Papazzoni, C.A., 2012. Mesophotic coral buildups in a prodelta setting (Late Eocene, southern Pyrenees, Spain): A mixed carbonate-siliciclastic system. Sedimentology 59, 766–794. https://doi.org/10.1111/j.1365-3091.2011.01275.x

Morsilli, M., Hairabian, A., Borgomano, J., Nardon, S., Adams, E., Gartner, G.B., 2017. The Apulia Carbonate Platform—Gargano Promontory, Italy (Upper Jurassic–Eocene). American

Association of Petroleum Geologists Bulletin 101, 523–531. https://doi.org/10.1306/011817DIG17031

Moum, J.N., Farmer, D.M., Smyth, W.D., Armi, L., Vagle, S., 2003. Structure and generation Structure and generation of turbulence at interfaces strained by internal solitary waves propagating shoreward over the continental shelf. Journal of Physical Oceanography 33, 2093–2112.

Munk, W., 1981. Internal waves and small-scale processes. In: Warren, B.A., Wunsch, C. (Eds.), Evolution of Physical Oceanography. MIT Press, Cambridge, pp. 264–291.

Mutti, M., Hallock, P., 2003. Carbonate systems along nutrient and temperature gradients: some sedimentological and geochemical constraints. International Journal of Earth Sciences 92, 465–475.

Nakayama, K., Sato, T., Shimizu, K., Boegman, L., 2019. Classification of internal solitary wave breaking over a slope. Physical Review Fluids 4, 14801-16.

Nash, J.D., Moum, J.N., 2005. River plumes as a source of large-amplitude internal waves in the coastal ocean. Nature 437, 400–403.
Nash, J.D., Kelly, S.M., Shroyer, E.L., Moum, J.N., Duda, T.F., 2012. The unpredictable nature of internal tides on continental shelves. Journal of Physical Oceanography 42,1981–2000.

Nebelsick, J.H., Bassi, D., Lempp, J., 2013. Tracking paleoenvironmental changes in coralline algal-dominated carbonates of the Lower Oligocene Calcareniti di Castelgomberto formation (Monti Berici, Italy). Facies 59, 133-148. http:// dx.doi.org/10.1007/s10347-012-0349-6.

Nichols, G., 2009. Sedimentology and Stratigraphy, Wiley and Sons, New York, 225-246.

Nunes, F., Norris, R.D., 2006. Abrupt reversal in ocean overturning during the Palaeocene/ Eocene warm period. Nature 439, 60–63.

Olivier, N., Carpentier, C., Martin-Garin, B., Lathuilière, B., Gaillard, C., Ferry, S., Hantzpergue, P., Geister, J., 2004. Coral-microbialite reefs in pure carbonate versus mixed carbonate-siliciclastic

depositional environments: The example of the Pagny-sur-Meuse section (Upper Jurassic, northeastern France). Facies 50, 229–255. https://doi.org/10.1007/s10347-004-0018-5

Olivier, N., Colombié, C., Pittet, B., Lathuilière, B., 2011. Microbial carbonates and corals on the marginal French Jura platform (Late Oxfordian, Molinges section). Facies 57, 469–492. https://doi.org/10.1007/s10347-010-0246-9

Olivier, N., Hantzpergue, P., Gaillard, C., Pittet, B., Leinfelder, R.R., Schmid, D.U., Werner, W., 2003. Microbialite morphology, structure and growth: a model of the Upper Jurassic reefs of the Chay Peninsula (western France). Palaeogeography, Palaeoclimatology, Palaeoecology 193, 383–404.

Olivier, N., Martin-Garin, B., Colombié, C., Cornée, J.J., Giraud, F., Schnyder, J., Kabbachi, B., Ezaidi, K., 2012. Ecological succession evidence in an Upper Jurassic coral reef system (Izwarn section, High Atlas, Morocco). Geobios 45, 555–572. https://doi.org/10.1016/j.geobios.2012.05.002

Olivier, N., Pittet, B., Gaillard, C., Hantzpergue, P., 2007. High-frequency palaeoenvironmental fluctuations recorded in Jurassic coral- and sponge-microbialite bioconstructions. Comptes Rendus Palevol 6, 21–36. https://doi.org/10.1016/j.crpv.2006.07.005

Olivier, N., Pittet, B., Werner, W., Hantzpergue, P., Gaillard, C., 2008. Facies distribution and coral-microbialite reef development on a low-energy carbonate ramp (Chay Peninsula, Kimmeridgian, western France). Sedimentary Geology 205, 14–33. https://doi.org/10.1016/j.sedgeo.2007.12.011

Olóriz, F., Reolid, M., Rodríguez-Tovar, F.J., 2003. A Late Jurassic carbonate ramp colonized by sponges and benthic microbial communities (External Prebetic, Southern Spain). Palaios 18, 528–545.

Pagani, M., Zachos, J.C., Freeman, K.H., Tipple, B., Bohaty, S., 2005. Marked decline in atmospheric carbon dioxide concentrations during the Paleogene. Science 309, 600-603.

Pandey, D.K., Fürsich, F.T., 2003. Jurassic corals of east-central Iran. Beringeria 32, 1–138.

Papastamatiou, Y.P., Meyer, C.G., Kosaki, R.K., Wallsgrove, N.J., Popp, B.N., 2015. Movements and foraging of predators associated with mesophotic coral reefs and their potential for linking ecological habitats. Mar. Ecol. Prog. Ser. 521, 155–170. https://doi.org/10.3354/meps11110

Pavan, G., Pirini, C., 1966. Stratigrafia del Foglio 157 ‘‘Monte S. Angelo’’. Bollettino del Servizio Geologico Italiano 86, 123–189.

Pearson, P.N., McMillan, I.K., Wade, B.S., Jones, T.D., Coxall, H.K., Bown, P.R., Lear, C.H., 2008. Extinction and environmental change across the Eocene-Oligocene boundary in Tanzania. Geology 36, 179-182. http://dx.doi.org/ 10.1130/g24308a.1.

Perrin, C., 2002. Tertiary: the emergence of modern reef ecosystems. In: Kiessling, W., Flügel, E., Golonka, J. (Eds.), Phanerozoic Reef Patterns, vol. 72. SEPM Special Publication, pp. 587-621.
Perrin, C., Bosellini, F.R., 2012. Paleobiogeography of scleractinian reef corals: changing patterns during the OligoceneeMiocene climatic transition in the Mediterranean. Earth-Sci. Rev. 111, 1-24. http://dx.doi.org/10.1016/j.earscirev. 2011.12.007.

Picotti, V., Cobianchi, M., 2017. Jurassic stratigraphy of the Belluno Basin and Friuli Platform: a perspective on far-field compression in the Adria passive margin. Swiss Journal of Geosciences 110, 833–850. https://doi.org/10.1007/s00015-017-0280-5

Pomar, L., 2001. Types of carbonate platforms, a genetic approach. Basin Res. 13, 313-334. http://dx.doi.org/10.1046/j.0950-091x.2001.00152.x.

Pomar, L., Baceta, J.I., Hallock, P., Mateu-Vicens, G., Basso, D., 2017. Reef building and carbonate production modes in the west-central Tethys during the Cenozoic. Marine and Petroleum Geology 83, 261–304. https://doi.org/10.1016/j.marpetgeo.2017.03.015

Pomar, L., Brandano, M., Westphal, H., 2004. Environmental factors influencing skeletal-grain sediment associations: a critical review of Miocene examples from the Western-Mediterranean. Sedimentology 51, 627-651. http:// dx.doi.org/10.1111/j.1365-3091.2004.00640.x.
Pomar, L., Hallock, P., 2008. Carbonate factories: a conundrum in sedimentary geology. Earth-Sci. Rev. 87, 134-169. http://dx.doi.org/10.1016/j.earscirev.2007.12.002.

Pomar, L., Hallock, P., 2008. Carbonate factories: A conundrum in sedimentary geology. Earth-Science Reviews 87, 134–169. https://doi.org/10.1016/j.earscirev.2007.12.002

Pomar, L., Morsilli, M., Hallock, P., Bádenas, B., 2012. Internal waves, an under-explored source of turbulence events in the sedimentary record. Earth-Science Reviews 111, 56–81. https://doi.org/10.1016/j.earscirev.2011.12.005

Ray, R.D., Mitchum, G.T., 1996. Surface manifestation of internal tides generated near Hawaii. Geophysical Research Letter 23, 2101–4.

Read, J.F., 1982. Carbonate platforms of passive (extensional) continental margins: types, characteristics and evolution. Tectonophysics 81, 195-212.

Read, J.F., 1998. Phanerozoic carbonate ramps from greenhouse, transitional and ice-house worlds: clues from field and modeling studies. In: Wright V.P. and Burchette T.P (Eds) Carbonate Ramps. Geological Society of London Special Publications 149,107–135.

Reolid, M., Gaillard, C., Lathuilière, B., 2007. Microfacies, microtaphonomic traits and foraminiferal assemblages from Upper Jurassic oolitic-coral limestones: Stratigraphic fluctuations in a shallowing-upward sequence (French Jura, Middle Oxfordian). Facies 53, 553–574. https://doi.org/10.1007/s10347-007-0121-5

Reolid, M., Gaillard, C., Olóriz, F., Rodríguez-Tovar, F.J., 2005. Microbial encrustations from the Middle Oxfordian-earliest Kimmeridgian lithofacies in the Prebetic Zone (Betic Cordillera, southern Spain): Characterization, distribution and controlling factors. Facies 50, 529–543. https://doi.org/10.1007/s10347-004-0030-9

Richardson, K., Visser, A.W., Pedersen, F.B., 2000. Subsurface phytoplankton blooms fuel pelagic production in the North Sea. Journal of Plankton Research 22 (9), 1663–1671.

Riding, R., 2002. Structure and composition of organic reefs and carbonate mud mounds: Concepts and categories. Earth-Science Reviews 58, 163–231. https://doi.org/10.1016/S0012-8252(01)00089-7

Rocha, L.A., Pinheiro, H.T., Shepherd, B., Papastamatiou, Y.P., Luiz, O.J., Pyle, R.L., Bongaerts, P., 2018. Mesophotic coral ecosystems are threatened and ecologically distinct from shallow water reefs. Science. 361, 281–284. https://doi.org/10.1126/science.aaq1614

Rosales, I., Pomar, L., Al-Awwad, S.F., 2018. Microfacies, diagenesis and oil emplacement of the Upper Jurassic Arab-D carbonate reservoir in an oil field in central Saudi Arabia (Khurais Complex). Marine and Petroleum Geology 96, 551–576. https://doi.org/10.1016/j.marpetgeo.2018.05.010

Rusciadelli, G., Ricci, C., Lathuilière, B., 2011. The Ellipsactinia Limestones of the Marsica area (Central Apennines): A reference zonation model for Upper Jurassic Intra-Tethys reef complexes. Sedimentary Geology 233, 69–87. https://doi.org/10.1016/j.sedgeo.2010.10.011

Russo, A., Morsilli, M., 2007. New insight on architecture and microstructure of *Ellipsactinia* and *Sphaeractinia* (demosponges) from the Gargano Promontory (southern Italy). Geologica Romana 40, 215–225.

Ryan, J.P., Chavez, F.P., Bellingham, J.G., 2005. Physical–biological coupling in Monterey Bay, California: topographic influences on phytoplankton ecology. Marine Ecology Progress Series 287, 23–32.

Sadeghi, R., Vaziri-Moghaddam, H., Taheri, A., 2011. Microfacies and sedimentary environment of the Oligocene sequence (Asmari Formation) in Fars sub-basin, Zagros Mountains, southwest Iran. Facies 57:431–446. doi:10.1007/s10347-010-0245-x

San Miguel, G., Aurell, M., Bádenas, B., 2017. Occurrence of high-diversity metazoan- to microbial-dominated bioconstructions in a shallow Kimmeridgian carbonate ramp (Jabaloyas, Spain). Facies 63, 1–21. https://doi.org/10.1007/s10347-017-0493-0

Schlager, W., 1981. The paradox of drowned reefs and carbonate platforms. Geological Society of America Bulletin 92, 197-211.

Schlager, W., 2000. Sedimentation rates and growth potential of tropical, cool water and mud mound carbonate factories. In: Insalaco, E., Skelton, P.W., Palmer, T.J. (Eds.), Carbonate Platform Systems: Components and Interactions. Geological Society London, Special Publication., 178, pp. 217–227. http://dx.doi.org/10.1144/GSL.SP.2000.178.01.14.

Schlager, W., 2005. Carbonate Sedimentology and Sequence Stratigraphy. SEPM Concepts in Sedimentology and Paleontology, 8, 200 p.

Schlager, W., 2003. Benthic carbonate factories of the Phanerozoic. International Journal of Earth Sciences. (Geol. Rundsch.) 92, 445–464. http://dx.doi.org/10.1007/s00531-003-0327-x.

Schlagintweit, F., Gawlick, H.J., 2008. The occurrence and role of microencruster frameworks in Late Jurassic to Early Cretaceous platform margin deposits of the Northern Calcareous Alps (Austria). Facies 54, 207–231.

Schlagintweit, F., Gawlick, H.J., Missoni, S., Lein, R., 2005. The reefal facies of the Upper Jurassic Plassen carbonate platform at Mt. Jainzen (Northern Calcareous Alps, Austria). Schriftenreihe der Deutschen Gesellschaft für Geowissenschaften 38, 130–131.

Schmid, D.U., 1996. Marine Mikrobolithe und Mikroinkrustierer aus dem Oberjura. Profil 9, 101–251.

Seilacher, A., 1982. General remarks about event deposits. In: Einsele, G., Seilacher, A.(Eds.), Cyclic and Event Stratification. Springer-Verlag, New York, pp. 161–174.

Shabafrooz, R., Mahboubi, A., Vaziri-Moghaddam, H., Ghabeishavi, A., Moussavi- Harami, R., 2015. Depositional architecture and sequence stratigraphy of the oligoeMiocene Asmari platform; southeastern Izeh zone, Zagros Basin, Iran. Facies 61, 1-32. http://dx.doi.org/10.1007/s10347-014-0423-3.

Shanmugam, G., 2013. Modern internal waves and internal tides along oceanic pycnoclines: Challenges and implications for ancient deep-marine baroclinic sands. American Association of Petroleum Geologists Bulletin 97, 799. https://doi.org/10.1306/10171212101

Shepard, F.P., 1976. Tidal components of currents in submarine canyons. Journal of Geology 84, 343–350.

Sherkati, S., Letouzey, J., 2004. Variation of structural style and basin evolution in the central Zagros (Izeh zone and Dezful Embay- ment), Iran. Mar Pet Geol 21,535–554.

Simmons, H.L., Hallberg, R.W., Arbic, B.K., 2004. Internal wave generation in a global baroclinic tide model. Deep-Sea Research II 51,3043–68.

Stastna, M., Lamb, K.G., 2008. Sediment resuspension mechanisms associated with internal waves in coastal waters. Journal Geophysical Research 113, C10016-19.

Strasser, A., Pittet, B., Hug, W., 2015. Palaeogeography of a shallow carbonate platform: The case of the Middle to Late Oxfordian in the Swiss Jura Mountains. Journal of Palaeogeography 4, 251–268. https://doi.org/10.1016/j.jop.2015.08.005

Strasser, A., Védrine, S., 2009. Controls on facies mosaics of carbonate platforms: a case study from the Oxfordian of the Swiss Jura. International Association of Sedimentologists, Special Publication 41, 199–214. https://doi.org/10.1002/9781444312065.ch13

Tucker, M., Wright,V.P., 1990. Carbonate Sedimentology. Blackwell Science.

Turnšek, D., Buser, S., Ogorolec, B., 1981. An upper Jurassic reef complex from Slovenia, Yugoslavia. In: Toomey, D.F. (Ed.), European Fossil Reef Models: SEPM Special Publication 30, 361–369.

Van Buchem, F.S.P., Allan, T.L., Laursen, G.V., Lotfpour, M., Moallemi, A., Monibi, S., Motiei, H., Pickard, N.A.H., Tahmasbi, A.R., Vedrenne, V., Vincent, B., 2010. Regional stratigraphic architecture and reservoir types of the Oligo-Miocene deposits in the dezful Embayment (Asmari and pabdeh formations) SW Iran. In: Van Buchem, F.S.P., Gerdes, K.D., Esteban, M. (Eds.), Mesozoic and Cenozoic Carbonate Systems of the Mediterranean and the Middle East:

Stratigraphic and Diagenetic Reference Models. Geol. Soc., vol. 329. Spec. Publ., London, pp. 219-263.
Vaziri-Moghaddam, H., Kimiagari, M., Taheri, A., 2006. Depositional environment and sequence stratigraphy of the Oligo–Miocene Asmari Formation in SW Iran. Facies 52,41–51.

White, M., Dorschel, B., 2010. The importance of the permanent thermocline to the cold water coral carbonate mound distribution in the NE Atlantic. Earth Planet. Sc. Lett. 296, 395-402. http://dx.doi.org/10.1016/j.epsl.2010.05.025.

Wilson, M.E.J., 2008. Global and regional influences on equatorial shallow-marine carbonates during the Cenozoic. Palaeogeogr. Palaeoclimatol. Palaeoecol. 265, 262-274. http://dx.doi.org/10.1016/j.palaeo.2008.05.012.
Wilson, J.L., 1975. Carbonate Facies in Geologic History. Springer Verlag, New York, 471p.

Wilson, M.E.J., Vecsei, A., 2005. The apparent paradox of abundant foramol facies in low latitudes: their environmental significance and effect on platform development. Earth-Science Reviews 69, 133–168.

Wood, R., 1999. Reef Evolution. Oxford University Press, Oxford, 414 pp.

Woodson, C.B., 2018. The Fate and Impact of Internal Waves in Nearshore Ecosystems. Annual Review of Marine Science 10, 421-441.

Wright, V.P., Burchette, T.P., 1996. Shallow-water carbonate environments. Sedimentary Environments: Processes, Facies and Stratigraphy. H. G. Reading. Oxford, Blackwell Sciences, 325 394.

Zachos, J.C., Pagani, M., Sloan, L., Thomas, E., Billups, K., 2001. Trends, rhythms, and aberrations in global climate 65 Ma to Present. Science 292, 686-693.

Zhao, Z., Alford, M.H., 2009. New altimetric estimates ofmode-1 M2 internal tides in the central North Pacific Ocean. Journal of Physical Oceanography 39,1669–84.